Lancaster Environment Centre

Lancaster University

Adsorption and release behavior of chemicals from microplastics during environmental aging

Xiaoxin Chen

Submitted for the degree of Doctor of Philosphy

July 2024

Abstract

Plastics are widely used in daily life due to their flexibility, durability and low cost. Due to their global usage, and poor handling at all stages of use from manufacture to disposal, an increasing quantity of microplastic debris has been detected in aquatic environments. As microplastics are composed of a wide range of chemical additives (e.g., plasticizers, flame retardants, fillers, etc.), with those chemicals are not tightly bound into the polymer, they can be released into the environment, and furthermore, due to the hydrophobicity of microplastics, contaminants present environment might be adsorbed by microplastics. Microplastics have been shown to undergo extensive aging after physical abrasion, UV irradiation, biodegradation, etc. The aging effect is an important process that determines the transport and transformation of microplastics in the environment, as well as their interactions with environmental contaminants. This study investigates the aging mechanism, factors affect the aging process, and evaluates how aging of microplastics (including UV irradiation, biofilms colonization, natural aging) affects their surface properties, adsorption/desorption performance, presence of additives, etc. Generally, the oxygen-containing groups on the surface of microplastics increase after aging, and sometimes the surface brightness and colour-difference are changed (e.g., yellowing). Together with the changes in surface roughness, all of them directly or indirectly affect the adsorption/desorption performance of bisphenols (typical endocrine-disrupting chemicals) on microplastics. The interaction mechanisms involved H-bonding, π-π interaction, hydrophobicity interaction, electrostatic

interaction. In addition, suspect screening analysis suggested that additives (e.g., antioxidants, light stabilizers, plasticizers) might be vital in controlling the aging process, and the aging of microplastics affects the present of additives, leading to the changes of leaching behavior of additives from microplastics to the aquatic environment. This study combined both laboratory and field work, providing direct evidence of microplastic particles aging processes and their potential environmental risks due as a transport vector and exposure medium.

Acknowledgements

Firstly, I would like to acknowledge my supervisors Andrew Sweetman and Crispin Halsall. I'm very grateful for the support and mentorship that two of you have provided over the course of the project. In particular, Andy was there to support me from the onset to the end. Thank you for your encouragement and trust in me, with your support, I felt positive and reassuring during the time that I purchased for the PhD degree. In addition, I'd especially like to thank Chang-Er Chen and his excellent research team for the support of my project. Thank you for your expert guidance and kind help, which help to go through challenges a few times.

I'd like to thank all friends that I met in Lancaster. I had a grateful and lovely time in the UK with all of you accompany. Meanwhile, thank you to all of my friends in China, you all supported me to spend the tough time for the last four years. Finally, I'd like to thank my family, whose support allowed me to follow my dream and purse the career in natural science.

Content

Statement on publications

This thesis contains papers which have been published in appropriate journals. These papers are listed below.

1. **Chen, X.**, Chen, C.-E, Guo, X. and Sweetman, A.J. 2022. Sorption and desorption of bisphenols on commercial plastics and the effect of UV aging. Chemosphere 310, 136867. (**Chapter 2**)

2. **Chen, X.** and Sweetman, A.J. 2024. An investigation into the effect of UV irradiation and biofilm colonization on adsorption and desorption behavior of polyurethane (PU) microplastics for bisphenol A (BPA). Environmental Technology & Innovation 35, 103662. (**Chapter 3**)

3. **Chen, X.**, Chen, C.-E., Cheng, S. and Sweetman, A.J. 2024. Bisphenol A sorption on commercial polyvinyl chloride microplastics: Effects of UV-aging, biofilm colonization and additives on plastic behavior in the environment. Environmental Pollution. 356, 124218. (**Chapter 5**)

Statement on research collaborations

The naturally aged microplastic samples in Chapter 4 were collected by Dr Alice Hortonand from Chessel Bay and Dr Andrew Turner from Whitsand and Exmouth beach. Suspect screening analysis in Chapter 5 and Chapter 6 were carried out by our collaborated research team in South Chian Normal University in Guangzhou.

1. Introduction

This Chapter provides an introduction to manufacture, life cycle, transport and fate of

plastics. Particular attention is given to plastic debris as transport vector for chemicals

and includes a review of previous research.

1.1 The challenges of plastics

1.1.1 The composition, types of plastics

Plastics as polymers are joined together by a series of repeating units known as monomers. Different types of polymers are made by linking together monomers with different chemical compositions using either linear or branched structures (Takada; and Bell, 2021). Before polymers become the final commercial plastic products, chemical additives are mixed into the polymers. Then the polymers treated with additives can be cast, extruded or otherwise shaped into the final plastic products (Figure 1).
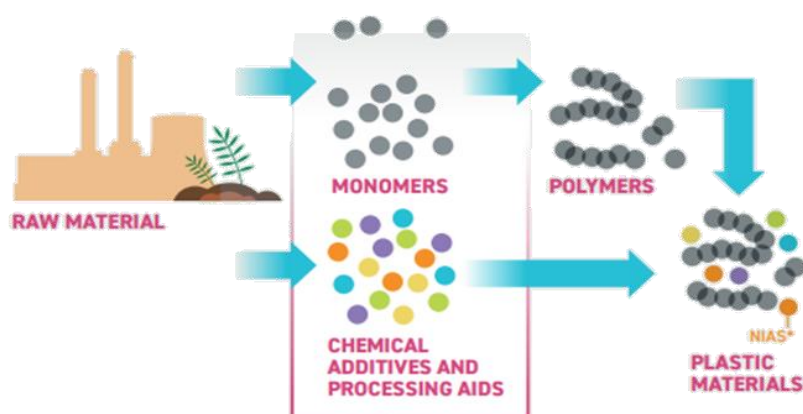
Figure 1. Manufacture process of plastics. Adapted from source: Chemicals-in Plastics - A Technical Report.

Additives can be divided into four main categories:

- Functions (plasticizers, flame retardants, stabilizers, etc.)

- Colorants (pigments, etc.)

- Fillers (mica, talc, kaolin, clay, calcium carbonate, etc.)

- Reinforcements (glass fibres, carbon fibres, etc.)

Table 1. Additives in plastics. Source: Andrade et al. (2021); Hahladakis et al. (2015).

Category	Purpose	Specific additive group	Typical chemicals	Percentage
Functional additives	Influence properties such as enhance softness, reduce flammability, resist to oxidization	Plasticizers	phthalates and short- and medium-chain chlorinated paraffins	10-70 %
		Flame retardants	brominated and chlorinated flame retardants	2-28 %
		Light stabilizers	UV absorber, hindered amine light stabilizers (HALS), phenolic benzotriazoles	0.1-10 %
		Antioxidants	amines, phenolic, phosphates	0.05-3 %
		Lubricants	fatty acid esters, hydrocarbon waxes, metal stearates	0.1-3 %
		Slip agents	erucamide, oleamide, stearamide	0.05-0.15 %
		Blowing agents	C,C'-azodi(formamide) (ADCA); fluorinated greenhouse gases: hydrofluorocarbons (HFCs)	0.05-20 %
		Curing agents	4,4'Diaminodiphenylmethane, 2,2'-dichloro-4,4'-methylenedianiline	0.1-2 %
		Biocides	organic tin compounds, arsenic compounds; triclosan	0.001-1 %
		Catalyst	chromium and chromium compounds (e.g., chromium trioxide), mercury and mercury compounds	0.1-0.3 %
Colorants	give colour to the plastic product	Pigments	cadmium compounds (e.g., cadmium sulfide), chromium compounds; lead chromates	0.01-5 %
		Soluble azocolorants	organic-based colorants	
Fillers	Enhance mechanical properties; reduce production costs	Calcium carbonate		
		Clay		
Reinforcements	Enhance mechanical properties	Glass fibres		15-30 %
		Carbon fibres		

Most additives are used to modify the features of plastic products by either enhancing the desirable properties of plastics or lessen the unwanted characteristics (Table 1). It is also worth noting that non-intentionally added substances (NIAS) include impurities, reaction by-products and degradation products which may also be potentially introduced during manufacture (Groh et al., 2019).
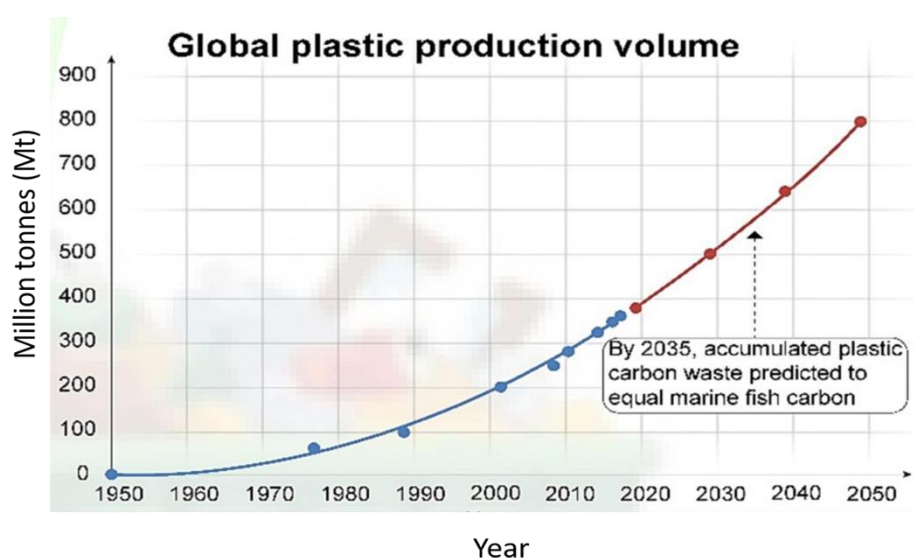
Figure 2. Evolution of the world plastics production. Source: Nayanathara Thathsarani Pilapitiya and Ratnayake (2024)

Owing to their versatility, flexibility, low cost, low weight, durability, and resistance to humidity, plastic products are widely used in both manufacturing and every day human activities (Hahladakis et al., 2015; Singla et al., 2020). Globally, the production of plastics has showed a growing trend with the manufacturing increasing from approximately 2 million tonnes in 1950 to 400.3 million tonnes in 2022, and the production is predicted over 800 million tonnes per year by 2050. (Nayanathara Thathsarani Pilapitiya and Ratnayake, 2024). Based on the different raw materials,

plastics can be divided into two broad categories— fossil-based plastics (conventional plastics) and bio-based plastics. The fossil-based plastics accounts for approximately 90 % of the world plastics production, the most commonly used fossil-based plastics are polyethylene (PE, 26.9 %), polypropylene (PP, 19.3 %), polyvinyl chloride (PVC, 12.9 %), polystyrene (PS, 8 %), polyethylene terephthalate (PET, 7 %) and polyurethane (PU, 5.5 %), which are classified into two categories: carbon-carbon backbone plastics and heteroatomic plastics (Janssens, 2021). Bio-based plastics represent plastics derived from non-petroleum biological resources (such as polylactic acid (PLA)), which are generally considered to more environment friendly compared with the traditional fossil-based plastics and are often proposed as a solution to reduce the total mass of non-biodegradable plastics, however, to date the production only accounted for about 1.5 % of the world plastics production in 2021 (Figure 2).
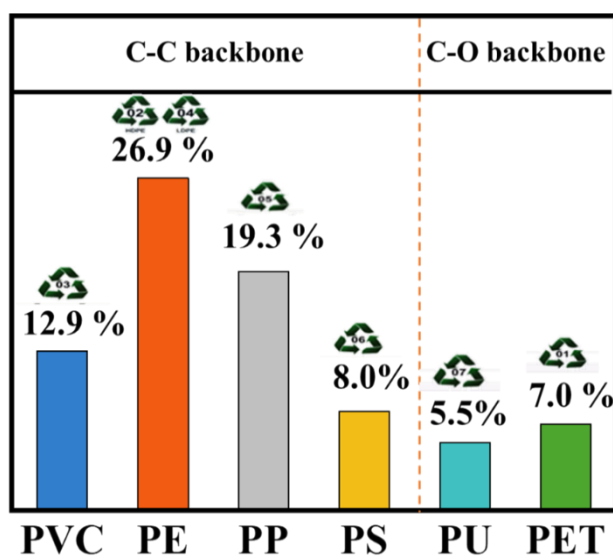
Figure 3. The commonly used types of plastics. Source: Janssens (2021).

Owing to the complex process use to convert plants (such as corn, sugarcane) into the building blocks for bio-based plastics, they are relatively expensive compared with traditional plastics. The weak strength also result in the use options are limited. In addition, due to the fertilizers and pesticides used in growing the crops and the chemical processing needed to turn organic material into bio-based plastic, the production of bioplastics might result in greater environmental impact (Pascoe Ortiz, 2023). Bio-based plastics are considered to produce significantly less greenhouse gas emissions than traditional plastics, as the plants that bio-based plastics are made from absorbed carbon dioxide via photosynthesis. Research has shown that the complete substitution of petroleum-based plastic with bio-based plastics would reduce greenhouse gas emissions by 369 Mt (Jin et al., 2023). As most bio-based plastics need high temperature industrial composting facilities to break down and very few cities have the infrastructure needed to deal with them, bio-based plastics often end up in landfills where they may release methane (a greenhouse gas 23 times more potent than CO_2) without enough oxygen. As a result, bio-based plastics can be considered unlikely to replace the traditional fossil-based plastics and which means it is difficult to solve the plastics problems in the short term.

The term of bio-based plastics and biodegradable plastics should be distinguished in that bio-based plastics might not biodegradable. For example, bio-based PE, PET, polyamide (PA) are not regarded as biodegradable plastics, and are not degraded by microorganisms (Figure 4). They are manufactured to replace similar plastics products

that are fossil based to save fossil fuel energy. Meanwhile, some biodegradable plastics are fossil-based for example polybutylene adipate terephthalate (PBAT). It worth noting that most biodegradable plastics (both bio-based and fossil-based) only degrade under very specialized conditions and therefore unlikely to naturally degrade in the environment (Miller, 2020).

1). Bio-based biodegradable plastics
2). Fossil-based biodegradable plastics **Bio-based**
3). Fossil-based conventional plastics
4). Bio-based non biodegradable plastics

4).

Such as bio-based PET, polyamide (PA) and PE

1).

Such as Polylactic acid (PLA) Polyhydroxyalkanoate (PHA)

Non biodegradable ---------- **Biodegradable**

3).

Such as PE, PVC, PS and PP

2).

Such as polybutylene adipate terephthalate (PBAT)

Fossil-based

Figure 4. The difference and associate between bio-based and biodegradable plastics. Source: Ahmad et al. (2024).

1.1.2 Life cycle of plastics

The life cycle of plastics is illustrated in Figure 5. After plastics are manufactured, they enter the market. Around 50 % of consumed plastic products are single-use plastics, including packaging and water bottles (Chen et al., 2021b; Giacovelli; et al., 2018), which suggests that plastic waste is easily generated during daily consumption. It is

estimated that around 6.3 billion tons of plastic wastes are produced from 1950 to 2015

(Kumi-Larbi et al., 2018).
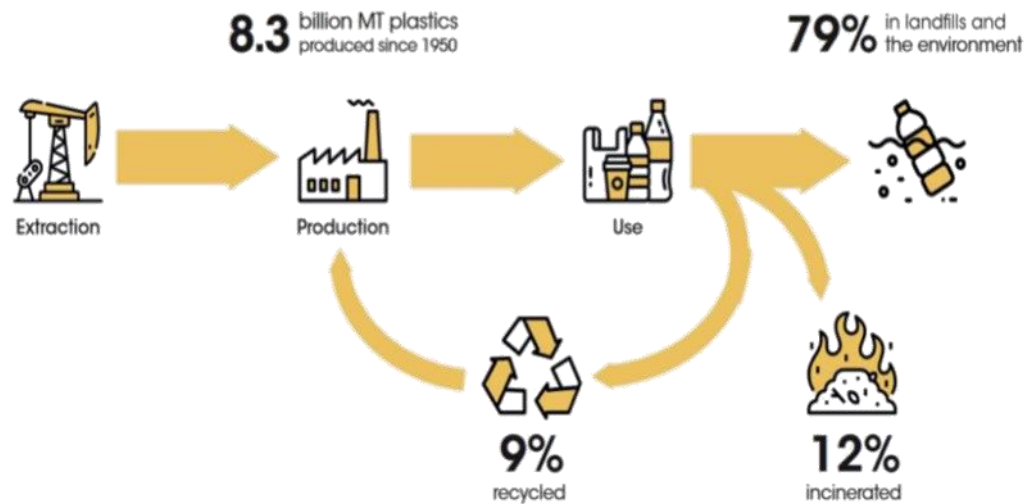
Figure 5. The life cycle of plastic products. Source: Geneva Beat Plastic Pollution.

Among the plastic wastes approximately 12 % are sent to incineration plants

(Geyer et al., 2017). In 2016, it was estimated that 11.3 million tons of plastic were

incinerated in the EU – a 61 % increase in a decade (Takada; and Bell, 2021).

Incineration of plastic waste is by far the greatest CO_2 emissions source of all plastic

end of life management options. Globally, it is estimated that around 40-50 million

metric tons of plastic are incinerated each year (CIEL, 2019). Each ton of plastic emits

about 2.5-3 tons of CO_2, this translates to approximately 100-150 million metric tons

of CO_2 emissions annually from plastic incineration worldwide (Zero Waste Europe,

2019). In addition to high volumes of greenhouse gases emission, toxic compounds are

also be produced such as dioxins and poly chlorinated compounds. Incineration is one

of the most polluting ways to solve the issue of plastic wastes, and so appears to not

have any role to play in the environmentally sound management of plastic waste in a circular economy (Takada; and Bell, 2021).

Table 2. Types of commonly found single-use plastic products. Source: Plastic Oceans.

Type of polymers	Application
PET	Water bottles, dispensing containers, biscuit trays
HDPE	Shampoo bottles, milk bottles, freezer bags, ice cream containers
LDPE	Bags, trays, containers, food packaging film
PP	microwave dishes, ice cream tubs, bottle caps, single-use face masks
PS/ expanded PS (EPS)	Cutlery, plates, cups, protective packaging (EPS), single-use EPS food containers

Recycling can be considered as a promising pathway to reduce the amount of virgin materials and energy required to make a new plastic product. Studies have shown that the recycling plastic products requires up to 44% less energy and with lower global warming potentials (GWP, saving 25 %–75 %) (Arena et al., 2003; Shen et al., 2010). However, only approximately 9 % plastics wastes are recycled (Geyer et al., 2017). Currently, fossil-carbon-based plastics with complex chemicals cannot readily be recycled or reused (Chen et al., 2021b). In theory, most plastics are recyclable, but there are many technical and economic barriers to recycling plastics, including energy use, contamination and toxic additives (Takada; and Bell, 2021). In order to impart specific characteristics (colour, pliability, durability, fire resistance, etc.) many polymers contain varying concentrations of chemical additives that are toxic and hazardous.

During the recycling process, those toxic additives are difficult to remove or decontaminate owing to lack of economic and technical solutions. Meanwhile, NIAS (from cross contamination during recollection of plastic materials, degradation products during recycling) might also be introduced during the recycling process. Mixing these together might result in a poor quality recycled material which is unlikely to meet the specific input needs of plastic manufacturers, and cause loss of structural integrity in the final product made from the recyclate (Takada; and Bell, 2021). In addition, most recycled plastics cannot safely be incorporated into materials such as food packaging, clothing, or children's toys because they contain toxic chemicals, which limits the application of recycled plastics in the products and dramatically reduces the possibility of recycled plastics to replace virgin materials.

As a result of good management and recovery systems, the large bulk of plastic wastes ends up in the landfills and the natural environment (around 79 %). Globally, approximately 22 million tonnes of plastics, along with the chemicals present in them, are released to the environment in 2019. This value is projected to double, reaching 44 Mt by 2060 (OECD, 2022).

1.2 Source, exposure, transport and fate of plastics in the environment

1.2.1 Source of plastics in the environment

The majority plastic debris are macroplastics (size > 25 mm), recognisable items including single-used plastic products such as beverage bottles, plastic bags. They are derived from the mismanagement of plastics wastes including inadequate collection and

disposal, which accounts for around 81.84 % of the source of plastic debris in the environment (Figure 6). Other leakage routes include littering or fly-tipping and marine activities (e.g., discarded fishing items including monofilament lines and nylon netting generated from commercial fishing) (Li et al., 2016).
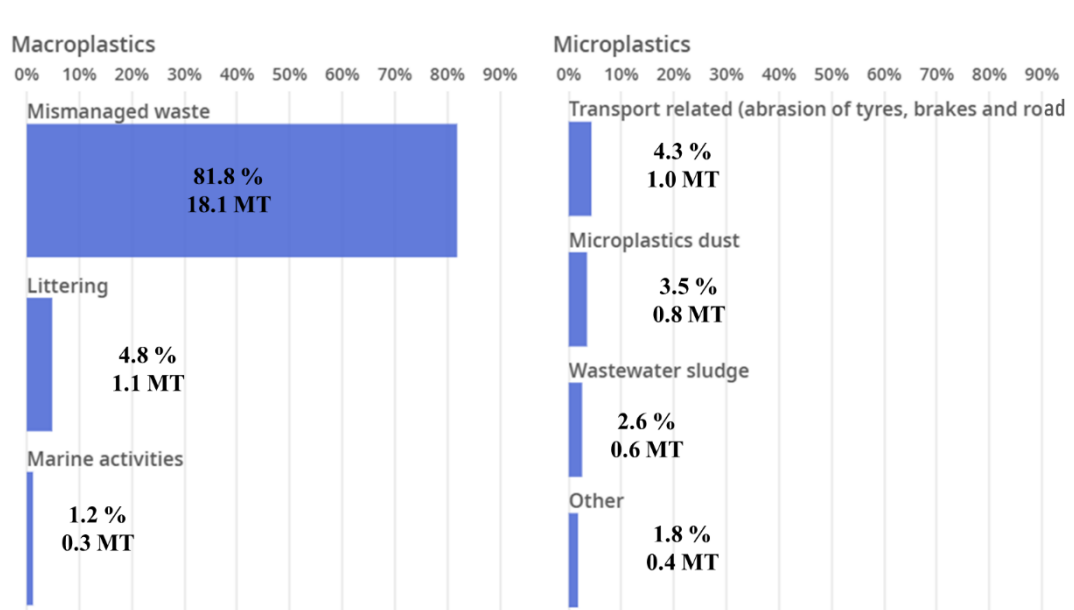
Figure 6. Leak of plastics debris in the environment in 2019. MT: million tons. Source: OECD (2022).

Microplastics contribute around 12.2 % of the total plastics found in the environment, these are defined as fragments less than 5 mm. Approximately 4.3 % microplastics reach the environment through wear to tyres and road markings wear. It has been reported that the total microplastics generated from the wear of automotive tyres in the European Union is around 0.5 million metric tonnes (MMT) per year (Eunomia and ICF 2018). In addition, city dust (originating from artificial turf, building paints, and industrial abrasives) is an important source of microplastics in the

environment, which accounts for around 3.5 % of the total plastics found in the environment. Microfibers or microbeads are easily entered into the sewage network along with washing wastewater due to their small size, insolubility in water, and slow degradation, which accounts for 2.6 % of the total plastics found in the environment. Those microbeads generally generate from accidental loss of plastic pellets, washing of synthetic textile fibres, consuming of personal care products (PCPs) and cosmetics, such as facial cleansers, toothpastes, sunscreen and shower gel (An et al., 2020). Although a previous study illustrated that more than 98 % of microplastics in influents could settle into the sewage sludge (Magnusson et al., 2016), owing to the sheer volume of microplastics and based on the screens size (2 mm – 50 mm) in wastewater treatment plants (WWTPs), smaller microplastics are not captured and so the release of microplastics to the environment is still significant (Duis and Coors, 2016). It has been estimated that each year 210 trillion microbeads are released into the aquatic environment in mainland China and more than 80 % of the source is from WWTP effluent (Cheung and Fok, 2017). Moreover, as most microplastics are found in sewage sludge, sludge composting and the use of sludge in agriculture results in the release of microplastics to soil (Corradini et al., 2019).

1.2.2 Exposure and degradation of plastics

Conventional fossil-based plastic materials are very resistant to degradation in general and plastics are estimated to persist for hundreds to even thousands of years in the environment. Although at a slow rate, environmental weathering breaks and reduces

the structural integrity of plastics debris (Browne et al., 2007). After exposure in the environment, macroplastics which have not been properly disposed of, will degrade into small plastic fragments (Pettipas et al., 2016). It's known that secondary sources of microplastic are a significant source of environmental microplastic. As a result, degradation is an important step after plastics are released into the environment, which induces changes in polymer physicochemical properties due to biological and/or abiotic processes (Figure 7).
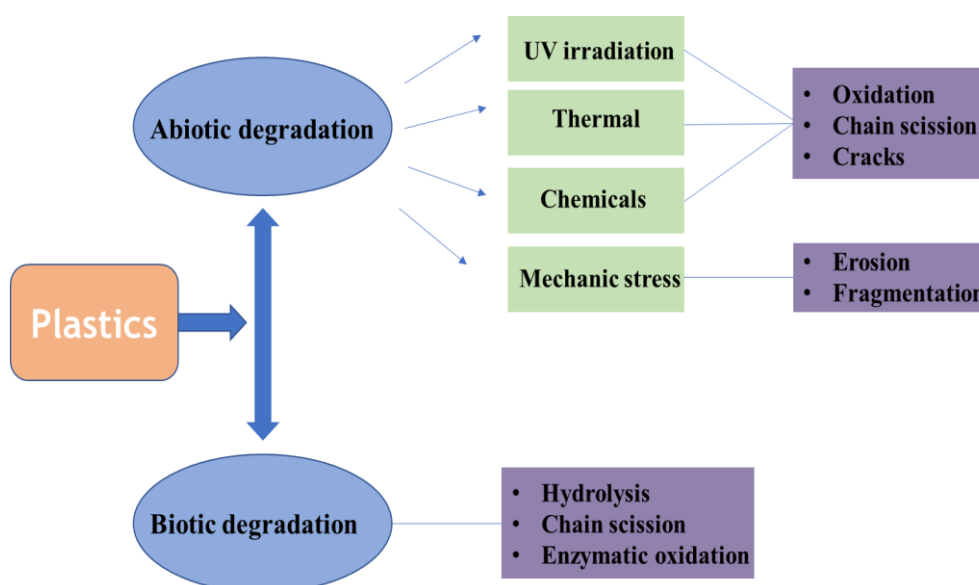
Figure 7. The schematic diagram showing the general pathways and process involved in the degradation of plastics. Source: Luo et al. (2022).

1.2.2.1 Abiotic degradation

Abiotic degradation occurs due to factors such as light, temperature, air, water and mechanical stress. In general, the action of abiotic processes breaks macro plastics into smaller fragments making them more accessible to biodegradation processes (Gewert et al., 2015). Abiotic degradation of plastics, producing products of lower molecular

weight and creates fractures and pores on the polymer surface, that can accelerate the biodegradation processes (Zhang et al., 2021). Thus, a synergy may exist between abiotic and biotic degradation (Bergmann et al., 2015).

Photodegradation is recognized as the most important process that initiates plastic degradation in the environment (Zhang et al., 2021). Photodegradation of plastics usually involves free radical mediated reactions initiated by solar irradiation, which cause molecular breakage and oxidative decomposition. The mechanism of plastic photodegradation involves three main stages: initiation, propagation and termination. During the initiation process, polymers adsorb light energy and chains are broken to produce free radicals (Yousif and Haddad, 2013). At this stage, polymers must contain unsaturated chromophoric groups that absorb light energy (Gewert et al., 2015; Gijsman et al., 1999). Although plastics such as PE and PP do not contain any unsaturated bonds, however, the presence of external impurities or structural abnormalities during manufacture can act as chromophores and provide the initiation step (Gijsman et al., 1999). Subsequently, polymer radicals react with oxygen and form peroxy radicals during the propagation stage. In addition to forming hydroperoxides, further complex radical reactions occur which result in auto-oxidation. Termination of radical reactions take place when inert products are formed from the combination of two radicals (Ali et al., 2021b). The photodegradation process results in the chain scission or crosslinking to form new structures.

Thermal degradation refers to the oxidation and degradation of plastics due to the energy input derived from elevated temperatures (Zhang et al., 2021). The long polymer chains can break and generate radicals when polymers absorb sufficient heat energy. These radicals can react with oxygen and produce hydroperoxides until inert products are formed, the process similar to photodegradation.

Chemical degradation involves hydrolytic degradation and oxidative degradation with hydrolysis being one of the main steps for the abiotic degradation pathway (Ali et al., 2021b). Hydrolysis susceptibility is determined by whether plastics contain hydrolysable covalent bonds (such as esters, ethers, anhydrides and amide groups). Meanwhile, other factors such as temperature and pH are also key factors affect hydrolysis rates (Lucas et al., 2008). Oxidative degradation is another important pathway for chemical degradation. The presence of ozone (O_3), sulfur dioxide (SO_2), nitrogen dioxide (NO_2) and volatile organic compounds (VOCs) in the atmosphere can directly attack plastics (e.g., O_3 attacks C=C bonds of polymers) or result in the formation radicals, which can also lead to degradation (Crawford and Quinn, 2016). In addition, advanced oxidation processes (AOPs) are also effective in degrading microplastics (Liu et al., 2022a) with the product of AOPs leading to chain breakage and formation of by-products (Du et al., 2021).

Mechanical degradation refers to the cracks or breakdown of plastics owing to the external forces, which can come from the collision and abrasion of plastics with rocks

and sands caused by wind and wave action (Zhang et al., 2021). Freezing and thawing of plastics in aquatic environment can also contribute to mechanical degradation.

1.2.2.2. Biotic degradation

Plastics biodegradation is the deterioration of plastics under the action of microorganisms, which are ubiquitous in natural environments such as bacteria, fungi and algae. The biodegradation of plastics is carried via five main steps: colonization, biodeterioration, bio- fragmentation, assimilation and mineralization (Ali et al., 2021b).
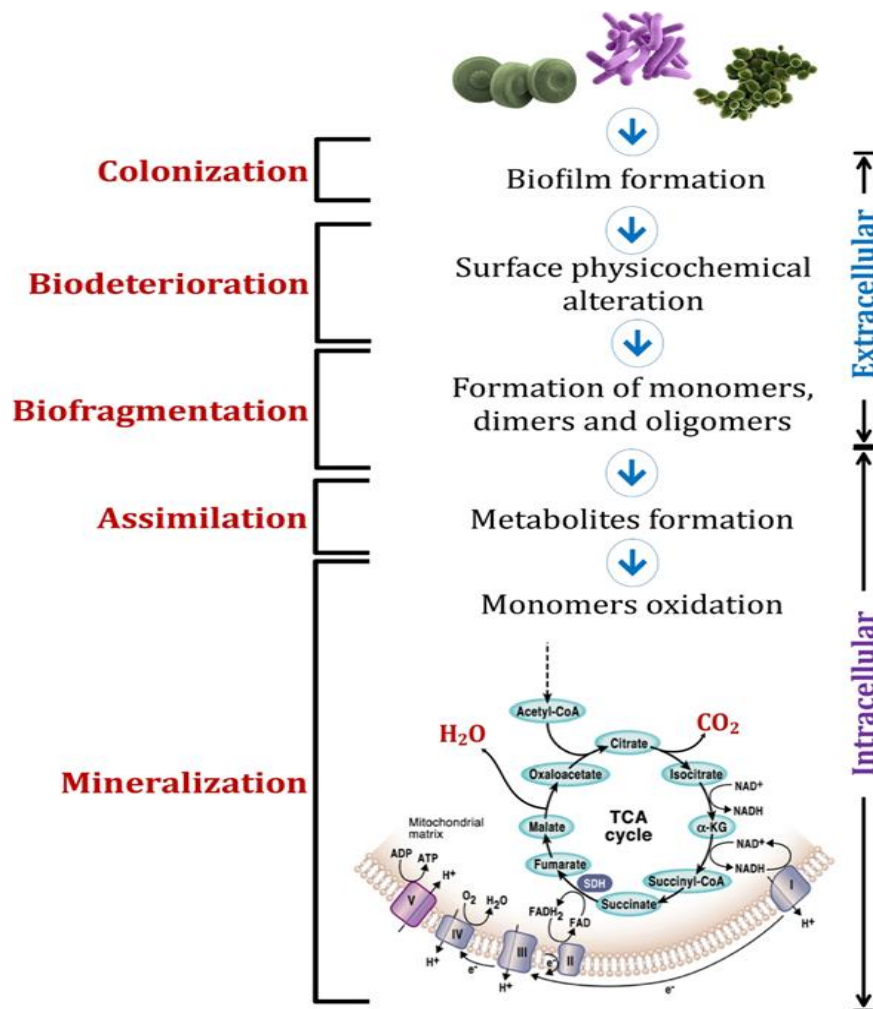
Figure 8. Biodegradation stages of plastics. Source: Ali et al. (2021b).

The first stage is the colonization of microorganisms on plastic surfaces. During this stage, microorganisms attach to the surface of plastics, then they secrete extracellular polymeric substances (EPS), which mainly includes polysaccharides, carbohydrates, proteins, lipids, and nucleic acids which facilitates the attachment of microorganisms (Flemming and Wingender, 2010). EPS can also protect microorganisms from physical and chemical stressors, such as sand abrasion and washing of waves (Demeter et al., 2016; Webb et al., 2009). EPS make plastics 'sticky' and so microorganisms can adhere onto the surface. Finally, biofilms mature with the proliferation of microorganisms (Wang et al., 2021).

Microorganisms and related substances, for example proteins and polysaccharides, infiltrate into the pores of plastics resulting in the pore physiochemical properties becoming altered and surface degradation (Ali et al., 2021b). For example, filamentous fungi utilize their mycelia to infiltrate into the polymers, which increase the size of pores and result in cracks, decreasing resistance and durability of plastics (Bonhomme et al., 2003a). Meanwhile, formation of acids and bases during the microorganism metabolic activity modify the pH and result in increased surface erosion (Lugauskas et al., 2003).

Fragmentation is a lytic process, essential for the degradation of polymers into monomers, dimers, or oligomers. A range of extracellular enzymes (such as Cutinases and Laccase) via hydrolytic and oxidative processes degrade plastics and result in chain scission, producing short-chain polymers and small molecular fragments (Zhang et al.,

2021). Small molecular degradation products can be assimilated and metabolized intracellularly (Wilkes and Aristilde, 2017). Finally, plastics can be mineralized into CO_2 and H_2O under aerobic conditions and into CH_4, CO_2, H_2O, NH_4 and organic acids under anaerobic conditions (Zhang et al., 2021).

1.2.3 Transport and fate of plastics

If plastic wastes are not treated properly they can enter terrestrial and aquatic systems. They can be transported by wind, deposited to surfaces during rainfall events, especially with stormwater run-off, and subsequently be transferred from land to water systems (Duis and Coors, 2016). In addition, through atmospheric deposition, very small microplastic particles or fibres can be transferred from the atmosphere to surface water and soil. It is estimated that only 20 % of plastic debris in the marine environment is sourced from marine actives and accidental losses, with 80 % being derived from land-based sources (Wayman and Niemann, 2021). Plastic debris are transported by wind and water flow from their sources via river systems to the marine environment, and can even be transported to remote locations such as the Arctic, ocean gyres and uninhabited islands via currents (Bergmann et al., 2022). As a result, once plastics are released to the environment, they can be transport by a series of pathways, including precipitation, atmospheric deposition, wind, wave and current action, etc., which has resulted in plastic debris being distributed all over the world. Many publications have reported that plastic debris distributed in freshwater and seawater, with some examples detailed in Table 3.

Table 3. Occurrence of plastic debris in water bodies. Source: Li et al. (2016).

Location	Region	Water bodies	Debris load	Plastic type	Reference
Baltic Sea	Baltic Sea	Marine, surface water	1.3 item ± 0.8/Ha	Macroplastics	(Galgani et al., 2000)
Atlantic Ocean	North Sea	Marine, surface water	1.6 items ± 0.4/Ha	Macroplastics	(Galgani et al., 2000)
	Channel East	Marine, surface water	1.2 ± 0.1 items/Ha	Macroplastics	(Galgani et al., 2000)
	French-Belgian-Dutch coastline	Marine, coast	0.4 items±0.3 /L	Microplastics	(Van Cauwenberghe et al., 2015)
	Bay of Seine	Marine, surface water	1.7 ± 0.1 items/Ha	Macroplastics	(Galgani et al., 2000)
	Celtic Sea	Marine, surface water	5.3 ± 2.5 items/Ha	Macroplastics	(Galgani et al., 2000)
	Rio de la Plata	River and estuary, coastal area and river bottom	0–15.1 items/Ha	-	(Acha et al., 2003)
	Offshore, Ireland	Marine, surface water	2.5 items/m3	Macroplastics and microplastics	(Lusher et al., 2014)
	Gioana estuary, Brazil	Estuary, surface and bottom water	0.3 items/m3	Microplastics	(Lima et al., 2014)
Mediterranean Sea	Gulf of Lion	Marine, surface water	1.4 ± 0.2 items/Ha	Macroplastics	(Lima et al., 2014)
	East Corsica	Marine, surface water	2.3 ± 0.7 items/Ha	-	(Galgani et al., 2000)
	Adriatic Sea	Marine, surface water	3.8 ± 2.5 items/Ha	Macroplastics	(Galgani et al., 2000)
	Greece Gulfs	Marine, seafloor	0.7–4.4 items/Ha	-	(Galgani et al., 2000)

	North Pacific Central Gyre	Marine, surface water	334271 items/km^2	Macroplastics and microplastics	(Moore et al., 2001)
	Waters around Australia	Marine, surface water	4256.4 items/km^2	Macroplastics and microplastics	(Reisser et al., 2013)
	Tokyo Bay	Marine, surface water	1.9–3.4 items/Ha	-	(Kuriyama et al., 2003)
	North Pacific offshore	River, surface water	0.4–2.2 items/m^3	-	(Moore et al., 2005)
	North Pacific central gyre	Marine, surface water	0.02 items/m^3		(Carson et al., 2013)
Pacific Ocean	North Pacific, inshore, surface	River, surface water	5.0–7.3 items/m^3	Macroplastics and microplastics	(Moore et al., 2005)
	Eastern China Sea	Marine, seafloor	-	-	(Lee et al., 2006)
	The South Pacific subtropical gyre	Marine, surface water	26898 items/Km^2	Macroplastics and microplastics	(Eriksen et al., 2013)
	Geoje Island, South Korea	Marine, surface water	16000 items/m^3	Microplastics	(Song et al., 2014)
	Lam Tsuen River, Hong Kong	River, surface water	7.428 pieces/m^3	Microplastics	(Cheung et al., 2018)

Table 4. The entanglement of plastics by organism. Source: Li et al. (2016).

Species	Location	Entangled material	Entanglement rate	Year	Reference
Antarctic Fur Seals	Subantarctic island, Bouvetøya	Fishing net (48.1%), polypropylene packaging strap (17.9%), rope or string (14.2%)	0.024–0.059%	1996-2002	(Hofmeyr et al., 2006)
	Marion Island	Polypropylene packaging strap (39.5%), synthetic string (10 mm diameter) (10.5%), synthetic rope (N10 mm diameter) (13.2%), and fishing net (21.1%).	0.15%	1991-1996	(Hofmeyr and Bester, 2002)
New Zealand fur seals	Kaikoura region	Green trawl net (42%), and plastic strapping tape (31%)	0.6–2.8%	1995-2005	(Boren et al., 2006)
	Cape Gantheaume, Kangaroo Island	Packing tape (30%), trawl netting (28%), lobster float rope (13%)	0.73%	1989-1991	(Page et al., 2004)
Steller sea lions	Southeast Alaska and northern British Columbia	Packing bands 54%, rubber bands (30%), net (7%), rope (7%)	0.26%	2000-2007	(Raum-Suryan et al., 2009)
Australian sea lions Seabirds	Seal Bay, Kangaroo Island	Monofilament netting (55%), packing tape (11%), trawl netting (11%), other rope (14%)	0.83%	1988-2002	(Page et al., 2004)
Northern gannets	Spanish Iberia and Mauritania	Fishing ropes (73.5%), nets (11.8%), nylon fishing lines (14.7%)	0.93%	2007-2010	(Rodríguez et al., 2013)
Seals Sea lions Gull Fulmar Turtle	United States	Fishing related (91.7%) such as fishing line, fishing hook, fishing string		2001-2005	(Moore et al., 2009)

During transport processes, plastic debris such as abandoned fishing gear might entangled with marine organisms (Table 4). Rodríguez et al. described and quantified the occurrence of marine debris entanglements in the northern gannets Morus bassanus at five of its main wintering areas between 2007 and 2010. They observed 34 entangled birds in total, representing 0.93% of all gannets counted (n = 3672 individuals). Entanglements might result in drowning, suffocation, laceration, a reduced ability to feed and even mortality of organisms (Li et al., 2016; van Emmerik and Schwarz, 2019).

In addition, plastic debris has been found in various species all over the world, including birds, fish, turtles and crustaceans (Table 5), which indicates that plastic debris might be accidently ingested by organisms during predation activities. Surface-foraging species, such as gulls are vulnerable to plastic ingestion (Codina-García et al., 2013). Zooplanktivorous species, for example, the little auk (Alle), are also susceptible to plastic ingestion because it is difficult to distinguish between zooplankton (e.g., amphipods, copepods, euphausiids) and small plastic particles (Avery-Gomm et al., 2013). The accumulation of plastic debris in bird's gastrointestinal tract will eventually lead to gastrointestinal blockage or problems with feeding stimuli and activity levels (Derraik, 2002). In addition, studies showed that the ingested plastic debris were white or transparent, which suggests it is possible that turtles mistake white plastic debris for jellyfish plastic and plastics take on the same smell as the ocean so it is also hard to separate (Bugoni et al., 2001; Da Silva Mendes et al., 2015). Macroplastics and microplastics have been detected in the tracts of multiple species of fish from different

locations, including the English Channel, the North Pacific Ocean and the North Sea (Boerger et al., 2010; Lusher et al., 2013; Van Cauwenberghe and Janssen, 2014). For example, 504 fish from the English Channel were examined by Lusher et al., 36.5 % of which contained synthetic polymers (including semi synthetic cellulosic material rayon and polyamide). High amounts of plastic debris ingested and accumulated in small organisms could lead to digestive system blocks (Hoss and Settle, 1990).

Table 5. Plastic debris ingestion by organism.

Species	Location	Ingestion material	Plastic type	Reference
Birds	Catalan coast, Mediterranean	fragments laminar plastics, filaments, industrial pellets and foamed plastics	Microplastics	(Codina-García et al., 2013)
	White Bay, Newfoundland	unidentifiable fragments, or bits of nylon fishing line	-	(Fife et al., 2015)
Turtle	South west Altantic	-	Macroplastics and microplastics	(Carman et al., 2014)
	Ubatuba, Brazilian coast	Soft plastic (54.3%), hard plastic (19%), nylon (21.4%), rubber (4.2%) and foam (1.1%)	Macroplastics and microplastics	(da Silva Mendes et al., 2015)
	Paranagua Estuary, Brazil	Plastic bags (44.7%), hard plastic (38.5%), nylon (7.73%), polystyrene (5.1%) and rubber (1.1%)	-	(Guebert-Bartholo et al., 2011)
	Tuscany coasts, Mediterranean Sea	User plastics (70.4%), fragments	-	(Campani et al., 2013)

		(20.3%), and threadlike (4.3%)		
Fish	English Channel	Semi synthetic cellulosic material rayon (58%), and polyamide (35%)	Macroplastics and microplastics	(Lusher et al., 2013)
	North Pacific	Fragments (94%), film (3%), fishing line (2%), and finally rope (woven filaments), Styrofoam and rubber (all b1%)	Microplastics	(Boerger et al., 2010)
	North Sea		Microplastics	(VanCauwenberghe and Janssen ,2014)
	Alappuzha, India	-	Microplastics	(Kripa et al., 2014)
Zooplankton	Portuguese coastal waters	Low density polyehtylene (98.1%)	Microplastic	(Frias et al., 2014)
Neocalanus cristatus	Northeast Pacific Ocean	-	Microplastic	(Desforges et al., 2015)
Euphausia pacifica	Northeast Pacific Ocean	-	Microplastic	(Desforges et al., 2015)
Brown shrimp (Crangon crangon)	Belgium	Fibres (95%), films (5%)	Microplastic	Devriese et al. (2014)
Blue mussel (Mytilus edulis)	Belgium, The Netherlands	Fibres	Microplastic	(De Witte et al., 2014)
Gooseneck barnacles (Lepas spp.)	North Pacific Subtropical Gyre	Fragments (99%), monofilament line (1%)	Microplastic and macroplastic	(Goldstein and Goodwin, 2013)
Franciscana dolphins (Pontoporia blainvillei)	Northern coast of Argentina	Packaging debris (64.3%), fishery-related fragments (35.7%	Macroplastic	(Denuncio et al., 2011)

As mentioned in section 1.2.2, although plastic debris can be degraded by various pathways, the majority of the fragments will remain in the environment as smaller

pieces of the same polymer, which indicates that plastic debris can persist in the natural environment and complete degradation is very difficult (Li et al., 2016). Ironically, the degradation of plastic debris into small fragments (microplastics) may pose an increasing ingestion risk for smaller organism. Thus, plastic debris in the natural environment can be transported over long distances resulting in entanglement by organisms and accidental ingestion by biota. It can thus enter food webs and even be consumed by humans via food chain transfer (Landrigan et al., 2023).

1.3. Plastics as a vector for chemicals

1.3.1 Carrier for chemicals

Additives are infused into polymers during the plastic manufacturing process. Concentration of additives typically ranges from 0.001 % to 50 % but up to 70 % by weight (Andrady and Rajapakse, 2019; Costa et al., 2023). As plastic waste is unintentionally released into the environment, it is inevitable that the chemical additives are transported along with plastics resulting in distribution all over the world. For example, benzotriazole UV stabilizers (BUVSs) have been detected in polypropylene pellets collected from 36 beaches worldwide, including Europe, Africa, Asia, Oceania, etc. Among them, 17 samples were even collected from remote islands (Figure 9). It suggests that plastics as a carrier can result in long-range transport hydrophobic additives across the world.
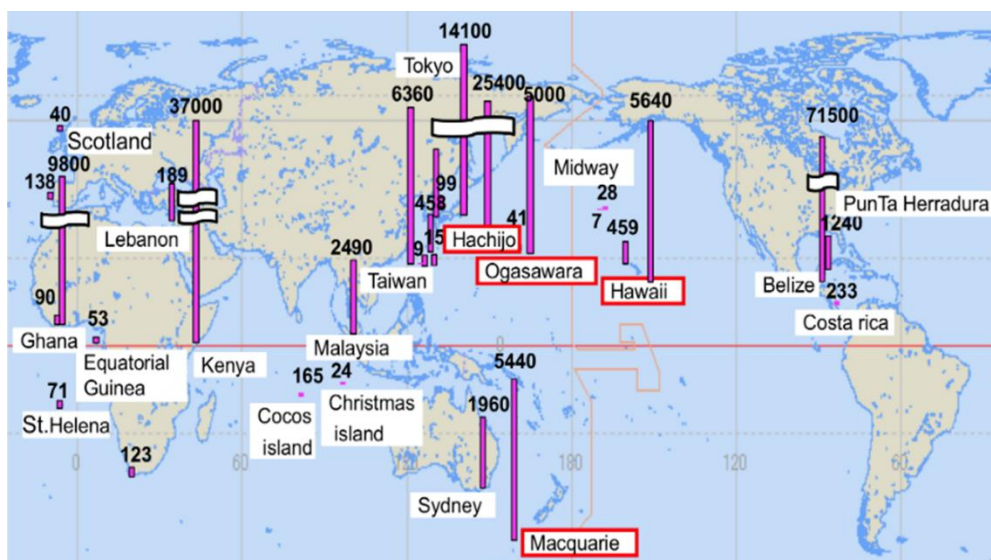
Figure 9. Concentration (ng/g) of total benzotriazole UV stabilizers (BUVSs) in PP pellets on the world beach. Source: International Pellet Watch.

In addition to providing a transport vector for plastic additives, a number of studies have suggested that plastics can adsorb chemicals that exist in the environment. Those plastic particles were identified in different ecosystems, including beaches, river and seawater (Bouhroum et al., 2019; Leon et al., 2018; Rodriguez et al., 2020). Types of adsorbed chemicals include persistent organic pollutants (POPs, including PBDEs, PCBs, OCPs and PAHs), PCPs, pharmaceuticals, and hydrophobic organic compounds (HOCs) (Fang et al., 2019; Guo and Wang, 2019a; Ho and Leung, 2019; Lee et al., 2014; Llorca et al., 2018; Ma et al., 2016; Velzeboer et al., 2014). The concentrations of organic pollutants on plastics have been reported to lie within the range of 0.1-3814 ng/g (Table 6). More specifically, the concentrations of PAHs in studies spanned from 0.2 to 3814 ng/g, while those of PCBs varied from 0.1 to 187.8 ng/g. Pharmaceuticals on plastics exhibited concentrations of 33-111 ng/g. Significant amounts of PAHs adsorbed on plastics were probably due to their hydrophobic

properties and high environmental concentrations. It has also shown that partitioning involving halogen bonding, dative bonding, hydrophobic interaction, Van der Waals interactions, π-π interaction, and electrostatic interactions are the common adsorption mechanisms of chemical pollutants on plastics (Elizalde-Velazquez et al., 2020).

Table 6. Organic contaminants in plastic samples collected in the environment.

Study area	Type of ecosystem	Plastic type	Chemical type	Specific chemicals	Sorption concentration (ng/g)	Reference
Canary Islands, Spain	Beaches	-	pharmaceuticals	CP, TAM, NIC, CAF, PRX, GEM, ATL, CMZ, TMP, ERY	Range from 34–111 ng/g	(Santana-Viera et al., 2021)
Punta del Diablo, Uruguay	Beaches	PP, PE, PVC, PS	POPs, HOCs	PCBs, PAHs, OCPs	Range of 0.6 – 3814 ng/g	(Rodriguez et al., 2020)
Southwestern coast, Taiwan	River, seawater	PE, PP, PS, PA, PVC	POPs, HOCs	PAHs	Range of 104 – 3595 ng/g	(Chen et al., 2020)
Central coast, Chile	Beach	PE, PP	POPs, HOCs	PBDEs, PCBs, OCPs	Range of 0.1–133 ng/g	(Pozo et al., 2020)
Indonesian coast and North Atlantic gyre	Seawater	PE, PP, PS PET	POPs, HOCs	PAHs and PCBs	Range of 0.2–255 ng/g	(Bouhroum et al., 2019)
Mediterranean coast, Southeastern Spanish	Beach	PE, PP, PET, PA, PU, PS	POPs, PCPs, HOCs	PAHs, PCBs, OCPs, Triclosan	Range of 0.29 – 605.59 ng/g	(Leon et al., 2019)
Atlantic coast, Uruguayan	Beach	PP, PE, PET, PVC	POPs, HOCs	PAHs, PCBs	Range of 16.7–758 ng/g	(Lozoya et al., 2016)

CP: cyclophosphamide; TAM: tamoxifen; NIC: nicotine; CAF: caffeine; PRX: paraxanthine; GEM: gemfibrozil; ATL: atenolol; CMZ: carbamazepine; TMP: trimethoprim; ERY: erythromycin; PCBs: polychlorinated biphenyls; PAHs: polycyclic aromatic hydrocarbons; OCPs: organochlorine pesticides; PBDEs: polybrominated diphenyl ethers.

1.3.2 Chemicals release from plastics

As most chemical additives and adsorbed pollutants are typically not covalently bound to the polymer matrix they can be released from plastics over time, leading to ecosystem exposures to chemicals during the lifecycle of plastics (Roland Weber et al., 2023). Therefore, plastic-associated chemical pollution is a transboundary issue of global concern. In addition to the potential release behavior of chemicals from plastic matrices, substantial amounts of associated additives might also be transported with the plastic debris over long distances. These associated chemicals might then be released to the environment along the way. In addition, as mentioned in section 1.2.3, those plastic debris ingested by organisms can also impart their chemical burden to organisms.

1.3.3 Potential toxicity

The chemicals associated with plastics include a range of endocrine-disrupting chemicals (EDCs) and POPs, many of which have been verified to have potential toxicity for organisms.

1.3.3.1 Chemical additives

Out of the range of chemical additives (such as plasticizers, stabilizers and flame retardants.), some are of greater concern due to their potential or known toxic effect, and are summarized in the following chapter.

Flame retardants (FRs) are functional additives that are widely used to reduce flammability of plastic products (such as electronic devices, vehicles and insulation foams) with many incorporated at high concentrations in polymers (Takada; and Bell, 2021). For example, dashboards, seating and upholstery are always treated with flame retardants to reduce the fire risk. Flame retardants may have different compositions including; halogenated flame retardants (bromine flame retardants (BFRs), chlorinated flame retardants (CFRs), organophosphorous flame retardnats (OPFRs), and inorganic flame retardants (such as aluminum and boron) (van der Veen and de Boer, 2012). Many BFRs (such as polybrominated dipheyl ethers (PBDE), hexabromocyclododecane (HBCD or HBCDD)) have been identified as POPs according to Stockholm Convention and have well documented concerns about their toxicity (Takada; and Bell, 2021). For example, PBDEs as POPs have attracted great attention with concerns over human health owing to being ubiquitous, persistent, bioaccumulate and exhibiting various toxicity traits including endocrine disruption, developmental neurotoxicity and reproductive disorders (Wu et al., 2020). In addition, tetrabromobisphenol A (TBBPA) is the most commonly used BFR in the world, which has been shown to disrupt the endocrine system, thyroid hormones, and

neurobehavioral functions even at low doses (Sunday et al., 2022). OPFRs (such as tris(2-chloroisopropyl) phosphate (TCPP), tris(2-butoxyethyl) phosphate (TBOEP) and triphenyl phosphate (TPhP)) has also been shown to exhibit toxicological effects and be associate with adverse health issues. For example, tris(1,3-dichloro-2-propyl) phosphate (TDCPP) has been determined to be a carcinogen and TDCPP exposure has been shown to alter pathways related to DNA damage, including cell cycle, DNA replication, DNA repair pathways and to induce apoptosis (Chen et al., 2019).

Plasticizers are a functional additive to enhance flexibility and softness of plastic products but have also been shown to have potential to impact human health. They as a group are dominated by phthalates or phthalic acid esters and are mainly present in PVC plastics (10–60 % by weight) (Roland Weber et al., 2023). Phthalates are not covalently bound to polymers and can easily leach or migrate out of the polymer structure. Phthalates (such as di-(2-ethylhexyl) phthalate (DEHP), dibutyl phthalate (DBP), benzyl butyl phthalate (BBP) and diisobutyl phthalate (DIBP)) are known EDCs and disrupt the hormonal system of biota. Research has found that phthalate concentrations in human urine positively correlate with both abnormal serum thyroid hormone levels and increased risks of thyroid cancer and nodules (Liu et al., 2020a). In addition, serum phthalate exposure levels were related to decreased serum testosterone levels, semen quality, total sperm count and inducing DNA damage in sperm. DEHP is classified as reprotoxic (category 1B) in the EU (Roland Weber et al., 2023), which suggests potential neurotoxicity towards aquatic organisms. A previous study also

showed a positive association between the level of DEHP metabolites in urine samples and benign prostate hyperplasia and prostatic enlargement in humans (Chang et al., 2019). Some countries have restricted or labelling requirements for some phthalates. For example, the EU has restricted DEHP, DBP, BBP, and DIBP in toys, childcare articles, and all indoor or outdoor products with prolonged contact with human skin (Roland Weber et al., 2023). However, there are few restrictions in most developing countries or countries with economies in transition (UNEP, 2017). Resulting in differing exposure risks between economic zones.

Bisphenols (BPs) are a group of aromatic compounds with two hydroxyphenyl functionalities. Bisphenol A (BPA) is the most widely produced and representative member of the BPs chemical class with production of BPA over three million tonnes each year (Laing et al., 2016). BPA is the monomer used to make polycarbonate plastic products (such as water bottles, sports equipment and medical devices) and epoxy resins (liners of aluminium cans). In addition, BPA is also used as an additive (such as plasticizers and stabilizers) in plastics. BPA is one of the typical range of EDCs that impacts both male and female reproductive system. In addition, it's also associated with cardiovascular diseases, various cancers and obesity. (Glaussusz, 2014; Ortiz-Villanueva et al., 2018). In recent years, infant feeding bottles that contain BPA have been banned in some countries and regions, such as the EU, Canada, North America and Israel (Roland Weber et al., 2023). However, owing to its widespread use, BPA can be frequently detected in the environment. Over the past years, multiple studies have

determined BPA concentrations in the environment, including sediments, sludge and water systems. The highest concentration of BPA (29920 ng/L) was found in rivers located in the northeastern Mediterranean region in Turkey (Ozhan and Kocaman, 2019). In recent years, bisphenol analogues (such as bisphenol F (BPF) and bisphenol S (BPS)) have been used as substitute for BPA. For example, bisphenol F (BPF) is a widely used substitute for BPA in the manufacture of epoxy resins, water pipes, food packaging, polycarbonate plastics. BPs have been detected in the environment, many household and personal care products such as body wash and toothpaste, along with surface waters, sewage and human urine samples (Rochester and Bolden, 2015). The highest concentration of BPF (399 ng/L) and BPS (121 ng/L) were found in the Pearl River Estuary's coast in China (Zhao et al., 2019b). BPA analogues (including BPF, BPS, BPB and BPAP) have been detected in PCPs that were purchased from retail stores in China and the United States (concentrations ranged from to 0.354-0.707 ng/g) (Liao and Kannan, 2014), which indicates those chemicals have been widely used in daily consumption products. In addition, BPA substitutes were also detected in the urine samples that were collected from Saudi Arabia and the concentrations varied from 0.15 ng/mL to 13.3 ng/mL (Asimakopoulos et al., 2016). However, research shows that hormonal activities of BPF are similar to BPA with similar endocrine-disrupting effects (Rochester and Bolden, 2015). Animal tests have showed that BPF affects uterine growth and weight of testes, suggesting that BPF impacts the estrogen and androgen pathways (Higashihara et al., 2007). BPS also disrupts hormonal pathways in many ways, including changing uterine growth patterns, changing sex hormone

concentrations, alterations to egg production and sperm count, weight gain and altering

hormone metabolic activity (Ivry Del Moral et al., 2016; Naderi et al., 2014; Rochester

and Bolden, 2015).

Table 7. Concentration of bisphenol analogues in environmental related samples, foods,

consumer products, and humans. Source: Catenza et al. (2021); Chen et al. (2016)

	Matrix	Region	BPA	BPF	BPS	BPB	BPAP	Reference
		India	7.58–2026	-	-	-	-	(Mukhopadhyay et al., 2020)
	Sediment (ng/g)	China	0.11–359	0.02–36.4	0.06–45.4	-	-	(Huang et al., 2018)
		China	26.6–1860	16.0–1390	nd–5.6	-	-	(Huang et al., 2020a)
		Croatia	1.84-81.39	-	-	-	-	(Anđelić et al., 2020)
Environment	Wastewater (ng/L)	Slovenia	-	16.4 (mean, influents), <0.47 (mean, effluents)	21.3, <0.317	8.46, 0.755	74.9, 4.91	(Česen et al., 2018)
		USA	90.0 (mean, influents), 42.9 (mean, effluents)	90.2, 64.9	31.2, 23.6	-	-	(Xue and Kannan, 2019)
		China	412 (mean, influents), 42.9 (mean, effluents)	66.4, <4.97	109, 11.9	<6.79, nd	1.16, nd	(Sun et al., 2018)
	Sludge (ng/g)	China	43.0 (average)	4.73	1.50	0.25	0.51	Pang et al. (2019)
		USA	238–961	140	7.76–15.8	-	-	(Xue and Kannan, 2019)
	Freshwater (ng/L)	India	16.7–14800	16.7–209	16.7–341	-	-	(Lalwani et al., 2020)
		China	19.0–2180	0.24–255	0.07–122	-	-	(Huang et al., 2020a)

Category	Type	Country						Reference
		Turkey	4620–29920	-	-	-	-	(Ozhan and Kocaman, 2019)
		Slovenia and Croatia	-	-	1.68–35.2	-	0.540–0.903	(Česen et al., 2019)
	Seawater (ng/L)	China	12.5–176	9.58–399	3.14–121	0.36–18.1	-	(Zhao et al., 2019a; Zhao et al., 2019b)
		Turkey	12800–15340	-	-	-	-	(Ozhan and Kocaman, 2019)
Consumer products	Thermal paper (ng/g)	Nigeria	1.50×10^6 – 3.16×10^6	-	-	-	-	(Adeyemi et al., 2020)
		Brazil	$<1.7 \times 10^5$ – 1.69×10^7	-	$<3.0 \times 10^4$ – 8.93×10^6	-	-	(Molina-Molina et al., 2019)
	Personal care products (ng/g)	China, USA	0.354 (mean)	0.707	0.354	0.707	0.354	(Liao and Kannan, 2014a)
	Canned and non-canned foods (ng/g)	Spain	<0.17-88.66	-	-	<0.17–4.19	-	(González et al., 2020)
Food	Meat (ng/g)	China	0.1 (mean)	0.03	<0.01	0.01	<0.01	(Liao and Kannan, 2014b)
	Soft drink (ng/L)	Spain	nd-607	nd-218	-	-	-	(Gallart-Ayala et al., 2011)
Human	Urine (ng/mL)	Saudi Arabia	4.92 (mean)	0.19	13.3	0.05	0.3	(Asimakopoulos et al., 2016)
	Serum (ng/mL)	Italy	2.91 (mean)	-	-	5.15	-	(Cobellis et al., 2009)

nd: not detected; BPB: bisphenol B; BPAP: bisphenol AP

Light stabilizers play important role for preventing the degradation of plastics by adsorbing UV irradiation or removing free radicals. The most common UV stabilizers includie benzophenones, benzotriazoles (BZTs) and hindered amine light stabilizers (HALS). Benzophenones are of concern due to their potential ecotoxicity. For example, benzophenone-3 (BP-3, 2-hydroxy-4-methoxybenzophenone) is one of the widely used benzophenones light stabilizers has been frequently reported as an endocrine disruptor (Fent et al., 2008; Kunz et al., 2006; Schreurs et al., 2005; Schultz et al., 2009). Animal and in vitro experiments have suggested that BP-3 influences reproduction and sex hormone signalling (Blair et al., 2000; Kunz et al., 2006; Schreurs et al., 2005; Suzuki et al., 2005). BZTs are of growing concern as chemical additives as they could bind with the human oestrogen receptors and have the potential to exert endocrine disrupting activity (Takada; and Bell, 2021). The BZT family, such as UV-326, UV-327 and UV-328 also demonstrate with persistent, bioaccumulate and toxic properties, among them UV-328 has been listed as POPs under the Stockholm Convention (under Annex A) (UNEP, 2023), which is the first non-halogenated POP.

1.3.3.2 Other chemicals

In addition to those chemical additives already described, other chemicals that are associated with plastics have been shown to be of concern due to their toxicity. PAHs are an important class of HOCs, which are ubiquitously distributed in aquatic and terrestrial ecosystems and preferentially associated with solid particles due to their low solubility. PAHs are known as one of the most toxic organic pollutants and having been

shown to be lipophilic, carcinogenic, and have mutagenic properties. They can cause serious adverse health effects on organisms including tumors, reproduction development, and immunity effects (Abdel-Shafy and Mansour, 2016; Mihankhah et al., 2020). The US Environmental Protection Agency has listed 16 PAHs family as priority pollutants. Among them, 7 compounds were classified as probable human carcinogens, including Benzo(a)anthracene, Benzo(a)pyrene, Benzo(b)fluoranthene, Benzo(k) fluoranthene, Chrysene, Dibenzo(ah)anthracene and Indeno(1,2,3-cd) pyrene (Mihankhah et al., 2020).   In addition, PCBs and OCPs have also been frequently detected on plastic debris (Figure 6), with these chemicals being in the spotlight owing to their toxicity, high environmental persistence, widespread emission, bioaccumulation capacity and they are listed as POPs (Vasseghian et al., 2021).

1.4 Aims, objectives and thesis outline

Globally, approximately 22 million tonnes of plastics, along with the chemicals present in them, are released to the environment every year (OECD, 2022). As noted, large pieces of plastic can break down into smaller fragments to form microplastics by the effect of mechanical wear (such as wearing of road or sand, washing of waves and turbulence), UV oxidation, which can alter the surface functional groups of plastics particles. Biological enzymes, bacterial, algae or fungi can also interact/bind with plastics to form biofilms on the surface of plastic polymers, which could cause the erosion and biodegradation of plastic materials. The degradation of plastics results in the modification of their physicochemical characteristics and might further affect the

36

adsorption and release behavior of associated chemicals on and within microplastics. As microplastic debris can be considered an important transport vector for a wide range of chemicals that could result in a long-term risk of the release of hazardous chemicals from microplastic waste in the environment or into organisms (Figure 10), exploring the degradation of microplastics to determine the interaction behavior between chemicals and microplastics is vital to assess the risks posed by plastic debris in the environment. Therefore, this study was designed around a series of experiments, described in the following Chapters, to help understanding the exposure risks from aged microplastics in the environment.
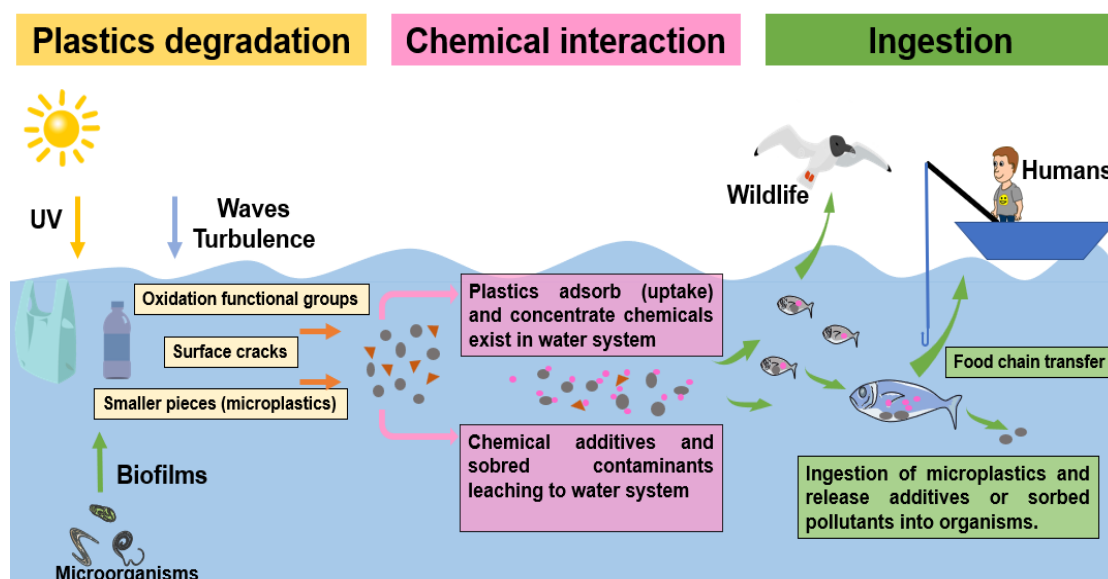
Figure 10. The release of plastic debris in the environment.

For this study, bisphenols were selected as a target chemical group to understand the interaction behavior of chemicals on aged microplastics. These substances can be considered to be representative of typical EDCs widely used as plastic additives and

frequently detected in the aquatic environment (Table 7). Up to now, detailed studies on the adsorption and release behavior of bisphenols on microplastic debris are limited, and so further studies are required. Chapters 2, 3 and 4 presents result from a series of laboratory-based experiments designed to investigate the interaction behavior and mechanism of bisphenols on aged microplastics. The microplastic samples used in Chapter 2 were obtained from UV irradiation of virgin materials, to assess the most important and common abiotic degradation process on the adsorption and release behavior of bisphenols on microplastics. In Chapter 3, a more complex aging experiment was designed, which included abiotic (artificial UV aging) and biotic (biofilms colonization) aging processes and their combination to obtain more environmentally representative particles to investigate their interaction behavior with the most frequently detected bisphenol — BPA. As for Chapter 4, naturally aged microplastic debris was collected from field locations to help better understanding the degradation behavior of 'real' plastic and the potential relationship between the aging of plastics and the adsorption/release of chemicals in the natural environment, providing more realistic data. In addition to the target analysis, suspect screening analysis techniques were also adopted in this study to determine additives in microplastics and how could they change or release from microplastics during the aging process. For example, in Chapter 5 and Chapter 6, we explored how additives (such as plasticizers and UV stabilizers) affect microplastics degradation and the how could they further affect the adsorption and release behavior of plastics during the degradation process by suspect screening analysis. The results will be useful to provide a better

understanding of the fate of plastic debris and associated chemicals in the natural environment.

Overall, this study undertook a combination of laboratory based and field experiments were carried out to explore the aging mechanisms of plastics under different aging conditions and to clarify the potential relationship between the aging of plastics and the uptake/release of chemicals. By probing the mechanisms of sorption/desorption and leaching behavior between additives and aged plastics under different environmental conditions we will be able to better assess the potential risks of the exposure of plastic fragments in the aquatic environment and ingestion by biota.

References

Abdel-Shafy, H.I., Mansour, M.S.M., 2016. A review on polycyclic aromatic hydrocarbons: Source, environmental impact, effect on human health and remediation. Egyptian Journal of Petroleum 25, 107-123.

Acha, E.M., Iribarne, H.W.M.O., Gagliardini, D.A., Lasta, C., Daleo, P., 2003. The role of the R ıo de la Plata bottom salinity front in accumulating debris. Marine Pollution Bulletin 46, 197-202.

Adeyemi, J.A., Gallimberti, M., Olise, C.C., Rocha, B.A., Adedire, C.O., Barbosa Jr, F., 2020. Evaluation of bisphenol A levels in Nigerian thermal receipts and estimation of daily dermal exposure. Environmental Science and Pollution Research 27, 37645-37649.

Ahmad, A., Banat, F., Alsafar, H., Hasan, S.W., 2024. An overview of biodegradable poly (lactic acid) production from fermentative lactic acid for biomedical and bioplastic applications. Biomass Conversion and Biorefinery 14, 3057-3076.

Ali, S.S., Elsamahy, T., Koutra, E., Kornaros, M., El-Sheekh, M., Abdelkarim, E.A., Zhu, D., Sun, J., 2021. Degradation of conventional plastic wastes in the environment: A review on current status of knowledge and future perspectives of disposal. Sci Total Environ 771, 144719.

An, L., Liu, Q., Deng, Y., Wu, W., Gao, Y., Ling, W., 2020. Sources of Microplastic in the Environment, in: He, D., Luo, Y. (Eds.), Microplastics in Terrestrial Environments: Emerging Contaminants and Major Challenges. Springer International Publishing, Cham, pp. 143-159.

Anđelić, I., Roje-Busatto, R., Ujević, I., Vuletić, N., Matijević, S., 2020. Distribution of bisphenol A in sediment and suspended matter and its possible impact on marine life in Kaštela Bay, Adriatic Sea, Croatia. Journal of Marine Science and Engineering 8, 480.

Andrade, H., Glüge, J., Herzke, D., Ashta, N.M., Nayagar, S.M., Scheringer, M., 2021. Oceanic long-range transport of organic additives present in plastic products: an overview. Environmental Sciences Europe 33.

Andrady, A.L., Rajapakse, N., 2019. Additives and Chemicals in Plastics, in: Takada, H., Karapanagioti, H.K. (Eds.), Hazardous Chemicals Associated with Plastics in the Marine Environment. Springer International Publishing, Cham, pp. 1-17.

Arena, U., Mastellone, M.L., Perugini, F., 2003. Life Cycle Assessment of a Plastic Packaging Recycling System. The International Journal of Life Cycle Assessment 8, 92-98.

Asimakopoulos, A.G., Xue, J., De Carvalho, B.P., Iyer, A., Abualnaja, K.O., Yaghmoor, S.S., Kumosani, T.A., Kannan, K., 2016. Urinary biomarkers of exposure to 57 xenobiotics and its association with oxidative stress in a population in Jeddah, Saudi Arabia. Environmental research 150, 573-581.

Avery-Gomm, S., Provencher, J., Morgan, K., Bertram, D., 2013. Plastic ingestion in marine-associated bird species from the eastern North Pacific. Marine pollution bulletin 72, 257-259.

Benson, N.U., Fred-Ahmadu, O.H., 2020. Occurrence and distribution of microplastics-sorbed phthalic acid esters (PAEs) in coastal psammitic sediments of tropical Atlantic Ocean, Gulf of Guinea. Science of the Total Environment 730.

Bergmann, M., Collard, F., Fabres, J., Gabrielsen, G.W., Provencher, J.F., Rochman, C.M., van Sebille, E., Tekman, M.B., 2022. Plastic pollution in the Arctic. Nature Reviews Earth & Environment 3, 323-337.

Bergmann, M., Gutow, L., Klages, M., 2015. Marine Anthropogenic Litter.

Blair, R.M., Fang, H., Branham, W.S., Hass, B.S., Dial, S.L., Moland, C.L., Tong, W., Shi, L., Perkins, R., Sheehan, D.M., 2000. The Estrogen Receptor Relative Binding Affinities of 188 Natural and Xenochemicals: Structural Diversity of Ligands. TOXICOLOGICAL SCIENCES 54, 138-153.

Boerger, C.M., Lattin, G.L., Moore, S.L., Moore, C.J., 2010. Plastic ingestion by planktivorous fishes in the North Pacific Central Gyre. Marine pollution bulletin 60, 2275-2278.

Bonhomme, S., Cuer, A., Delort, A., Lemaire, J., Sancelme, M., Scott, G., 2003. Environmental biodegradation of polyethylene. Polymer degradation and Stability 81, 441-452.

Boren, L.J., Morrissey, M., Muller, C.G., Gemmell, N.J., 2006. Entanglement of New Zealand fur seals in man-made debris at Kaikoura, New Zealand. Marine pollution bulletin 52, 442-446.

Bouhroum, R., Boulkamh, A., Asia, L., Lebarillier, S., Halle, A.T., Syakti, A.D., Doumenq, P., Malleret, L., Wong-Wah-chung, P., 2019. Concentrations and

fingerprints of PAHs and PCBs adsorbed onto marine plastic debris from the Indonesian Cilacap coast and theNorth Atlantic gyre. Regional Studies in Marine Science 29.

Browne, M.A., Galloway, T., Thompson, R., 2007. Microplastic--an emerging contaminant of potential concern? Integr Environ Assess Manag 3, 559-561.

Bugoni, L., Krause, L.g., Petry, M.V.n., 2001. Marine debris and human impacts on sea turtles in southern Brazil. Marine pollution bulletin 42, 1330-1334.

Campani, T., Baini, M., Giannetti, M., Cancelli, F., Mancusi, C., Serena, F., Marsili, L., Casini, S., Fossi, M.C., 2013. Presence of plastic debris in loggerhead turtle stranded along the Tuscany coasts of the Pelagos Sanctuary for Mediterranean Marine Mammals (Italy). Marine Pollution Bulletin 74, 225-230.

Carman, V.G., Acha, E.M., Maxwell, S.M., Albareda, D., Campagna, C., Mianzan, H., 2014. Young green turtles, Chelonia mydas, exposed to plastic in a frontal area of the SW Atlantic. Marine Pollution Bulletin 78, 56-62.

Carson, H.S., Nerheim, M.S., Carroll, K.A., Eriksen, M., 2013. The plastic-associated microorganisms of the North Pacific Gyre. Marine pollution bulletin 75, 126-132.

Catenza, C.J., Farooq, A., Shubear, N.S., Donkor, K.K., 2021. A targeted review on fate, occurrence, risk and health implications of bisphenol analogues. Chemosphere 268, 129273.

Česen, M., Ahel, M., Terzić, S., Heath, D.J., Heath, E., 2019. The occurrence of contaminants of emerging concern in Slovenian and Croatian wastewaters and receiving Sava river. Science of the Total Environment 650, 2446-2453.

Česen, M., Lenarčič, K., Mislej, V., Levstek, M., Kovačič, A., Cimrmančič, B., Uranjek, N., Kosjek, T., Heath, D., Dolenc, M.S., 2018. The occurrence and source identification of bisphenol compounds in wastewaters. Science of the Total Environment 616, 744-752.

Chang, W.H., Tsai, Y.S., Wang, J.Y., Chen, H.L., Yang, W.H., Lee, C.C., 2019. Sex hormones and oxidative stress mediated phthalate-induced effects in prostatic enlargement. Environ Int 126, 184-192.

Chen, C.-F., Ju, Y.-R., Lim, Y.C., Hsu, N.-H., Lu, K.-T., Hsieh, S.-L., Dong, C.-D., Chen, C.-W., 2020. Microplastics and their affiliated PAHs in the sea surface connected to the southwest coast of Taiwan. Chemosphere 254.

Chen, D., Kannan, K., Tan, H., Zheng, Z., Feng, Y.L., Wu, Y., Widelka, M., 2016. Bisphenol Analogues Other Than BPA: Environmental Occurrence, Human Exposure, and Toxicity-A Review. Environmental Science & Technology 50, 5438-5453.

Chen, R., Hou, R., Hong, X., Yan, S., Zha, J., 2019. Organophosphate flame retardants (OPFRs) induce genotoxicity in vivo: A survey on apoptosis, DNA methylation, DNA oxidative damage, liver metabolites, and transcriptomics. Environ Int 130, 104914.

Chen, Y., Awasthi, A.K., Wei, F., Tan, Q., Li, J., 2021. Single-use plastics: Production, usage, disposal, and adverse impacts. Sci Total Environ 752, 141772.

Cheung, P.K., Fok, L., 2017. Characterisation of plastic microbeads in facial scrubs and their estimated emissions in Mainland China. Water Res 122, 53-61.

Cheung, P.K., Hung, P.L., Fok, L., 2018. River Microplastic Contamination and Dynamics upon a Rainfall Event in Hong Kong, China. Environmental Processes 6, 253-264.

CIEL, 2019. Plastic & Climate: The Hidden Costs of a Plastic Planet.

Cobellis, L., Colacurci, N., Trabucco, E., Carpentiero, C., Grumetto, L., 2009. Measurement of bisphenol A and bisphenol B levels in human blood sera from healthy and endometriotic women. Biomedical Chromatography 23, 1186-1190.

Codina-García, M., Militão, T., Moreno, J., González-Solís, J., 2013. Plastic debris in Mediterranean seabirds. Marine pollution bulletin 77, 220-226.

Corradini, F., Meza, P., Eguiluz, R., Casado, F., Huerta-Lwanga, E., Geissen, V., 2019. Evidence of microplastic accumulation in agricultural soils from sewage sludge disposal. Sci Total Environ 671, 411-420.

Costa, J.P.d., Avellan, A., Mouneyrac, C., Duarte, A., Rocha-Santos, T., 2023. Plastic additives and microplastics as emerging contaminants: Mechanisms and analytical assessment. TrAC Trends in Analytical Chemistry 158

Crawford, C.B., Quinn, B., 2016. Microplastic pollutants. Elsevier.

Da Silva Mendes, S., de Carvalho, R.H., de Faria, A.F., de Sousa, B.M., 2015. Marine debris ingestion by Chelonia mydas (Testudines: Cheloniidae) on the Brazilian coast. Marine pollution bulletin 92, 8-10.

De Witte, B., Devriese, L., Bekaert, K., Hoffman, S., Vandermeersch, G., Cooreman, K., Robbens, J., 2014. Quality assessment of the blue mussel (Mytilus edulis):

Comparison between commercial and wild types. Marine pollution bulletin 85, 146-155.

Derraik, J.G., 2002. The pollution of the marine environment by plastic debris: a review. Marine pollution bulletin 44, 842-852.

Demeter, M.A., Lemire, J.A., Turner, R.J., Harrison, J.J., 2016. Biofilm survival strategies in polluted environments. Biofilms in bioremediation: current research and emerging technologies, 43-56.

Denuncio, P., Bastida, R., Dassis, M., Giardino, G., Gerpe, M., Rodríguez, D., 2011. Plastic ingestion in Franciscana dolphins, Pontoporia blainvillei (Gervais and d'Orbigny, 1844), from Argentina. Marine pollution bulletin 62, 1836-1841.

Desforges, J.-P.W., Galbraith, M., Ross, P.S., 2015. Ingestion of microplastics by zooplankton in the Northeast Pacific Ocean. Archives of environmental contamination and toxicology 69, 320-330.

Du, H., Xie, Y., Wang, J., 2021. Microplastic degradation methods and corresponding degradation mechanism: Research status and future perspectives. J Hazard Mater 418, 126377.

Duis, K., Coors, A., 2016. Microplastics in the aquatic and terrestrial environment: sources (with a specific focus on personal care products), fate and effects. Environ Sci Eur 28, 2.

Eriksen, M., Maximenko, N., Thiel, M., Cummins, A., Lattin, G., Wilson, S., Hafner, J., Zellers, A., Rifman, S., 2013. Plastic pollution in the South Pacific subtropical gyre. Marine pollution bulletin 68, 71-76.

Eunomia and ICF (2018) Investigating options for reducing releases in the aquatic environment of microplastics emitted by (but not intentionally added in) products.

Fang, S., Yu, W., Li, C., Liu, Y., Qiu, J., Kong, F., 2019. Adsorption behavior of three triazole fungicides on polystyrene microplastics. Science of the Total Environment 691, 1119-1126.

Fent, K., Kunz, P.Y., Gomez, E., 2008. UV Filters in the Aquatic Environment Induce Hormonal Effects and Affect Fertility and Reproduction in Fish. Chimia 62.

Fife, D.T., Robertson, G.J., Shutler, D., Braune, B.M., Mallory, M.L., 2015. Trace elements and ingested plastic debris in wintering dovekies (Alle alle). Marine pollution bulletin 91, 368-371.

Flemming, H.-C., Wingender, J., 2010. The biofilm matrix. Nature Reviews Microbiology 8, 623-633.

Frias, J.P., Otero, V., Sobral, P., 2014. Evidence of microplastics in samples of zooplankton from Portuguese coastal waters. Marine Environmental Research 95, 89-95.

Galgani, F., Leaute, J.P., Moguedet, P., Souplet, A., Verin, Y., Carpentier, A., Goraguer, H., Latrouite, D., Andral, B., Cadiou, Y., Mahe, J.C., Poulard, J.C., Nerisson, P., 2000. Litter on the Sea Floor Along European Coasts. Marine Pollution Bulletin 40, 516-527.

Gallart-Ayala, H., Moyano, E., Galceran, M., 2011. Analysis of bisphenols in soft drinks by on-line solid phase extraction fast liquid chromatography–tandem mass spectrometry. Analytica Chimica Acta 683, 227-233.

Gewert, B., Plassmann, M.M., MacLeod, M., 2015. Pathways for degradation of plastic polymers floating in the marine environment. Environ Sci Process Impacts 17, 1513-1521.

Geyer, R., Jambeck, J.R., Law, K.L., 2017. Production, use, and fate of all plastics ever made. Sci. Adv.1-5.

Giacovelli;, C., Zamparo;, A., Wehrli;, A., Alverson, K., 2018. Single-Use Plastic sustainability. UN Environment Programme report

Gijsman, P., Meijers, G., Vitarelli, G., 1999. Comparison of the UV-degradation chemistry of polypropylene, polyethylene, polyamide 6 and polybutylene terephthalate. Polymer Degradation and Stability 65, 433±441.

Glaussusz, J., 2014. THE PLASTICS PUZZLE. Nature 508, 306-308.

Goldstein, M.C., Goodwin, D.S., 2013. Gooseneck barnacles (Lepas spp.) ingest microplastic debris in the North Pacific Subtropical Gyre. Peerj 1, e184.

González, N., Cunha, S.C., Ferreira, R., Fernandes, J.O., Marquès, M., Nadal, M., Domingo, J.L., 2020. Concentrations of nine bisphenol analogues in food purchased from Catalonia (Spain): Comparison of canned and non-canned foodstuffs. Food and Chemical Toxicology 136, 110992.

Groh, K.J., Backhaus, T., Carney-Almroth, B., Geueke, B., Inostroza, P.A., Lennquist, A., Leslie, H.A., Maffini, M., Slunge, D., Trasande, L., Warhurst, A.M., Muncke, J., 2019. Overview of known plastic packaging-associated chemicals and their hazards. Sci Total Environ 651, 3253-3268.

Guebert-Bartholo, F., Barletta, M., Costa, M., Monteiro-Filho, E., 2011. Using gut contents to assess foraging patterns of juvenile green turtles Chelonia mydas in the Paranaguá Estuary, Brazil. Endangered Species Research 13, 131-143.

Guo, X., Wang, J., 2019. Sorption of antibiotics onto aged microplastics in freshwater and seawater. Marine Pollution Bulletin 149.

Hahladakis, J.N., Velis, C.A., Weber, R., Iacovidoua, E., Purnell, P., 2015. An overview of chemical additives present in plastics: Migration,release, fate and environmental impact during their use, disposal and recycling. J. Hazard. Mater. 344, 179-199.

Higashihara, N., Shiraishi, K., Miyata, K., Oshima, Y., Minobe, Y., Yamasaki, K., 2007. Subacute oral toxicity study of bisphenol F based on the draft protocol for the "Enhanced OECD Test Guideline no. 407". Arch Toxicol 81, 825-832.

Ho, W.-K., Leung, K.S.-Y., 2019. Sorption and desorption of organic UV filters onto microplastics in single and multi-solute systems. Environmental Pollution 254.

Hofmeyr, G., Bester, M., 2002. Entanglement of pinnipeds at Marion Island. South African Journal of Marine Science 24, 383-386.

Hofmeyr, G.G., Bester, M.N., Kirkman, S.P., Lydersen, C., Kovacs, K.M., 2006. Entanglement of antarctic fur seals at Bouvetøya, Southern Ocean. Marine pollution bulletin 52, 1077-1080. Hoss, D.E., Settle, L.R., 1990. Ingestion of plastics by teleost fishes, Proceedings of the second international conference on marine debris. NOAA technical memorandum. NOAA-TM-NMFS-SWFSC-154. Miami, FL, pp. 693-709.

Huang, C., Wu, L.-H., Liu, G.-Q., Shi, L., Guo, Y., 2018. Occurrence and ecological risk assessment of eight endocrine-disrupting chemicals in urban river water and sediments of South China. Archives of environmental contamination and toxicology 75, 224-235.

Huang, Z., Zhao, J.-L., Yang, Y.-Y., Jia, Y.-W., Zhang, Q.-Q., Chen, C.-E., Liu, Y.-S., Yang, B., Xie, L., Ying, G.-G., 2020. Occurrence, mass loads and risks of bisphenol analogues in the Pearl River Delta region, South China: Urban rainfall runoff as a potential source for receiving rivers. Environmental Pollution 263, 114361.

Ivry Del Moral, L., Le Corre, L., Poirier, H., Niot, I., Truntzer, T., Merlin, J.F., Rouimi, P., Besnard, P., Rahmani, R., Chagnon, M.C., 2016. Obesogen effects after perinatal exposure of 4,4'-sulfonyldiphenol (Bisphenol S) in C57BL/6 mice. Toxicology 357-358, 11-20.

Janssens, V., 2021. Plastics – the Facts 2022. Plastics Europe.

Jin, Y., Lenzen, M., Montoya, A., Laycock, B., Yuan, Z., Lant, P., Li, M., Wood, R., Malik, A., 2023. Greenhouse gas emissions, land use and employment in a future global bioplastics economy. Resources, Conservation and Recycling 193.

Kripa, V., Nair, P.G., Dhanya, A., Pravitha, V., Abhilash, K., Mohammed, A.A., Vijayan, D., Vishnu, P., Mohan, G., Anilkumar, P., 2014. Microplastics in the gut of anchovies caught from the mud bank area of Alappuzha, Kerala. Marine Fisheries Information Service; Technical and Extension Series, 27-28.

Kumi-Larbi, A.J., Yunana, D., Kamsouloum, P., Webster, M., Wilson, D.C., Cheeseman, C., 2018. Recycling waste plastics in developing countries: Use of low-density polyethylene water sachets to form plastic bonded sand blocks. Waste Manag 80, 112-118.

Kunz, P.Y., Galicia, H.F., Fent, K., 2006. Comparison of in vitro and in vivo estrogenic activity of UV filters in fish. Toxicol Sci 90, 349-361.

Kuriyama, Y., Tokai, T., Tabata, K., Kanehiro, H., 2003. Distribution and composition of litter on seabed of Tokyo Bay and its age analysis. Nippon Suisan Gakkaishi 69, 770-781.

Laing, L.V., Viana, J., Dempster, E.L., Trznadel, M., Trunkfield, L.A., Uren Webster, T.M., van Aerle, R., Paull, G.C., Wilson, R.J., Mill, J., Santos, E.M., 2016. Bisphenol A causes reproductive toxicity, decreases dnmt1 transcription, and reduces global DNA methylation in breeding zebrafish (Danio rerio). Epigenetics 11, 526-538.

Lalwani, D., Ruan, Y., Taniyasu, S., Yamazaki, E., Kumar, N.J., Lam, P.K., Wang, X., Yamashita, N., 2020. Nationwide distribution and potential risk of bisphenol analogues in Indian waters. Ecotoxicology and Environmental Safety 200, 110718.

Landrigan, P., Symeonides, C., Raps, H., Dunlop, S., 2023. The global plastics treaty: why is it needed? Lancet.

Lee, D.-I., Cho, H.-S., Jeong, S.-B., 2006. Distribution characteristics of marine litter on the sea bed of the East China Sea and the South Sea of Korea. Estuarine, Coastal and Shelf Science 70, 187-194.

Lee, H., Shim, W.J., Kwon, J.-H., 2014. Sorption capacity of plastic debris for hydrophobic organic chemicals. Science of the Total Environment 470, 1545-1552.

Leon, V.M., Garcia-Aguera, I., Molto, V., Fernandez-Gonzalez, V., Llorca-Perez, L., Andrade, J.M., Muniategui-Lorenzo, S., Campillo, J.A., 2019. PAHs, pesticides, personal care products and plastic additives in plastic debris from Spanish Mediterranean beaches. Sci Total Environ 670, 672-684.

Li, W.C., Tse, H.F., Fok, L., 2016. Plastic waste in the marine environment: A review of sources, occurrence and effects. Sci Total Environ 566-567, 333-349.

Liao, C., Kannan, K., 2014a. A survey of alkylphenols, bisphenols, and triclosan in personal care products from China and the United States. Arch Environ Contam Toxicol 67, 50-59.

Liao, C., Kannan, K., 2014b. A survey of bisphenol A and other bisphenol analogues in foodstuffs from nine cities in China. Food Additives & Contaminants: Part A 31, 319-329.

Lima, A.R., Costa, M.F., Barletta, M., 2014. Distribution patterns of microplastics within the plankton of a tropical estuary. Environ Res 132, 146-155.

Liu, C., Deng, Y.L., Zheng, T.Z., Yang, P., Jiang, X.Q., Liu, E.N., Miao, X.P., Wang, L.Q., Jiang, M., Zeng, Q., 2020. Urinary biomarkers of phthalates exposure and risks of thyroid cancer and benign nodule. J Hazard Mater 383, 121189.

Liu, L., Xu, M., Ye, Y., Zhang, B., 2022. On the degradation of (micro)plastics: Degradation methods, influencing factors, environmental impacts. Sci Total Environ 806, 151312.

Llorca, M., Schirinzi, G., Martinez, M., Barcelo, D., Farre, M., 2018. Adsorption of perfluoroalkyl substances on microplastics under environmental conditions. Environmental Pollution 235, 680-691.

Lozoya, J.P., Teixeira de Mello, F., Carrizo, D., Weinstein, F., Olivera, Y., Cedres, F., Pereira, M., Fossati, M., 2016. Plastics and microplastics on recreational beaches in Punta del Este (Uruguay): Unseen critical residents? Environ Pollut 218, 931-941.

Lucas, N., Bienaime, C., Belloy, C., Queneudec, M., Silvestre, F., Nava-Saucedo, J.E., 2008. Polymer biodegradation: mechanisms and estimation techniques. Chemosphere 73, 429-442.

Lugauskas, A., Levinskait̃, L., Pečiulyt̃, D., 2003. Micromycetes as deterioration agents of polymeric materials. International Biodeterioration & Biodegradation 52, 233-242.

Luo, H., Liu, C., He, D., Xu, J., Sun, J., Li, J., Pan, X., 2022. Environmental behaviors of microplastics in aquatic systems: A systematic review on degradation, adsorption, toxicity and biofilm under aging conditions. Journal of Hazardous Materials 423, 126915.

Lusher, A.L., Burke, A., O'Connor, I., Officer, R., 2014. Microplastic pollution in the Northeast Atlantic Ocean: validated and opportunistic sampling. Mar Pollut Bull 88, 325-333.

Lusher, A.L., Mchugh, M., Thompson, R.C., 2013. Occurrence of microplastics in the gastrointestinal tract of pelagic and demersal fish from the English Channel. Marine pollution bulletin 67, 94-99.

Ma, Y., Huang, A., Cao, S., Sun, F., Wang, L., Guo, H., Ji, R., 2016. Effects of nanoplastics and microplastics on toxicity, bioaccumulation, and environmental fate of phenanthrene in fresh water. Environmental Pollution 219, 166-173.

Magnusson, K., Eliasson, K., Fråne, A., Haikonen, K., Hultén, J., Olshammar, M., Stadmark, J., Voisin, A., Miljöinstitutet, I.S., 2016. Swedish sources and pathways for microplastics to the marine environment.

Mihankhah, T., Saeedi, M., Karbassi, A., 2020. Contamination and cancer risk assessment of polycyclic aromatic hydrocarbons (PAHs) in urban dust from different land-uses in the most populated city of Iran. Ecotoxicol Environ Saf 187, 109838.

Miller, S.A., 2020. Five Misperceptions Surrounding the Environmental Impacts of Single-Use Plastic. Environ Sci Technol 54, 14143-14151.

Molina-Molina, J., Jiménez-Díaz, I., Fernández, M., Rodriguez-Carrillo, A., Peinado, F., Mustieles, V., Barouki, R., Piccoli, C., Olea, N., Freire, C., 2019. Determination of bisphenol A and bisphenol S concentrations and assessment of estrogen-and anti-androgen-like activities in thermal paper receipts from Brazil, France, and Spain. Environmental research 170, 406-415.

Moore, C.J., Lattin, G., Zellers, A., 2005. A brief analysis of organic pollutants sorbed to pre and post-production plastic particles from the Los Angeles and San Gabriel

river Watersheds, Proceedings of the Plastic Debris Rivers to Sea Conference, Algalita Marine Research Foundation, Long Beach, CA.

Moore, C.J., Moore, S.L., Leecaster, M.K., Weisberg, S.B., 2001. A Comparison of Plastic and Plankton in the North Paci®c Central Gyre. Marine Pollution Bulletin 42, 1297-1300.

Moore, E., Lyday, S., Roletto, J., Litle, K., Parrish, J.K., Nevins, H., Harvey, J., Mortenson, J., Greig, D., Piazza, M., 2009. Entanglements of marine mammals and seabirds in central California and the north-west coast of the United States 2001–2005. Marine pollution bulletin 58, 1045-1051.

Mukhopadhyay, M., Sampath, S., Muñoz-Arnanz, J., Jiménez, B., Chakraborty, P., 2020. Plasticizers and bisphenol A in Adyar and Cooum riverine sediments, India: occurrences, sources and risk assessment. Environmental Geochemistry and Health 42, 2789-2802.

Nayanathara Thathsarani Pilapitiya, P.G.C., Ratnayake, A.S., 2024. The world of plastic waste: A review. Cleaner Materials 11.

Naderi, M., Wong, M.Y., Gholami, F., 2014. Developmental exposure of zebrafish (Danio rerio) to bisphenol-S impairs subsequent reproduction potential and hormonal balance in adults. Aquat Toxicol 148, 195-203.

OECD, 2022. Plastic leakage to the environment - projections.

Ortiz-Villanueva, E., Jaumot, J., Martinez, R., Navarro-Martin, L., Pina, B., Tauler, R., 2018. Assessment of endocrine disruptors effects on zebrafish (Danio rerio)

embryos by untargeted LC-HRMS metabolomic analysis. Science of the Total Environment 635, 156-166.

Ozhan, K., Kocaman, E., 2019. Temporal and spatial distributions of bisphenol A in marine and freshwaters in Turkey. Archives of environmental contamination and toxicology 76, 246-254.

Page, B., McKenzie, J., McIntosh, R., Baylis, A., Morrissey, A., Calvert, N., Haase, T., Berris, M., Dowie, D., Shaughnessy, P.D., 2004. Entanglement of Australian sea lions and New Zealand fur seals in lost fishing gear and other marine debris before and after Government and industry attempts to reduce the problem. Marine pollution bulletin 49, 33-42.

Pascoe Ortiz, S., 2023. Are bioplastics the solution to the plastic pollution problem? PLoS Biology 21.

Pettipas, S., Bernier, M., Walker, T.R., 2016. A Canadian policy framework to mitigate plastic marine pollution. Marine Policy 68, 117-122.

Pozo, K., Urbina, W., Gomez, V., Torres, M., Nunez, D., Pribylova, P., Audy, O., Clarke, B., Arias, A., Tombesi, N., Guida, Y., Klanova, J., 2020. Persistent organic pollutants sorbed in plastic resin pellet - "Nurdles" from coastal areas of Central Chile. Mar Pollut Bull 151, 110786.

Rai, P.K., Sonne, C., Brown, R.J.C., Younis, S.A., Kim, K.H., 2022. Adsorption of environmental contaminants on micro- and nano-scale plastic polymers and the influence of weathering processes on their adsorptive attributes. J Hazard Mater 427, 127903.

Raum-Suryan, K.L., Jemison, L.A., Pitcher, K.W., 2009. Entanglement of Steller sea lions (Eumetopias jubatus) in marine debris: Identifying causes and finding solutions. Marine pollution bulletin 58, 1487-1495.

Reisser, J., Shaw, J., Wilcox, C., Hardesty, B.D., Proietti, M., Thums, M., Pattiaratchi, C., 2013. Marine plastic pollution in waters around Australia: characteristics, concentrations, and pathways. Plos One 8, e80466.

Rodriguez, B., Becares, J., Rodríguez, A., Arcos, J.M., 2013. Incidence of entanglements with marine debris by northern gannets (Morus bassanus) in the non-breeding grounds. Marine Pollution Bulletin 75, 259-263.

Rochester, J.R., Bolden, A.L., 2015. Bisphenol S and F: A Systematic Review and Comparison of the Hormonal Activity of Bisphenol A Substitutes. Environmental Health Perspectives 123, 643-650.

Rodríguez, B., Bécares, J., Rodríguez, A., Arcos, J.M., 2013. Incidence of entanglements with marine debris by northern gannets (Morus bassanus) in the non-breeding grounds. Marine Pollution Bulletin 75, 259-263.

Rodriguez, C., Fossatti, M., Carrizo, D., Sanchez-Garcia, L., Teixeira de Mello, F., Weinstein, F., Lozoya, J.P., 2020. Mesoplastics and large microplastics along a use gradient on the Uruguay Atlantic coast: Types, sources, fates, and chemical loads. Sci Total Environ 721, 137734.

Roland Weber, Narain M. Ashta, Nicolò Aurisano, Zhanyun Wang, Magali Outters, Kimberley De Miguel, Martin Schlummer, Markus Blepp, Helene Wiesinger,

Helena Andrade, Martin Scheringer, Fantke, P., 2023. Chemicals-in-Plastics. United Nations Environment Programme.

Santana-Viera, S., Montesdeoca-Esponda, S., Torres-Padron, M.E., Sosa-Ferrera, Z., Santana-Rodriguez, J.J., 2021. An assessment of the concentration of pharmaceuticals adsorbed on microplastics. Chemosphere 266, 129007.

Schreurs, R.H., Sonneveld, E., Jansen, J.H., Seinen, W., van der Burg, B., 2005. Interaction of polycyclic musks and UV filters with the estrogen receptor (ER), androgen receptor (AR), and progesterone receptor (PR) in reporter gene bioassays. Toxicol Sci 83, 264-272.

Schultz, T.W., Seward, J.R., Sinks, G.D., 2009. Estrogenicity of benzophenones evaluated with a recombinant yeast assay: Comparison of experimental and rules-based predicted activity. Environmental Toxicology and Chemistry 19, 301-304.

Shen, L., Worrell, E., Patel, M.K., 2010. Open-loop recycling: A LCA case study of PET bottle-to-fibre recycling. Resources, Conservation and Recycling 55, 34-52.

Singla, M., Diaz, J., Broto-Puig, F., Borros, S., 2020. Sorption and release process of polybrominated diphenyl ethers (PBDEs) from different composition microplastics in aqueous medium: Solubility parameter approach. Environmental Pollution 262.

Song, Y.K., Hong, S.H., Jang, M., Kang, J.-H., Kwon, O.Y., Han, G.M., Shim, W.J., 2014. Large accumulation of micro-sized synthetic polymer particles in the sea surface microlayer. Environmental science & technology 48, 9014-9021.

Sun, X., Peng, J., Wang, M., Wang, J., Tang, C., Yang, L., Lei, H., Li, F., Wang, X., Chen, J., 2018. Determination of nine bisphenols in sewage and sludge using dummy molecularly imprinted solid-phase extraction coupled with liquid chromatography tandem mass spectrometry. Journal of Chromatography A 1552, 10-16.

Sunday, O.E., Bin, H., Guanghua, M., Yao, C., Zhengjia, Z., Xian, Q., Xiangyang, W., Weiwei, F., 2022. Review of the environmental occurrence, analytical techniques, degradation and toxicity of TBBPA and its derivatives. Environ Res 206, 112594.

Suzuki, T., Kitamura, S., Khota, R., Sugihara, K., Fujimoto, N., Ohta, S., 2005. Estrogenic and antiandrogenic activities of 17 benzophenone derivatives used as UV stabilizers and sunscreens. Toxicol Appl Pharmacol 203, 9-17.

Takada;, H., Bell, L., 2021. ipen-plastic-waste-management-hazards.

UNEP, 2017. Overview Report III:Existing national, regional, and global regulatory frameworks addressing Endocrine Disrupting Chemicals (EDCs). Prepared by: The International Panel on Chemical Pollution (IPCP). United Nations Environment Programme.

UNEP, 2023. Report of the Conference of the Parties to the Stockholm Convention on Persistent Organic Pollutants on the work of its eleventh meeting.

Van Cauwenberghe, L., Claessens, M., Vandegehuchte, M.B., Janssen, C.R., 2015. Microplastics are taken up by mussels (Mytilus edulis) and lugworms (Arenicola marina) living in natural habitats. Environ Pollut 199, 10-17.

Van Cauwenberghe, L., Janssen, C.R., 2014. Microplastics in bivalves cultured for human consumption. Environmental Pollution 193, 65-70.

Van der Veen, I., de Boer, J., 2012. Phosphorus flame retardants: properties, production, environmental occurrence, toxicity and analysis. Chemosphere 88, 1119-1153.

Van Emmerik, T., Schwarz, A., 2019. Plastic debris in rivers. WIREs Water 7.

Vasseghian, Y., Hosseinzadeh, S., Khataee, A., Dragoi, E.N., 2021. The concentration of persistent organic pollutants in water resources: A global systematic review, meta-analysis and probabilistic risk assessment. Sci Total Environ 796, 149000.

Velzeboer, I., Kwadijk, C.J.A.F., Koelmans, A.A., 2014. Strong Sorption of PCBs to Nanoplastics, Microplastics, Carbon Nanotubes, and Fullerenes. Environmental Science & Technology 48, 4869-4876.

Wang, J., Guo, X., Xue, J., 2021. Biofilm-Developed Microplastics As Vectors of Pollutants in Aquatic Environments. Environ Sci Technol 55, 12780-12790.

Wayman, C., Niemann, H., 2021. The fate of plastic in the ocean environment - a minireview. Environ Sci Process Impacts 23, 198-212.

Webb, H.K., Crawford, R.J., Sawabe, T., Ivanova, E.P., 2009. Poly(ethylene terephthalate) polymer surfaces as a substrate for bacterial attachment and biofilm formation. Microbes Environ 24, 39-42.

Wilkes, R.A., Aristilde, L., 2017. Degradation and metabolism of synthetic plastics and associated products by Pseudomonas sp.: capabilities and challenges. J Appl Microbiol 123, 582-593.

Wu, Z., He, C., Han, W., Song, J., Li, H., Zhang, Y., Jing, X., Wu, W., 2020. Exposure pathways, levels and toxicity of polybrominated diphenyl ethers in humans: A review. Environ Res 187, 109531.

Xue, J., Kannan, K., 2019. Mass flows and removal of eight bisphenol analogs, bisphenol A diglycidyl ether and its derivatives in two wastewater treatment plants in New York State, USA. Science of the Total Environment 648, 442-449.

Xue, J., Wu, Q., Sakthivel, S., Pavithran, P.V., Vasukutty, J.R., Kannan, K., 2015. Urinary levels of endocrine-disrupting chemicals, including bisphenols, bisphenol A diglycidyl ethers, benzophenones, parabens, and triclosan in obese and non-obese Indian children. Environmental research 137, 120-128.

Yousif, E., Haddad, R., 2013. Photodegradation and photostabilization of polymers, especially polystyrene: review. Springerplus, 1-33.

Zero Waste Europe, 2019. The Impact of Waste-to-Energy Incineration on Climate.

Zhang, K., Hamidian, A.H., Tubic, A., Zhang, Y., Fang, J.K.H., Wu, C., Lam, P.K.S., 2021. Understanding plastic degradation and microplastic formation in the environment: A review. Environ Pollut 274, 116554.

Zhao, Q., Howard, E.W., Parris, A.B., Ma, Z., Xing, Y., Yang, X., 2019a. Bisphenol AF promotes estrogen receptor-positive breast cancer cell proliferation through amphiregulin-mediated crosstalk with receptor tyrosine kinase signaling. Plos One 14, e0216469.

Zhao, X., Qiu, W., Zheng, Y., Xiong, J., Gao, C., Hu, S., 2019b. Occurrence, distribution, bioaccumulation, and ecological risk of bisphenol analogues,

parabens and their metabolites in the Pearl River Estuary, South China. Ecotoxicology and environmental safety 180, 43-52.

2. Adsorption and desorption of bisphenols on commercial microplastics and the effect of UV aging

This chapter presents the study of the adsorption/desorption behavior of four kinds of bisphenols (BPF, BPA, BPB, BPAP) on plastics particles and evaluated the UV irradiation for the effect of the interaction behavior. It provides information to assess the potential exposure risk of plastic debris that undergoing UV degradation in the natural environment.

This chapter was published in the journal Chemosphere in 2023 as a research article in volume 310.

The candidate's contribution was designing and conducting the experiments, samples and data analysis, draft preparation.

Graphical abstract
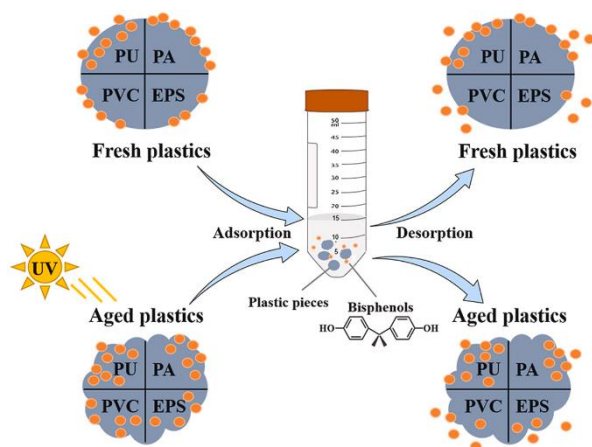
Abstract

Plastics gradually degrade in the natural environment from the effect of irradiation, which can change the surface properties of plastics and affect the migration behavior of pollutants. Up to now, studies on the adsorption/desorption behavior of organic pollutants on aged microplastics are still limited. In this study, several types of commercial plastics (polyurethane (PU), polyamide (PA), polyvinyl chloride (PVC), expanded polystyrene (EPS)) were selected to investigate the adsorption and release behavior for four kinds of bisphenols (bisphenol-F, A, B, AP). The results from Raman spectroscopy and scanning electron microscopy (SEM) analysis showed evidence of oxidization and surface cracks of plastics after irradiation. The adsorption behavior for both fresh and aged microplastics were dominated by hydrophobicity. In addition, the electrostatic force, H-bonding interaction, and π-π interaction were also the important factors impacting the adsorption process. The desorption kinetics behavior indicates that desorption becomes faster after aging. Hydrophobicity is also an important factor

that affects desorption behavior. This study showed that sorption capacity for most fresh and aged microplastics was enhanced by the impact of salinity and dissolved organic matter (DOM). Increased temperature could increase the desorption of bisphenols on both fresh and aged microplastics, which illustrated that warm environments would promote more pollutants be released from plastics to water bodies.

2.1 Introduction

Commercial plastics are intensively used in daily life owing to their versatile, flexible, light and durable properties (Hahladakis et al., 2015; Singla et al., 2020). Globally, over 320 million tons of plastics are produced each year (Wright and Kelly, 2017).Whilst only a small amount of plastics are recycled, the majority of plastics are sent to landfills, incineration plants or even discarded into the natural environment (Liang et al., 2021). Due to the lack of an effective recovery and management system, plastic debris is easily transferred to marine, lake, soil or sediment systems. It has been reported that approximately 5.25 trillion pieces of plastic are present in marine environments, which accounts for 60-80 % of marine litter, even reaching 90 - 95 % in some regions (Singla et al., 2020). These plastic materials can not only cause physical effects for biota (e.g. entanglement of marine species) (Li et al., 2018a), but also result in biotoxicity (Hamlin et al., 2015; Wang et al., 2020a). Various chemical additives (e.g. plasticizers, antioxidants, fillers) are added to polymers to enhance their properties, and as those additives are not tightly bound to plastics they are easily released to the environment. Many additives (such as phthalates, brominated flame retardants and UV-

stabilizers) are endocrine-disrupting chemicals (EDCs) which have a negative effect on normal hormone function, potentially affecting growth, causing obesity and even breast cancer (Suhrhoff and Scholz-Böttcher, 2015). Furthermore, owing to the hydrophobic nature of many plastics, additives and other organic chemicals released into the environment could be adsorbed and desorbed by plastics. As a result, plastics need to be considered a potentially important carrier of contaminants to and within the environment.

When plastics enter the environment, they can gradually break into micro-size (1 μm – 5 mm) or even nano-size (< 1 μm) particles as a result of weathering, with photoaging being a vital factor for the degradation of plastics (Luo et al., 2022c). With irradiation, the hydrophobicity of plastics might be changed, forming oxidation functional groups. In addition, the surface of plastics might crack, which could affect their interaction with chemicals in the natural environment. For example, a study found that the adsorption behavior of 9-Nitroanthrene (9-Nant) on polystyrene (PS) and polyethene (PE) microplastics decreased after artificial aging by UV lamps (Zhang et al., 2020a). This may be related to the supply of oxygen-containing functional groups, which increased the surface polarity of plastics and reduced the affinity of hydrophobic organic pollutants on the surface of microplastic particles.

Bisphenol A (BPA) is one of the typical EDCs that has commonly been used in many consumer products including food containers, paper products (e.g., thermal receipts), water pipes, toys, medical equipment, etc (Chen et al., 2016). It is also the monomer used for polycarbonate (PC) skeletons (Sun et al., 2021). As a result, BPA is

a widely used chemical and frequently detected in water bodies (Wu and Seebacher, 2020). Owing to its toxicity to biota (Naveira et al., 2021; Wu and Seebacher, 2020), BPA use has been limited as an additive in some regions. As a result, some bisphenol analogues (e.g. BPF, BPB, BPAP) have been used in plastics as a substitute for BPA. These bisphenol analogues have been detected in plastics fibres (Sait et al., 2021), rivers (Wang et al., 2022b) and fish (Barboza et al., 2020). Unfortunately, those analogues can also cause negative effects in biota and generate the similar toxicity to BPA (Chen et al., 2016). Nevertheless, studies on the interaction behavior between plastics and bisphenol analogues is limited. As a result, the fate, adsorption/desorption behavior of bisphenols in the presence of aged plastics is still unclear.

Therefore, in this study, selected commercial microplastic particles — polyurethane (PU), polyamide (PA), expanded polystyrene (EPS) and polyvinyl chloride (PVC), have been artificial aged in a Suntest CPS+ chamber for 48 h and 168 h to investigate the adsorption/desorption behavior of bisphenols (BPF, BPA, BPB, BPAP) on fresh and aged microplastics. The objectives of this study were to (i) explore the interaction mechanism of bisphenols on fresh and aged commercial microplastics to clarify the potential relationship between the ageing of microplastics and the uptake/release behavior of bisphenols; (ii) probe the adsorption/desorption behavior for different types of microplastics to assess the potential risk for exposure from plastic fragments to the environment; (iii) examine the influence of environmental conditions (temperature, DOM, artificial seawater) on the adsorption and desorption behaviors of bisphenols by microplastics.

2.2 Material and methods

2.2.1 Materials and chemicals

Standards of BPF, BPA, BPB and BPAP (purity > 98.0 %) were purchased from Sigma-Aldrich Co. LLC (UK), details of the four bisphenols are shown in Table S1. Acetonitrile (HPLC grade) and Methanol (HPLC grade) were purchased from Fisher Scientific Ltd (UK). Stock bisphenol solutions (100 mg/L) were prepared in methanol and kept at 4 °C. The Humic acid (HA) was purchased from Sigma-Aldrich Co. LLC (UK). The artificial seawater was obtained from Brightwell Aquatics (USA), the average concentration of Mg, Ca, K, and Sr are 1290 mg/L, 413 mg/L, 399 mg/L, and 8 mg/L, respectively.

Seven different kinds of commercial plastics (Table S2) related to food and general use (daily necessities) were collected in a local market (Guangzhou, China) or "Taobao.com". The preliminary experiment (Figure S1) demonstrated that PU, PA, PVC and EPS had good adsorption ability for bisphenols. This allowed further study of the interaction behavior between bisphenols and plastics to be observed along with the aging process for four selected plastics. The structures of the four plastics are given in Figure S2. All plastics were cut into small pieces approximately 5×5 mm to obtain micro-sized plastics.

2.2.2 Artificial aging and characterization of microplastics

A Suntest CPS+ xenon chamber (Atlas Material Testing Technology LLC, USA) was configured at 500 W m^{-2}, 35 °C for the degradation of microplastic pieces. The

wavelength of radiation ranged from 300 nm to 800 nm (including the range of UV-A and part UV-B radiation), and was performed for 48 h and 168 h respectively, which are similar as exposure 146 and 511 days under the European mean irradiance (Gewert et al., 2018), the equation is shown in the Supporting information-M1. Raman and SEM were used to characterize the aged microplastics.

2.2.3 Adsorption experiments

Bisphenols stock solutions (100 mg/L) were diluted to 1 mg/L with ultrapure water with the volume ratio of methanol kept below 0.1 % to reduce solvent effects. Before the kinetic experiments, three control experiments were performed: (1) 60 mg original microplastic pieces were added to 15 mL ultrapure water to determine if plastic materials contained and leached bisphenol additives. (2) 15 mL bisphenol solutions were placed into polypropylene (PP) centrifuge tubes to confirm if the centrifuge tubes would adsorb bisphenols. (3) 15 mL ultrapure water, artificial seawater and humic acid water were placed into PP centrifuge tubes to ensure that the tubes didn't leach bisphenols. Results showed that no bisphenols leached from both plastic materials and tubes, the loss of bisphenols in centrifuge tubes was less than 5 %.

For the adsorption kinetic experiments, 60 mg of microplastics and 15 mL 1 mg/L bisphenols were added into PP centrifuge tubes. All centrifuge tubes were placed on the shaker at 180 rpm (25 ± 1 °C). The supernatants were collected after 4 h, 12 h, 24 h, 48 h, 72 h, 108 h, 156 h, 204 h, 256 h, 308 h and 360 h, and filtered through a 0.2 μm PTFE membrane (Figure S3). In addition, 1 mg/L single solution of each bisphenol

were prepared to investigate the competitive absorption behavior on plastics. Environmental conditions are important factors in the interaction between contaminants and microplastics. As a result, the adsorption experiments of fresh and aged 168 h microplastics were carried out in three different matrices—ultrapure water, artificial seawater and 15 mg/L humic acid water to simulate the adsorption behavior of plastics under the impact of freshwater, seawater and the presence of DOM. The initial pH values of ultrapure water, artificial seawater and HA water were 6.8 ± 0.1, 8.2 ± 0.1 and 6.5 ± 0.1. Moreover, the impacts of different temperatures including 15 ℃, 25 ℃ and 35 ℃ were investigated. Three replicates were conducted for each treatment.

2.2.4 Desorption experiments

After adsorption equilibrium was achieved, desorption experiments were further carried out to investigate the release kinetics of bisphenols from microplastics. Microplastics from the adsorption experiment were transferred into centrifuge tubes containing 15 mL ultrapure water, artificial seawater or 15 mg/L HA water, and shaken at 180 rpm. The desorption experiments were carried out at 15 ℃, 25 ℃, 35℃, respectively. Three replicates were implemented for each treatment. The supernatants were collected from 0 h to 156 h.

2.2.5 Chemical analysis

All samples were analysed using a Shimadzu NexeraX2 UHPLC with fluorescence detector (Shimadzu, Japan) and a Phenomenex C18 column (4 μm, 150 × 4.6 mm). Chromatographic separation was performed with a mobile phase of A:

ultrapure water and B: acetonitrile (ACN). The gradient began at 40 % ACN, then increased to 60 % ACN within 9 min, followed by reaching 90 % ACN at 12 min and decreased to 40 % ACN at 15 min, finally, 5 min of post-ran ensured equilibrium of the column before the next injection. Samples were prepared in ultrapure water and methanol (4:1, v/v). Other parameters are available in Table S3.

2.2.6 Statistical analysis

T-test and ANOVA were used to analyse significant differences and statistical significance was set as $p < 0.05$. All statistical analysis was performed using SPSS 22.0 software and Microsoft Office Excel 2020. Figures were plotted with Origin 2020.

The adsorption efficiency of bisphenols was calculated according to Eq. (2):

$$\% \text{ A} = \left(\frac{C_0 - C_e}{C_0}\right) \times 100 \qquad (2)$$

where A represents the adsorption efficiency of each bisphenol; C_0 and C_e (μg/L) are the initial concentration and equilibrium concentration of bisphenols in the solution respectively.

The capacities of 4 types of bisphenols adsorbed to microplastics was calculated to Eq. (3) as below.

$$q_e = \frac{C_0 - C_e}{m} V \qquad (3)$$

where q_e (μg/g) refers to the equilibrium adsorption capacity of microplastics for each bisphenol; m (mg) is the mass of microplastics and V (mL) is the volume of the solution used in adsorption experiments.

The adsorption kinetics can be fitted using a pseudo-first order model and a pseudo-second order model. The linear form of equations are as follows:

Pseudo-first order model:

$$\log (q_e - q_t) = \log q_e - k_1 t / 2.303 \tag{4}$$

Pseudo-second order model:

$$\frac{t}{q_t} = \frac{1}{k_2 q_e^2} + \frac{t}{q_e} \tag{5}$$

where q_t (µg/g) is the adsorption amount of bisphenols per gram of microplastics at a given time t (h); k_1 and k_2 represent the rate constant for pseudo-first order and pseudo-second order kinetics respectively. The pseudo-first order model represents a physical process, where the intermolecular force (Van der Waals' force) is the main interaction between particles, and the pseudo-second-order model relies on chemical processes, such as the formation of chemical bonds, electron transfer, etc. (Wu et al., 2019).

The desorption efficiency of each bisphenol was calculated using:

$$\%D = \left(\frac{C_{desorb}}{C_{adsorb}} \right) \times 100 \tag{6}$$

where C_{desorb} (µg/L) is the desorption concentration of bisphenols from microplastics and C_{adsorb} (µg/L) is the adsorbed equilibrium concentration of bisphenols on microplastics at the beginning of the desorption experiment.

2.3 Results and discussion

2.3.1 Surface changes and characterization of aged plastics

The Raman spectra (Figure 1) showed that there were significant changes for aged PA and PVC microplastics compared with the virgin microplastics.
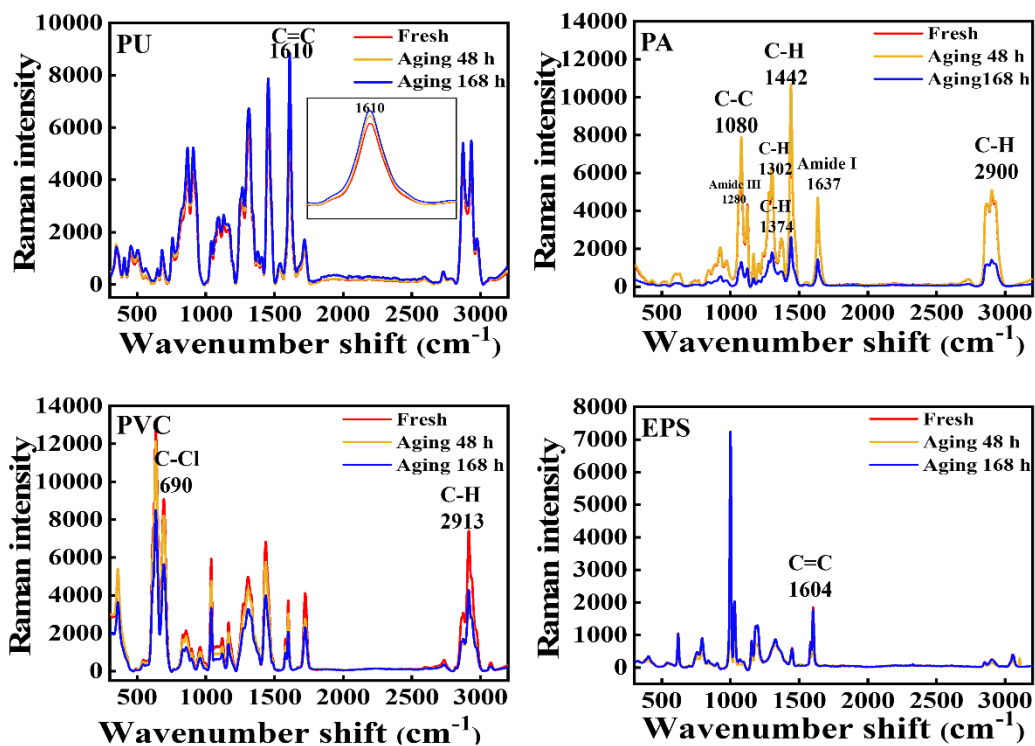
Figure 1. Raman spectra of microplastics. The spectral range of 300–3200 cm^{-1} (785 nm laser, 15 mW, x50 objective, 10 s collection).
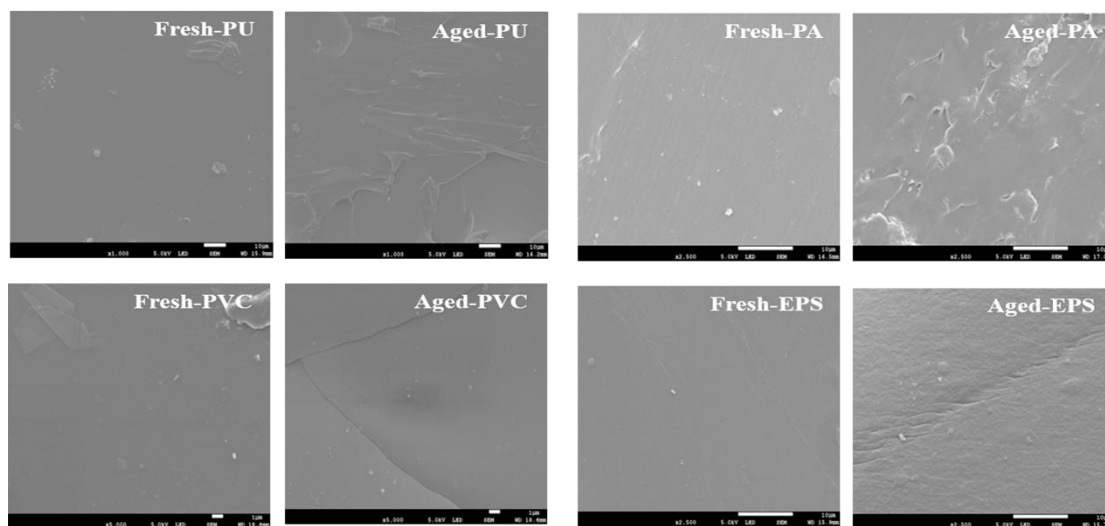
Figure 2. SEM images for fresh and aged 168 h microplastics.

The reduced intensities of stretching (2900 cm^{-1}), twisting (1301 cm^{-1}), wagging (1374 cm^{-1}) and bending (1442 cm^{-1}) of methylene (–CH$_2$) suggests the oxidation of PA plastics which would convert C–H bonding to carbonyl bonding (C=O) (Uematsu

73

et al., 2021; Zou et al., 2020).The reduced peak for amide I (C=O) and amide III (N–H, C–N) represents amide bending (C=O–N–H) breaks during the aging process. For PVC microplastics, there is an obvious reduction for the stretching vibration of carbon-chlorine (C–Cl) (690 cm^{-1}) and C–H (2913 cm^{-1}) (Kappler et al., 2016)，which would be due to oxidation. As for EPS plastics, Raman spectra showed a slight reduction of C=C in benzene ring intensity. For PU microplastics the intense band between 1570 cm^{-1} and 1660 cm^{-1} with a maximum at 1610 cm^{-1} can be ascribed to the C=C stretching vibrations of aromatic rings. A broadening with increased aged time could be observed, which illustrates degradation of aromatic rings (Bruckmoser and Resch, 2014). Changes for PU plastics were also visually observed as they became yellow with the light irradiation (Figure S4). This might be related to oxidation reactions and the creation of quinone-imide structures (chromophore) (Rosu et al., 2009). In addition, Photo-Fries rearrangement is another mechanism for the formation of chromophores.

Figure 2 illustrates the surface changes after irradiation. The surfaces of fresh microplastics are smooth, whilst in contrast, the surfaces became rough after aging. For aged PU and PA microplastics, surfaces showed more pits compared with fresh microplastics, while the surface change of aged PVC and EPS were mainly due to the appearance of cracks. The surface changes observed for plastics after UV-aging was similar to the aged plastics from previous studies (Fan et al., 2021b; Mao et al., 2020). With surface erosion, there are more voids appearing compared to the fresh microplastics.

2.3.2 Adsorption and desorption behavior of bisphenols on microplastics

2.3.2.1 Adsorption ability of commercial microplastics

Data from a preliminary experiment (Figure S1), where several types of commercial plastics were assessed, showed that only a few showed obvious adsorption for bisphenols. This result was different from a previous study on the adsorption behavior of BPA on a range of plastic particles (Liu et al., 2019d). Commercial plastics are composed of resins and a wide range of additives. It is possible that the additives might change the structure or properties of polymers which would lead to different adsorption behavior. Moreover, the particle size might also be an important factor affecting the adsorption behavior. The size of plastic pieces used in this study are much larger than those used in the previous study (nano-level particles), which owing to the decrease specific surface area and less adsorption sites, leading to lower adsorption capacity (Liu et al., 2019d).

It is noticeable that although two types of PS plastics were firstly selected for the preliminary study, only the expanded polystyrene (EPS) showed adsorption affinity for bisphenols. It was also found that the weight of EPS increased 3.6 times (increased from 60 mg to 216 mg) after being soaked in water for 5 minutes. This effect was not observed for the other plastics which showed no weight changes. The strong water retention capacity by EPS was also observed in a previous study on the adsorption of a lipophilic toxin (Costa et al., 2020). The high-water retention ability of plastics could increase their external surface contact area with contaminants, which would improve the adsorption process and result in potential adsorption for bisphenols.

2.3.2.2 Adsorption kinetics of bisphenols on microplastics

The adsorption kinetics for BPA, BPF, BPB and BPAP in fresh and aged microplastics are given in Figure 3. Fresh EPS plastics didn't show obviously adsorption ability for BPF and BPA in the multi-solute system, which was likely to be related to the competitive adsorption behavior. This demonstrated that adsorption is improved in a single solution system rather than a multi-system for EPS plastics (Figure S5). Previous studies have suggested that the uptake of hydrophobic organic compounds on plastics are expected to be competitive (Bakir et al., 2012). Chemicals with similar structures show strong competition, which illustrates the adsorption for compounds are selective (Pignatello, 1998).
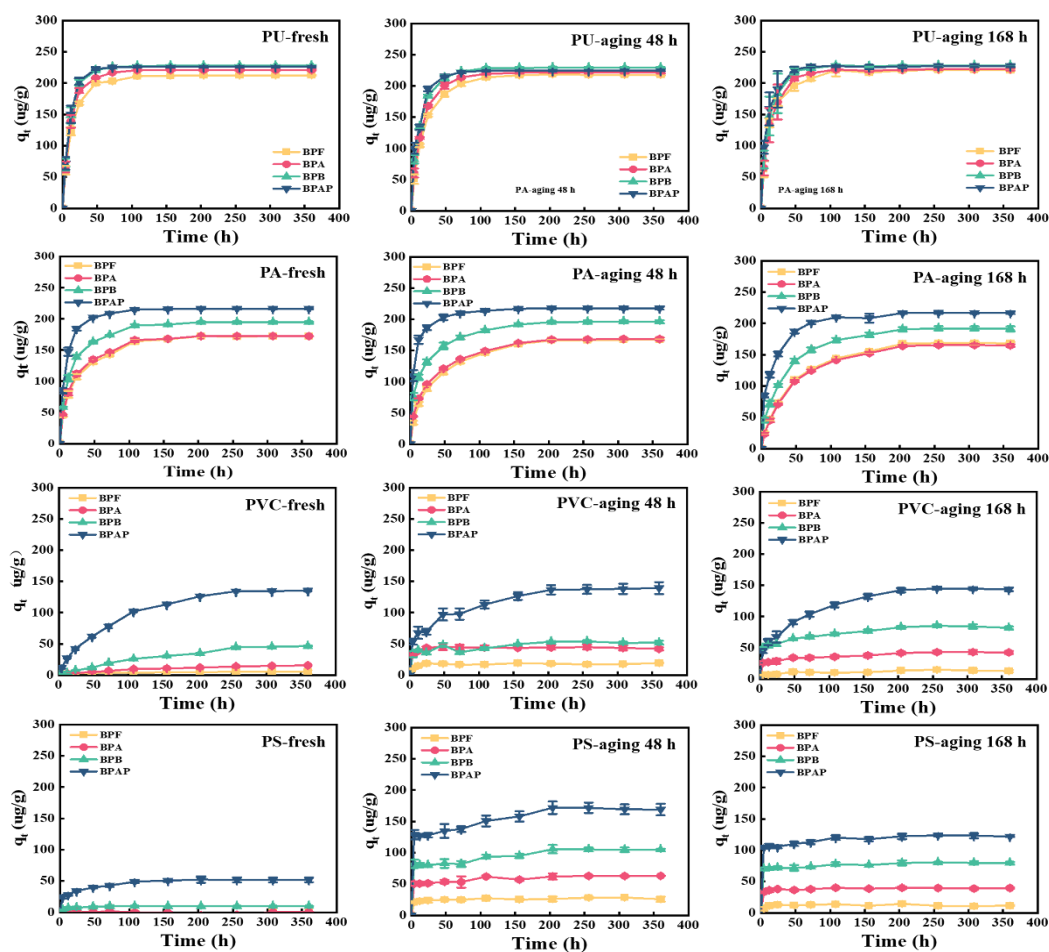
Figure 3. Adsorption kinetics of BPF, BPA, BPB and BPAP on fresh and aged microplastics. Error bars are the means ± standard deviation (SD) of three repeats. (60 mg microplastics, 15 mL 1 mg/L bisphenols, 25 °C, 180 rpm).

The adsorption data has been fitted using both the pseudo-first model and pseudo-second models (Figure S6 and Figure S7), the fitting parameters are shown in Table S4. The kinetics for fresh and aged microplastics were better described by the pseudo-second-order model (R^2 range from 0.979 to 0.999) except for fresh PVC microplastics, suggesting that chemical adsorption was likely to be the dominant factor for the adsorption process of bisphenols onto microplastics. Whereas, fresh PVC plastics could be better described by the pseudo-first-order model, similar to that in a previous study (Liu et al., 2019b), which indicates the adsorption behavior for fresh PVC microplastics was a single adsorption process and the adsorption capacity limited by the adsorption sites (Zhang et al., 2018).

2.3.2.3 Adsorption mechanism

According to Figure 4, the equilibrium adsorption efficiency of the four bisphenols on PVC microplastics (except aging for 48 h), EPS plastics (except fresh) and PA plastics are positively correlated ($R^2 > 0.9$, $p < 0.05$) with their octanol/water partition coefficients ($\log K_{ow}$), which illustrates that hydrophobicity was an important factor dominating the adsorption behavior for most fresh and aged microplastics.
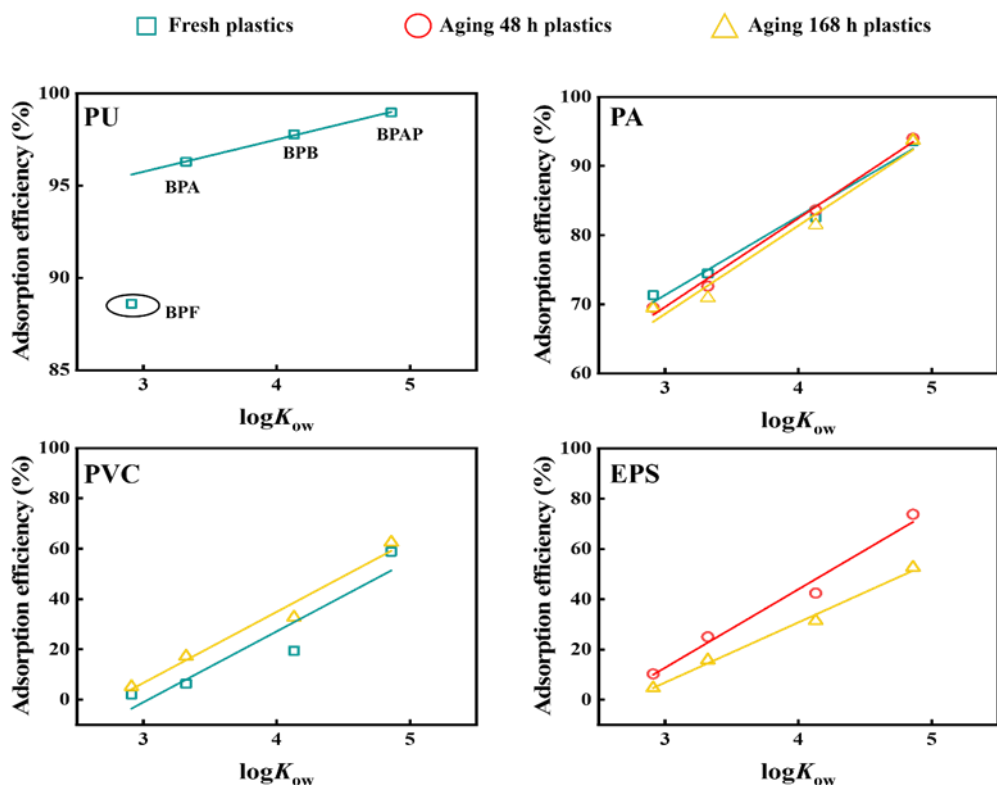
Figure 4. The correlation between $\log K_{ow}$ and adsorption efficiency values for four bisphenols partitioning on fresh and aged microplastics.
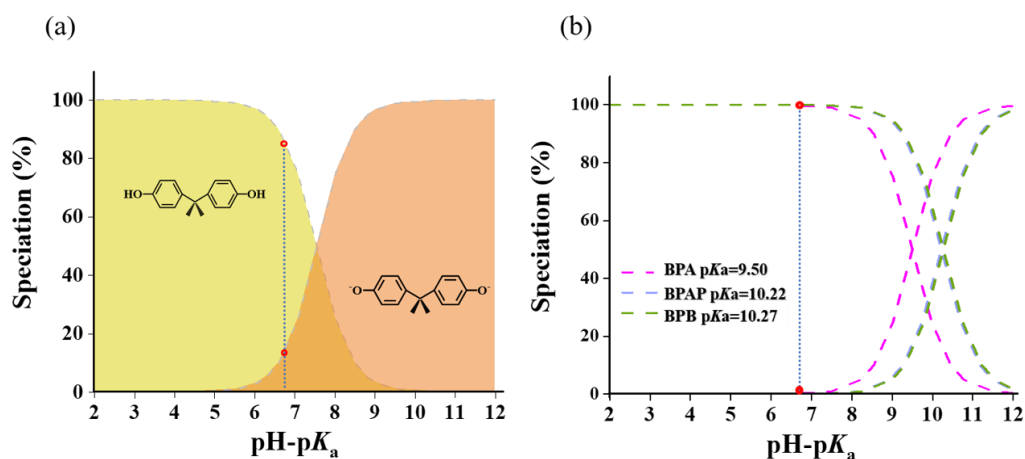

Figure 5. (a) Speciation of BPF at different pH values. (b) Speciation of BPA, BPB and BPAP at different pH values.

For fresh PU plastics (Figure 4), good correlations (R^2=0.999, $p < 0.05$) were evident if the data for BPF were excluded. The $\log K_{ow}$ of BPA (3.32) is only slightly

higher than BPF (2.91), but the adsorption rate of BPA (96.29 %) on fresh PU microplastics was much higher than BPF (88.59 %), which suggested that except for hydrophobicity, there were other factors that affect the uptake behavior of BPF onto PU microplastics. Surface electrostatic interactions might also be an important factor affecting adsorption ability for bisphenols. As illustrated in Figure 5a, BPF was present in both non-ionized form and anionic form at the pH of ultrapure water (6.8). Whereas, BPA, BPB and BPAP were mostly present in the non-ionized form (Figure 5b) as their pK_a values (range from 9.50-10.27) are much higher than BPF (7.55). Moreover, plastics are negatively charged in most water bodies, which indicates that an electrostatic repulsive-force existed between PU microplastic particles and BPF, leading to the reduced adsorption efficiency. Therefore, both hydrophobicity and electrostatic interaction are important factors affect the adsorption behavior of bisphenols on fresh PU microplastics.

2.3.2.4 Adsorption capacity with the aging of microplastics
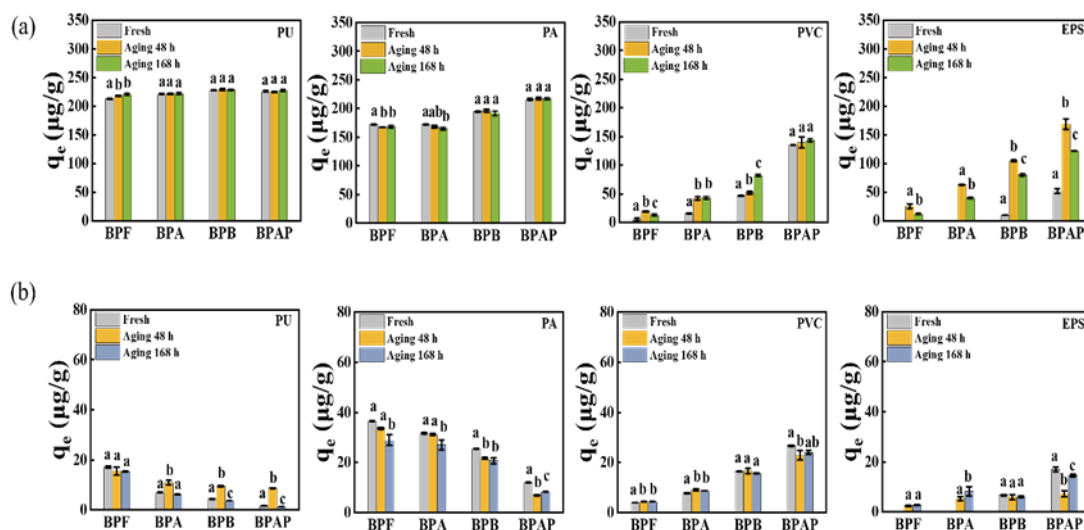
Figure 6. (a) The adsorption capacity of four bisphenols on PU, PA, PVC and EPS microplastics before and after UV- aging. (b) The desorption capacity of four bisphenols on PU, PA, PVC and EPS microplastics before and after UV- aging. Error bars are the means ± standard deviation (SD) of three repeats. (60 mg microplastics, 15 mL 1 mg/L bisphenols, 25 °C, 180 rpm). Values not sharing common letters (a-c) are significantly different from each other ($p < 0.05$).

According to Figure 6a, the adsorption capacity for bisphenols on aged PVC and EPS microplastics are significantly higher ($p < 0.05$) than fresh microplastics, which might be due to the cracks in the plastics offering more available adsorption sites. Moreover, according to the Raman data, the reduction of –Cl for PVC microplastics could increase the free volume, which would further increase the adsorption sites for bisphenols on PVC microplastics after irradiation. For EPS microplastics the abundance of aromatic rings might have reduced with the degree of aging, which could reduce the

π-π interaction with bisphenols (Liu et al., 2020b). As a result, the adsorption amount decreased with the increased aging degree of EPS microplastics. For PA microplastics, the adsorption for BPF and BPA reduced after irradiation, which could be due to the effect of H-bonding interaction. Several studies have demonstrated that the adsorption behavior of polyamide plastics strongly relied on hydrogen boding interaction between the amide group (–CO–NH–) and study chemicals (e.g. sulfamethoxazole, 17β-oestradiol, amoxicillin, tetracycline, etc.) (Guo et al., 2019; Li et al., 2018b; Liu et al., 2019e). As shown in Figure 1, the reduction of amid III (N–H, C–N) would weaken the H-bond interaction and further effect the adsorption ability for bisphenols. Whilst for PU plastics, the adsorption ability for most bisphenols did not change with the aging process, which illustrates that aging had very limited impact for adsorption behavior of bisphenols on PU microplastics.

Table 1. Desorption efficiency (%) of bisphenols on fresh and aged microplastics.

	PU				PA				PVC				EPS			
	BPF	BPA	BPB	BPAP	BPF	BPA	BPB	BPAP	BPF	BPA	BPB	BPAP	BPF	BPA	BPB	BPAP
Fresh	8.1	3.2	2.0	0.7	21.2	18.4	13.1	5.6	77.4	50.5	35.6	19.8	-	-	67.8	32.7
Aging 48 h	7.1	5.0	4.2	3.9	20.2	18.5	11.1	3.2	23.0	21.8	32.1	16.5	9.7	8.2	5.7	4.3
Aging 168 h	7.0	2.8	1.6	0.5	17.2	16.5	10.9	3.8	35.2	20.6	19.3	16.7	24.3	20.9	7.7	12.0

2.3.2.5 Desorption of bisphenols on microplastics with aging

The time needed to reach desorption equilibrium became shorter for most microplastics after irradiation (Figure S8). For example, BPF, BPA need approximately 96 h and BPB, BPAP need 120 h to reach equilibrium on fresh PVC microplastics,

which reduced to around 72 h (BPF, BPA, BPAP) and 48 h (BPB) after aging 168 h (one-way ANOVA analysis, $p > 0.05$). According to the data in Table 1, the desorption efficiency for both fresh and aged microplastics followed the order: BPF> BPA> BPB> BPAP, which is negatively correlated with the hydrophobicity.

For most microplastics, the desorption efficiency decreased after the aging process (Table 1). Due to cracks in the plastics, more bisphenols could diffuse to the inside of the structure (Sun et al., 2021) or the narrow pores of the plastics (Fan et al., 2021a), which suggests it is more difficult for aged microplastics to release bisphenols compared with those bisphenols sorbed on the surface of fresh plastics. As a result, the lower desorption efficiency was expected after aging. Although the desorption efficiency of BPF and BPA on PVC microplastics decreased sharply after irradiation, the desorption capacity showed an increasing trend owing to the increased uptake ability for PVC plastics after aging (Figure 6b). For example, the desorption efficiency of BPA on PVC microplastics decreased from 50.5 % to 21.8 % after aging 48 h, whereas the desorption capacity increased from 7.8 μg/g to 9.2 μg/g. As a result, the aging of microplastics might suggest that greater pollutant loadings could be released to the environment.

2.3.3 Effects of environmental factors

2.3.3.1 Water matrix

The pH value (8.2) of artificial seawater suggests that BPF was mostly present in the anionic form, and BPA, BPB, BPAP also showed the anion potential, so the

repulsive-force between bisphenols and microplastics would be increased compared with ultrapure water (Figure 5), which should lead to the decreased adsorption capacity of bisphenols on microplastics. However, the adsorption capacity of BPF and other bisphenols increased for most fresh and aged microplastics in seawater (Figure 7a), which might be due to the salting-out effect. The salting-out effect would reduce the solubility of bisphenols in seawater (non-polar organic compounds), which would enhance the hydrophobic interactions between plastics and bisphenols, leading to the increased adsorption capacity of bisphenols to plastics (Liu et al., 2019a; Xiong et al., 2020).
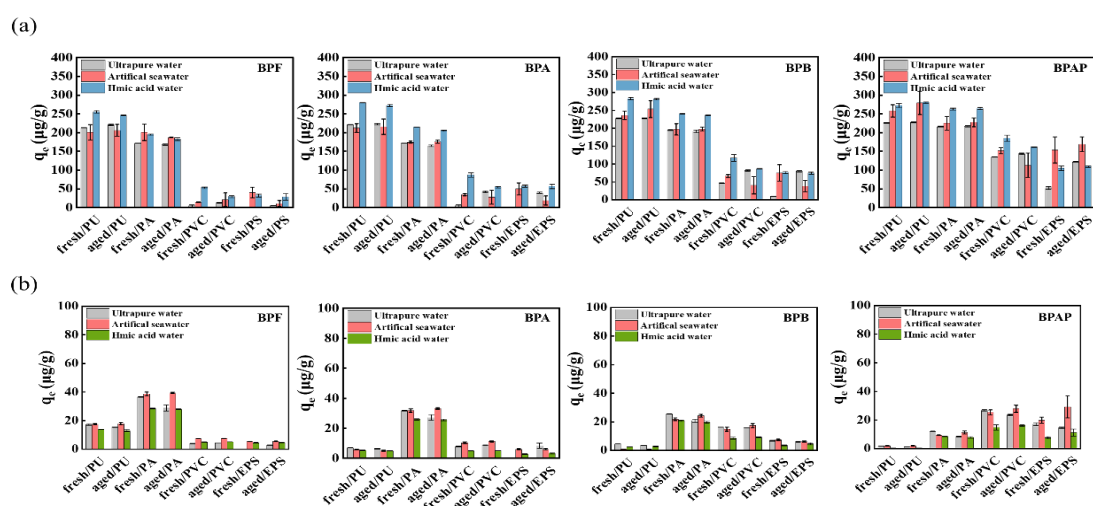
Figure 7. (a) The effect of water matrix on the adsorption of bisphenols on fresh and aged 168 h microplastics. (b) The effect of water bodies on the desorption of bisphenols on fresh and aged 168 h microplastics (n=3, 60 mg microplastics, 25 °C, 180 rpm).

HA is the main component of natural dissolved organic matter (DOM) (Xiong et al., 2020), and is composed of carboxyl-substituted benzene rings, hydroxy-substituted benzene rings, carbonyl-substituted benzene rings, etc. Carboxyl-substituted benzene

rings act as electron acceptors which could bind through n-π interaction with carbonyl groups of amides (Lara et al., 2021). In addition to that, the aromatic structure of DOM could interact with EPS polymers via π-π interaction resulting in a highly conjugated structure (Chen et al., 2018). HA could also bond with bisphenols by π-π interaction and H-bond interaction (Lara et al., 2021). As a result, HA can act as a bridge between bisphenols and plastics (Figure S9), leading to higher adsorption capacity of bisphenols on microplastics (Tourinho et al., 2019). Moreover, the introduction of HA makes the solution weakly acidic (pH=6.5) and reduces the anionic form of BPF (Figure 5a), which could reduce the repulsive force and also result in the enhanced adsorption capacity compared with in ultrapure water.

The adsorption capacity for fresh and aged microplastics showed no significant difference (T-test, $p > 0.05$) in seawater. Whilst the sorption capacity of bisphenols on most aged microplastics decreased compared with fresh plastics in HA water (T-test, $p < 0.05$). This might be due to the reduction of functional groups impacting the interaction behavior between plastics and bisphenols/HA after irradiation. For example, the reduction of amide I (C=O) and amide III (–NH–, –CN–) after aging (Figure 1) would weaken the bonding of microplastics with HA (n-π interaction) and bisphenols (H-bonding interaction), which could further reduce the adsorption of bisphenols on aged microplastics. According to the data in Table S5 and Table S6, hydrophobicity still dominated the sorption behavior of most fresh and aged microplastics in both seawater and HA water.

According to Figure 7b, the desorption capacities for most bisphenols were relatively high in seawater, which might exert potential risks to aquatic ecosystems since the desorbed contaminants could re-enter the seawater, sediments, or even organisms (Lu et al., 2020). The desorption capacity in HA water is low, which might be due to the strong affinity of HA towards pollutants (Lian et al., 2015), resulting in lower release of bisphenols to water bodies.

2.3.3.2 Temperature effect
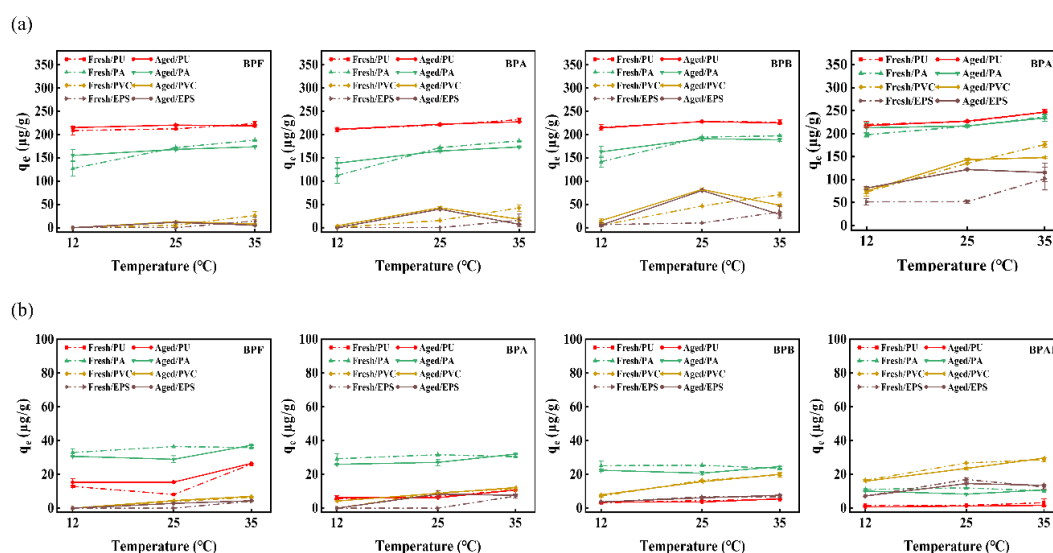
Figure 8. (a) The relationship between temperature and the adsorption behavior of bisphenols on plastics. (b) The relationship between temperature and the desorption of bisphenols (n=3, 60 mg microplastics, 15 mL ultrapure water, 180 rpm).

The sorption capacity for most fresh and aged microplastics (Figure 8a) was enhanced with increased temperature (one-way ANOVA analysis, $p < 0.05$), while for aged PVC and EPS microplastics, the sorption capacity for most bisphenols increased at first and then decreased when the temperature was higher than 25 °C, which might be due to the simultaneous desorption behavior (Dong et al., 2019; Zhang et al., 2018).

In addition, increased temperature could increase the mobility of molecules, reducing the bonding between chemicals and plastics (Xu et al., 2019). For both fresh and aged microplastics, the desorption capacity increased with increased temperature (Figure 8b), which indicates the potential for considerable transfer of bisphenols adsorbed to plastics in warmer regions.

2.4 Conclusions

In this study, the adsorption/desorption behavior of bisphenols on microplastics were investigated, with special emphasis on the influence of irradiation/aging and a range of environmental factors. After irradiation, adsorption capacity increased for PVC and EPS microplastics, whilst the desorption efficiency showed a decreasing trend after irradiation. Environmental factors had significant effects on the interaction behavior between bisphenols and microplastics. The adsorption capacity was higher for most microplastics under artificial seawater and humic acid water compared to ultrapure water. For both fresh and aged microplastics, desorption quantity increased in artificial seawater and enhanced temperature, which indicates a potential exposure risk of plastics in the natural environment.
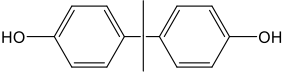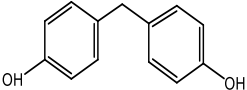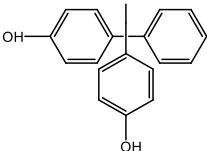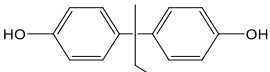
Supporting information

M1: Calculation equation for the simulate exposure days

The mean UV-irradiance in Europe is approximate 60 kWh/ (m^2/year), the equation to

calculate the simulate days is

$$\text{Simulated day} = \frac{\text{Total irradiance expose in exp } (0.5 \text{ kW/m}^2 \times \text{expose hours})}{\text{Mean UV irradiance in Europe } (60 \text{ kW h/ } (\text{m}^2/\text{year}))} \times 365$$

Expose hours	Total irradiance	Simulated exposure days under European mean irradiance
48 h	24 kWh/m^2	146
168 h	84 kWh/m^2	511

Table S1. Properties and structures of bisphenols used in this study

Chemicals	Molecular formula	Structure	Molecular weight	logK_{ow}	pK_a
BPA	$C_{15}H_{16}O_2$		228.29	3.32	9.50±0.1
BPF	$C_{13}H_{12}O_2$		200.23	2.91	7.55±0.1
BPAP	$C_{20}H_{18}O_2$		290.36	4.86	10.22±0.1
BPB	$C_{16}H_{18}O_2$		242.31	4.13	10.27±0.1

LogK_{ow} is calculated by Estimation Program Interface (EPI)

http://www.epa.gov/oppt/exposure/pubs/episuite.htm

Table S2. Details of collected plastic samples

Plastic polymer	Type	Category
PE	Storage boxes (HDPE)	General
	Garbage bags (LDPE)	General
PP	Straws	Food
	Sauce boxes	Food
	Milk boxes	Food
PS	Spoons (non-expanded polystyrene)	Food
	Disposable fast-food boxes (EPS)	Food
PVC	Table mats	General
PA	High-pressure pipes (PA 6)	General
PET	Water bottles	Food
PU	Sheets	General

Table S3. The parameters of HPLC for detecting four bisphenols

Injection volume (μL)	Flow rate (mL/min)	Tray temperature (°C)	Excitation wavelength (nm)	Emission wavelength (nm)
20	0.5 mL/min	30	226 nm	315 nm

Table S4. Kinetics parameters of bisphenols on fresh and aged microplastics

Types		q_e* (μg/g)	pseudo-first order parameters			pseudo-second order parameters		
			q_e (μg/g)	k_1 (/h)	R^2	q_e (μg/g)	k_2 (μg/(g.h))	R^2
Fresh PU	BPF	212.55	72.7	2.41×10^{-2}	0.877	205.34	1.86×10^{-3}	**0.988**

88

	BPA	221.07	59.22	2.39×10^{-2}	0.877	224.72	1.04×10^{-3}	**0.999**
	BPB	227.94	50.72	2.73×10^{-2}	0.901	230.95	1.18×10^{-3}	**0.999**
	BPAP	226.09	20.91	2.90×10^{-2}	0.698	228.83	1.36×10^{-3}	**0.999**
	BPF	217.77	83.90	1.63×10^{-2}	0.863	226.24	4.25×10^{-4}	**0.999**
	BPA	221.38	69.71	1.93×10^{-2}	0.861	227.79	5.74×10^{-4}	**0.999**
Aging 48 h	BPB	229.06	61.24	2.25×10^{-2}	0.867	233.64	7.76×10^{-4}	**0.999**
	BPAP	224.68	57.56	2.71×10^{-2}	0.877	228.31	1.08×10^{-3}	**0.999**
	BPF	220.65	70.70	2.15×10^{-2}	0.720	226.76	5.83×10^{-4}	**0.999**
	BPA	222.21	68.03	2.27×10^{-2}	0.778	228.31	6.24×10^{-4}	**0.999**
Aging 168 h	BPB	228.23	50.83	2.49×10^{-3}	0.780	233.10	7.90×10^{-4}	**0.999**
	BPAP	227.36	36.05	1.89×10^{-2}	0.721	230.41	1.13×10^{-3}	**0.999**
	BPF	172.21	141.06	2.39×10^{-2}	0.967	171.82	5.24×10^{-4}	**0.984**
	BPA	172.12	108.69	2.16×10^{-2}	0.898	178.57	5.16×10^{-4}	**0.998**
Fresh PA	BPB	194.61	116.19	9.9258	0.882	200	6.51×10^{-4}	**0.999**
	BPAP	216.22	60.87	3.13×10^{-2}	0.907	219.30	1.23×10^{-3}	**0.999**
	BPF	167.26	189.93	2.56×10^{-2}	0.947	179.53	2.52×10^{-4}	**0.999**
	BPA	168.44	123.63	1.87×10^{-2}	0.980	178.57	3.04×10^{-4}	**0.999**
Aging 48 h	BPB	196.34	112.95	1.93×10^{-2}	0.975	203.67	4.37×10^{-4}	**0.999**
	BPAP	217.76	66.80	2.53×10^{-2}	0.902	220.75	1.21×10^{-3}	**0.999**
	BPF	168.25	170.90	2.15×10^{-2}	0.923	186.57	1.67×10^{-4}	**0.998**
	BPA	164.69	156.44	2.27×10^{-2}	0.697	183.15	1.67×10^{-4}	**0.998**
Aging 168 h	BPB	191.32	137.17	1.80×10^{-2}	0.944	204.50	2.44×10^{-4}	**0.999**
	BPAP	216.78	96.84	1.84×10^{-2}	0.914	223.21	5.08×10^{-4}	**0.999**

	BPF	5.09	3.57	9.01×10^{-3}	**0.934**	3.54	-1.16	0.566
	BPA	15.50	15.91	8.84×10^{-3}	**0.973**	21.94	2.70×10^{-4}	0.374
Fresh PVC	BPB	46.40	46.40	1.14×10^{-2}	**0.919**	154.80	9.26×10^{-6}	0.087
	BPAP	135.32	135.32	1.23×10^{-2}	**0.981**	154.80	1.25×10^{-4}	0.976
	BPF	19.26	3.20	5.28×10^{-3}	0.145	18.36	1.34×10^{-2}	**0.993**
	BPA	42.06	5.59	4.70×10^{-3}	0.244	42.81	1.59×10^{-2}	**0.998**
Aging 48 h	BPB	51.89	19.66	8.45×10^{-3}	0.632	53.94	1.50×10^{-3}	**0.992**
	BPAP	139.34	104.05	1.50×10^{-2}	0.975	147.28	2.98×10^{-4}	**0.995**
	BPF	12.73	7.70	5.20×10^{-3}	0.698	13.78	4.05×10^{-3}	**0.979**
	BPA	42.66	24.14	1.38×10^{-2}	0.855	44.19	1.57×10^{-3}	**0.996**
Aging 168 h	BPB	82.02	38.33	9.72×10^{-3}	0.845	86.13	9.35×10^{-4}	**0.997**
	BPAP	143.42	109.77	1.47×10^{-2}	0.922	155.76	2.46×10^{-4}	**0.996**
	BPB	9.92	3.74	1.40×10^{-2}	0.877	10.05	1.46×10^{-2}	**0.999**
Fresh EPS	BPAP	51.94	25.33	1.38×10^{-2}	0.910	53.22	1.97×10^{-3}	**0.998**
	BPF	25.65	6.54	6.49×10^{-3}	0.383	26.69	1.47×10^{-2}	**0.992**
	BPA	62.96	21.92	1.65×10^{-2}	0.833	63.90	1.56×10^{-2}	**0.998**
Aging 48 h	BPB	104.99	44.08	1.31×10^{-2}	0.881	107.87	8.34×10^{-4}	**0.996**
	BPAP	168.94	66.15	1.19×10^{-2}	0.732	173.91	5.80×10^{-4}	**0.997**
	BPF	11.56	2.92	7.68×10^{-4}	0.011	11.21	1.74×10^{-2}	**0.984**
	BPA	39.56	5.63	9.19×10^{-3}	0.518	39.48	1.52×10^{-2}	**0.999**
Aging 168 h	BPB	79.74	15.05	9.51×10^{-3}	0.758	80.58	1.24×10^{-2}	**0.999**
	BPAP	121.86	25.14	1.05×10^{-2}	0.748	123.92	2.06×10^{-3}	**0.999**

**Table S5.** Correlations between $\log K_{ow}$ of bisphenols and the adsorption efficiency under seawater

	PU		PA		PVC		EPS	
	F/SW	A/SW	F/SW	A/SW	F/SW	A/SW	F/SW	A/SW
Pearson Correlation coefficient	0.538	0.855	0.989	0.984	0.977	0.918	0.964	0.899
P value (2-tailed)	0.462	0.145	0.011*	0.016*	0.023*	0.082	0.036*	0.101

F/SW and A/SW represent fresh plastics/seawater and aged plastics/seawater

Table S6. Correlations between $\log K_{ow}$ of bisphenols and the adsorption efficiency under seawater

	PU		PA		PVC		EPS	
	F/HAW	A/HAW	F/HAW	A/HAW	F/HAW	A/HAW	F/HAW	A/HAW
Pearson Correlation coefficient	0.895	0.911	0.989	0.995	0.979	0.975	0.988	0.983
P value (2-tailed)	0.105	0.089	0.011*	0.005*	0.025*	0.025**	0.012*	0.017*

F/HAW and A/HAW represent fresh plastics/humic acid water and aged plastics/humic acid water.
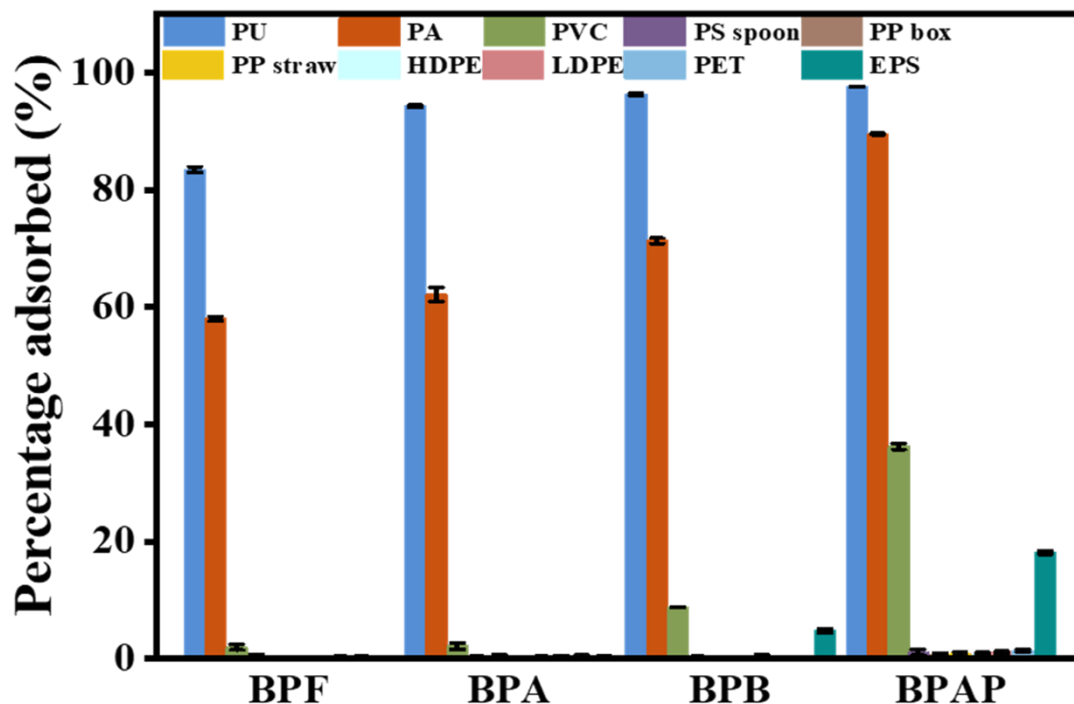
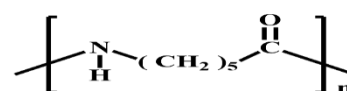**Figure S1.** The preliminary experiment for the adsorption ability of BPF, BPA, BPB and BPAP onto different commercial microplastics (n=2). Experimental conditions: mass of microplastics=60 mg, initial concentration: 1mg/L temperature=25 °C, shaker speed=180 rpm, contact time=72 h.
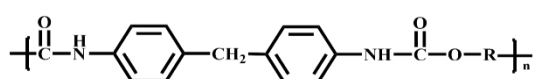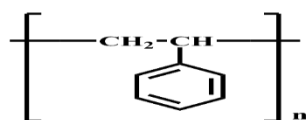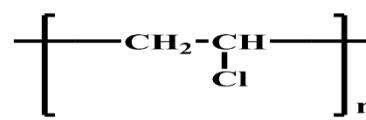
Figure S2. The structures and types of polyurethane (PU), polyamide (PA), polystyrene (PS) and polyevinyl chloride (PVC).
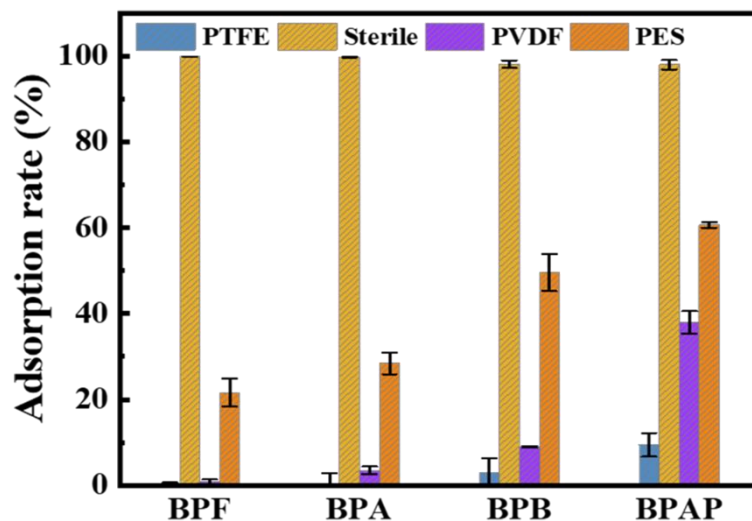
Figure S3. Adsorption (%) of PTFE, Sterile, PVDF and PES filter membranes for four

bisphenols.Error bars were calculated from the SD of two replciates.
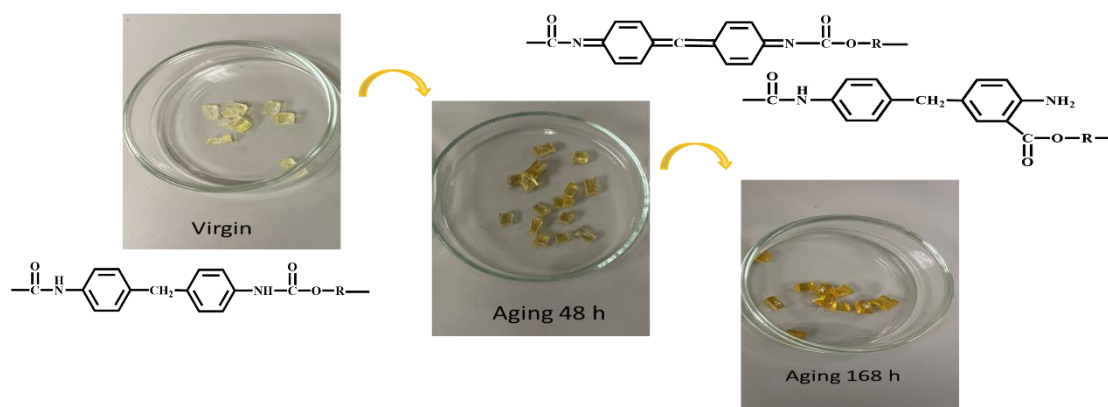
Figure S4.   Changes of PU microplastics after irradiating 48 h and 168 h.
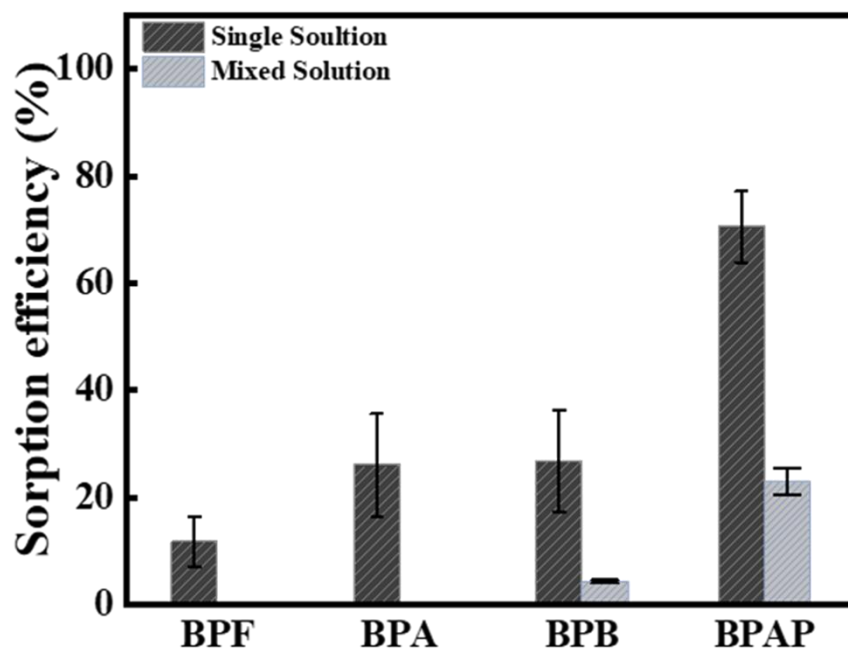
Figure S5. The competitive adsorption of bisphenols on fresh EPS microplastics. The experiment was implemented by 60 mg microplastic pieces into 15 mL 1 mg/L single and mixed bisphenol solution at 25 ℃, 180 rpm for 360 h.
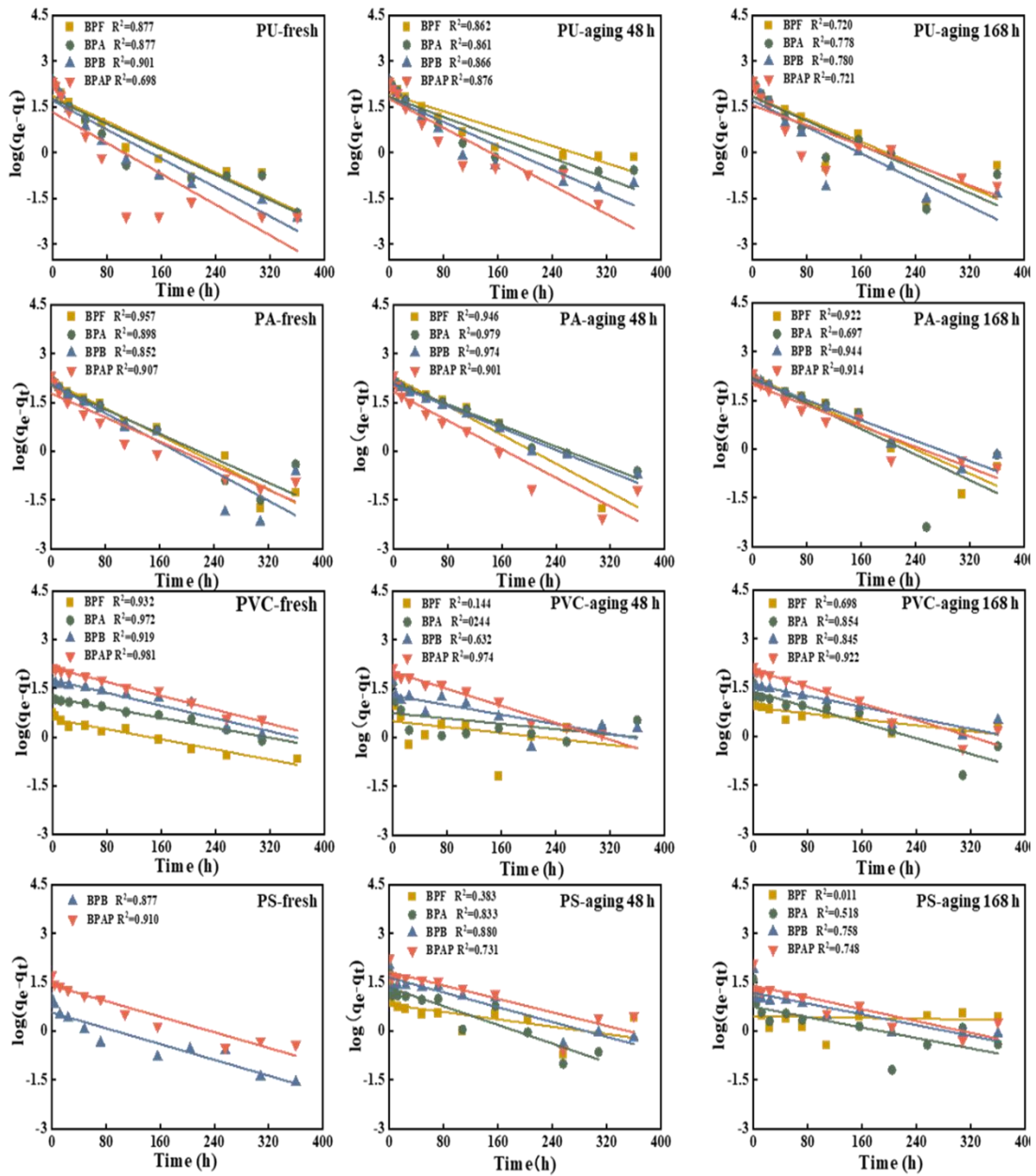
Figure S6. Pseudo-first-order model of fresh and aged microplastics.
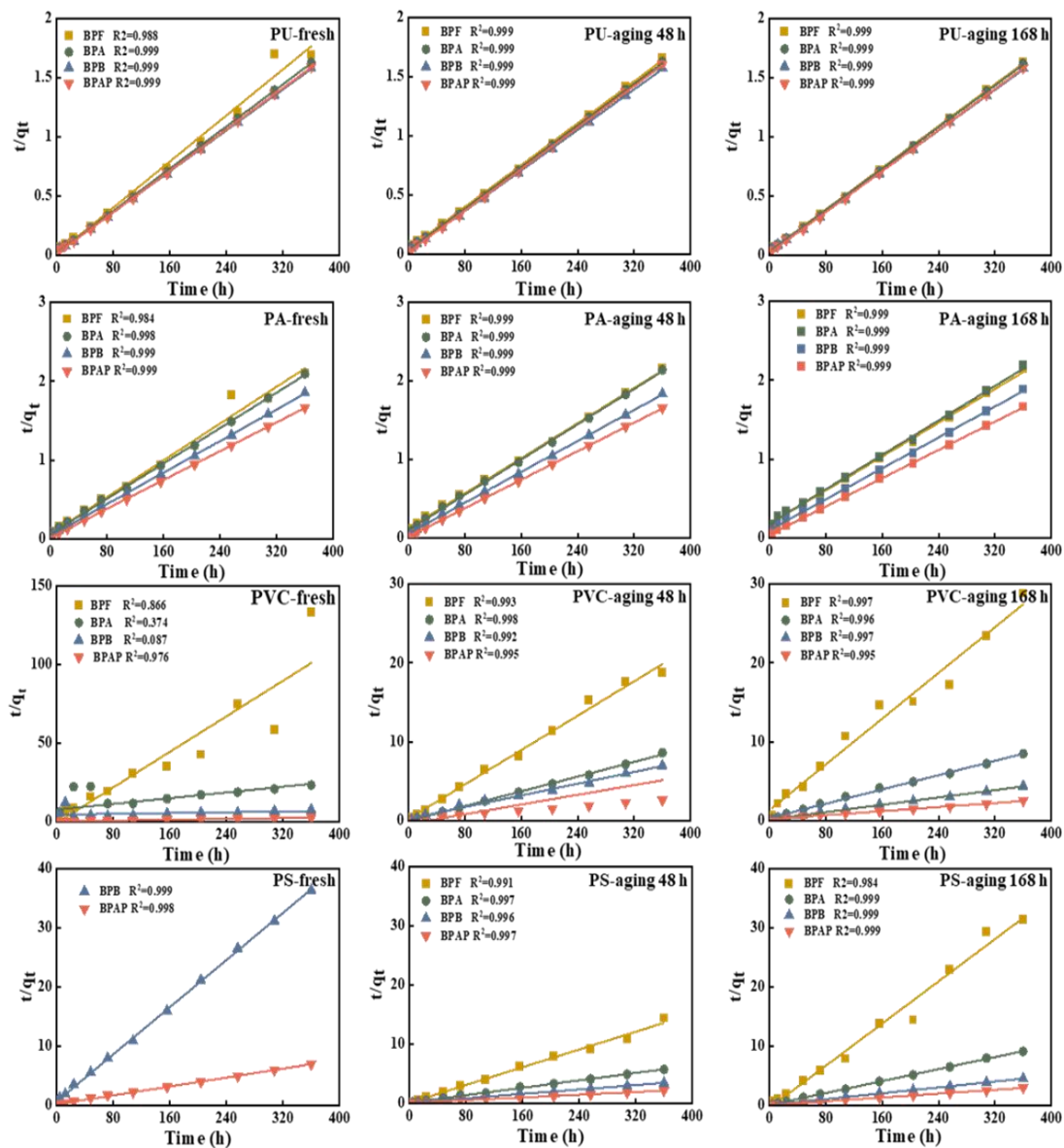
Figure S7. Pseudo-second-order model of fresh and aged microplastics.
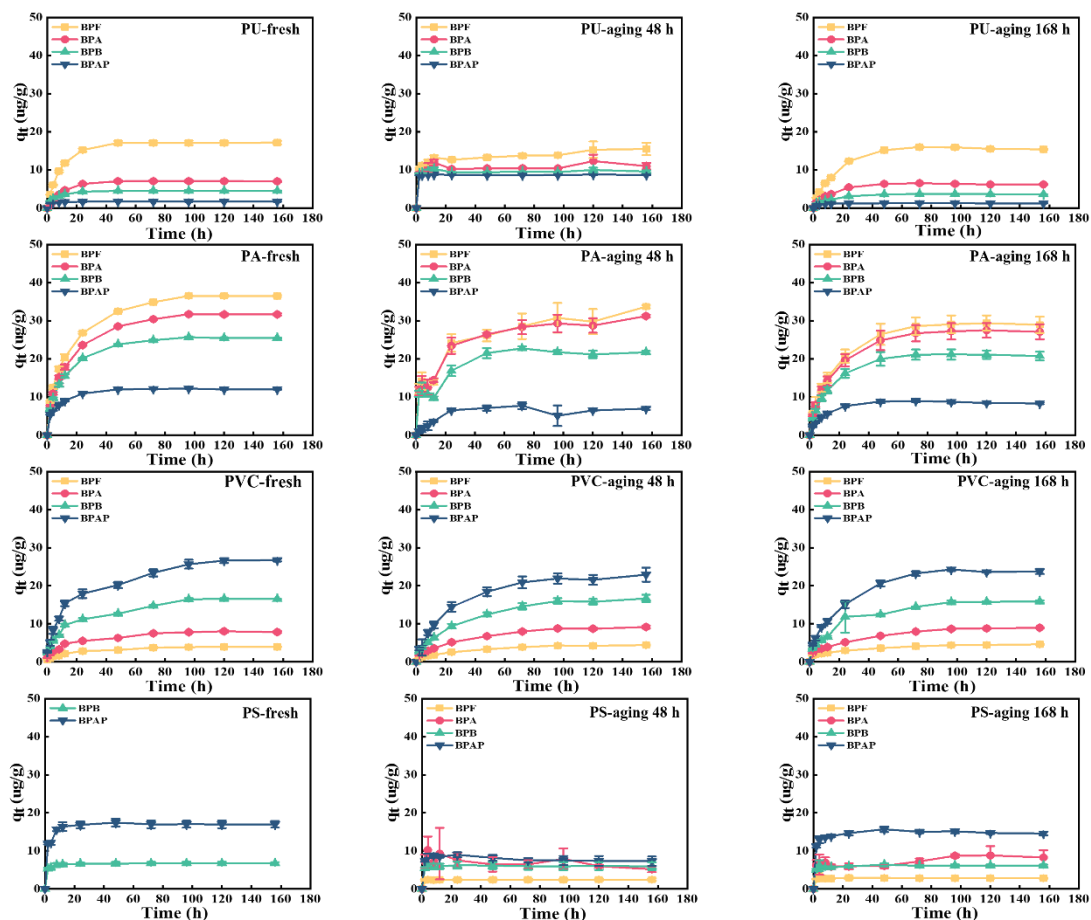
Figure S8. Desorption kinetics of BPF, BPA, BPB and BPAP on fresh and aged microplastics. Error bars are the means ± standard deviation (SD) of three repeats. (60 mg microplastics, 15 mL ultrapure water, 25 °C, 180 rpm).
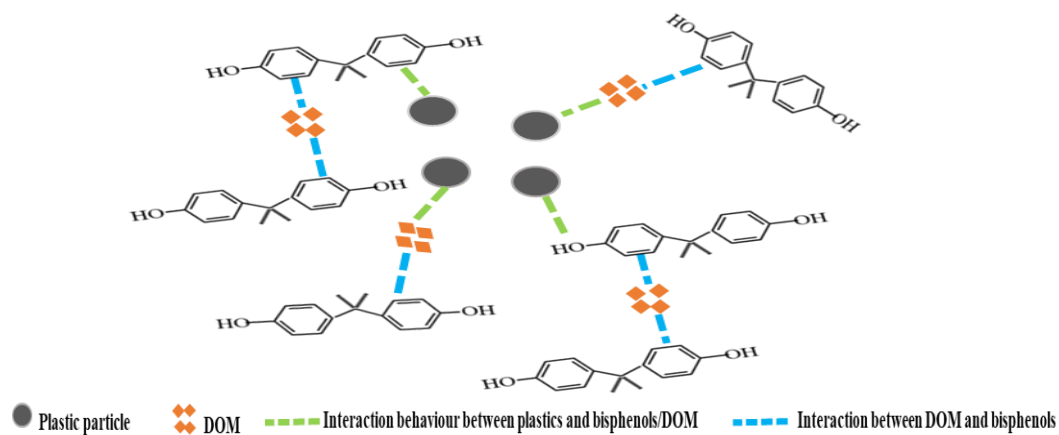
Figure S9. Effects of HA (DOM) for the sorption of bisphenols on plastic particles.

References

Bakir, A., Rowland, S.J., Thompson, R.C., 2012. Competitive sorption of persistent organic pollutants onto microplastics in the marine environment. Marine Pollution Bulletin 64, 2782-2789.

Barboza, L.G.A., Cunha, S.C., Monteiro, C., Fernandes, J.O., Guilhermino, L., 2020. Bisphenol A and its analogs in muscle and liver of fish from the North East Atlantic Ocean in relation to microplastic contamination. Exposure and risk to human consumers. J. Hazard. Mater. 393.

Bruckmoser, K., Resch, K., 2014. Investigation of Ageing Mechanisms in Thermoplastic Polyurethanes by Means of IR and Raman Spectroscopy. Macromolecular Symposia 339, 70-83.

Chen, D., Kannan, K., Tan, H., Zheng, Z., Feng, Y.L., Wu, Y., Widelka, M., 2016. Bisphenol Analogues Other Than BPA: Environmental Occurrence, Human Exposure, and Toxicity-A Review. Environmental Science & Technology 50, 5438-5453.

Chen, W., Ouyang, Z.-Y., Qian, C., Yu, H.-Q., 2018. Induced structural changes of humic acid by exposure of polystyrene microplastics: A spectroscopic insight. Environmental Pollution 233, 1-7.

Costa, S.T., Rudnitskaya, A., Vale, C., Guilhermino, L., Botelho, M.J., 2020. Sorption of okadaic acid lipophilic toxin onto plastics in seawater. Marine Pollution Bulletin 157.

Dong, X., Zheng, M., Qu, L., Shi, L., Wang, L., Zhang, Y., Liu, X., Qiu, Y., Zhu, H., 2019. Sorption of Tonalide, Musk Xylene, Galaxolide, and Musk Ketone by microplastics of polyethylene and polyvinyl chloride. Marine Pollution Bulletin 144, 129-133.

Fan, X., Gan, R., Liu, J., Xie, Y., Xu, D., Xiang, Y., Su, J., Teng, Z., Hou, J., 2021a. Adsorption and desorption behaviors of antibiotics by tire wear particles and polyethylene microplastics with or without aging processes. Science of the Total Environment 771, 145451.

Fan, X., Zou, Y., Geng, N., Liu, J., Hou, J., Li, D., Yang, C., Li, Y., 2021b. Investigation on the adsorption and desorption behaviors of antibiotics by degradable MPs with or without UV ageing process. J. Hazard. Mater. 401, 123363.

Gewert, B., Plassmann, M., Sandblom, O., MacLeod, M., 2018. Identification of Chain Scission Products Released to Water by Plastic Exposed to Ultraviolet Light. Environ. Sci. Technol. Lett. 5, 272-276.

Guo, X., Chen, C., Wang, J., 2019. Sorption of sulfamethoxazole onto six types of microplastics. Chemosphere 228, 300-308.

Hahladakis, J.N., Velis, C.A., Weber, R., Iacovidoua, E., Purnell, P., 2015. An overview of chemical additives present in plastics: Migration,release, fate and environmental impact during their use, disposal and recycling. J. Hazard. Mater. 344, 179-199.

Hamlin, H.J., Marciano, K., Downs, C.A., 2015. Migration of nonylphenol from food-grade plastic is toxic to the coral reef fish species Pseudochromis fridmani. Chemosphere 139, 223-228.

Kappler, A., Fischer, D., Oberbeckmann, S., Schernewski, G., Labrenz, M., Eichhorn, K.J., Voit, B., 2016. Analysis of environmental microplastics by vibrational microspectroscopy: FTIR, Raman or both? Anal Bioanal Chem 408, 8377-8391.

Lara, L.Z., Bertoldi, C., Alves, N.M., Fernandes, A.N., 2021. Sorption of endocrine disrupting compounds onto polyamide microplastics under different environmental conditions: Behaviour and mechanism. Science of the Total Environment 796, 148983.

Li, J., Liu, H., Chen, J.P., 2018a. Microplastics in freshwater systems: A review on occurrence, environmental effects, and methods for microplastics detection. Water Research 137, 362-374.

Li, J., Zhang, K., Zhang, H., 2018b. Adsorption of antibiotics on microplastics. Environmental Pollution 237, 460-467.

Lian, F., Sun, B., Chen, X., Zhu, L., Liu, Z., Xing, B., 2015. Effect of humic acid (HA) on sulfonamide sorption by biochars. Environmental Pollution 204, 306-312.

Liang, Y., Tan, Q., Song, Q., Li, J., 2021. An analysis of the plastic waste trade and management in Asia. Waste Management 119, 242-253.

Liu, F.-f., Liu, G.-z., Zhu, Z.-l., Wang, S.-c., Zhao, F.-f., 2019a. Interactions between microplastics and phthalate esters as affected by microplastics characteristics and solution chemistry. Chemosphere 214, 688-694.

Liu, G., Zhu, Z., Yang, Y., Sun, Y., Yu, F., Ma, J., 2019b. Sorption behavior and mechanism of hydrophilic organic chemicals to virgin and aged microplastics in freshwater and seawater. Environmental Pollution 246, 26-33.

Liu, P., Lu, K., Li, J., Wu, X., Qian, L., Wang, M., Gao, S., 2020. Effect of aging on adsorption behavior of polystyrene microplastics for pharmaceuticals: Adsorption mechanism and role of aging intermediates. Journal of Hazardous Materials 384.

Liu, X., Shi, H., Xie, B., Dionysiou, D., Zhao, Y., 2019c. Microplastics as Both a Sink and a Source of Bisphenol A in the Marine Environment. Environ. Sci. Technol. 53, 10188-10196.

Liu, X., Xu, J., Zhao, Y., Shi, H., Huang, C.-H., 2019d. Hydrophobic sorption behaviors of 17 beta-Estradiol on environmental microplastics. Chemosphere 226, 726-735.

Lu, J., Wu, J., Wu, J., Zhang, C., Luo, Y., 2020. Adsorption and Desorption of Steroid Hormones by Microplastics in Seawater. Bulletin of environmental contamination and toxicology 107, 730–735.

Luo, H., Liu, C., He, D., Xu, J., Sun, J., Li, J., Pan, X., 2022. Environmental behaviors of microplastics in aquatic systems: A systematic review on degradation, adsorption, toxicity and biofilm under aging conditions. Journal of Hazardous Materials 423, 126915.

Mao, R., Lang, M., Yu, X., Wu, R., Yang, X., Guo, X., 2020. Aging mechanism of microplastics with UV irradiation and its effects on the adsorption of heavy metals. Journal of Hazardous Materials 393.

Naveira, C., Rodrigues, N., Santos, F.S., Santos, L.N., Neves, R.A.F., 2021. Acute toxicity of Bisphenol A (BPA) to tropical marine and estuarine species from different trophic groups. Environmental Pollution 268, 115911.

Pignatello, J.J., 1998. Soil organic matter as a nanoporous sorbent of organic pollutants. Advances in Colloid and Interface Science, 445-467.

Rosu, D., Rosu, L., Cascaval, C.N., 2009. IR-change and yellowing of polyurethane as a result of UV irradiation. Polym. Degrad. Stab. 94, 591-596.

Sait, S.T.L., Sorensen, L., Kubowicz, S., Vike-Jonas, K., Gonzalez, S.V., Asimakopoulos, A.G., Booth, A.M., 2021. Microplastic fibres from synthetic textiles: Environmental degradation and additive chemical content. Environmental Pollution 268.

Singla, M., Diaz, J., Broto-Puig, F., Borros, S., 2020. Sorption and release process of polybrominated diphenyl ethers (PBDEs) from different composition microplastics in aqueous medium: Solubility parameter approach. Environmental Pollution 262.

Suhrhoff, T.J., Scholz-Böttcher, B.M., 2015. Qualitative impact of salinity, UV radiation and turbulence on leaching of organic plastic additives from four common plastics — A lab experiment. Marine Pollution Bulletin 102, 84-94.

Sun, P., Liu, X., Zhang, M., Li, Z., Cao, C., Shi, H., Yang, Y., Zhao, Y., 2021. Sorption and leaching behaviors between aged MPs and BPA in water: the role of BPA binding modes within plastic matrix. Water Research 195, 116956.

Tourinho, P.S., Koci, V., Loureiro, S., van Gestel, C.A.M., 2019. Partitioning of chemical contaminants to microplastics: Sorption mechanisms, environmental distribution and effects on toxicity and bioaccumulation. Environmental Pollution 252, 1246-1256.

Uematsu, H., Kawasaki, T., Koizumi, K., Yamaguchi, A., Sugihara, S., Yamane, M., Kawabe, K., Ozaki, Y., Tanoue, S., 2021. Relationship between crystalline structure of polyamide 6 within carbon fibers and their mechanical properties studied using Micro-Raman spectroscopy. Polymer 223.

Wang, Q., Bai, J., Ning, B., Fan, L., Sun, T., Fang, Y., Wu, J., Li, S., Duan, C., Zhang, Y., Liang, J., Gao, Z., 2020. Effects of bisphenol A and nanoscale and microscale polystyrene plastic exposure on particle uptake and toxicity in human Caco-2cells. Chemosphere 254, 126788-126788.

Wang, Q., Zhang, Y., Feng, Q., Hu, G., Gao, Z., Meng, Q., Zhu, X., 2022. Occurrence, distribution, and risk assessment of bisphenol analogues in Luoma Lake and its inflow rivers in Jiangsu Province, China. Environmental Science and Pollution Research 29, 1430-1445.

Wright, S.L., Kelly, F.J., 2017. Plastic and human health: a micro issue? Environmental Science & Technology 51, 6634-6647.

Wu, N.C., Seebacher, F., 2020. Effect of the plastic pollutant bisphenol A on the biology of aquatic organisms: A meta-analysis. Global Change Biology 26, 3821-3833.

Wu, P., Cai, Z., Jin, H., Tang, Y., 2019. Adsorption mechanisms of five bisphenol analogues on PVC microplastics. Science of the Total Environment 650, 671-678.

Xiong, Y., Zhao, J., Li, L., Wang, Y., Dai, X., Yu, F., Ma, J., 2020. Interfacial interaction between micro/nanoplastics and typical PPCPs and nanoplastics removal via electrosorption from an aqueous solution. Water Research 184, 116100-116100.

Xu, P., Ge, W., Chai, C., Zhang, Y., Jiang, T., Xia, B., 2019. Sorption of polybrominated diphenyl ethers by microplastics. Marine Pollution Bulletin 145, 260-269.

Zhang, J., Chen, H., He, H., Cheng, X., Ma, T., Hu, J., Yang, S., Li, S., Zhang, L., 2020. Adsorption behavior and mechanism of 9-Nitroanthracene on typical microplastics in aqueous solutions. Chemosphere 245.

Zhang, X., Zheng, M., Wang, L., Lou, Y., Shi, L., Jiang, S., 2018. Sorption of three synthetic musks by microplastics. Marine Pollution Bulletin 126, 606-609.

Zou, W., Xia, M., Jiang, K., Cao, Z., Zhang, X., Hu, X., 2020. Photo-Oxidative Degradation Mitigated the Developmental Toxicity of Polyamide Microplastics to Zebrafish Larvae by Modulating Macrophage-Triggered Proinflammatory Responses and Apoptosis. Environmental Science & Technology 54, 13888-13898.

3. An investigation into the effect of UV irradiation and biofilm colonization on adsorption and desorption behavior of polyurethane (PU) microplastics for bisphenol A (BPA)

This chapter presents the study of the adsorption/desorption behavior of BPA on PU microplastics particles and evaluated not only abiotic aging treatment, but biotic and a combination of both for the effect of the interaction behavior. More environmentally representative particles will be helpful to better understand the environmental behavior of microplastics as a carrier for the migration and transformation of BPA, also potentially to the assessment of exposure risk of microplastic debris in the environment.

This chapter was published in the journal Environmental Technology & Innovation in 2024 as a research article in volume 35.

The candidate's contribution was designing and conducting the experiments, samples and data analysis, draft preparation.

Graphical abstract
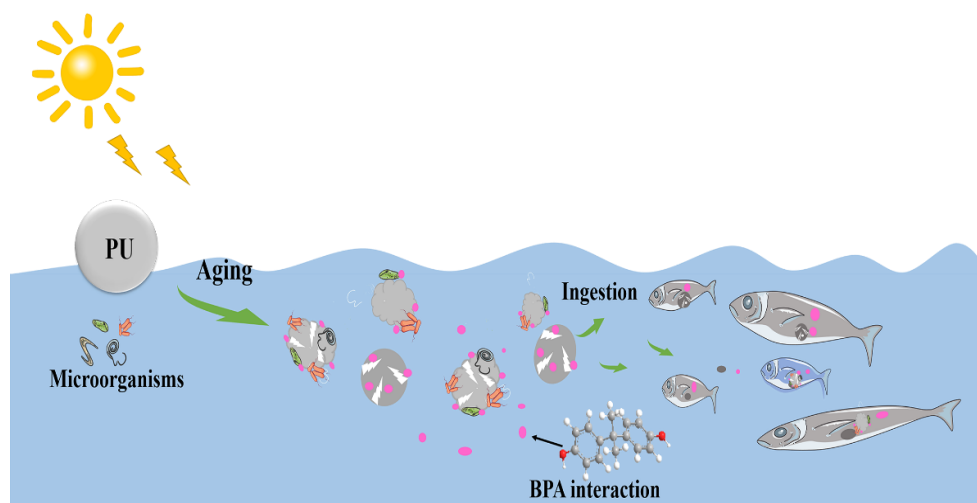
Abstract

Recent studies have demonstrated that microplastics can act as a transport vector for pollutants in the environment. However, most studies have focused on carbon-carbon backbone polymers, with little known about heteroatom backbone polymers. In this study, polyurethane (PU) microplastics were modified by UV irradiation and microorganism colonization to assess the different aging treatments on the interaction behavior (adsorption/desorption) between PU microplastics and bisphenol A (BPA). The results of the adsorption kinetics experiment illustrated that the adsorption process of BPA could be described well by a pseudo-second order kinetic equation on both fresh and aged PU microplastics. Although fresh PU microplastics revealed the highest saturated adsorption capacity, at low BPA exposure concentrations ($\leq$ 100 μg/L) the adsorption capacities for UV aged and biofilm colonized PU microplastics were very similar to fresh microplastics or even slightly higher than for fresh microplastics, the main adsorption mechanisms including H-bonding interactions and π–π interactions.

106

Fourier-transform infrared spectroscopy (FTIR) and scanning electron microscopy (SEM) investigations suggested obvious physicochemical property changes (e.g., generation of new functional groups, erosion, etc.) after UV irradiation and biofilm colonization. This study also showed that different exposure environments (ultrapure water, artificial seawater, simulated gastric fluid) could affect BPA adsorption/desorption via hydrophobic and electrostatic interaction on PU surfaces. These results further clarify the adsorption mechanisms of BPA on PU microplastics that have undergone different aging treatments, and provides a theoretical basis for the assessment of environmental behavior and exposure risks when PU microplastics and BPA coexist.

3.1 Introduction

With the increasing use of single use plastic products, plastic pollution has become a global issue owing to the lack of good management of plastic wastes. A previous study suggested that only 9 % plastics have been recycled from 1950 to 2015, with 60 % of plastic products discarded and accumulating in landfills or in the natural environment (Geyer et al., 2017b). Once plastic wastes are released into the environment, they decompose into plastic fragments under the action of abiotic (e.g., UV irradiation) and biotic processes (e.g., microorganism colonization). These fragments are defined as microplastics when the diameter is less than 5 mm (Andrady, 2011). A number of studies have demonstrated that microplastics could provide a transport vector for a range of chemical pollutants in the natural environment (e.g.,

polycyclic aromatic hydrocarbon (PAHs), perfluoroalkyl acids (PFAAs), etc.) (Wang et al., 2015; Zuo et al., 2019). In addition, the aging process of microplastics could be an important variable that affects the interaction behavior between microplastics and pollutants as biotic and abiotic factors can alter the physicochemical properties of microplastics. For example, a previous study has established that the aging process of microplastics (UV irradiation, biofilm colonization) could generate oxygen-containing functional groups, which could change the hydrophobicity and further affect the interaction behavior with chemical pollutants (Bhagwat et al., 2021; Liu et al., 2019b). Therefore, investigating the interaction of aged microplastics with coexisting pollutants could further improve their environmental risk assessment.

Bisphenol A (BPA) is commonly used for the production of polycarbonate polymers, epoxy resins, food containers, medical equipment, toys and electronics (Vandenberg et al., 2007). Previous studies have reported the widespread occurrence of BPA in rivers, personal care products, human serum, urine, and even placental tissue, revealing a global exposure (Huang et al., 2020b; Jala et al., 2022; Jimenez-Diaz et al., 2010; Tang et al., 2020; Tschersich et al., 2021). BPA has been defined as an endocrine disrupting chemical (EDC) and exhibiting adverse effects on reproduction, development, neural networks, cardiovascular, and metabolic (Crain et al., 2007; Richter et al., 2007; Vom Saal et al., 2007). BPA has also been a widely detected environmental estrogen associated with cardiovascular disease, obesity, and breast cancer (Glausiusz, 2014; Ortiz-Villanueva et al., 2018). Previous studies have

suggested that BPA could be adsorbed on fresh microplastics (e.g., polystyrene (PS),

polyvinyl chloride (PVC), polyethylene (PE), polypropylene (PP). etc.) (Liu et al.,

2019d; Wu et al., 2019), and thus, microplastics could as vectors for BPA transport.

Undertaking BPA adsorption experiments on microplastics will contribute to our

understanding of the vector effects of microplastics on pollutants and potential

ecological risks. Up to now, only a few studies have assessed the interaction behavior

between BPA and aged microplastics to evaluate the aging process on adsorption

behavior of BPA (Chen et al., 2022; Liu et al., 2021; Sun et al., 2021; Xiong et al.,

2020). However, most research has only focused on abiotic aging on microplastics

adsorption behavior, and ignored the role of biotic factors. Therefore, further studies

are required to obtain more environmentally representative particles (for example,

combine abiotic and biotic treatments) to explore the adsorption/desorption mechanism

of BPA on microplastics.

Polyurethane (PU) is a polymeric material that can be used in many different

items, such as paints, elastomers, insulators, elastic fibres, foams, etc. (Akindoyo et al.,

2016).   The demand from plastic products manufacturers for PU accounted for 8.2 %

of total plastics demand in Europe in 2021 and ranked fifth among all types of plastics

(Janssens, 2021). However, limited studies have been carried on heteroatom backbone

PU polymers compared to carbon-carbon backbone polymers such as PE, PP, PS. As a

result, PU was selected as a typical microplastic for this study. PU microplastic particles

were modified by abiotic (artificial UV), biotic (biofilm colonization) aging processes

and their combination to obtain more environmentally representative particles to investigate their interaction behavior with BPA. The objectives of this study were to (i); investigate the adsorption behavior of PU microplastics for BPA, including kinetics and isothermal equilibrium, (ii) explore the changes of adsorption/desorption behavior after UV irradiation and biofilm colonization to clarify the interaction mechanism; and (iii) to examine the interaction behavior of BPA with PU microplastics under artificial seawater and simulated gastric fluid to assess the potential exposure risk of microplastics in marine environments and organisms.

3.2 Materials and methods

3.2.1 chemicals and reagents

Acetonitrile and Methanol (HPLC grade) were purchased from Fisher Scientific Ltd (UK).   BPA (purity $\geq$ 99 %) was purchased from Sigma-Aldrich Co. LLC (UK) and the detailed information of BPA is shown in Table S1. Stock BPA solution (100 mg/L) was prepared in methanol and kept at 4 ℃.

The artificial seawater was obtained from Brightwell Aquatics (USA), the pH value is 8.2 $\pm$ 0.1. Crystal violet solution was purchased from Sigma-Aldrich Co. LLC (UK). The pepsin A was purchased from Sigma-Aldrich Co. LLC (UK), and the simulated gastric fluid was prepared according to the formula in a previous study (Liu et al., 2020c). In brief, 1.6 g pepsin was added into 500 mL artificial seawater for a final concentration of 3.2 g/L. The pH of the solution was adjusted to 2.0 by the addition 1 M HCl to simulate the acidic stomach environment.

3.2.2 Preparation of commercial PU microplastics and samples characterization

3.2.2.1 Fresh PU microplastics

Commercial polyester PU sheets were obtained from a market (Guangzhou, China), which are commonly used for sports equipment, building materials, etc. The structure of PU plastic polymers is given in Figure S1. In order to obtain micro-sized plastics, the PU sheet was cut into small pieces with uniform size, washed with ultrapure water to remove surface impurities and then air-dried.

3.2.2.2 UV aged PU microplastics

A Suntest CPS+ xenon chamber (Atlas Material Testing Technology LLC, USA) was configured at 750 W/m^2, 35 °C for the degradation of PU pieces. Appropriate glass filters were employed to restrict the transmission of irradiation wavelengths below 290 nm giving a wavelength spectrum similar to that of natural solar light. The accelerated aging experiment was performed for 7 days, which are similar as exposure 767 days under the European mean irradiance (Gewert et al., 2018), the equation is shown in the Supporting Information-M1. The final obtained samples of microplastics were cleaned with ultrapure water, dried and collected for use.

3.2.2.3 Biofilm colonized PU microplastics

Activated sludge was collected from Wastewater Treatment Plant (WWTP) in Lancaster (UK). The laboratory biofilm incubation work was carried out with both fresh and UV aged PU microplastics. 800 mg samples were put into flasks with 200 mL activated sludge (110 rpm), temperature was setting at 23 ± 1 °C and incubated on a

shaker for four weeks. After four weeks incubation, the biofilm colonized microplastics were separated from sludge and washed with ultrapure water and kept sealed at 4 °C until further analysis.

In addition, field deployments were also carried out to incubate biofilms on fresh and UV aged microplastics. Fifty fragments of fresh and UV aged PU microplastics were packed into filter bags (8 cm × 10 cm) which were placed into a large mesh nylon bag (11 cm × 17 cm) to exclude large organisms. All bags were finally fixed into metal cages. The metal cages were placed into River Conder (54°00'29.8"N 2°46'17.9"W, Lancaster, UK) and the active sludge plant of WWTP (54°00'29.8"N 2°46'17.9"W, Lancaster, UK), respectively. After four weeks incubation (May-June), the metal cages were transported to the laboratory. The microplastics samples were washed with ultrapure water and kept at 4 °C for further analysis.

3.2.2.4 PU microplastics characterization

PU samples with different aging treatments were characterized by Fourier-transform infrared spectroscopy (FTIR, Agilent, USA) and recorded in the range of 4000–400 cm^{-1} to identify transformations of the functional groups. Scanning electron microscopy (SEM, JEOL JSM 7800F) was performed to identify and surface changes. Biofilm biomass was quantified with a modified crystal violet (CV) method which is described in the Supporting Information-M2 (Lobelle and Cunliffe, 2011). Differential scanning calorimetry (DSC, NETZSCH DSC 3500 Sirius) tests were performed to

determine glass transition temperatures (T_g), the scan range from -96 to 200 °C at a rate of 5 °C /min under ambient nitrogen at a flow rate of 50 mL/ min.

3.2.3 Adsorption and desorption experiments

A 100 mg/L BPA stock solution was diluted into seven different concentrations (20, 50, 100, 200, 500, 700 and 1000 μg/L). The volume percentage of methanol was kept below 0.1% (v/v) to yield negligible solvent effects. For the kinetics experiments, 50 mg of PU microplastics and 10 mL of 100 μg/L BPA solutions were added into 20 mL glass tubes. All the glass tubes were shaken at 140 rpm and conducted at room temperature (25 ± 1 °C). The supernatants were collected at different times (0, 12 h, 24 h, 48 h, 72 h, 96 h, 120 h, 168 h, 216 h, and 264 h), and filtered through a 0.2 μm PTFE membrane. Before the batch experiments, 10 mL 100 μg/L BPA solution was placed into glass tubes to assess the loss of BPA caused by volatilization and adsorption to glass surfaces. fifty mg PU microplastics were placed into 10 mL ultrapure water to determine if PU could leach BPA. Results showed that the loss of BPA in glass tubes was less than 1 % and PU microplastics not leach BPA. The impact of artificial seawater for the adsorption behavior were further carried using 50 mg fresh and aged PU microplastics in 10 mL 100 μg/L BPA solutions and performed for 264 h. After adsorption equilibrium was achieved, PU microplastics from the adsorption experiments were transferred into glass tubes containing 10 mL ultrapure water, artificial seawater and simulated gastric, shaken at 140 rpm (25 ± 1 °C) to simulate the desorption behavior of BPA from PU microplastics to river, marine and the body of

organisms. The supernatants were collected from 0 h to 120 h. Experiments for the adsorption isotherms were performed with 50 mg PU microplastics and 10 mL BPA solutions at different concentrations ranging from 20 to 1000 μg/L, and then shaken at 140 rpm, 25 °C for 264 h. Three replicates were carried out for each experiment.

3.2.4 Ultra high-performance liquid chromatography (UHPLC) analysis

Samples were analysed using a Shimadzu NexeraX2 UHPLC with fluorescence detector (Shimadzu, Japan) and a Phenomenex C18 column (4 μm, 150 × 4.6 mm). Chromatographic separation was performed with a mobile phase of A: ultrapure water and B: acetonitrile (ACN). The isocratic procedure was set: 50 % ultrapure water (A) and 50 % ACN (B), held 10 min. The injection volume was 50 μg/L and the tray temperature was kept at 30 °C. The excitation wavelength and emission wavelength were 226 nm and 315 nm, respectively. Flow rate was 0.5 mL/min. Samples were prepared in ultrapure water/artificial seawater/simulated gastric fluid and methanol (4:1, v/v).

3.2.5 Statistical analysis

Data were compared by T-test and one-way analysis of variance (ANOVA) using SPSS version 22.0. Figures were plotted with Origin version 2019. All calculation equations are listed in the Supporting Information-M3.

3.3 Results and discussion

3.3.1 PU microplastics characterization

The estimation of biofilm biomass using the CV method indicated an obvious increase for both fresh and UV aged PU microplastics after incubation for four weeks (Figure 1a). It was clear that biomass growth was higher on UV aged PU microplastics compared with fresh PU (T-test, $p < 0.05$). Recent studies suggested that the increased surface roughness and hydrophilicity of microplastics after irradiation could promote the colonization of microorganism on microplastics (Ho et al., 2020; Hossain et al., 2019). The initial binding of CV, as seen in fresh and UV aged PU samples was perhaps due to the highly polar amide (−CONH−) functional groups in PU, which provide sites for hydrogen bonding to ionic and polar groups in the dye molecules (Bhagwat et al., 2021).
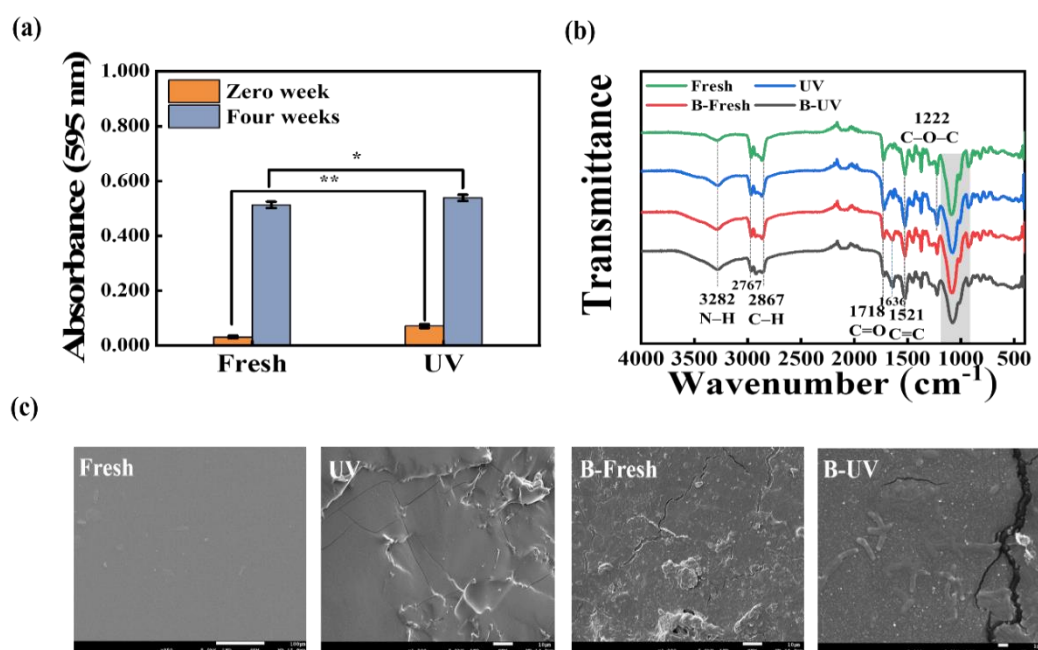
Figure 1. (a) Changes in absorbances of crystal violet dye for fresh and UV aged PU microplastics after incubated biofilm in the laboratory for four weeks. Error bars are

the means ± standard deviation (SD) of three repeats. $* p < 0.05$, $** p < 0.01$, $*** p < 0.001$. (b) FTIR spectrogram of fresh, UV aged, biofilm colonized fresh (B-Fresh) and UV aged (B-UV) PU microplastics. (c) SEM images of PU microplastics with different aging treatments.

The FTIR spectra for PU microplastics are illustrated in Figure 1b. The peaks of typical PU could be observed at around 3282 cm^{-1} (N–H), 1718 cm^{-1} (C=O), 1521 cm^{-1} (C=C), 1222 cm^{-1} (C–O–C), 2967 cm^{-1} and 2867 cm^{-1} (asymmetric and symmetric stretching of C–H) (Badri et al., 2010; de Oliveira et al., 2017; Gao et al., 2010; Santos et al., 2020). In general, UV aging of polymers involves degradation by chain scission, oxidation, and depolymerization, resulting in the formation of new functional groups, or structural defects (Xue et al., 2021). The vibration of N–H stretching, C=O stretching, C=C stretching, C–O–C stretching increased, and C–H stretching slightly decreased after UV aging, which suggests breakage of polymer chains. In addition, an obvious yellow coloration could be observed for UV aged PU microplastics as showed in Figure S2, which would be related to the oxidation and degradation of PU microplastics, leading to the generation of chromophores (e.g., quinone-imide structures) (Rosu et al., 2009). After the colonization of biofilm, the peak at 3282 cm^{-1} (N–H) was enhanced and peaks at 2867 cm^{-1} (C–H) and 1718 cm^{-1}(C=O) were obviously decreased. New peak was generated at around 1636 cm^{-1} (C=O, amide I), which represent characteristic peak for proteins and indicated biofilm formation on PU microplastics (Bonhomme et al., 2003b; Maquelin et al., 2002). In addition, the

peak changes between 900 cm^{-1} and 1180 cm^{-1} (grey area in Figure 1b) after biofilm colonization might be associated with polysaccharides, which are the usual metabolites produced by microorganisms and major constituents of biofilms (Bonhomme et al., 2003b; Sandt et al., 2021). Figure 1c illustrates the surface changes after UV irradiation and biofilm colonization. The surfaces of fresh PU microplastics were smooth, whilst the surfaces were eroded with more pits and wrinkles after UV aging. After the colonization of biofilm, surface changes and microorganisms were observed in SEM images, which confirmed biofilm colonization.

3.3.2 Adsorption kinetics and isotherm of PU microplastics with different aging treatments

3.3.2.1 Adsorption kinetics

The adsorption kinetics curves of PU microplastics with different aging treatments are shown in Figure 2a. The kinetics data suggested that adsorption equilibrium of BPA on fresh PU microplastics was achieved within 120 h (one-way ANOVA analysis, $p > 0.05$), and the time needed to reach adsorption equilibrium became shorter after UV irradiation and biofilm colonization (range from 48 h to 96 h), which suggested UV aging and biofilm colonization could accelerate the adsorption of BPA on PU microplastics.

The experimental data for BPA adsorption kinetics were fitted using the intraparticle diffusion model (Figure 2b), which assumed the adsorption process was controlled by the diffusion of adsorbate into the internal particles. The intraparticle

diffusion plots for BPA adsorption onto microplastics can be divided into two or three linear segments, which is line with previous studies (Qi et al., 2021; Wang et al., 2020b). The initial linear segments represent external mass transfer from the solution to the external surface of the adsorbent and the subsequent linear segments are related with intraparticle diffusion (Fierro et al., 2008). According to Table S2, the k values from the UV aging and biofilm colonization treatments increased when compared with those for the fresh PU microplastics. For example, the k_{p1} of BPA to PU microplastics increased from 1.681 to 2.250 ($\mu g/ (g.h^{0.5})$), and the k_{p2} increased from 0.114 to 0.590 ($\mu g/ (g.h^{0.5})$) after UV aging. It is likely that the erosion and cracks appearing within the PU microplastics after aging treatments, result in easier diffusion for the BPA, which leaded to the shorter adsorption equilibrium time compared with fresh PU microplastics.
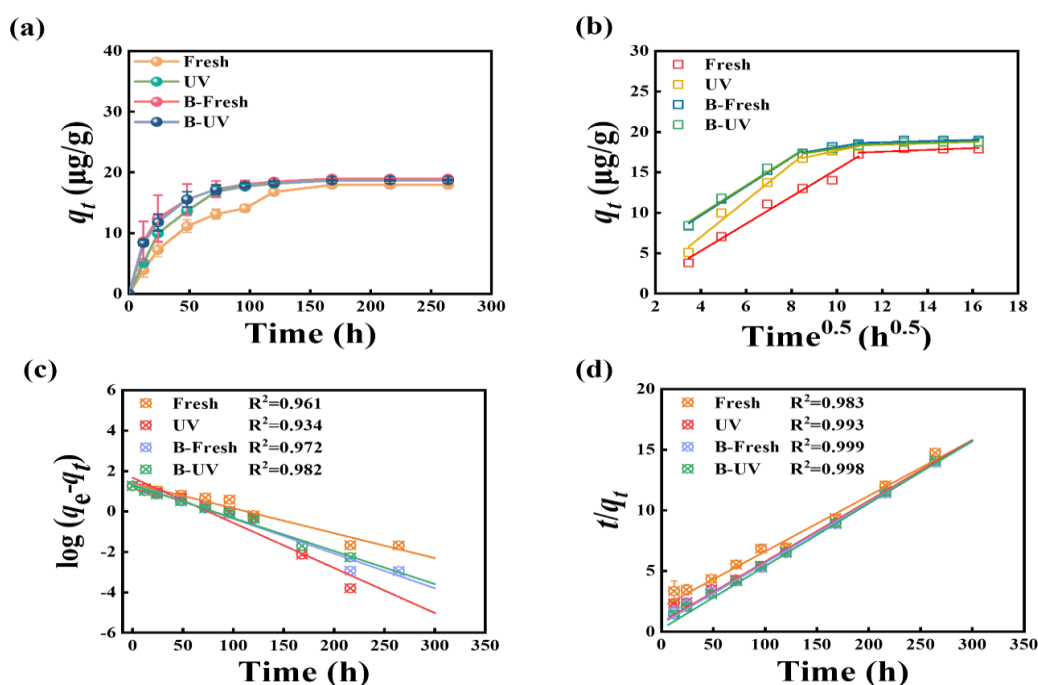
Figure 2. (a) Adsorption kinetics of BPA on fresh and aged PU microplastics (b) Intraparticle diffusion mole of fresh and aged PU microplastics. (c) Pseudo-first-order

model of fresh and aged PU microplastics. (d) pseudo-second-order model of fresh and aged PU microplastics. Error bars are the means ± standard deviation (SD) of three repeats. (50 mg PU microplastics, 10 mL 100 μg/L, 25 °C, 140 rpm). B-fresh and B-UV represent fresh and UV aged PU microplastics colonized biofilm, respectively.

The adsorption data has been fitted using both the pseudo-first model and pseudo-second order models (Figure 2c and Figure 2d). The kinetics for fresh, UV irradiated and biofilm colonized PU microplastics were better described by the pseudo-second-order model as illustrated in Table S3 (R^2 range from 0.983 to 0.999), suggesting that chemical adsorption was likely to be the dominant factor for the adsorption process of BPA onto fresh and aged PU microplastics.

3.3.2.2 Adsorption isotherms
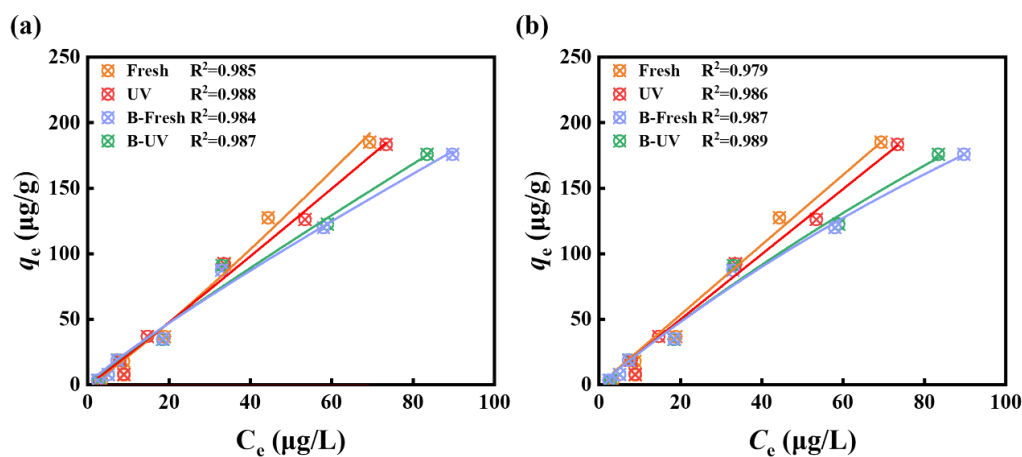
Figure 3. Equilibrium data of BPA adsorption on fresh and aged microplastics fitted by Freundlich (a) and Langmuir (b) models. B-fresh and B-UV represent fresh and UV aged PU microplastics colonized biofilm, respectively.

The adsorption isotherm has been assessed using both the Freundlich model and Langmuir models (Figure 3), with the relevant parameters summarized in Table 1. The results suggest that the Freundlich isotherm model was the most appropriate model to describe the adsorption of BPA on fresh and UV aged PU microplastics which indicates that the adsorption of BPA on fresh and UV aged PU microplastics are multi-layer adsorption on heterogeneous surfaces affected by both chemical and physical adsorption processes (Wu et al., 2019).

Table 1. Parameters of the isotherm models for adsorption of BPA on PU microplastics.

Isotherms	Parameters	Microplastics			
		Fresh	UV aged	B-Fresh	B-UV
Freundlich	K_F [(µg/g) (L/µg)$^{1/n}$]	1.64	2.10	3.01	3.32
	n	0.89	0.95	1.08	0.88
	R^2	**0.985**	**0.988**	0.984	0.987
Langmuir	q_m (µg/g)	2.39×10^5	9.76×10^4	9.76×10^2	7.52×10^2
	K_L (L/g)	1.11×10^{-5}	2.55×10^{-5}	2.59×10^{-3}	3.40×10^{-3}
	R^2	0.979	0.986	**0.987**	**0.989**

The data in Table 1 provide values for n which is the surface heterogeneity factor. If n > 1, the adsorption is favourable, otherwise it is unfavourable (Meghea et al., 1998). The value of n for fresh and UV aged microplastics was less than 1 (0.89 and 0.95 respectively), which indicated that the adsorption will decrease with increasing amounts of BPA in solution. As for biofilm colonized PU microplastics, the Langmuir isotherm provided a better fitting for BPA adsorption. The Langmuir model is used to describe nonlinear adsorption behavior in monolayers, and it assumes adsorption sites are

energetically constant and limited (Meghea et al., 1998). Thus, the monolayer coverage might be the predominant mechanism for PU microplastics after colonized biofilm.

3.3.3 Adsorption mechanism and capacity of fresh and different aging treatments PU microplastics

Using data from previous studies (Table S6) the saturated adsorption capacity of BPA on fresh PU microplastics (Table 1) was clearly higher than for carbon-carbon backbone microplastics (e.g., PVC, PS, PE). As the glass transition temperature (T_g) of PU microplastics is -50.29 °C (Table S5), which is much lower than the experimental temperature, the state of the PU can be classed as rubbery. This represents PU microplastics as having high free volume, with chain segments that can move freely and can be considered to be present in a flexible state. These factors can be considered to be responsible for the excellent adsorption ability. In addition, strong H-bonding interactions behavior might be observed between BPA and PU microplastics owing to the heteroatom backbone of PU microplastics, which might also result in better adsorption ability (Liu et al., 2019d). In order to get more detailed information about the adsorption mechanism of BPA on PU microplastics, FTIR scans were undertaken. As shown in Figure 4a, the peak at 3282 cm^{-1} (N–H) stretching vibrations of amide groups became broad and the intensity of the peak at 1718 cm^{-1} (C=O) and 1521 cm^{-1} (C=C) reduced after adsorption, which indicated H-bonding interactions and π-π interactions between BPA and PU microplastics. The vibration of phenolic hydroxyl groups (O–H) is around 3348 cm^{-1} for the BPA molecule (Figure S3). These functional

groups could act as H-bond donors and bind with H-acceptors (e.g., amide groups) on PU microplastics via H-bonding interactions (Liu et al., 2019d). The broad vibration band between 3700 cm^{-1} and 3078 cm^{-1} might also suggest strong H-bonding (O–H N) between BPA and PU microplastics. In addition, the aromatic ring vibration of BPA range 1604 — 1442 cm^{-1} (Figure S3) (Liu et al., 2022e), which could form π-π interactions with PU microplastics (e.g., C=C, C=O) (Zhang et al., 2020b; Zhao et al., 2020). As a result, all transformations of the FTIR spectrum suggest the interaction mechanisms between BPA and fresh PU microplastics involve H-bonding and π-π interactions. UV aged PU microplastics exhibited similar changes in infrared peaks after adsorption of BPA (Figure 4a), which suggests the H-bonding interactions and π-π interactions are still the main mechanisms for the UV aged PU microplastics.
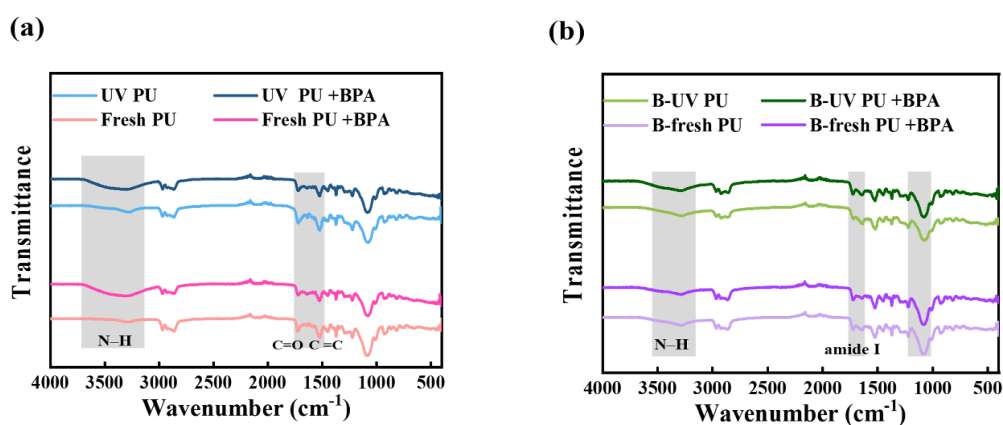
Figure 4. (a) FTIR spectrogram of fresh and UV aged PU microplastics before and after adsorption of BPA. (b) FTIR spectrogram of biofilm colonized PU microplastics before and after adsorption. B-Fresh and B-UV represent biofilm colonized fresh and UV aged microplastics.

Figure 4b illustrates the FTIR spectra of biofilm colonized PU microplastics after adsorption of BPA. The intensity and vibration of the biofilm characteristic peaks at 3282 cm^{-1} (N–H) and 1636 cm^{-1} (amide I) decreased after adsorption, it could be inferred that C=O, N–H still play important roles in the adsorption process after biofilm colonization and the main mechanisms also be involved H-bonding interactions and π–π interactions. In addition, the vibration of the polysaccharide band (900 cm^{-1} and 1180 cm^{-1}) changed for the biofilm colonized UV aged PU microplastics and vibration of the peak at 1076 cm^{-1} shifted to 1083 cm^{-1} after BPA adsorption, which suggested that adsorption behavior might be impacted by microorganisms for both fresh and UV aged PU microplastics after biofilm colonization. In order to further investigate the effect of microorganisms on the adsorption behavior of PU microplastics, adsorption experiments for the field biofilm colonized PU microplastics were also carried out. As illustrated in Figure S4a, field derived biofilms successfully colonized the microplastics with the UV aged PU microplastics showing higher biomass than fresh microplastics after biofilm colonization. The adsorption capacity increased with the increased biomass for PU microplastics (Figure S4b) and showed a positive correlation ($p < 0.05$) between biomass and adsorption capacity (Figure S4c). This indicates that biofilms play an important role for the adsorption behavior of PU microplastics after microorganism colonization.

The saturated adsorption capacity (q_m) of BPA on fresh PU microplastics was 2.39×10^5 µg/g (Table 1), but decreased after UV aging and biofilm colonization. This

might indicate that adsorption behavior is inhibited after aging treatments. As shown in

Figure 3, the adsorption capacities of BPA on fresh microplastics were 185.8 μg/g with

a 1000 μg/L initial BPA exposure concentration, which was significantly higher than

UV aged (183.4 μg/g) and biofilm colonized fresh and UV aged PU microplastics

(175.1 μg/g and 175.9 μg/g, respectively). The reason might be due to the limited

adsorption sites inhibiting adsorption ability. UV irradiation and biofilm colonization

increased the T_g of PU microplastics (Table S5), which decreased internal free spaces

and mobility of inner molecular segments in the microplastics, thus providing less

accessibility, which is similar to results obtained in a previous study (Zhang et al.,

2020b). In addition to this, information on biofilms will be important owing to their

effect on adsorption behavior as mentioned previously. Adsorption behavior of PU

microplastics could be better fitted by the Langmuir isothermal model which also

suggests that adsorption sites are limited, and hence, will result in the obvious decrease

of the saturated adsorption capacity compared to fresh PU microplastics. However, it is

worth noting that the adsorption capacity on UV aged and biofilm colonized PU

microplastics did not show a dramatic difference and even suggested a slight increase

($p < 0.05$) compared with fresh PU microplastics at the relatively low initial BPA

exposure concentration (Figure S5). Specific surface area should always be considered

as an important factor that could affect the adsorption behavior of microplastics. In this

study, we attempted to measure the specific area using an ASAP 2020 instrument

(Micromeritics, USA). Unfortunately, the surface of our PU material did not interact

with the N_2 (adsorbate) and thus the surface area of PU microplastics wasn't

successfully measured. Previous studies have suggested that specific surface area increased after UV irradiation and biofilm colonization (Bhagwat et al., 2021; Fan et al., 2021a; Fan et al., 2021b; Zafar et al., 2023), which could promote the adsorption of pollutants on microplastics. Although we haven't obtained the porosimeter data for the PU microplastics, it could be inferred that the surface area might have increased after aging treatments which might be a potential factor affecting the adsorption of BPA. Another potential explanation is that the breakage of chains and formation of new functional groups (Figure 1b, e.g., N–H, C=O, etc.) might enhance the H-bonding interactions and further promote affinity for BPA. Hence, bond interactions might play an important role for the adsorption behavior on PU microplastics at low BPA exposure concentrations, whilst the adsorption behavior will be dominated by the available adsorption sites with the increased BPA concentration in the aquatic environment. In the natural environment, concentration of BPA ranges from around 0.11 ng/L to 30 µg/L in surface waters worldwide (Abraham and Chakraborty, 2020; Catenza et al., 2021), which indicates that saturated adsorption capacity BPA exposure concentration is very unlikely. As a result, the adsorption capacity of BPA might only very slightly difference after UV aging and biofilm colonization in the environment.

3.3.4 Desorption behavior of PU microplastics with aging treatments

As shown in Table S4, the desorption efficiencies decreased after UV irradiation and biofilm colonization. As a result of the erosion of PU microplastics after UV aging, increasing amounts of BPA diffused into the structure or the narrow pores of the

microplastics (Fan et al., 2021a; Sun et al., 2021), which results in it being more difficult for UV aged PU microplastics to release BPA compared with BPA sorbed on fresh PU microplastics surfaces. Moreover, the desorption efficiency also decreased after biofilm colonization. The adsorption behavior of PU microplastics colonized by biofilm was dominated by the properties of the biofilms, which suggested that the interaction behavior reflected enhanced H-bonding interaction compared to fresh PU microplastics. This may have the result of increased affinity of BPA to microplastics resulting in lower desorption efficiencies compared to PU microplastics without microorganism colonization.

3.3.5 Effect of artificial seawater and simulated gastric fluid

The adsorption capacity for PU microplastics was found to decrease in seawater by a small but significant amount compared with ultrapure water (Figure 5a), which might be due to electrostatic interactions. As illustrated in Figure 5c, the pH in seawater (pH=8.2) was higher than ultrapure water (pH=6.8), resulting in the anionic speciation of BPA in seawater being slightly higher than in the ultrapure water. The point of zero charge (pH_{pzc}) of PU is around 6 (Xue et al., 2021) and the pH_{pzc} of biofilms is commonly around 4.5 (Qi et al., 2021), which suggests that PU surfaces would be negatively charged in artificial seawater. Although limited, the enhanced electrostatic repulsive-force between BPA and PU microplastics in artificial seawater could lead to a reduction in the adsorption capacity. In addition to this effect, the negative PU surface will attract cations such as Na^+ and Ca^{2+} in the seawater which could easily be adsorbed

onto PU surfaces by electrostatic attraction (Guo et al., 2019). These inorganic exchangeable cations could substitute the H^+ of acidic groups and inhibit the H-bonding interactions (Aristilde et al., 2010).
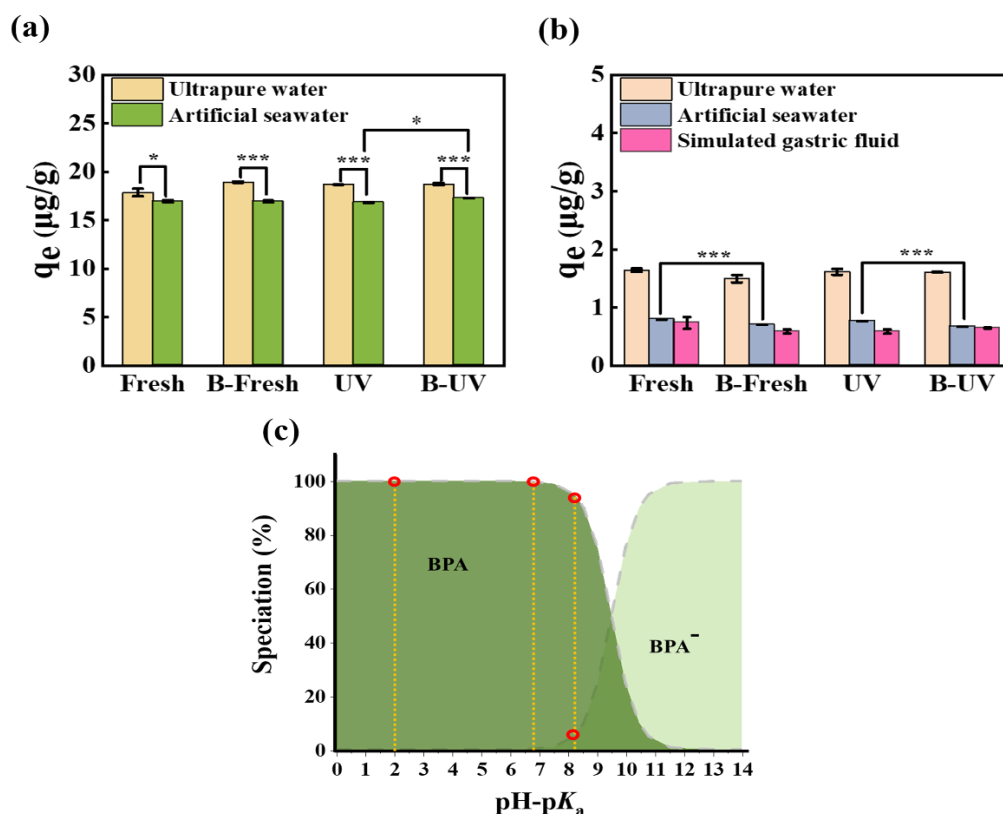
Figure 5. (a) The adsorption capacity of BPA on fresh, UV aged, biofilm colonized fresh (B-Fresh) and UV aged (B-UV) PU microplastics under ultrapure water and artificial seawater. (b) The desorption capacity of BPA on fresh, UV aged, biofilm colonized fresh (B-Fresh) and UV aged (B-UV) PU microplastics under ultrapure water, artificial seawater and simulated gastric fluid. (n=3, 50 mg microplastics, 25 ℃, 140 rpm). * $p < 0.05$, ** $p < 0.01$, *** $p < 0.001$. (c) Speciation of BPA at different pH values.

Previous research has suggested that microplastics could be accidentally ingested marine organisms (e.g., fish) (Peters et al., 2017), and that chemicals might be released causing potential biotoxicity. As a result, the desorption experiment was repeated in simulated gastric fluid to help assess the potential exposure risk of microplastics to organisms. The desorption capacity of microplastics was observed to decrease in seawater after the colonization of biofilm (Figure 5b), which showed a similar trend with ultrapure water. However, this trend became weak and not significant in simulated gastric fluid for both fresh and UV aged PU microplastics after biofilm formation. The pepsin in simulated gastric fluid contained several hydrophobic residues and residues with aromatic rings (Liu et al., 2022c) and it is possible that hydrophobic and π-π interactions between the biofilms and pepsin might have occupied the adsorption sites of microplastics promoting the release of BPA.

The desorption capacity (Figure 5b) and efficiency (Table S4) mostly followed the trend: ultrapure water > artificial seawater > simulated gastric fluid, which has also been reported in a previous study (Liu et al., 2019d). The salting-out effect enhanced the hydrophobic interaction between BPA and microplastics, which would increase affinity of BPA to microplastics, leading to a decreased desorption ability in artificial seawater compared with ultrapure water. Although desorption was lowest in simulated gastric fluid, colonization by microorganism could lead to microplastics acquiring chemical signals which could be attractive to those species (such as marine copepods, procellariiform seabirds and foraging fish) that use chemosensory mechanisms when

locating, identifying, and ingesting food (Procter et al., 2019; Savoca et al., 2016). For example, the presence of dimethyl sulfide (DMS) — a marine trace gas is derived from dimethylsuoniopropionate (DMSP) produced by phytoplankton, has been observed to increase the ingestion rate of microplastics in zooplankton (Botterell et al., 2020; Procter et al., 2019). As a result, colonization by biofilm might enhance bioavailability of microplastics to marine organisms and therefore increase the bioavailability of pollutants sorbed in microplastics increasing the potential exposure risk.

3.4 Conclusions

In this study, PU microplastics were modified by UV irradiation and microorganism colonization to obtain more realistic polymers for the investigation of the adsorption/desorption behavior of BPA. π-π and H-bonding interactions contribute to the adsorption of BPA on fresh and aged PU microplastics. In addition, our results suggest that biofilms might play an important role in adsorption behavior and that the adsorption capacity might be determined by the available adsorption sites on biofilms. Environmental factors were also shown to have effects on the interaction behavior between BPA and microplastics. Whilst the desorption capacity/efficiency was lowest in simulated gastric fluid, the colonization of biofilm on microplastics may increase the possibility of accidental ingestion of microplastic particles by organisms, and so this potential exposure pathway cannot be ignored. PU microplastics could be expected to exhibit strong interaction behavior with BPA in aquatic environments owing to their

complex structures (e.g., carbamate groups). With aging by sunlight and microorganism actives in the natural environment, structural changes might occur that may further influence the transfer and fate of BPA. These findings will be helpful to understand the environmental behavior of PU as a carrier for the migration and transformation of BPA, also potentially to the assessment of exposure risk of microplastic debris in the environment.

Supporting information

M1: Calculation equation for the simulate exposure days

The mean UV-irradiance in Europe is approximate 60 kWh/ (m²/year), the equation to calculate the simulate days is

$$\text{Simulated day} = \frac{\text{Total irradiance expose in exp } (0.75 \text{ kW/m}^2 \times \text{expose hours})}{\text{Mean UV irradiance in Europe } (60 \text{ kW h/ } (\text{m}^2/\text{year}))} \times 365$$

Expose hours	Total irradiance	Simulated exposure days under European mean irradiance
168 h	126 kWh/m²	767

M2: Crystal violet (CV) method

0.5 g plastics were transferred to the tube with 1 mL crystal violet (1 % W/V) and stain for at least 45 min. The stained plastic samples were rinsed with ultrapure water until the filtrate was clear. The stained samples were then air-dried for 45 min in sterile dishes and transferred to new vials containing 2.0 mL of 95% ethanol. After 10 min, 1.5 mL of the ethanol solution was transferred into a cuvette, and the optical density was measured with an ultraviolet-visible spectrophotometer at 595 nm.

M3: Calculation equations

The adsorption capacity of BPA on microplastics:

$$q_e = \frac{C_0 - C_e}{m} V$$

where q_e (µg/g) refers to the equilibrium adsorption capacity of microplastics for BPA; C_0 and C_e (µg/L) are the initial concentration and equilibrium concentration of BPA in the solution respectively; m (mg) is the mass of plastics and V (mL) is the volume of the solution used in adsorption experiments.

Intraparticle diffusion model:

$$q_t = k_p t^{0.5} + C$$

Pseudo-first order model:

$$\log (q_e - q_t) = \log q_e - k_1 t / 2.303$$

Pseudo-second order model:

$$\frac{t}{q_t} = \frac{1}{k_2 q_e^2} + \frac{t}{q_e}$$

where k_P (µg/ (g·h$^{0.5}$)) is the rate constant of the intraparticle diffusion model; q_t (µg/g) is the adsorption amount of BPA on per gram microplastics at a given time t (h); k_1 and

k_2 represent the rate constant for pseudo-first order and pseudo- second order kinetics respectively.

Langmuir equation:

$$q_e = \frac{q_m K_L C_e}{1 + C_e K_L}$$

Freundlich equation:

$$q_e = K_F C_e^{1/n}$$

where q_m is the maximum adsorption capacity of the monolayer (μg/g); n is surface heterogeneity factor. K_L (L/g) and K_F [(μg/g) (L/μg)$^{1/n}$] represent the affinity constants of the Langmuir and Freundlich equations, respectively.

The desorption efficiency:
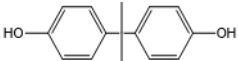
$$\%D = \left(\frac{C_{desorb}}{C_{adsorb}}\right) \times 100$$

where C_{desorb} (μg/L) is the desorption concentration of BPA from microplastics and C_{adsorb} (μg/L) is the adsorbed equilibrium concentration of BPA on microplastics at the beginning of the desorption experiment.

The desorption capacity:

$$q_{\mathrm{d}} = \frac{C_{desorb}}{m} V$$

Where q_{d} (μg/g) is the desorption capacity of BPA from microplastics.

Table S1. Properties and structures of BPA used in this study

Chemicals	Molecular formula	Structure	Molecular weight	$\log K_{\mathrm{ow}}$	pK_{a}
BPA	$C_{15}H_{16}O_2$		228.29	3.32	9.50±0.10

Table S2. Parameters of the intraparticle diffusion model

Parameters	Fresh	UV	B-fresh	B-UV
k_{p1} (μg/ (g ·h$^{0.5}$))	1.681	2.250	1.795	1.773
C_1	-1.438	-1.983	2.476	2.744
R^2	0.980	0.979	0.989	0.981
k_{p2} (μg/ (g ·h$^{0.5}$))	0.114	0.590	0.468	0.410
C_2	16.218	11.771	13.466	13.832
R^2	0.900	0.991	0.964	0.999
k_{p3} (μg/ (g ·h$^{0.5}$))	-	0.089	0.075	0.076
C_3	-	17.340	17.814	17.580
R^2	-	0.664	0.650	0.689

Table S3. Kinetic parameters for BPA adsorption by PU microplastics.

Types	q_e* (μg/g)	pseudo-first order parameters			pseudo-second order parameters		
		q_e (μg/g)	k_1	R^2	q_e (μg/g)	k_2	R^2
	Fresh	17.89	24.58	2.84×10^{-2}	0.961	21.80	1.03×10^{-3}	0.983
	UV	18.69	46.34	5.14×10^{-2}	0.934	20.99	3.25×10^{-3}	0.993
PU	B-Fresh	18.95	22.85	3.96×10^{-2}	0.972	20.28	1.08×10^{-2}	0.999
	B-UV	18.74	20.16	3.76×10^{-2}	0.982	19.95	3.77×10^{-3}	0.998

q_e* represent the adsorption capacity of BPA measured in experiments.

Table S4. Desorption efficiency (%) of BPA in ultrapure water (UW), artificial seawater (AS) and simulated gastric fluid (SGF).

Type		UW	AS	SGF
PU	Fresh	9.196 ± 0.162	4.680 ± 0.006	4.421 ± 0.603
	B-Fresh	7.903 ± 0.331	4.164 ± 0.011	3.784 ± 0.164
	UV	8.644 ± 0.270	4.570 ± 0.022	3.545 ± 0.214
	B-UV	8.560 ± 0.023	3.879 ± 0.007	3.813 ±0.049

Table S5. Glass transition temperature of PU microplastics with different aging treatment.

Sample	Treatment	T_g (°C)
PU	Fresh	-50.29
	UV	-48.55
	B-Fresh	-49.22
	B-UV	-48.90

Table S6. Summary of saturated adsorption capacity (q_m) of BPA on carbon-carbon backbone microplastics according to previous studies.

Type	q_m (µg/g)	Reference
PVC	923, 4.16×10^3	(Jiang et al., 2023; Wu et al., 2019)
PS	6.66×10^3, 1.24×10^4	(Jiang et al., 2023; Xiong et al., 2020)
PE	1.206×10^3	(Jiang et al., 2023)
HDPE	163	(Tang et al., 2023)
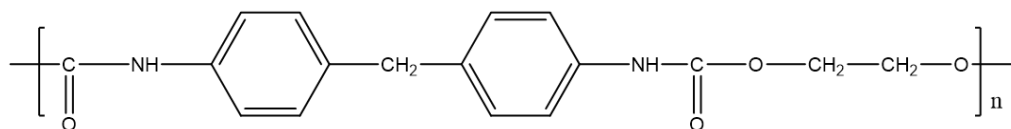
Figure S1. The structures of PU microplastics.
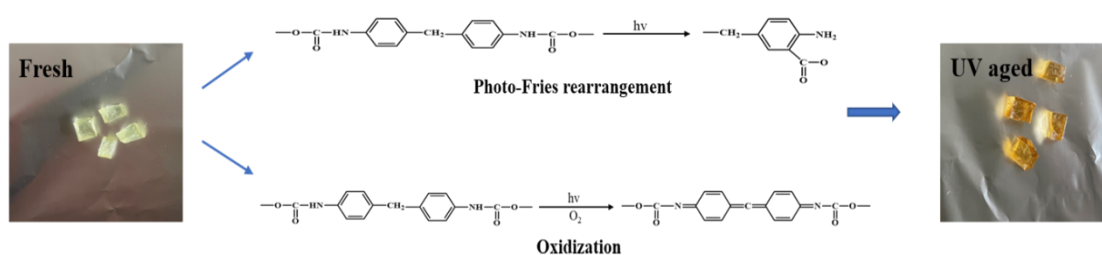
Figure S2. The degradation mechanism of PU microplastics. The degradation mechanism was cited from (Rosu et al., 2009)
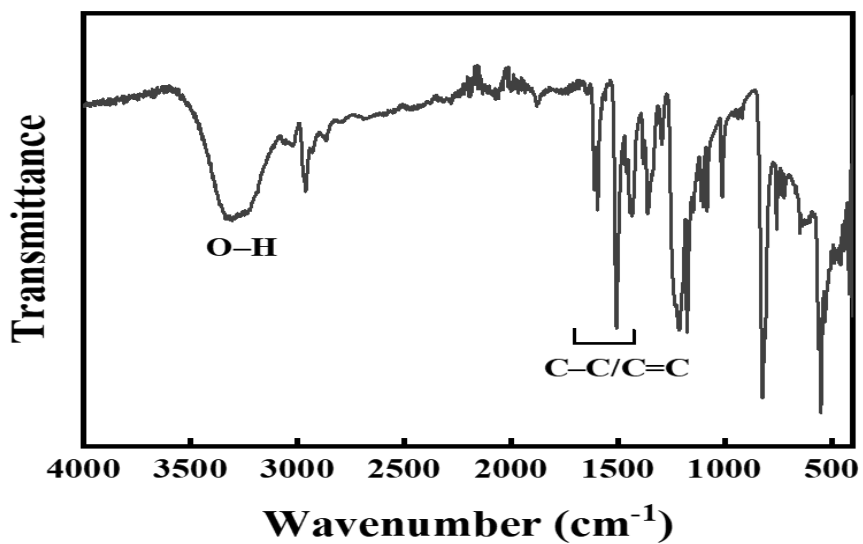
Figure S3. FTIR spectrogram of BPA.
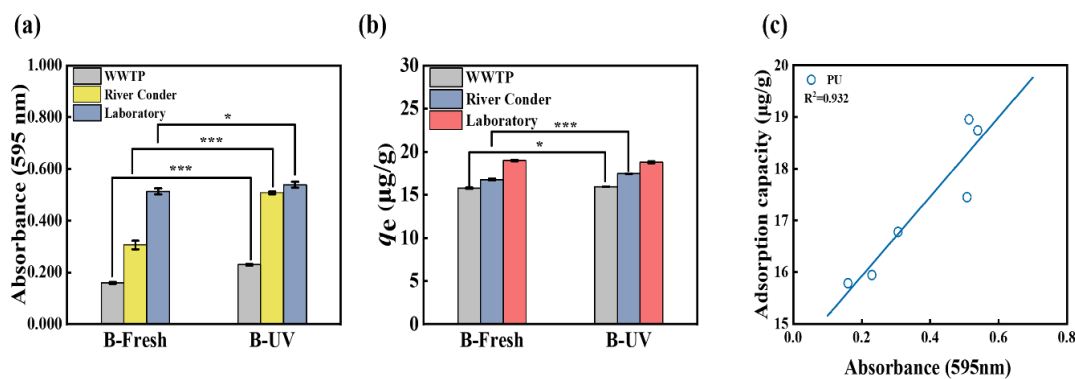
Figure S4. (a) Changes in absorbance of crystal violet dye for biofilm colonized fresh (B-Fresh) and UV aged (B-UV) PU microplastics that incubated in active sludge plant of wastewater treatment plant (WWTP), River Conder. (b) The adsorption capacity of BPA on biofilms colonized (field and laboratory) fresh and UV aged PU microplastics. (n=3, 50 mg MPs, 25 °C, 140 rpm). $*$ $p < 0.05$, $**$ $p < 0.01$, $***$ $p < 0.001$. (c) The positive correlation ($p < 0.05$) between absorbance (an indirect measure of biofilm biomass) and the adsorption capacity of PU microplastics that incubated biofilm among different sites.
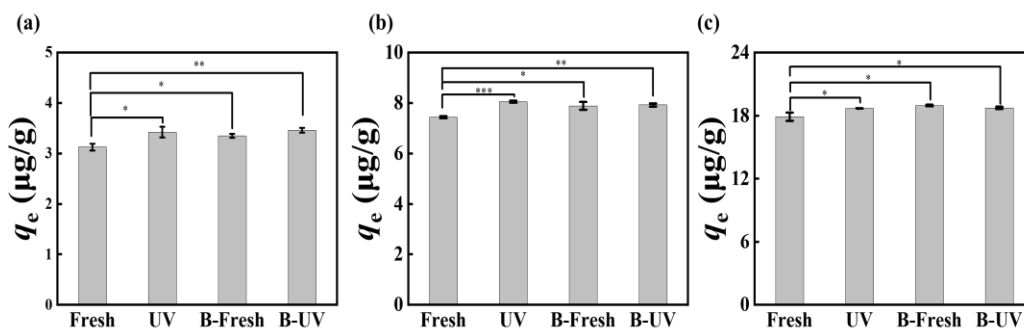
Figure S5. Adsorption capacity of BPA on PU microplastics under initial exposure concentration of 20 µg/L (a), 50 µg/L (b) and 100 µg/L (c).

References

Abraham, A., Chakraborty, P., 2020. A review on sources and health impacts of bisphenol A. Rev. Environ. Health. 35, 201-210.

Akindoyo, J.O., Beg, M.D.H., Ghazali, S., Islam, M.R., Jeyaratnam, N., Yuvaraj, A.R., 2016. Polyurethane types, synthesis and applications – a review. RSC Adv. 6, 114453-114482.

Andrady, A.L., 2011. Microplastics in the marine environment. Marine Pollution Bulletin 62, 1596-1605.

Aristilde, L., Marichal, C., Jocelyne, Miehe-Brendle, Lanson, B., Charlet, L., 2010. Interactions of Oxytetracycline with a Ametctite Clay: A Spectroscopic Study with Molecular Simulations. Environ. Sci. Technol. 44, 7839-7845.

Badri, K.B.H., Sien, W.C., Shahrom, M.S.B.R., Hao, L.C., Baderuliksan, N.Y., Norzali, N.R.A., 2010. FTIR spectroscopy analysis of the prepolymerization of palm-based polyurethane. J. Solid State Sci. Technol. 18, 1-8.

Bhagwat, G., Tran, T.K.A., Lamb, D., Senathirajah, K., Grainge, I., O'Connor, W., Juhasz, A., Palanisami, T., 2021. Biofilms Enhance the Adsorption of Toxic Contaminants on Plastic Microfibers under Environmentally Relevant Conditions. Environ. Sci. Technol. 55, 8877-8887.

Bonhomme, S., Cuer, A., Delort, A.M., Lemaire, J., Sancelme, M., Scott, G., 2003. Environmental biodegradation of polyethylene. Polym. Degrad. Stab. 81, 441-452.

Botterell, Z.L.R., Beaumont, N., Cole, M., Hopkins, F.E., Steinke, M., Thompson, R.C., Lindeque, P.K., 2020. Bioavailability of Microplastics to Marine Zooplankton: Effect of Shape and Infochemicals. Environ. Sci. Technol. 54, 12024-12033.

Catenza, C.J., Farooq, A., Shubear, N.S., Donkor, K.K., 2021. A targeted review on fate, occurrence, risk and health implications of bisphenol analogues. Chemosphere 268, 129273.

Chen, X., Chen, C., Guo, X., Sweetman, A.J., 2022. Sorption and desorption of bisphenols on commercial plastics and the effect of UV aging. Chemosphere 310, 136867.

Crain, D.A., Eriksen, M., Iguchi, T., Jobling, S., Laufer, H., LeBlanc, G.A., Guillette, L.J., Jr., 2007. An ecological assessment of bisphenol-A: evidence from comparative biology. Reproductive Toxicology 24, 225-239.

de Oliveira, G.L., Ariza Gomez, A.J., Caire, M., Vaz, M.A., da Costa, M.F., 2017. Characterization of seawater and weather aged polyurethane elastomer for bend stiffeners. Polymer Testing 59, 290-295.

Fan, X., Gan, R., Liu, J., Xie, Y., Xu, D., Xiang, Y., Su, J., Teng, Z., Hou, J., 2021a. Adsorption and desorption behaviors of antibiotics by tire wear particles and polyethylene microplastics with or without aging processes. Science of the Total Environment 771, 145451.

Fan, X., Zou, Y., Geng, N., Liu, J., Hou, J., Li, D., Yang, C., Li, Y., 2021b. Investigation on the adsorption and desorption behaviors of antibiotics by degradable MPs with or without UV ageing process. J. Hazard. Mater. 401, 123363.

Fierro, V., Torné-Fernández, V., Montané, D., Celzard, A., 2008. Adsorption of phenol onto activated carbons having different textural and surface properties. Micropor. Mesopor. Mat. 111, 276-284.

Gao, Q., Li, H., Zeng, X., 2010. Preparation and characterization of UV-curable hyperbranched polyurethane acrylate. J. Coat. Technol. Res. 8, 61-66.

Gewert, B., Plassmann, M., Sandblom, O., MacLeod, M., 2018. Identification of Chain Scission Products Released to Water by Plastic Exposed to Ultraviolet Light. Environ. Sci. Technol. Lett. 5, 272-276.

Geyer, R., Jambeck, J.R., Law, K.L., 2017. Production, use, and fate of all plastics ever made. Sci. Adv. 3, 1-5.

Glausiusz, J., 2014. THE PLASTICS PUZZLE. Nature 508, 306-308.

Guo, X., Chen, C., Wang, J., 2019. Sorption of sulfamethoxazole onto six types of microplastics. Chemosphere 228, 300-308.

Ho, W.K., Law, J.C., Zhang, T., Leung, K.S., 2020. Effects of Weathering on the Sorption Behavior and Toxicity of Polystyrene Microplastics in Multi-solute Systems. Water Research 187, 116419.

Hossain, M.R., Jiang, M., Wei, Q., Leff, L.G., 2019. Microplastic surface properties affect bacterial colonization in freshwater. Journal of Basic Microbiology 59, 54-61.

Huang, Z., Zhao, J., Yang, Y., Jia, Y., Zhang, Q., Chen, C., Liu, Y., Yang, B., Xie, L., Ying, G., 2020. Occurrence, mass loads and risks of bisphenol analogues in the

Pearl River Delta region, South China: Urban rainfall runoff as a potential source for receiving rivers. Environmental Pollution 263, 114361.

Jala, A., Varghese, B., Dutta, R., Adela, R., Borkar, R.M., 2022. Levels of parabens and bisphenols in personal care products and urinary concentrations in Indian young adult women: Implications for human exposure and health risk assessment. Chemosphere 297, 134028.

Janssens, V., 2021. Plastics – the Facts 2022. Plastics Europe.

Jiang, H., Li, Q., Sun, J., Mao, Y., Liu, X., Que, S., Yu, W., Kan, Y., 2023. The Adsorption and Desorption Behavior of Bisphenol A on Five Microplastics Under Simulated Gastrointestinal Conditions. WAT. AIR AND SOIL POLL. 234, 1-14.

Jimenez-Diaz, I., Zafra-Gomez, A., Ballesteros, O., Navea, N., Navalon, A., Fernandez, M.F., Olea, N., Vilchez, J.L., 2010. Determination of Bisphenol A and its chlorinated derivatives in placental tissue samples by liquid chromatography-tandem mass spectrometry. J. Chromatogr. B 878, 3363-3369.

Liu, G., Zhu, Z., Yang, Y., Sun, Y., Yu, F., Ma, J., 2019a. Sorption behavior and mechanism of hydrophilic organic chemicals to virgin and aged microplastics in freshwater and seawater. Environmental Pollution 246, 26-33.

Liu, P., Dai, J., Bie, C., Li, H., Zhang, Z., Guo, X., Zhu, L., 2022a. Bioaccessibility of Microplastic-Associated Antibiotics in Freshwater Organisms: Highlighting the Impacts of Biofilm Colonization via an In Vitro Protocol. Environ. Sci. Technol. 56, 12267−11227.

Liu, P., Wu, X., Liu, H., Wang, H., Lu, K., Gao, S., 2020. Desorption of pharmaceuticals from pristine and aged polystyrene microplastics under simulated gastrointestinal conditions. J. Hazard. Mater. 392, 122346.

Liu, T., Wang, C., Han, Y., Bai, C., Ren, H., Liu, Y., Han, X., 2022b. Oxidative polymerization of bisphenol A (BPA) via H-abstraction by $Bi_{2.15}WO_6$ and persulfate: Importance of the surface complexes. J. Chem. Eng. 435, 134816.

Liu, X., Shi, H., Xie, B., Dionysiou, D., Zhao, Y., 2019b. Microplastics as Both a Sink and a Source of Bisphenol A in the Marine Environment. Environ. Sci. Technol. 53, 10188-10196.

Liu, X., Sun, P., Qu, G., Jing, J., Zhang, T., Shi, H., Zhao, Y., 2021. Insight into the characteristics and sorption behaviors of aged polystyrene microplastics through three type of accelerated oxidation processes. J. Hazard. Mater. 407, 124836.

Lobelle, D., Cunliffe, M., 2011. Early microbial biofilm formation on marine plastic debris. Marine Pollution Bulletin 62, 197-200.

Maquelin, K., Kirschner, C., Choo-Smith, L.P., Braak, N.v.d., Endtz, H.P., Naumann, D., Puppels, G.J., 2002. Identification of medically relevant microorganisms by vibrational spectroscopy. Journal of Microbiological Methods, 255–271.

Meghea, A., Rehner, H.H., Peleanu, I., Mihalache, R., 1998. Test-fitting on adsorption isotherms of organic pollutants from waste waters on activated carbon. J. Radioanal. Nucl. Chem. 229, 105-110.

Ortiz-Villanueva, E., Jaumot, J., Martinez, R., Navarro-Martin, L., Pina, B., Tauler, R., 2018. Assessment of endocrine disruptors effects on zebrafish (Danio rerio)

embryos by untargeted LC-HRMS metabolomic analysis. Science of the Total Environment 635, 156-166.

Peters, C.A., Thomas, P.A., Rieper, K.B., Bratton, S.P., 2017. Foraging preferences influence microplastic ingestion by six marine fish species from the Texas Gulf Coast. Marine Pollution Bulletin 124, 82-88.

Procter, J., Hopkins, F.E., Fileman, E.S., Lindeque, P.K., 2019. Smells good enough to eat: Dimethyl sulfide (DMS) enhances copepod ingestion of microplastics. Marine Pollution Bulletin 138, 1-6.

Qi, K., Lu, N., Zhang, S., Wang, W., Wang, Z., Guan, J., 2021. Uptake of Pb(II) onto microplastic-associated biofilms in freshwater: Adsorption and combined toxicity in comparison to natural solid substrates. J. Hazard. Mater. 411, 125115.

Richter, C.A., Birnbaum, L.S., Farabollini, F., Newbold, R.R., Rubin, B.S., Talsness, C.E., Vandenbergh, J.G., Walser-Kuntz, D.R., vom Saal, F.S., 2007. In vivo effects of bisphenol A in laboratory rodent studies. Reproductive Toxicology 24, 199-224.

Rosu, D., Rosu, L., Cascaval, C.N., 2009. IR-change and yellowing of polyurethane as a result of UV irradiation. Polym. Degrad. Stab. 94, 591-596.

Sandt, C., Waeytens, J., Deniset-Besseau, A., Nielsen-Leroux, C., Rejasse, A., 2021. Use and misuse of FTIR spectroscopy for studying the bio-oxidation of plastics. Spectrochim. Acta - A: Mol. Biomol. Spectrosc. 258, 119841.

Santos, O.S.H., Yoshida, M.I., Hussene, C.M.B., da Silva, M.C., 2020. Demulsification and Oil Removal from Metalworking Fluids by Polyurethane Foam as Sorbent. J. Polym. Environ. 29, 441-449.

Savoca, M.S., Wohlfeil, M.E., Ebeler, S.E., Nevitt, G.A., 2016. Marine plastic debris emits a keystone infochemical for olfactory foraging seabirds. Sci. Adv. 2, 1-8.

Sun, P., Liu, X., Zhang, M., Li, Z., Cao, C., Shi, H., Yang, Y., Zhao, Y., 2021. Sorption and leaching behaviors between aged MPs and BPA in water: the role of BPA binding modes within plastic matrix. Water Research 195, 116956.

Tang, S., He, C., Thai, P.K., Heffernan, A., Vijayasarathy, S., Toms, L., Thompson, K., Hobson, P., Tscharke, B.J., O'Brien, J.W., Thomas, K.V., Mueller, J.F., 2020. Urinary Concentrations of Bisphenols in the Australian Population and Their Association with the Per Capita Mass Loads in Wastewater. Environ. Sci. Technol. 54, 10141-10148.

Tang, S., Ma, S., Zhang, T., Liu, X., Nahid Pervez, M., Cao, C., Zhao, Y., 2023. Sorption of bisphenol A onto microplastics and associated environmental risks in comparison to engineered carbonous materials and natural media. Gondwana Res. 117, 295-306.

Tschersich, C., Murawski, A., Schwedler, G., Rucic, E., Moos, R.K., Kasper-Sonnenberg, M., Koch, H.M., Bruning, T., Kolossa-Gehring, M., 2021. Bisphenol A and six other environmental phenols in urine of children and adolescents in Germany - human biomonitoring results of the German Environmental Survey 2014-2017 (GerES V). Science of the Total Environment 763, 144615.

Vandenberg, L.N., Hauser, R., Marcus, M., Olea, N., Welshons, W.V., 2007. Human exposure to bisphenol A (BPA). Reproductive Toxicology 24, 139-177.

Vom Saal, F.S., Akingbemi, B.T., Belcher, S.M., Birnbaum, L.S., Crain, D.A., Eriksen, M., Farabollini, F., Guillette, L.J., Jr., Hauser, R., Heindel, J.J., Ho, S.M., Hunt, P.A., Iguchi, T., Jobling, S., Kanno, J., Keri, R.A., Knudsen, K.E., Laufer, H., LeBlanc, G.A., Marcus, M., McLachlan, J.A., Myers, J.P., Nadal, A., Newbold, R.R., Olea, N., Prins, G.S., Richter, C.A., Rubin, B.S., Sonnenschein, C., Soto, A.M., Talsness, C.E., Vandenbergh, J.G., Vandenberg, L.N., Walser-Kuntz, D.R., Watson, C.S., Welshons, W.V., Wetherill, Y., Zoeller, R.T., 2007. Chapel Hill bisphenol A expert panel consensus statement: integration of mechanisms, effects in animals and potential to impact human health at current levels of exposure. Reproductive Toxicology 24, 131-138.

Wang, F., Shih, K., Li, X., 2015. The partition behavior of perfluorooctanesulfonate (PFOS) and perfluorooctanesulfonamide (FOSA) on microplastics. Chemosphere 119, 841-847.

Wang, Y., Wang, X., Li, Y., Li, J., Wang, F., Xia, S., Zhao, J., 2020. Biofilm alters tetracycline and copper adsorption behaviors onto polyethylene microplastics. J. Chem. Eng. 392.

Wu, P., Cai, Z., Jin, H., Tang, Y., 2019. Adsorption mechanisms of five bisphenol analogues on PVC microplastics. Science of the Total Environment 650, 671-678.

Xiong, Y., Zhao, J., Li, L., Wang, Y., Dai, X., Yu, F., Ma, J., 2020. Interfacial interaction between micro/nanoplastics and typical PPCPs and nanoplastics

removal via electrosorption from an aqueous solution. Water Research 184, 116100-116100.

Xue, X.D., Fang, C.R., Zhuang, H.F., 2021. Adsorption behaviors of the pristine and aged thermoplastic polyurethane microplastics in Cu(II)-OTC coexisting system. J. Hazard. Mater. 407, 124835.

Zafar, R., Arshad, Z., Eun Choi, N., Li, X., Hur, J., 2023. Unravelling the complex adsorption behavior of extracellular polymeric substances onto pristine and UV-aged microplastics using two-dimensional correlation spectroscopy. J. Chem. Eng. 470.

Zhang, P., Huang, P., Sun, H., Ma, J., Li, B., 2020. The structure of agricultural microplastics (PT, PU and UF) and their sorption capacities for PAHs and PHE derivates under various salinity and oxidation treatments. Environmental Pollution 257.

Zhao, L., Rong, L., Xu, J., Lian, J., Wang, L., Sun, H., 2020. Sorption of five organic compounds by polar and nonpolar microplastics. Chemosphere 257, 127206-127206.

Zuo, L., Li, H., Lin, L., Sun, Y., Diao, Z., Liu, S., Zhang, Z., Xu, X., 2019. Sorption and desorption of phenanthrene on biodegradable poly(butylene adipate co-terephtalate) microplastics. Chemosphere 215, 25-32.

4. Investigation into the adsorption and desorption behavior of BPF and BPA onto naturally aged microplastics

This chapter presents a study of the adsorption/desorption behavior of BPF and BPA on plastics particles and their interaction mechanisms. An important difference in this chapter is that the studies in Chapter 2 and Chapter 3 have used artificially aged plastic particles whereas in this study naturally aged microplastics collected in two UK estuaries have been used to carry out the adsorption/desorption experiments, providing more real environmental- related data.

Graphical abstract
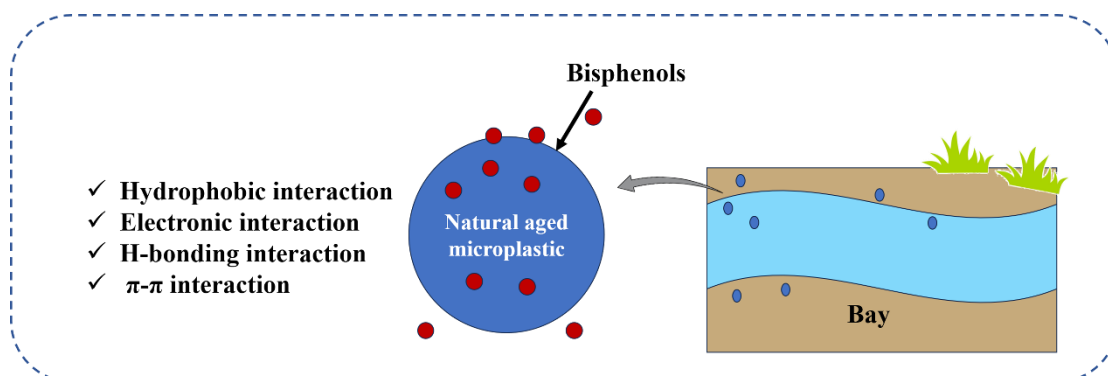
Abstract

In this study, the adsorption behavior of bisphenols on naturally aged and fresh microplastics (polyethene (PE), polypropylene (PP), expanded polystyrene (EPS)) was investigated. The results demonstrated that naturally aged microplastics exhibited higher adsorption capacity for bisphenols compared to fresh microplastics, with the adsorption mechanism involving H-bonding interaction, π-π interaction. The adsorption kinetics were better described by the pseudo-second order model. The adsorption isotherm of bisphenols onto microplastics could be described well by the Langmuir model, with the adsorption process being monolayer adsorption. In addition, the adsorption ability of BPF was higher than BPA following the order: BPF > BPA for both fresh and naturally aged microplastics, which indicates hydrophobicity is an important factor affecting the sorption/desorption behavior. This study also showed that the adsorption capacity of bisphenols was higher in artificial seawater and humic acid solutions than ultrapure water, which indicates that stronger carrier effects of bisphenols could be expected in marine environments and with dissolved organic matter (DOM) in surface waters. This study expands our understanding on the environmental

risks from microplastic debris and help the evaluation the interaction behavior of naturally aged microplastics with pollutants in the environment.

4.1 Introduction

It has been widely reported that microplastics have been found in oceans, lakes, rivers, reservoirs, and even polar regions (Di and Wang, 2018). The widespread distribution of microplastics could pose a potential threat to aquatic biota and human health as microplastics debris have been shown to be an important vector for chemical pollutant transport in the environment. Thus, exploring adsorption and desorption mechanisms of aged microplastics could help assess the potential exposure risk. Chapter 2 and Chapter 3 assessed UV irradiation and biofilms colonization on the effect of microplastics interaction behavior with bisphenols. However, these studies were all based on the laboratory aging experiments, whilst little is known about the adsorption/desorption behavior of naturally aged microplastics.

In this study, the naturally aged microplastics were collected from two estuaries located in Plymouth and Southampton in the United Kingdom. We carried out the adsorption/desorption experiments and compared them to virgin microplastics to investigate the interaction mechanism of naturally aged microplastics, also comparing the results with our laboratory aged plastic particles. Bisphenol A (BPA) and bisphenol F (BPF) are two widely used bisphenols and were selected as target contaminants to explore the interaction behavior with microplastics (Rochester and Bolden, 2015). Changing environmental conditions are also critical factors in the adsorption/desorption

150

of contaminants on microplastics. Salinity, pH, and dissolved organic matter (DOM) are some factors that influence adsorption characteristics in the aquatic environment and are thus important aspects that need to be evaluated. As a result, the adsorption and desorption behavior were also assessed under different aquatic conditions (ultrapure water, artificial seawater, humic acid (HA) water) to clarify different exposure environments on microplastic adsorption/desorption behaviors.

4.2 Materials and methods

4.2.1 Materials and chemicals

Naturally aged microplastics were collected along the edge of two estuaries located in Plymouth (United Kingdom) and Southampton (United Kingdom), respectively. These naturally aged microplastics were sent back to the laboratory for further characterization and analysis. The microplastic surface was carefully rinsed with ultrapure water to eliminate the attached surface impurities and air-dried before further study. Fourier-transform infrared spectroscopy ((FTIR, Agilent, USA) was used to confirm the types of microplastics, scanning from 4000 to 400 cm^{-1} with 4 cm^{-1} resolutions. The FTIR spectra showed that the types of those microplastics mainly including polyethylene (PE), expanded polystyrene (EPS) and polypropylene (PP). We classified and labelled them as A-PE1 (naturally aged PE1), A-PE2 (naturally aged PE1), A-EPS (naturally aged EPS) and A-PP (naturally aged PP), details about sampling sites are contained in Table S1. Fresh PE and PP microplastic pellets were

purchased from Poli Plastic Pellets Ltd. UK, fresh EPS was collected from a shockproof packaging and cut into small pieces that similar with A-EPS.

Acetonitrile and Methanol (HPLC grade) were purchased from Fisher Scientific Ltd (UK). Standards of BPF and BPA (purity ≥ 98 %) were purchased from Sigma-Aldrich Co. LLC (UK). Stock BPF and BPA mixed solution (100 mg/L) was prepared in methanol and diluted into 20, 50, 100, 200, 500, 700 and 1000 μg/L with ultrapure water. To avoid solvent effects, the volume percentage of methanol was kept less than 0.1 % (v/v), and all solutions were kept at 4 ℃. The Humic acid (HA) was purchased from Sigma-Aldrich Co. LLC (UK). The artificial seawater was obtained from Brightwell Aquatics (USA).

4.2.2 Characterization of microplastics

The surface morphological and structural differences between fresh and naturally aged microplastics were characterized via scanning electron microscope (SEM, JEOL JSM 7800F). Surface functional groups of microplastics in different states were qualitatively detected by FTIR and recorded in the range of 4000–400 cm^{-1}.

4.2.3 Adsorption and desorption experiments

Prior to the adsorption experiments, three control experiments were performed: (1) 100 mg microplastic samples (20 mg for EPS) were added to 15 mL ultrapure water to determine if microplastic materials contained and leached BPF and BPA. (2) 15 mL 100 μg/L BPF and BPA mixed solutions were placed into glass tubes to confirm if the glass tubes would adsorb bisphenols. Results showed that no BPF and BPA leached

from both plastic materials and tubes, the loss of bisphenols in tubes was less than 2 %. In the adsorption experiments, fresh and aged microplastic (100 mg for PE and PP microplastics, 20 mg for EPS owing to the light weight) and 15.0 mL of bisphenol solution (BPF and BPA) were added to glass tubes and placed on an orbital shaker at room temperature (25 °C) and 150 rpm. Owing to the sensitivity of the HPLC instrument being used to assess the interaction behavior and mechanism between bisphenols and microplastics the adsorption experiments were conducted at higher concentrations of the bisphenols than those typically found in the environment. Adsorption kinetic experiments were conducted with the BPF and BPA mixed solution concentration fixed at 100 μg/L, and time was assessed at 2, 4, 8, 12, 24, 48, 72, 120, 168 h. Adsorption isotherm experiments were performed with bisphenol concentrations set as 20, 50, 100, 200, 500, 700 and 1000 μg/L. All experiments were performed in triplicate. Before analyses, the samples were filtered with 0.2 μm PTFE filters to remove the suspended microplastics in the solution.

After the adsorption kinetics experiment, the microplastic samples were collected and a total of 100 mg of dried PE, PP microplastics, 20 mg EPS and 15 mL ultrapure water were added in glass tubes, shaken at 150 rpm. At present time intervals from 0 to 120 h, samples were collected and filtered through PTFE filter membranes, and the concentration of bisphenols was analyzed by HPLC instrument.

In addition to experiments carried out in ultrapure water to assess the adsorption behavior in fresh water systems, additional experiments were also carried out in two

further matrices: (1) artificial seawater (ASW) to assess the adsorption/desorption behavior of BPA in marine systems; (2) humic acid solution (HA, a typical representation of DOM in the environment) at a concentration of 15 mg L^{-1} to assess the present of DOM for the effect of adsorption/desorption behavior. Since DOM is present in natural waters with concentrations much higher than organic pollutants, preloading MPs with DOM can give more realistic insights on the adsorption behavior of microplastics in natural water systems (Ateia et al., 2020). The methods used for sample preparation and analysis of bisphenols was the same as those described above.

4.2.4 Instrument analysis

The analyses were performed on a Shimadzu NexeraX2 ultra high-performance liquid chromatography (UHPLC) with RF-20AXS fluorescence detector. The excitation wavelength and emission wavelength were set at 226 nm and 315 nm. Phenomenex C18 column (4 μm, 150 × 4.6 mm) was used for samples analysis. Chromatographic separation was performed with a mobile phase of A: ultrapure water and B: acetonitrile (ACN). The gradient began at 50% ACN, then decreased to 60% ACN within 4 min, followed by reaching 90% ACN at 7 min and decreased to 50% ACN at 10 min, finally, 2 min of post-ran ensured equilibrium of the column before the next injection. The injection volume was 50 μg/L and the tray temperature was kept at 30 °C. Samples were prepared in ultrapure water/artificial seawater/HA water and methanol (4:1, v/v).

4.3 Results and discussions

4.3.1 Characterization of microplastics

The morphology of the naturally aged microplastics is shown in Figure S1. It was obvious that the most of the naturally aged microplastics showed yellowing or degradation compared to fresh microplastics. The SEM images of fresh and aged microplastics are shown in Figure 1. The surface of F-PE had a few bumps and dents, while the surface of aged PE had undergone some changes with the surface becoming a little rougher for A-PE1 compared with F-PE. For A-PE2, cracks and pits were obvious on the surface. Similar changes were also observed for PP microplastics. The surface of F-PP was relatively smooth, but became rough after aging. For F-EPS, some holes were observed on the surface. After the natural aging process, more voids crinkles appeared on the surface of EPS.
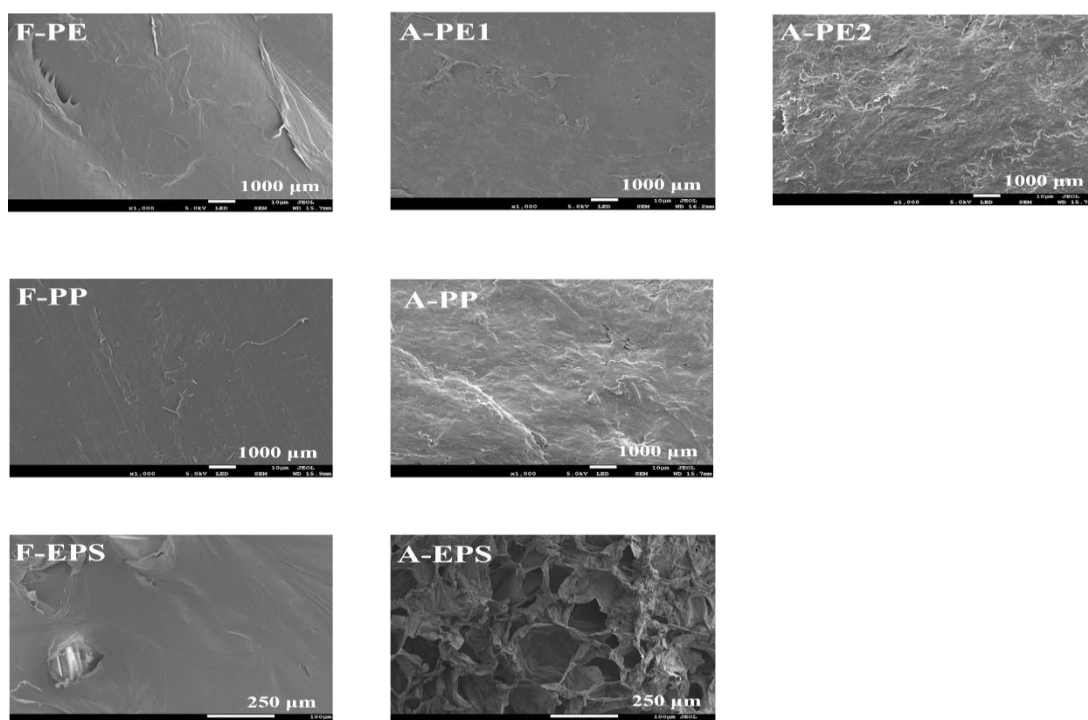
Figure 1. SEM images of fresh and naturally aged microplastics.
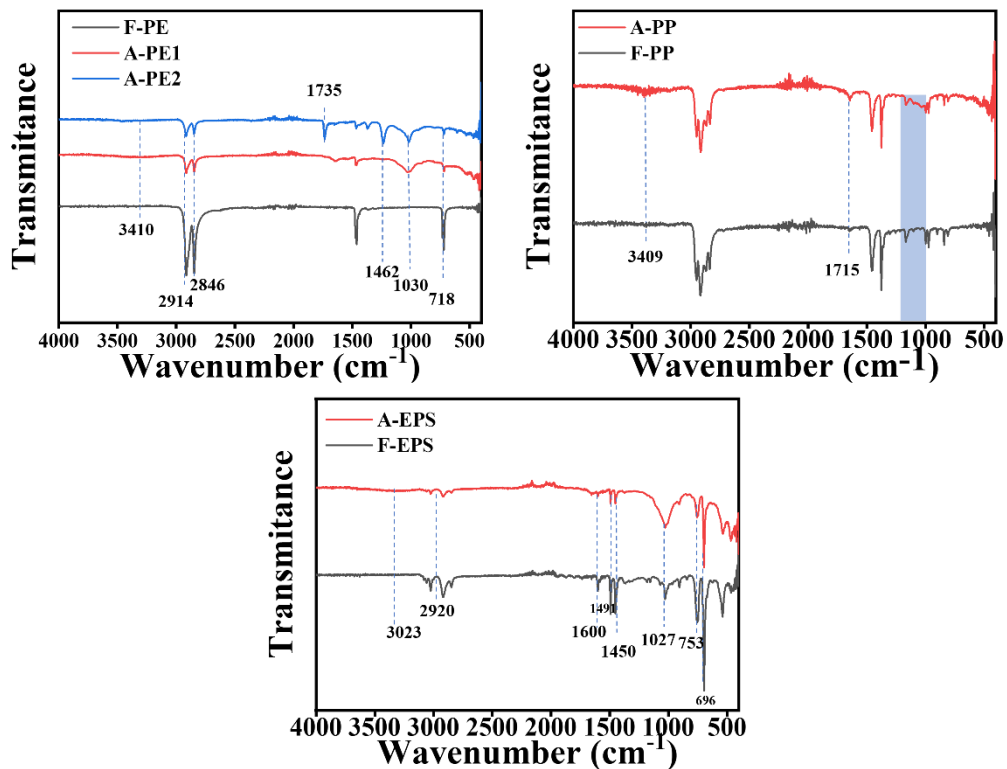
Figure 2. FTIR spectrum of fresh and naturally aged microplastics.

The surface functional groups of fresh and naturally aged microplastics were characterized by FTIR and the results shown in Figure 2. Previous studies have suggested that free radicals are formed from the breaking of C–H bonds in the aging process of microplastics with oxidation of functional groups generated by the reaction between oxygen and radicals (Guo and Wang, 2019b; Liu et al., 2019c). For PE, the peaks at 2914 cm^{-1}, 2846 cm^{-1}, 1462 cm^{-1} and 718 cm^{-1} corresponded to the C–H stretching vibration, which attributed to –CH$_2$ asymmetric stretching, symmetric stretching, bending deformation, and rocking deformation, respectively (Gulmine et al., 2002). All band intensity decreased in naturally aged PE microplastics compared to fresh microplastics. The intensity of the peaks at 3410 cm^{-1} slightly increased, with the peak corresponding to O–H. Compared to F-PE, a broadened peak located at 1030 cm^{-1}

was observed on the A-PE, which may be attributed to the C–O–C stretching of ester (Liu et al., 2022d). In addition, a new peak at around 1735 cm^{-1} was generated for A-PE1, which corresponds to C=O stretching. As for PP microplastics, the new peaks generated at 3409 cm^{-1} and 1715 cm^{-1} represent O–H and C=O bonds, respectively. In addition, the peaks between 1300-1000 cm^{-1} originated from the C–O stretching vibration (Liu et al., 2022b), which showed an obvious change after aging. The results indicated that the functional groups on the surface of the aged microplastics were oxidized by the aging process. For EPS, the characteristic peaks at 3023 cm^{-1} and 2920 cm^{-1} corresponded to the extension of =C–H bond of the benzene ring and single bond of –CH$_2$ asymmetric stretching vibration, respectively, with the vibration decreasing for A-EPS (Wang et al., 2022c). Compared with F-EPS, the stretching at 1600 cm^{-1}, 1491 cm^{-1} and 1450 cm^{-1} obviously changed for A-EPS, which represented the deformation vibration of the C=C of benzene ring skeleton (Wang et al., 2023b). The vibration bands at 1027 cm^{-1}, 753 cm^{-1} and 696 cm^{-1} were attributed to the C–H bending vibration for the benzene ring, which also showed obvious differences after aging (Budlayan et al., 2021; Hou et al., 2021; Osman et al., 2022).

4.3.2 Adsorption kinetics and isotherms of microplastics

The results of the adsorption kinetics experiments are shown in Figure S2. The adsorption of BPF and BPA by microplastics is rapid in the initial stages, and then gradually slows down. For both BPF and BPA, adsorption increased substantially in the first 4 h after the beginning of the adsorption experiments, and then slowed down

until reaching adsorption equilibrium. The time needed for reaching adsorption equilibrium was within 12 h for BPF and BPA on most fresh and aged microplastics.

Table 1. Kinetic parameters for BPF and BPA adsorption by fresh and naturally aged microplastics.

Chemicals	Microplastics	q_e* (µg/g)	pseudo-first order parameters			pseudo-second order parameters		
			q_e	k_1	R^2	q_e	k_2	R^2
	F-PE		0.097	0.0343	0.554	0.396	1.066	**0.999**
	A-PE1		0.167	0.019	0.356	0.851	0.665	**0.999**
	A-PE2		0.347	0.018	0.302	0.957	1.208	**0.999**
BPF	F-PP		0.030	0.101	0.335	0.356	0.551	**0.996**
	A-PP		0.079	2.531	0.349	0.713	1.904	**0.999**
	F-EPS		0.740	0.001	0.127	5.388	1.208	**0.996**
	A-EPS		9.764	0.033	0.274	28.876	0.008	**0.996**
	F-PE		0.163	0.024	0.453	0.672	0.590	**0.998**
	A-PE1		0.224	0.030	0.541	1.457	0.385	**0.999**
	A-PE2		0.136	0.016	0.491	1.457	0.476	**0.999**
BPA	F-PP		0.060	0.158	0.899	0.530	0.485	**0.996**
	A-PP		0.283	0.030	0.646	1.201	0.434	**0.999**
	F-EPS		1.936	0.022	0.274	16.015	0.0371	**0.999**
	A-EPS		0.283	0.030	0.990	35.435	0.002	**0.992**

The kinetics data were fitted by pseudo-first order models and pseudo-second order models (Figure S3 and Figure S4), with the values of kinetic models' parameters listed in Table 1. According to the R^2 values, the pseudo-second-order model fits better

than the pseudo-first order model, which was similar to the results of the adsorption

kinetics experiments with laboratory aged microplastics described in Chapter 2 and

Chapter 3.

The adsorption isothermal curves of BPF and BPA onto microplastics at different

initial concentrations (20 – 1000 μg/L) are shown in Figure 3. The results indicated that

the adsorption amount of both BPF and BPA increased with the equilibrium

concentrations, and the adsorption process showed an obvious non-liner trend. The

adsorption rate was fast at the relatively low concentration (less than 100 μg/L), which

may be attributed to adequately available adsorption sites for bisphenols at low

concentrations. When the concentration of bisphenols continued to increase, the

adsorption tendency slowed down because the adsorption reached a certain amount

affecting subsequent adsorption (Liu et al., 2022d).
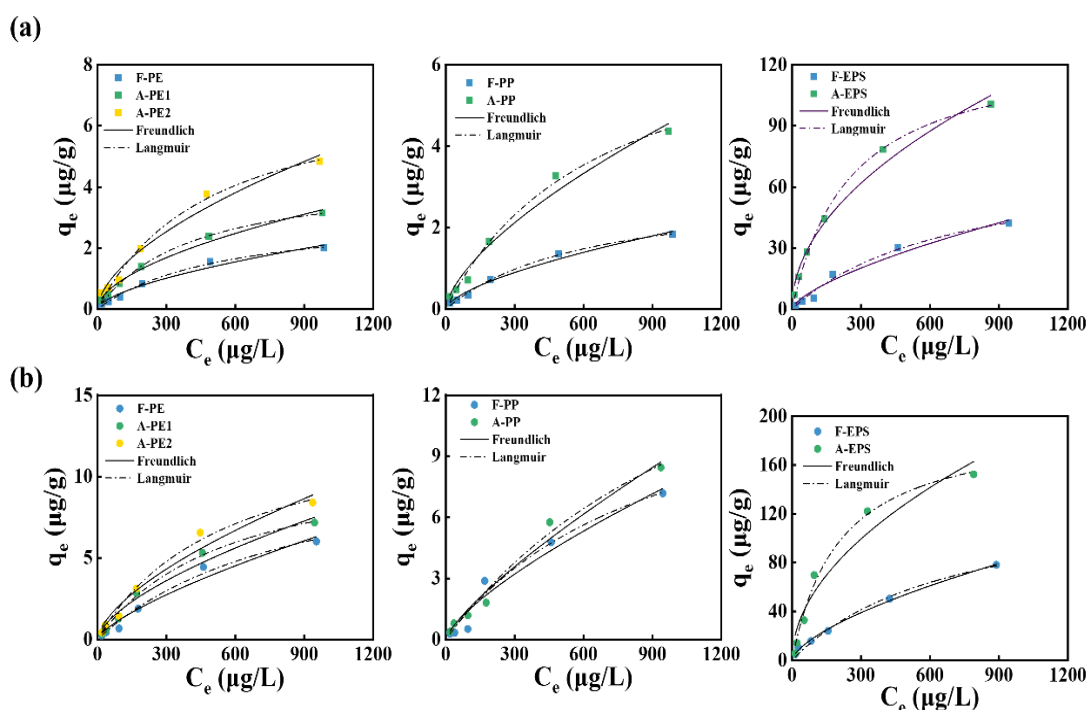
Figure 3. Adsorption isotherms of BPF (a) and BPA (b) on fresh and aged microplastics.

Table 2. Parameters of the isotherm models for adsorption of BPF and BPA on microplastics.

| Chemicals	Microplastics	Freundlich			Langmuir		
		K_F	n	R^2	q_m	K_L	R^2
BPF	F-PE	0.030	1.631	0.976	3.180	0.0017	**0.994**
	A-PE1	0.070	1.796	0.988	4.464	0.0024	**0.998**
	A-PE2	0.089	1.703	0.975	7.435	0.0019	**0.988**
	F-PP	0.024	1.582	0.984	3.037	0.0015	**0.996**
	A-PP	0.051	1.533	0.978	7.516	0.0014	**0.993**
	F-EPS	0.427	1.479	0.969	74.464	0.0014	**0.986**
	A-EPS	3.581	2.002	0.983	129.322	0.0039	**0.997**
BPA	F-PE	0.044	1.383	0.968	12.035	0.0011	**0.986**
	A-PE1	0.094	1.567	0.974	11.649	0.0017	**0.995**
	A-PE2	0.117	1.583	0.967	13.779	0.0017	**0.990**
	F-PP	0.049	1.369	0.957	14.282	0.0010	**0.970**
	A-PP	0.041	1.277	0.978	21.531	0.0007	**0.986**
	F-EPS	0.987	1.835	0.996	138.832	0.0014	**0.999**
	A-EPS	5.440	1.963	0.941	194.733	0.00048	**0.990**

The Langmuir and Freundlich isotherms are shown in Figure 3, and the relevant parameters are summarized in Table 2. The Langmuir model's R^2 value (0.970-0.999) was higher than the Freundlich models (range from 0.941-0.996), which indicates that Langmuir could more accurately describe the adsorption process. As the Langmuir isotherm assumes a homogenous adsorbent surface covered by a monolayer of adsorbate molecules, and a finite number of adsorption sites (Wagstaff et al., 2022),

monolayer coverage might be the predominant mechanism for the adsorption of bisphenols on fresh and aged PE, PP and EPS microplastics, which is similar to results reported in a recent study about sorption of BPA on microplastics (Jiang et al., 2023).

4.3.3 Adsorption capacity and mechanism

As illustrated in Figure 3, the adsorption capacity of naturally aged microplastics were higher than fresh microplastics, which might be related to the physiochemical property changes during the aging process. The cracks in the plastics shown in SEM images (Figure 1) indicates that aging could offer more available adsorption sites. In addition, the generation of oxidation functional groups might suggest enhanced interaction behavior between bisphenols and microplastics. Figure 4 shows the FTIR spectrum of microplastics after adsorption bisphenols. As for naturally aged PE and PP microplastics, the vibration of characteristic O–H peak slightly increased after adsorbing BPA and BPF, indicating the H-bonding interaction between bisphenols and A-PE1, A-PE2 and A-PP. Generally, the adsorption of both BPF and BPA were higher on A-PE2 microplastics compared with A-PE1, which might be due to more cracks and pits on the surface of A-PE2 which offer more available adsorption sites than A-PE1. F-PE and F-PP, only have simple C–H in their structure, so there was no significant change in the chemical functional groups after adsorption. Although π-π interactions were expected to exist between F-EPS and bisphenols, no obvious changes on FTIR spectrum after adsorption bisphenols were observed (Figure 4). This means that π-π interactions did not dominate the adsorption mechanism for BPA on F-EPS. The high

adsorption ability of F-EPS for bisphenols might be due to the high-water retention ability increasing external surface contact area with bisphenols. Moreover, the holes in the structure of EPS might also increase the available adsorption sites. As for A-EPS, the O–H stretching and C=C stretching vibration was enhanced after adsorption of bisphenols, which indicates H-bonding interaction and π-π interaction was involved in the adsorption of bisphenols on A-EPS.
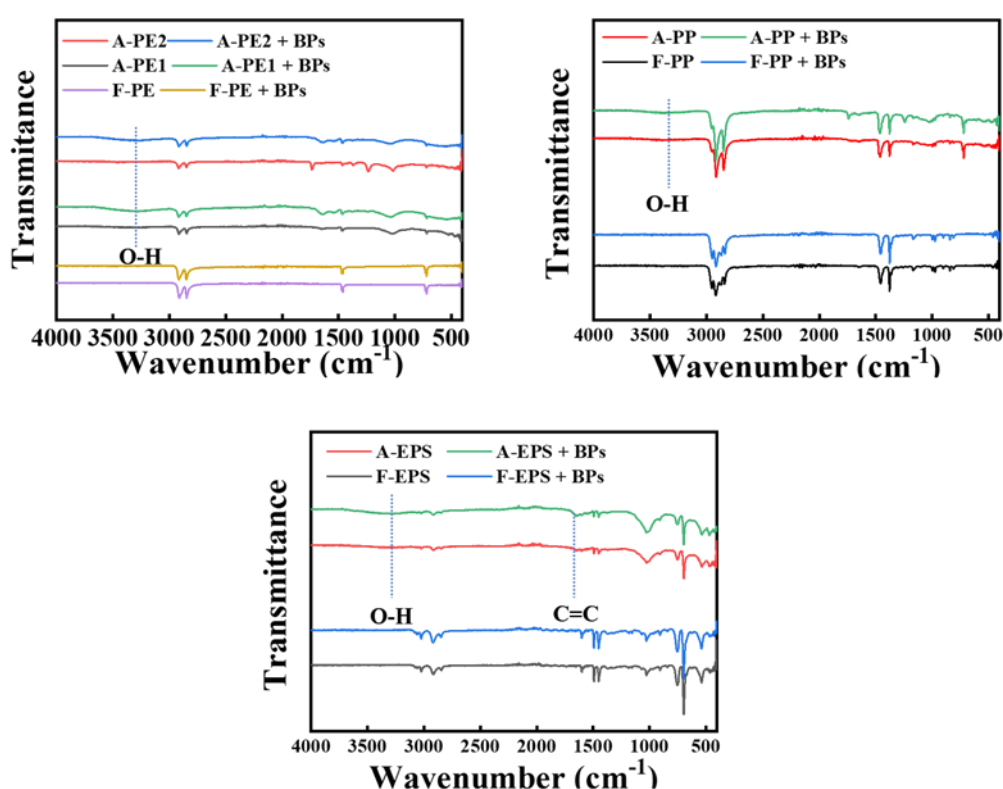
Figure 4. FTIR spectrum of the fresh and aged microplastics after adsorbing bisphenols (BPs).

For both fresh and aged microplastics, the adsorption ability followed the order: BPA > BPF, which is positively correlated with their octanol/water partition coefficients ($\log K_{ow}$), and illustrates that hydrophobicity was also an important factor affecting the adsorption behavior for fresh and aged microplastics. Moreover, as

illustrated in chapter 2 (section 2.3.2.3), BPF was present in both non-ionized and anionic forms in ultrapure water. The pH point of zero charges (pH_{pzc}) for PE, PP and PS microplastics are at around 5.76, 5.59 and 5.85, respectively (Li et al., 2019). In this study, the pH_{pzc} of the microplastics was lower than the pH of the ultrapure water (pH= 6.8) and therefore carried a negative surface charge under the experimental pH value. Thus, electrostatic repulsive-forces might also exist between microplastics and BPF, leading to the reduced adsorption ability of BPF on microplastics.

4.3.4 Desorption behavior

Data on the desorption kinetics are shown in Figure S5. and the desorption capacity date are contained in Table 3. The desorption efficiency for both fresh and naturally aged plastics followed the order: BPF > BPA, which is negatively correlated with their hydrophobicity. The microplastics aging process reduced the desorption efficiency of bisphenols. Owing to the cracks in the microplastics, more bisphenols were able to diffuse to the inside of the structure (Sun et al., 2021) or the narrow pores (Fan et al., 2021a) of the plastics, which indicates it is more difficult for aged microplastics to release bisphenols compared with those bisphenols sorbed on the surfaces of fresh plastics. In addition, the enhanced chemical bonding interaction resulted in the increased affinity of bisphenols to aged microplastics and leading to lower desorption efficiency compared with fresh microplastics.

Table 3. The desorption efficiency of BPF and BPA on microplastics.

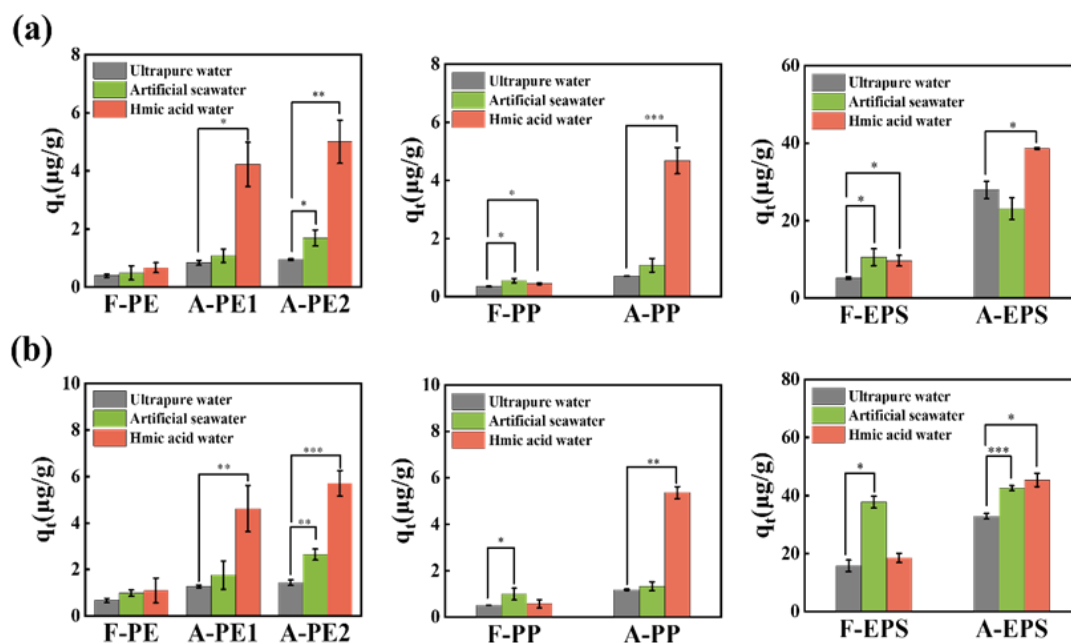| Microplastics	BPF	BPA
F-PE	68.4 %	43.8 %
A-PE1	41.6 %	35.8 %
A-PE2	39.5 %	36.1 %
F-PP	81.6 %	58.5 %
A-PP	44.8 %	29.0 %
F-EPS	47.8 %	26.1 %
A-EPS	16.7 %	15.8 %

Although the desorption efficiency decreased after the aging process, the increased adsorption capacity could potentially lead to greater pollutant release to the environment. For example, the desorption efficiencies of BPF and BPA on F-EPS were 47.8 % and 26.1 %, respectively, which decreased to 16.7 % and 15.8 % after aging. Whereas, the desorption capacity showed an increased trend as the adsorption capacity of BPF increased from 2.4 μg/g to 4.6 μg/g and BPA increased from 4.1 μg/g to 5.2 μg/g after aging.

4.3.5 Effect of relevant environmental factors

As shown in Figure 5, the adsorption capacity of naturally aged microplastics was still higher than fresh microplastics in both artificial seawater and HA solution ($p < 0.05$), which indicates a higher pollutant loading potential for microplastics in aquatic systems. Moreover, the adsorption capacity increased for most fresh and aged plastics in seawater and the HA solution compared with ultrapure water (T-test, $p < 0.05$), which

showed a similar adsorption trend with the laboratory aged microplastics described in chapter 2 (section 2.3.3.1).

Figure 5. The effect of water matrix on the adsorption of BPF (a) and BPA (b) on fresh and naturally aged microplastics.

Salting-out effect could reduce the solubility of bisphenols (hydrophobic compounds) in artificial seawater, which would enhance their hydrophobic interactions with microplastics (Liu et al., 2019a). It is possible that HA could act as a bridge between bisphenols and microplastics via bond interactions (H-bonding interaction, π-π interaction), leading to higher adsorption capacity. As F-PE and F-PP do not interact with HA via chemical bonds, adsorption was only marginally affected by HA on F-PE and F-PP microplastics (T-test, $p > 0.05$). However, the adsorption of BPF in the HA solution was significantly higher than in ultrapure water (T-test, $p < 0.05$) for F-PP microplastics. This might be due to the reduced repulsive force between BPF and

microplastics in the HA solution which could also result in the enhanced adsorption affinity. In addition, the adsorption capacity of BPA was still higher than BPF, which suggest that hydrophobicity is still important for the adsorption behavior of fresh and aged microplastics in both seawater and HA solution.
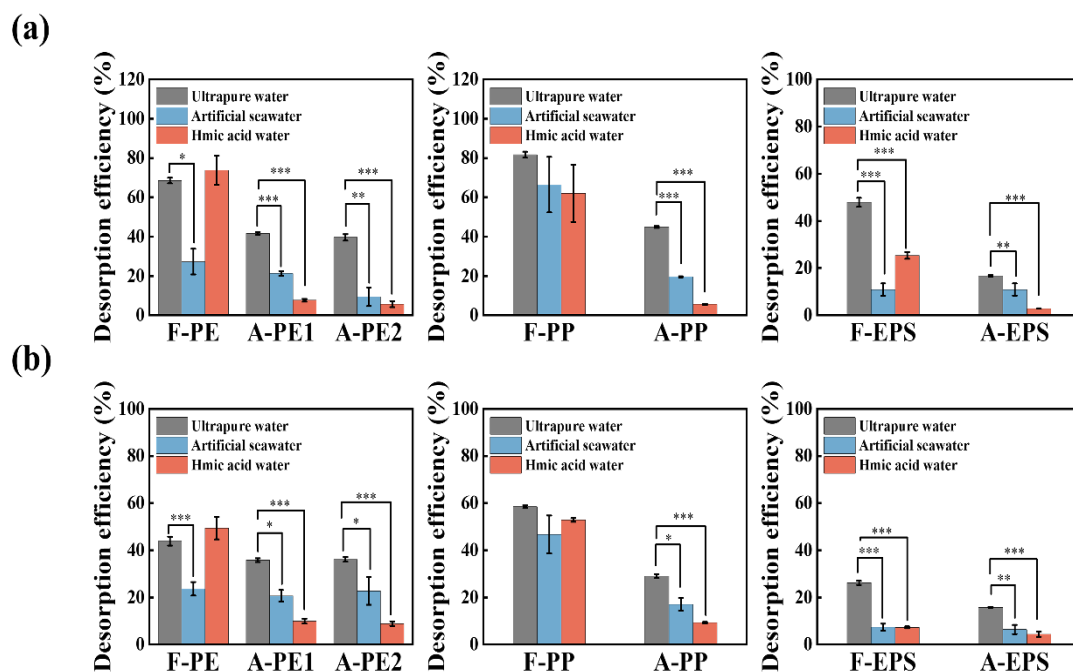
Figure 6. The effect of water matrix on the desorption efficiency of BPF (a) and BPA (b) on fresh and naturally aged microplastics.

The desorption efficiency also followed the order: BPF > BPA in both artificial seawater and HA solution (Figure 6), which is negative related to the hydrophobicity of bisphenols. In addition, the desorption efficiency of bisphenols decreased for most fresh and aged microplastics in artificial seawater and HA solution, which might be due to the salinity and DOM enhanced affinity of bisphenols, leading to a decreased desorption ability compared with ultrapure water.

4.4 Conclusions

This study investigated BPF and BPA adsorption/desorption performance and interaction mechanisms on naturally aged microplastics. The data generated revealed that the morphology of microplastics changed and new structural groups were produced after aging, and that the sorbing capacity increased. It can be seen that aging substantially affects the adsorption of microplastics. Although, the desorption efficiency decreased after microplastics aging, desorption capacity might be increased owing to potentially higher pollutant loading on aged microplastics. As a result, aging of plastic debris might increase the potential release risk of pollutants to the aquatic environment. In addition, artificial seawater and the presence of HA increased the adsorption capacity of bisphenols on most fresh and aged microplastics. These results indicate that environmental factors (e.g., salinity, pH, DOM) can affect the adsorption behavior between microplastics and pollutants. These findings are similar to the results presented in Chapter 2 and Chapter 3, where the adsorption mechanisms involved chemical bonding interactions (e.g., H-bonding interaction, π-π interaction). Moreover, electrostatic interaction, hydrophobicity of pollutants and roughness of microplastics were also important factors that affect the adsorption/desorption behavior of bisphenols onto aged plastic particles.
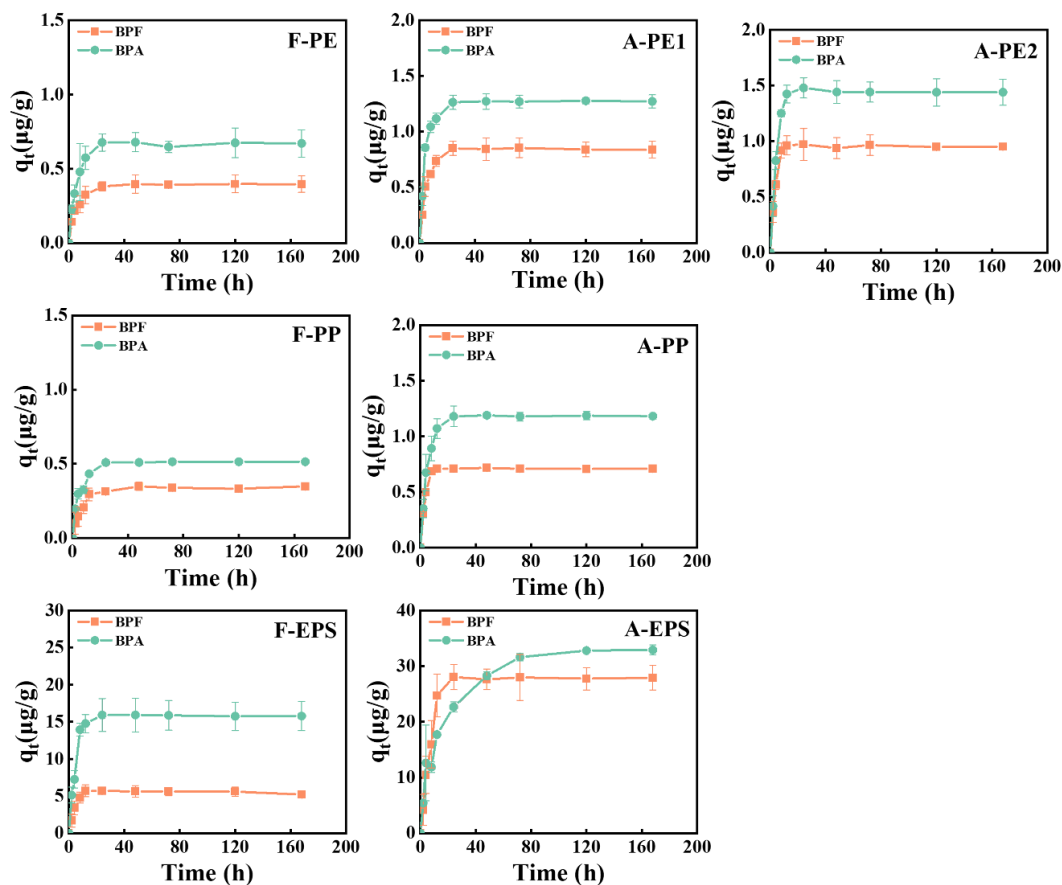
Table S1. Sampling sites of naturally aged microplastics.

Microplastic type	Sampling location
A-PE1	Chessel Bay
A-PE2	Whitsand Bay
A-EPS	Chessel Bay
A-PP	Whitsand Bay

Figure S1. Fresh and naturally aged microplastics.

Figure S2. Adsorption kinetics of BPF and BPA on fresh and aged plastics. Error bars

are the means ± standard deviation (SD) of three repeats.
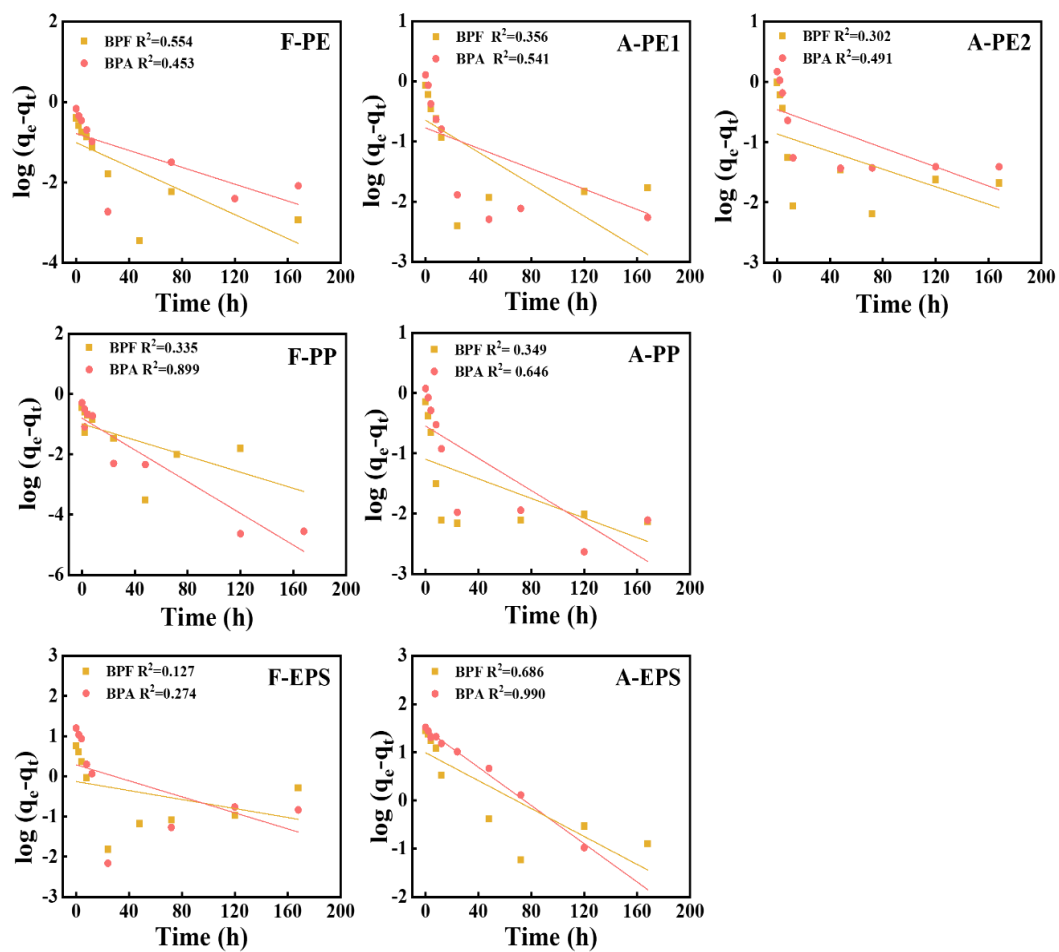
Figure S3. Pseudo-first order model of fresh and naturally aged microplastics.
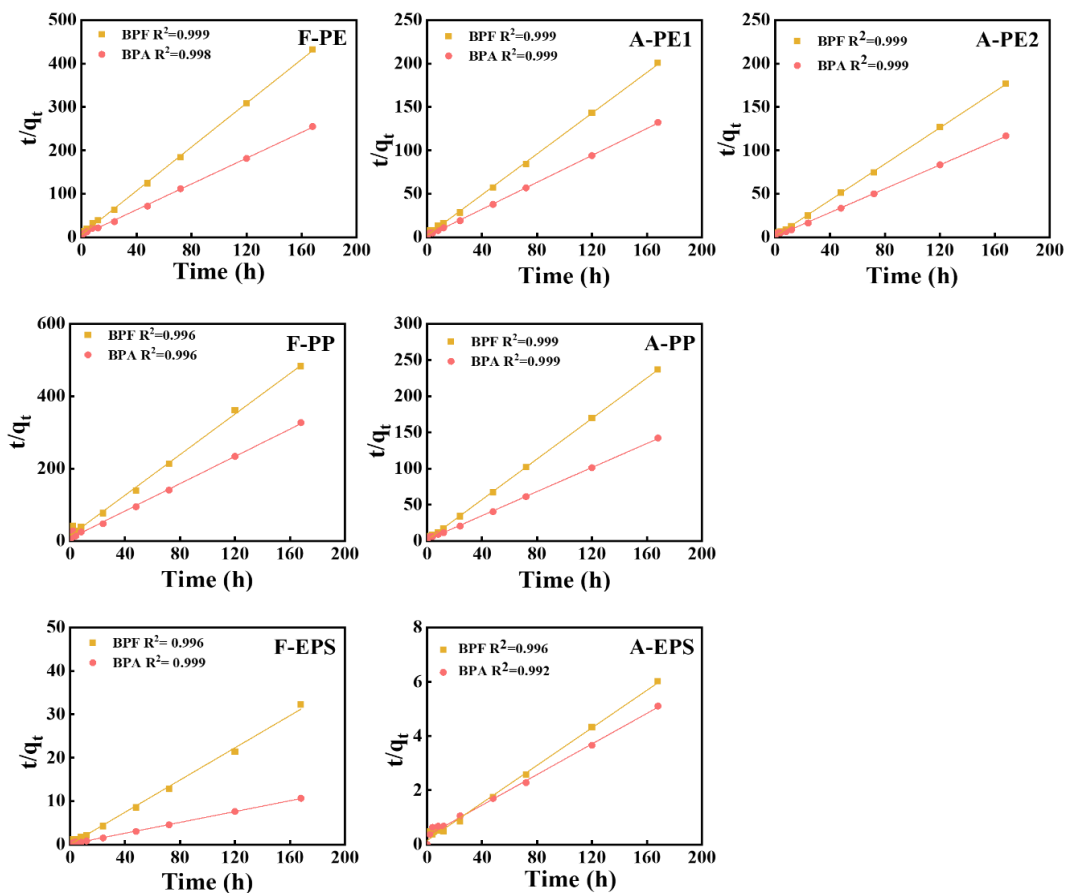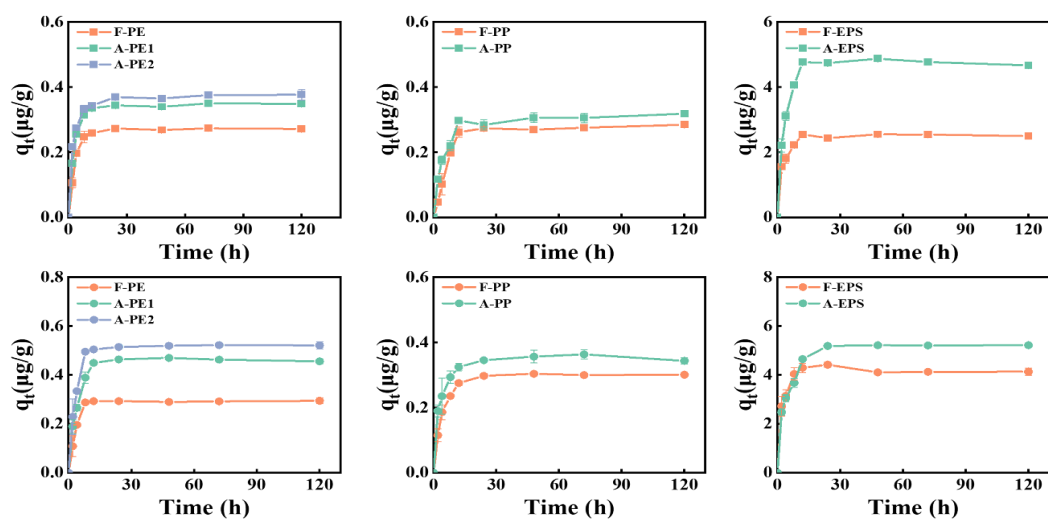
Figure S4. Pseudo-second order model of fresh and naturally aged microplastics

Figure S5. Desorption kinetics of bisphenols from fresh and naturally aged microplastics.

References

Ateia, M., Zheng, T., Calace, S., Tharayil, N., Pilla, S., Karanfil, T., 2020. Sorption behavior of real microplastics (MPs): Insights for organic micropollutants adsorption on a large set of well-characterized MPs. Science of the Total Environment 720.

Budlayan, M.L.M., Patricio, J.N., Lagare-Oracion, J.P., Arco, S.D., Alguno, A.C., Basilio, A., Latayada, F.S., Capangpangan, R.Y., 2021. Improvised centrifugal spinning for the production of polystyrene microfibers from waste expanded polystyrene foam and its potential application for oil adsorption. Journal of Engineering and Applied Science 68.

Di, M., Wang, J., 2018. Microplastics in surface waters and sediments of the Three Gorges Reservoir, China. Science of the Total Environment 616, 1620-1627.

Fan, X., Gan, R., Liu, J., Xie, Y., Xu, D., Xiang, Y., Su, J., Teng, Z., Hou, J., 2021. Adsorption and desorption behaviors of antibiotics by tire wear particles and polyethylene microplastics with or without aging processes. Science of the Total Environment 771, 145451.

Gulmine, J., Janissek, P., Heise, H., Akcelrud, L., 2002. Polyethylene characterization by FTIR. Polymer testing 21, 557-563.

Guo, X., Wang, J., 2019. Sorption of antibiotics onto aged microplastics in freshwater and seawater. Marine Pollution Bulletin 149, 110511.

Hou, P., Qu, Y., Li, P., Wang, Q., Luo, S.H., 2021. Controllable synthesis of polystyrene microspheres used as template and in-situ carbon source for Li2MnSiO4 cathode material to boost lithium-ion batteries performance. International Journal of Energy Research 46, 1711-1721.

Jiang, H., Li, Q., Sun, J., Mao, Y., Liu, X., Que, S., Yu, W., Kan, Y., 2023. The Adsorption and Desorption Behavior of Bisphenol A on Five Microplastics Under Simulated Gastrointestinal Conditions. WAT. AIR AND SOIL POLL. 234, 1-14.

Li, X., Mei, Q., Chen, L., Zhang, H., Dong, B., Dai, X., He, C., Zhou, J., 2019. Enhancement in adsorption potential of microplastics in sewage sludge for metal pollutants after the wastewater treatment process. Water Research 157, 228-237.

Liu, F.-f., Liu, G.-z., Zhu, Z.-l., Wang, S.-c., Zhao, F.-f., 2019a. Interactions between microplastics and phthalate esters as affected by microplastics characteristics and solution chemistry. Chemosphere 214, 688-694.

Liu, G., Zhu, Z., Yang, Y., Sun, Y., Yu, F., Ma, J., 2019b. Sorption behavior and mechanism of hydrophilic organic chemicals to virgin and aged microplastics in freshwater and seawater. Environmental Pollution 246, 26-33.

Liu, N., Yu, F., Wang, Y., Ma, J., 2022a. Effects of environmental aging on the adsorption behavior of antibiotics from aqueous solutions in microplastic-graphene coexisting systems. Sci Total Environ 806, 150956.

Liu, S., Huang, J., Zhang, W., Shi, L., Yi, K., Zhang, C., Pang, H., Li, J., Li, S., 2022b. Investigation of the adsorption behavior of Pb(II) onto natural-aged microplastics as affected by salt ions. Journal of Hazardous Materials 431.

Osman, A.F., Badawi, M.S., Roumie, M., Awad, R., 2022. Effect of PbO Incorporation with Different Particle Sizes on Structural and Mechanical Properties of Polystyrene.

Rochester, J.R., Bolden, A.L., 2015. Bisphenol S and F: A Systematic Review and Comparison of the Hormonal Activity of Bisphenol A Substitutes. Environmental Health Perspectives 123, 643-650.

Sun, P., Liu, X., Zhang, M., Li, Z., Cao, C., Shi, H., Yang, Y., Zhao, Y., 2021. Sorption and leaching behaviors between aged MPs and BPA in water: the role of BPA binding modes within plastic matrix. Water Research 195, 116956.

Wagstaff, A., Lawton, L.A., Petrie, B., 2022. Polyamide microplastics in wastewater as vectors of cationic pharmaceutical drugs. Chemosphere 288, 132578.

Wang, L., Guo, C., Qian, Q., Lang, D., Wu, R., Abliz, S., Wang, W., Wang, J., 2023. Adsorption behavior of UV aged microplastics on the heavy metals Pb(II) and Cu(II) in aqueous solutions. Chemosphere 313, 137439.

Wang, X., Zhang, R., Li, Z., Yan, B., 2022. Adsorption properties and influencing factors of Cu(II) on polystyrene and polyethylene terephthalate microplastics in seawater. Sci Total Environ 812, 152573.

5. Bisphenol A sorption on polyvinyl chloride microplastics: Effects of UV-aging, biofilm colonization and additives on plastic behavior in the environment

This chapter reveals the role of plastic additives (light stabilizers, antioxidants, plasticizers) on the aging process and how they could further affect the adsorption/desorption behavior of co-exist pollutants on microplastics. This study provides important new insights into the evaluation of commercial plastic particles in the natural environment.

This chapter was published in the journal Environmental Pollution in 2024 as a research article in volume 356.

The candidate's contribution was designing and conducting the experiments, samples and data analysis, draft preparation.

Graphical abstract
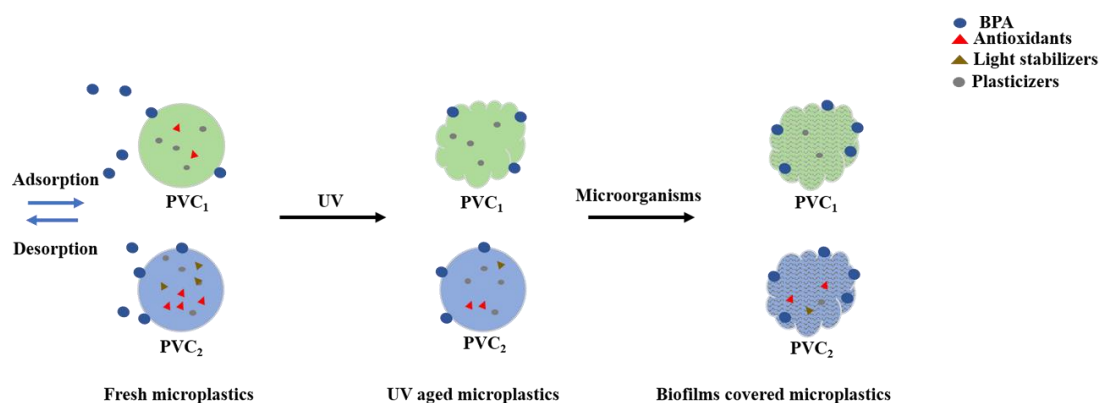
Abstract

Chemical additives are important components in commercial microplastics and their leaching behavior has been widely studied. However, little is known about the potential effect of additives on the adsorption/desorption behavior of pollutants on microplastics and their subsequent role as vectors for pollutant transport in the environment. In this study, two types of commercial polyvinyl chloride (PVC_1 and PVC_2) microplastics were aged by UV irradiation and biotic modification via biofilm colonization to investigate the adsorption and desorption behavior of bisphenol A (BPA). Surface cracks and new functional groups (e.g., O–H) were found on PVC_1 after UV irradiation, which increased available adsorption sites and enhanced H-bonding interaction, resulting in an adsorption capacity increase from 1.28 μg/L to 1.85 μg/L. However, the adsorption and desorption capacity not showed significant changes for PVC_2, which might be related to the few characteristic changes after UV aging with the protection of light stabilizers and antioxidants. The adsorption capacity ranged from

176

1.28 µg/L to 2.06 µg/L for PVC_1 and PVC_2 microplastics, and increased to 1.62 µg/L—

2.95 µg/L after colonization by biofilms. The increased adsorption ability might be

related to the N–H functional group, amide groups generated by microorganisms

enhancing the affinity for BPA. The opposite effect was observed for desorption.

Plasticizers can be metabolized during biofilm formation processes and might play an

important role in microorganism colonization. In addition, antioxidants and UV

stabilizers might also indirectly influence the colonization of microorganisms' on

microplastics by controlling the degree to which PVC microplastics age under UV. The

amount of biomass loading on the microplastics would further alter the

adsorption/desorption behavior of contaminants. This study provides important new

insights into the evaluation of the fate of plastic particles in natural environments.

5.1 Introduction

Commercial plastic products are widely used in both manufacturing and human

activities (Hahladakis et al., 2015; Singla et al., 2020). Although plastic products bring

convenience, they also result in large amounts of plastic waste. It has been reported

only about 20 % of plastic waste is recycled or incinerated, with the majority of plastic

wastes accumulating in landfills or released into the environment (Geyer et al., 2017a).

Plastic fragments with a diameter of less than 5 mm are typically defined as

microplastics (Arthur et al., 2009). Owing to their specific properties (e.g., small

particle size, large specific area, strong hydrophobicity, etc.), microplastics are prone

to act as important transport vectors for pollutants in the natural environment (Chen et al., 2020; Gorman et al., 2019).

Microplastic particles gradually age under abiotic processes (e.g., ultraviolet radiation) and biotic processes (e.g., biofilm colonization) in the natural environment (Sutkar et al., 2023), with chemical additives having the potential to affect these aging processes   (Luo et al., 2022a). For example, a previous study revealed that the presence of the Irgafos 168 (antioxidant) that is added could prevent the formation of radicals and inhibit the UV aging effects for microplastics (Wu et al., 2021). In addition, studies have revealed that plasticizers (e.g., phthalates) could increase the attachment of microorganisms on plastic surfaces and promote the colonization of biofilm (Debroy et al., 2021; Wang et al., 2022a). Additives play important role in the aging process of microplastics, and studies have shown that aging could be an important variable that affects the interaction between microplastics and pollutants by altering the physicochemical properties of microplastics debris (He et al., 2023; Zafar et al., 2023). The presence of additives might therefore affect the adsorption/desorption behavior of microplastics debris for chemical pollutants through controlling the aging process of microplastics. Up to now, most studies have only focussed on environmental exposure factors (e.g., water matrix, sun light strength, temperature, etc.) on the effect of the interaction behavior between pollutants and microplastics (Hanun et al., 2023; Pischedda et al., 2019; Qiu et al., 2022; Yao et al., 2023). To our knowledge, there have been no previous studies that have investigated how additives could impact the

adsorption/desorption behavior of chemical on microplastics when microplastic debris act as vectors for pollutant transport in the environment. As additives are an integral part of commercial plastic products, exploring the role of plastic additives on plastics' environmental behavior is necessary to assess the exposure risks of plastic debris in the environment.

Polyvinyl chloride (PVC) is one of the most widely consumed microplastics worldwide and is known to contain a high number of additives compared to other polymers. For example, plasticizers can make up over 50 % of the total weight of PVC microplastics (Net et al., 2015). In addition to that, PVC is one of the most difficult plastics to manage (Takada; and Bell, 2021) as it is not easy to recycle (Liu et al., 2020d; Ragaert et al., 2017). As a result, PVC has been shown to result in a high environmental exposure risk and is an ideal material to investigate the role of additives on environmental behavior of microplastics. In this study, two types of commercial PVC that were purchased from two different sources were modified by abiotic (artificial UV), biotic (biofilms colonization) aging processes and their combination to obtain more environmentally representative particles. Meanwhile, additives changes of two different PVC microplastics during aging process were determined by liquid chromatography-mass spectrometry (LC-MS) with suspect screening analysis. In addition, the interaction behavior between aged microplastics and bisphenol A (BPA) was investigated. Previous studies have shown that microplastics could as a transport vector for BPA as it has been reported in aquatic microplastic debris (Rani et al., 2015;

Rochman et al., 2014), and therefore   microplastics may be a source of BPA to wild

fish (Barboza et al., 2020). BPA has been defined as an endocrine disrupting chemical

(EDC). Exploring the interaction behavior between BPA and aged PVC microplastics

could help to explore the carrier effect of microplastics on BPA and their potential

ecological risk. The objectives of this study were therefore to explore different aging

pathways and their effect on adsorption/desorption capacity of BPA on PVC

microplastics in the aquatic environment, and to probe the role plastic additives play in

this process.

5.2 Materials and methods

5.2.1 Chemicals and reagents

Acetonitrile and Methanol (HPLC grade) were purchased from Fisher Scientific

Ltd (UK). Bisphenol A (BPA, purity $\geq$ 99 %) was purchased from Sigma-Aldrich Co.

LLC (UK). Stock BPA solution (100 mg/L) was prepared in methanol and kept at 4 ℃.

Crystal violet solution was purchased from Sigma-Aldrich Co. LLC (UK).

5.2.2 Preparation of microplastics and samples characterization

5.2.2.1 Fresh microplastic samples

Two types of PVC plastic (PVC_1 and PVC_2) were obtained from a market

(Guangzhou, China) and Hilltop Products Ltd (UK). PVC_1 is a soft material used in

table mats and PVC_2 is a granule used in the construction industry and present in the

electrical component (e.g., electrical insulation, wires, and cable coatings). The

structures of PVC plastic polymers are given in Figure S1. Samples of PVC_1 were

placed on a table and cut with a knife into small pieces (approximately 3-5 mm) which were similar particle size to the PVC_2 granules. All PVC microplastic samples were washed with ultrapure water to remove surface impurities and then air-dried before use.

5.2.2.2 UV aged microplastic samples

Fresh PVC_1 and PVC_2 microplastic materials were placed into crimp cap quartz vials (7 pieces of microplastics in each vial). All quartz vials were placed into a Suntest CPS+ xenon chamber (Atlas Material Testing Technology LLC (USA)) for the accelerated aging experiments. The Xenon arc lamp produced an irradiance of 750 W/m^2. The wavelength of radiation ranged from 300 nm to 800 nm, temperature was set at 35 °C and performed for one week (7 days).

5.2.2.3 Biofilm colonized microplastic samples

Fresh and UV aged PVC_1 and PVC_2 microplastics were incubated in flasks and shaken (110 rpm) with the addition of activated sludge obtained from the Lancaster Wastewater Treatment Plant (WWTP) at 23 ± 1 °C for four weeks (28 days). After four weeks incubation, the biofilms colonized microplastics were separated from the sludge and washed with ultrapure water and kept sealed at 4 °C until further analysis. In addition, the two types of PVC plastic sample were also incubated in ultrapure water for four weeks as the control group.

Additional field work was carried out to further explore the interaction behavior between BPA and microplastics colonized with biofilms. Two in situ sites selected were the River Conder (54°00'29.8"N 2°46'17.9"W, Lancaster, UK) and the active sludge

plant of WWTP (54°00'29.8"N 2°46'17.9"W, Lancaster, UK). Fifty fragments of fresh and UV aged microplastics were packed in filter bags (8 cm × 10 cm). Filter bags were placed into a large mesh nylon bag (11 cm × 17 cm) to exclude large organisms. All bags were finally loaded into metal cages, details are shown in Figure S2. After incubation for four weeks (May-June), the metal cages were transported to the laboratory. The microplastics samples were washed with ultrapure water and kept at 4 °C for further analysis.

5.2.2.4 Microplastics characterization

PVC$_1$ and PVC$_2$ microplastic samples after the different aging treatments were characterized by Fourier-transform infrared spectroscopy (FTIR, Agilent, USA) and recorded in the range of 4000–400 cm^{-1} to identify transformations of the surface functional groups. In addition, microplastics after removal of biofilms were also characterized by FTIR. The cleaning method of biofilm colonized microplastics followed the previously reported protocol of (Supporting Information-M1) (Sandt et al., 2021), which was demonstrated to have minimal impact on the oxidation of microplastics.

Biofilm biomass was quantified with a modified crystal violet (CV) method (Lobelle and Cunliffe, 2011). 0.5 g microplastics were transferred to the tube with 1 mL CV (1 % W/V) and stained for at least 45 min. The stained microplastic samples were rinsed with ultrapure water until the filtrate was clear. The stained samples were then air-dried for 45 min in sterile dishes and transferred to new vials containing 2.0

mL of 95% ethanol. After 10 min, 1.5 mL of the ethanol solution was transferred into a cuvette, and the optical density was measured with an ultraviolet-visible spectrophotometer at 595 nm.

Scanning electron microscopy (SEM, JEOL JSM 7800F) was performed to characterize the surface changes of PVC microplastics after UV irradiation and biofilms colonization.

5.2.3 Suspect screening for microplastic samples using LC-MS

In addition, mass spectrometry based suspect screening analysis was used to reveal the effect of additives on the aging process of PVC microplastics. Suspect screening was conducted on solvent extracts produced from both fresh and UV aged PVC_1 and PVC_2 microplastics to determine the additives present in the microplastics. Samples of each PVC microplastic (100 mg) were extracted with 5 mL methanol (ME), n-hexane and dichloromethane (DCM) respectively by ultrasonication for 30 min at room temperature. In addition, fresh PVC_1 and PVC_2 microplastics with colonized biofilms were also analysed with the same method using suspect screening analysis to identify plasticizers present and changes compared with fresh counterparts. During the extraction, glassware was used throughout to prevent the contamination of exogenous plastic additives. Solvent extracts were filtered by PTFE and the volume adjusted to approximately 800 μL in ME prior to liquid chromatography-mass spectrometry (LC-MS) analysis. ME, n-hexane and DCM without microplastic samples were used as a control. The extracts were analyzed using a HPLC system (Waters ACQUITY™, USA)

coupled to a QTOF MS system (Waters Xevos G2-S, USA). The analysis and qualitative method were modified from our previously published method (Qiu et al., 2021).

5.2.4 Adsorption and desorption experiments

BPA stock solution (100 mg/L) was diluted to 100 μg/L with ultrapure water, the pH value was kept at 6.8 ± 0.1. The volume ratio of methanol kept below 0.1 % to reduce solvent effects. Before the adsorption experiments, 10 mL 100 μg/L BPA solution was placed into glass tubes to assess the loss of BPA caused by volatilization and adsorption to glass surfaces. Results showed that the loss of bisphenols in centrifuge tubes was less than 1 %.

For the adsorption kinetic study, 50 mg of microplastics and 10 mL 100 μg/L BPA were added into glass tubes. All tubes were placed on the shaker at 140 rpm (25 ± 1 °C). The supernatants were collected after 12 h, 24 h, 48 h, 72 h, 96 h, 120 h, 168 h, 216 h, 264 h, and filtered through a 0.2 μm PTFE membrane. All the experiments were performed in triplicate. In addition, the adsorption behavior of biofilms colonized microplastics (between laboratory and field work) was also investigated.

After adsorption equilibrium was achieved, microplastics from the adsorption experiments were transferred into glass tubes containing 10 mL ultrapure water to explore the desorption behavior. For the biofilms colonized microplastics environment (laboratory and field) the desorption capacity of BPA was also assessed. The shaken

speed was kept at 140 rpm. Supernatants were collected from 0 h to 120 h. Three replicates were conducted for each treatment.

All supernatants collected from adsorption and desorption experiments were analysed by a Shimadzu NexeraX2 ultra high-performance liquid chromatography (UHPLC), details about UHPLC conditions are presented in Supporting Information-M2.

5.2.5 Statistical analysis

T-test and ANOVA were used to analyse significant differences. All statistical analysis was performed using SPSS 22.0 software and Microsoft Office Excel 2020. Figures were plotted with Origin 2019. All calculation equations are listed in the Supporting Information-M3.

5.3 Results and discussion

5.3.1 Physicochemical characteristic and changes to additives after aging treatments

5.3.1.1 UV aging

UV irradiation results in obvious changes to PVC_1 microplastics. As illustrated in Figure 1b, slight vibration occurred at 3431 cm^{-1} (O–H), a new peak appeared at 1634 cm^{-1} (C=C) and the vibration of C–Cl at 1254 cm^{-1} reduced slightly after UV aging, which might indicate that dehydrochlorination and oxidation reactions occurred for PVC_1 during the UV aging process (Wang et al., 2020). In addition, the CV also suggests the changes of functional groups of PVC_1 microplastics after UV aging (Figure 1a). The initial binding of CV significantly increased after UV aging for PVC_1

microplastics (T-test, $p < 0.001$). The generation of new functional groups (e.g., O–H, C=C, C=O, etc.) allows the bonding (H–bonding interaction, π–π interaction) with the dye molecules (Bhagwat et al., 2021).
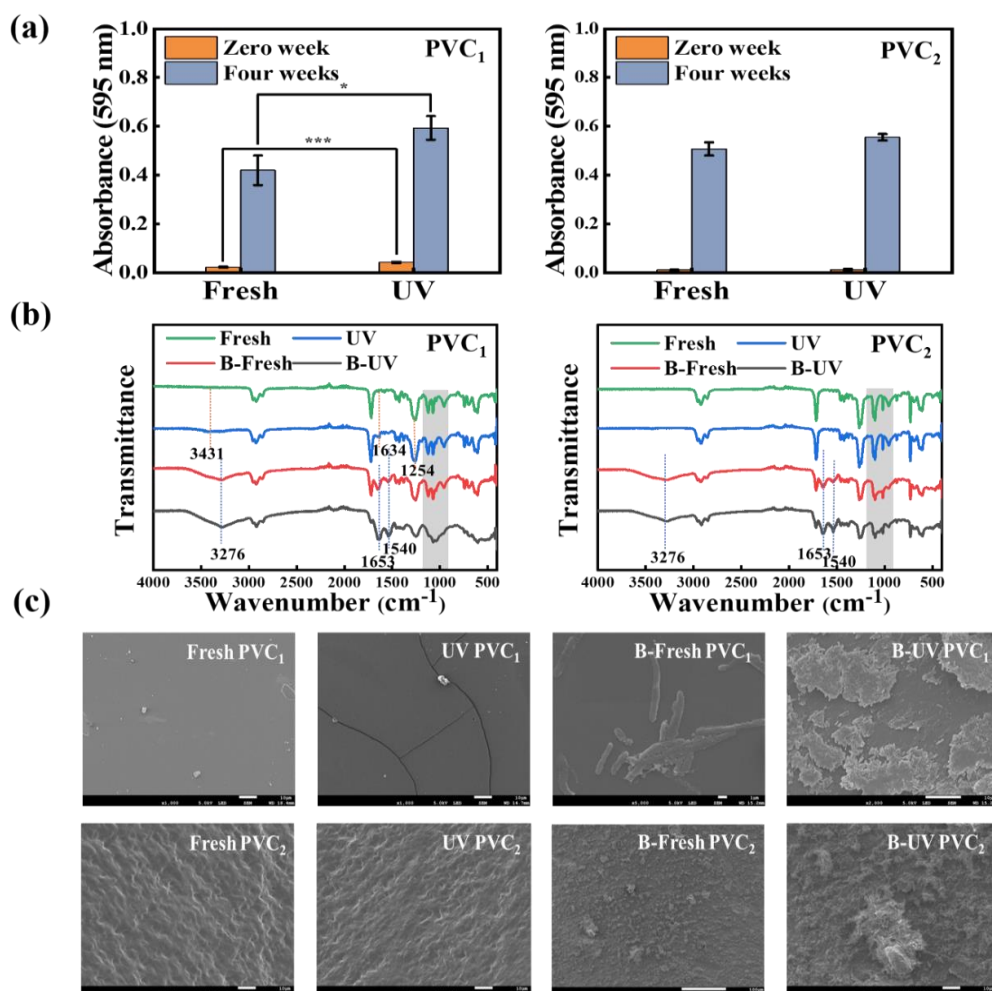
Figure 1. (a) Changes in absorbances of CV dye for fresh and UV aged PVC$_1$ and PVC$_2$ microplastics that incubated biofilms in the laboratory. Error bars are the means ± standard deviation (SD) of three repeats. * $p < 0.05$, ** $p < 0.01$, *** $p < 0.001$. (b) FTIR spectrogram of fresh, UV aged, biofilms colonized fresh (B-Fresh) and UV aged (B-UV) microplastics. (c) SEM images of microplastics with different aging treatment.

The SEM images also suggest changes after UV aging as the surfaces of fresh PVC$_1$ microplastics were smooth, whilst in contrast, the surfaces were cracked after UV irradiation (Figure 1c). However, few changes could be characterized by FTIR spectrum and SEM images for PVC$_2$ microplastics after UV aging treatment (Figure 1b and 1c), suggesting that UV aging resulted in very few changes to the structures and properties of PVC$_2$. The different changes between PVC$_1$ and PVC$_2$ microplastics after UV aging might be related to the additives used in the production of the plastics.

Table 1. Antioxidants and light stabilizers identified in fresh PVC$_1$ and PVC$_2$ microplastics.

Microplastics type	Antioxidants	Light stabilizers	
	Phenolic antioxidants	UV absorbers	HALS
PVC$_1$	Irganox 245	-	-
PVC$_2$	Irganox 1076 Isonox 132	Tinuvin 234	Tinuvin 144

Antioxidants (e.g., phenolic antioxidants, amine antioxidants, phosphorus antioxidants, etc.) and light stabilizers (e.g., UV absorbers, hindered amine light stabilizers (HALS), quenchers, etc.) are the most widely used additives to resist oxidation, UV degradation and improve the life cycle of polymers (Rani et al., 2017). According to the results of suspect screening analysis, a range of antioxidants and light

stabilizers were found in fresh PVC_1 and PVC_2 microplastics (Table 1). Irganox 1076 (phenolic antioxidants), Isonox 132 (phenolic antioxidants), Tinuvin 144 (HALS) and Tinuvin 234 (UV absorber) were detected in the solvent extracts of fresh PVC_2. However, only Irganox 245 (phenolic antioxidants) was detected for fresh PVC_1 microplastics.
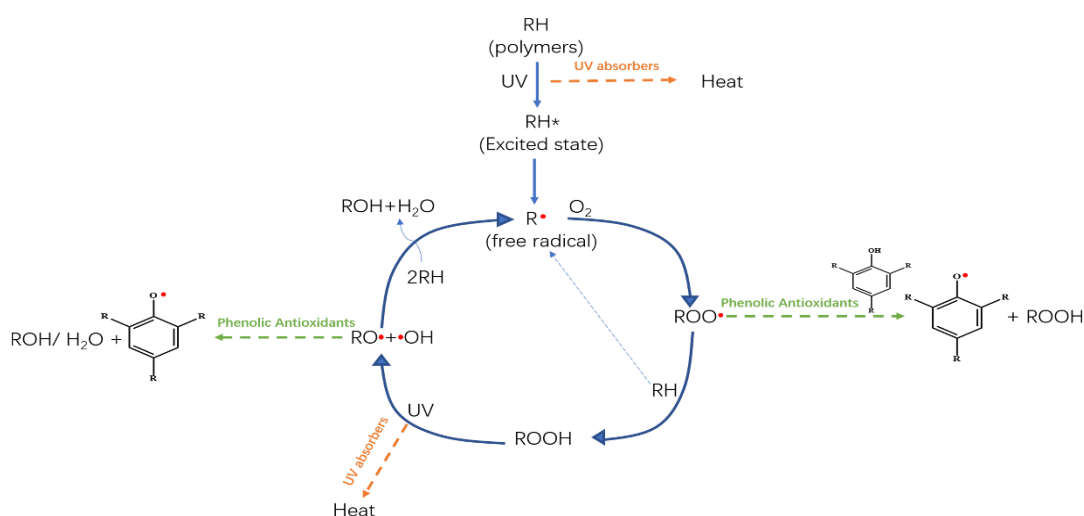
Figure 2. The aging mechanism of plastics and the function of antioxidants and light stabilizers.

After UV aging, the antioxidants cannot be detected in the extracts of PVC_1 microplastics (Figure S3), which indicates that phenolic antioxidants were all consumed and converted to their degradation products (Figure 2). However, all of the antioxidants and UV absorbers still remained in UV aged PVC_2 extracts (Figure S3). It's known that UV stabilizers can absorb UV and transfer irradiation to heat (Figure 2), with a previous study reporting a synergistic effect between UV stabilizers and antioxidants (Jiang et al., 2021), which might improve the UV aging resistance of PVC_2. As a result, with the

protection of antioxidants and light stabilizers, PVC_2 showed less changes to its properties compared with PVC_1 after UV irradiation.

5.3.1.2 Colonization by biofilms

The estimation of biomass using the CV method indicated an obvious colonization of biofilms after incubation over four weeks (Figure 1a). In addition, it was observed that biomass growth was higher on UV aged PVC_1 microplastics compared with fresh microplastics, whilst there was no significant difference for PVC_2 microplastics ($p > 0.05$), which might relate to few physiochemical property changes of PVC_2 microplastics. Recent studies showed that the increased roughness and hydrophilicity (generation of O–containing functional groups) of microplastics could promote the colonization of microorganisms on microplastics (Ho et al., 2020; Hossain et al., 2019). In the natural environment, the degradation of plastics is probably initiated with UV aging to reduce molecular weight and size of plastics, which can then be metabolized by microorganisms (Ali et al., 2021a). Therefore, UV degradation might be an important factor affecting the attachment of microorganisms on microplastics. As antioxidants and light stabilizers are vital factors to control the UV aging degree of microplastics, they could also indirectly affect the formation of biofilms on microplastics.

The FTIR spectrum illustrated new peaks were generated at 3293 cm^{-1} (N–H), 1653 cm^{-1} (C=O, amide I) and 1540 cm^{-1} (N–H and C–N, amide II) for both PVC_1 and PVC_2 microplastics after biofilms colonization (Figure 1b), which represent the

characteristic peaks from proteins, and as an indicator of biofilm formation (Sandt et al., 2021). In addition, the intensity of a spectral region between $1180 - 900$ cm^{-1} (shaded in grey) obviously changed after colonization by biofilms, which represents vibrations from polysaccharides (Sandt et al., 2021). For both PVC$_1$ and PVC$_2$ microplastics surface changes and microorganisms (e.g., rod-like bacteria) were observed in SEM images (Figure 1c), which confirmed biofilm formation on microplastics.

It is worth noting that the peak at 1720 cm^{-1} (C=O) of FTIR spectrum for fresh PVC$_1$ and PVC$_2$ microplastics represents the characteristic peak for plasticizers (Figure S8), which could also be observed in other plasticized PVC plastics but does not exist in the pure experimental unplasticized PVC plastics (Altenhofen da Silva et al., 2011; Patil and Jena, 2021). However, the intensity of C=O clearly reduced after removing the biofilms (Figure S8, red spectrum-b). The FTIR spectrum of PVC microplastic samples incubated in ultrapure water showed no obvious change of C=O (Figure S9), which excludes the effect of possible leaching behavior of plasticizers during the biofilm's incubation process. It suggests that the plasticizers could be metabolized by microorganisms. The biofilms colonized fresh PVC$_1$ and PVC$_2$ microplastics were also subjected to suspect screening analysis to further investigate any changes to the plasticizers after biofilm formation. Figure S4 and Figure S5 suggest that the presence of plasticizers (e.g., diisobutyl phthalate, di-n-octyl phthalate) decreased for PVC$_1$ and PVC$_2$ microplastics after colonization with biofilms. Dimethyl phthalate, dibutyl

phthalate, and diethyl phthalate co-existed in the extracts of fresh PVC_2 microplastics but could not be identified in the extracts after colonization. Results from the suspect screening analysis further indicates that plasticizers were consumed by the microorganisms present in the biofilms. Previous studies have suggested that plasticizers could act as a carbon source that can be utilized by many fungi or bacteria, hence promoting the initial colonization of microorganisms on PVC plastics (Ru et al., 2020; Singh Jadaun et al., 2022; Wang et al., 2022a). This indicates that the presence of plasticizers might also be important for the formation of biofilms on microplastics.

5.3.2 Adsorption and desorption behavior of BPA on microplastics

5.3.2.1 UV aging

The adsorption kinetics curves for BPA on PVC microplastics are shown in Figure 3a. The kinetics data demonstrate that adsorption equilibrium for BPA on fresh PVC_1 microplastics were achieved within 168 h (one-way ANOVA analysis, $p > 0.05$), and the time needed to reach adsorption equilibrium became shorter after UV irradiation (72 h). This suggested UV aging could accelerate the adsorption of BPA on PVC_1 microplastics. In addition, the fitting model (Figure 3b) suggested that the adsorption behavior of fresh PVC_1 microplastics could be better described by a pseudo-first-order model, whilst better described by a pseudo-second-order model after UV irradiation (Table S1). This indicates that the rate-limiting step was a physical process for fresh PVC_1, but after UV aging treatment relied on chemical processes which involved the

adsorption between the adsorbent and adsorbate (Mohan et al., 2006). However, the

adsorption behavior for PVC_2 microplastics didn't show such obvious changes after UV

irradiation as the adsorption equilibrium time both achieved equilibrium within 96 h

(Figure 3a), and adsorption behavior before and after UV aging was dominated by

physical process as the adsorption kinetics data both better described by a pseudo-first-

order model (R^2 values are 0.978 and 0.988, respectively).

(a)

(b)
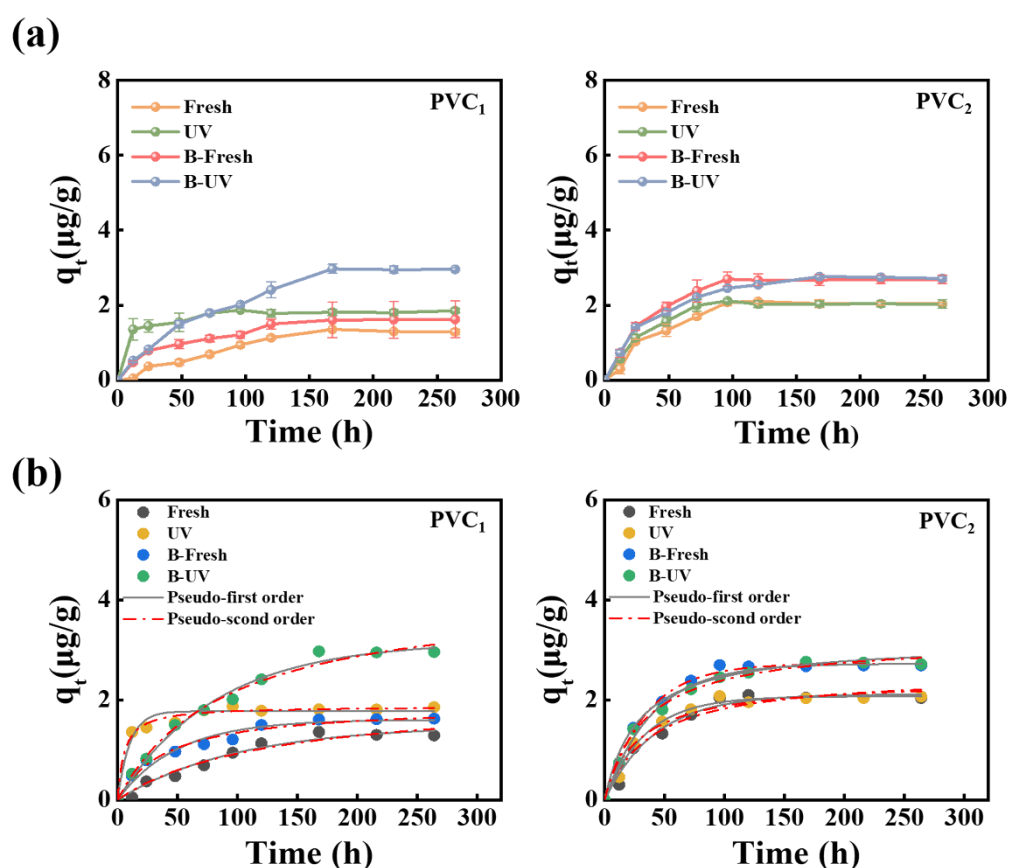
Figure 3. (a) Adsorption kinetics curves of PVC microplastics. Error bars are the means

± standard deviation (SD) of three repeats. (50 mg microplastics, 10 mL 0.1 mg/L BPA,

25 °C, 140 rpm). (b) Pseudo-first order and pseudo-second order model fitting curves

for PVC microplastics adsorbing BPA.

Adsorption kinetics studies have demonstrated that the adsorption capacity of BPA on PVC_1 microplastics significantly increased from 1.25 μg/g to 1.85 μg/g after UV aging (Figure 4a), with the generation of new functional groups (e.g., O–H) potentially enhancing the H–bonding between microplastics and BPA (Zhou et al., 2020). In addition, the cracks in UV aged microplastics can offer more available adsorption sites and enhance the adsorption capacity (Chen et al., 2022). Whilst, the adsorption capacity for fresh PVC_2 microplastics was 2.03 μg/g, which showed no significant changes after UV irradiation (T-test, $p > 0.05$). With the protection of antioxidants and light stabilizers, most chain degradation reactions could have been prevented leading to few changes in the physicochemical properties of PVC_2 microplastics (Figure 1), and thus further limiting changes in the adsorption behavior.
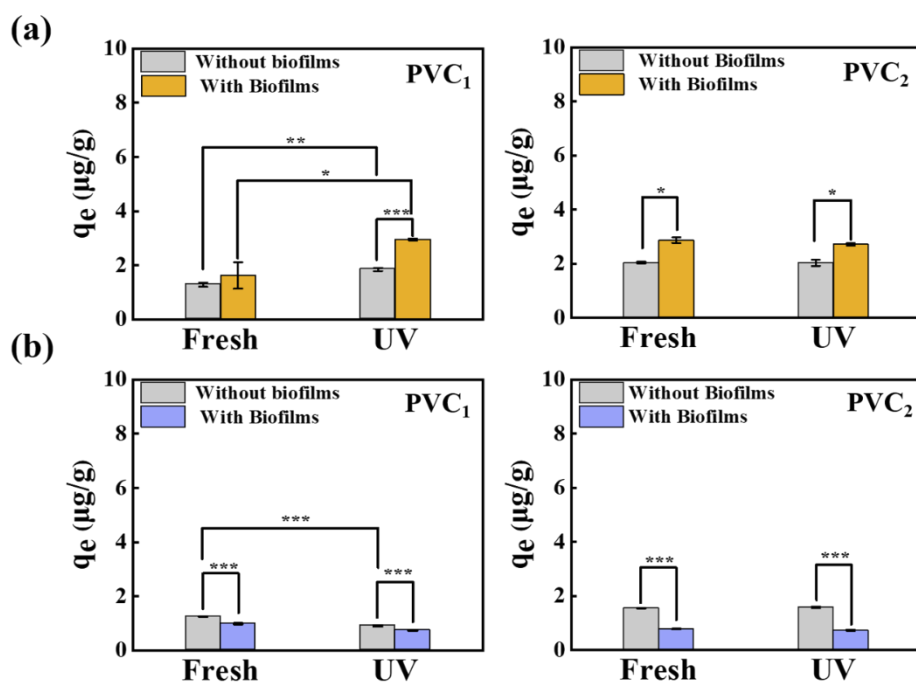
Figure 4. (a) The adsorption capacity of BPA on fresh and UV aged PVC_1 and PVC_2 with or without the colonization of biofilms. (b) The desorption capacity of BPA on

fresh and UV aged PVC_1 and PVC_2 with or without the colonization of biofilms. Error bars are the means ± standard deviation (SD) of three repeats. (50 mg microplastics, 10 mL 0.1 mg/L BPA, 25 °C, 140 rpm). * $p < 0.05$, ** $p < 0.01$, *** $p < 0.001$.

The aging degree also impacted the desorption behavior of BPA on microplastics. As shown in Figure 4b, the desorption capacity of PVC_1 significantly reduced from 1.25 µg/g to 0.91µg/g after UV aging (T-test, $p < 0.001$), where the cracks in the microplastics might allowed more BPA to diffuse into the structure or narrow pores rather than surface adsorption. This suggests it is more difficult for UV aged PVC_1 microplastics to release BPA compared to fresh microplastics (Fan et al., 2021a; Sun et al., 2021). In contrast, no significant change was observed for PVC_2 after UV aging (T-test, $p > 0.05$). This could also be attributed to no obvious changes to the physicochemical properties of PVC_2 after irradiation. As a result, plastic additives (antioxidants and light stabilizers) could not only affect the UV aging behavior of polymers but also indirectly impact the adsorption and desorption behavior of pollutants on polymers by controlling the aging process.

5.3.2.2 Biofilms colonization

The pseudo-second-order model (R^2 values range from 0.980 to 0.994) better described the adsorption process of BPA for both PVC_1 and PVC_2 microplastics after biofilm colonization (Table S1), which indicates that the adsorption process might mainly be controlled by chemical processes (Wang et al., 2023b).The adsorption capacity was enhanced (although no significant difference for fresh PVC_1) for both

fresh and UV aged microplastics after the colonization with biofilms (Figure 4a). This might be due to the formation of new functional groups (e.g., N–H, C=O, etc.) corresponding to biofilms that can further promote affinity for BPA. Figure S6 illustrates the FTIR spectra of PVC_1 and PVC_2 microplastics after adsorption of BPA. The intensity and vibration of the biofilm characteristic peaks (e.g., N–H, amide I, amide II) changes after adsorption. For example, decreased intensity of the peak at 3276 cm^{-1} (N–H), 1653 cm^{-1}(amide I) and 1540 cm^{-1} (amide II) could be observed for biofilms colonized on fresh and UV aged PVC_1 and PVC_2 microplastics after adsorption, which indicates interactions (e.g., H-bonding interaction, π-π interaction, etc.) may occur between BPA and biofilms colonized PVC microplastics. As BPA shows aliphatic C–H vibration at around 2962 cm^{-1} (Figure S7), the enhanced peak of C–H for biofilm colonized PVC_1 and PVC_2 microplastics after adsorption might also indicate the binding of BPA on PVC microplastics (Figure S6). As a result, adsorption behavior might be impacted by microorganisms for both fresh and UV aged microplastics after biofilm colonization. As shown in Figure 4b, the desorption capacity decreased for both fresh and UV aged PVC microplastics after colonization with biofilms. The enhanced H-bonding attraction could increase the affinity between BPA and PVC microplastics, which might result in the reduction of the desorption ability.

5.3.3 Field colonization by biofilms

As shown in Figure 5a, field derived biofilms successfully colonized the microplastics. The intensity of C=O also reduced after removing the biofilms from

PVC$_1$ and PVC$_2$ microplastics samples that were incubated in the River Conder and WWTP (Figure S8, orange spectrum-d, green spectrum-f), which further suggests that plasticizers may be degraded by microorganisms during the biofilm's colonization process and might be important for biofilm formation in the aquatic environment.
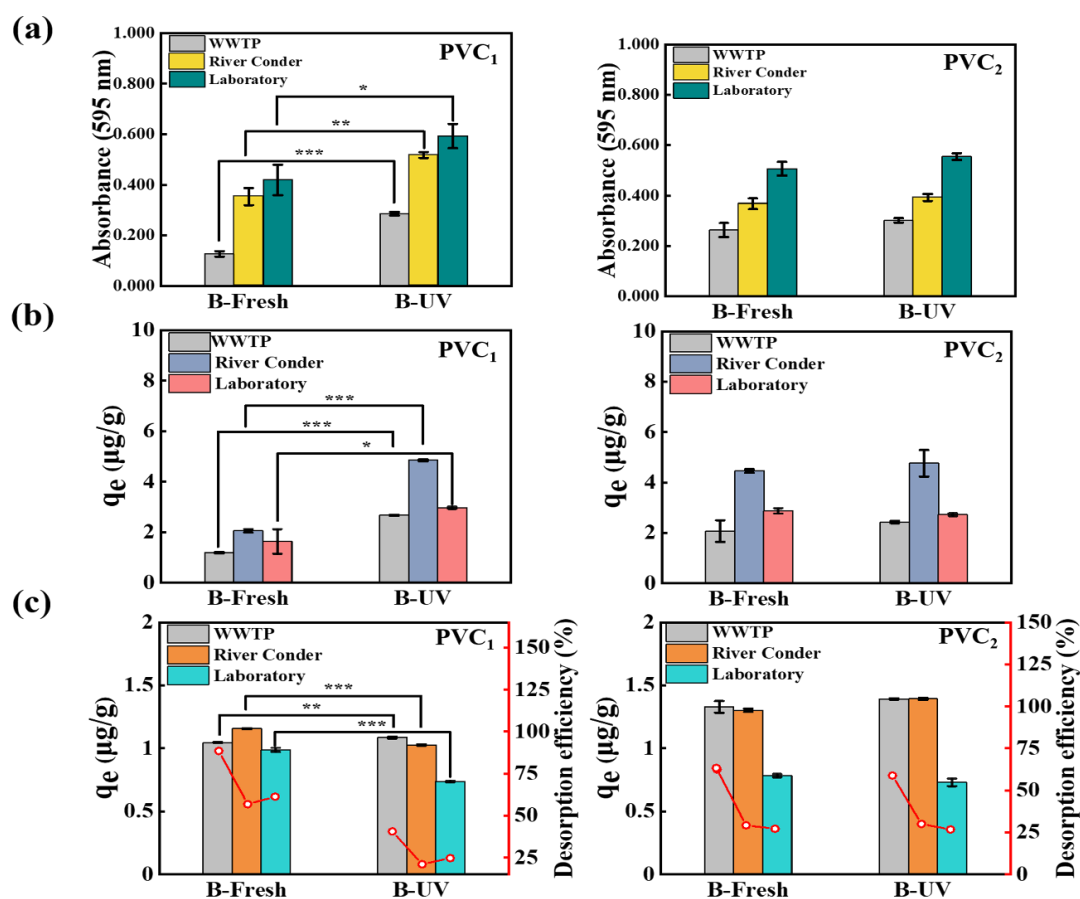
Figure 5. (a) Changes in absorbance of CV dye for biofilms colonized fresh (B-Fresh) and UV aged (B-UV) PVC$_1$ and PVC$_2$ microplastics that incubated in active sludge plant of wastewater treatment plant (WWTP), River Conder. (b) The adsorption capacity of BPA on biofilms colonized (field and lab) fresh and UV aged PVC plastics. (c) The desorption capacity of BPA on biofilms colonized (field and lab) fresh and UV aged PVC plastics. (n=3, 50 mg microplastics, 25 °C, 140 rpm). * $p < 0.05$, ** $p < 0.01$, *** $p < 0.001$.

The adsorption capacity of PVC microplastics was positively correlated with biofilm biomass in the same biofilm incubation site (Figure 5a and 5b), suggesting that higher biomass indicates higher affinity of BPA to PVC microplastics. Both filed and laboratory work showed that UV aging could promote the colonization of biofilms on PVC_1 microplastics (Figure 5a), thus which also verifies that the physiochemical properties changes as a result of UV irradiation could enhance the attachment of microorganism and further alter the adsorption behavior. As light stabilizers and antioxidants play an important role in the physiochemical property changes during the aging process, they are likely to have an indirect effect microorganism colonization. Thus, the presence of additives is likely to have an effect on the adsorption behavior of microplastics colonized by biofilms.

The data on desorption behavior suggested that UV aged PVC microplastics showed lower desorption efficiencies than fresh microplastics after colonization with biofilms under both field and laboratory conditions (Figure 5c). However, it is worth noting that the desorption capacity for PVC_1 microplastics with WWTP incubated biofilms increased after UV aging (T-test, $p < 0.01$), which is explained by enhanced sorption capacity. The sorption capacity of BPA on UV aged PVC_1 with WWTP incubated biofilms was significantly higher than fresh microplastics (Figure 5b), although the desorption efficiency decreased sharply from 88.0 % to 40.7 %, the desorption capacity still increased owing to the increased sorption capacity. As a result,

UV aging might result in microplastics accumulating higher biomass, leading to higher pollutant loadings and potentially greater pollutant release.

5.4 Conclusions

In this study, two types of PVC microplastics were modified by abiotic, biotic processes and a combination of both, to obtain more realistic polymers for the investigation of the sorption/desorption behavior of BPA. Special emphasis was placed on the influence of microplastic additives on the aging process and adsorption/desorption behavior. Although PVC_1 and PVC_2 were the same type of polymer, they were produced with different antioxidants and light stabilizers (chemical additives), which resulted in different aging profiles (UV aging degree and microorganism colonized level) under the same aging conditions. In addition, both field and laboratory biofilms incubation investigations provided evidence that plasticizers can be metabolized after the formation of biofilms, which suggests that plasticizers could affect the colonization behavior of microorganisms on PVC microplastics. As the aging of microplastics influences the adsorption/desorption behavior of BPA with interaction mechanisms involving H–bonding interaction, π–π interaction, etc., our results highlight that plastic additives can affect their environmental behavior (as a vector of pollutant transport). This is the first study to profile the role of plastic additives on adsorption/desorption behavior of plastic particles, and thereby lays a foundation for further study on the fate, potential exposure risk and toxicity of microplastics.

Supporting information

M1: Cleaning protocol of microplastics

Microplastics were washed with deionized water at first, then soaked in hot water (around 60 ℃) to remove proteins, after that rinsing in hot ethanol (50 %, 60 ℃) to remove lipids, then washed with NaOH (1 M) for 5 min in the ultrastatic instrument to solubilize carboxylic acid, finally rinsed in ultrapure water and air dried.

M2: Determinations for the concentration of BPA

Samples were analyzed using a Shimadzu NexeraX2 UHPLC with fluorescence detector (Shimadzu, Japan) and a Phenomenex C18 column (4 μm, 150 × 4.6 mm). Chromatographic separation was performed with a mobile phase of A: ultrapure water and B: acetonitrile (ACN). The isocratic procedure was set: 50 % ultrapure water (A) and 50 % ACN (B), held 10 min. The injection volume was 50 μg/L and the tray temperature was kept at 30 ℃. The excitation wavelength and emission wavelength were 226 nm and 315 nm, respectively. Flow rate was 0.5 mL/min. Samples were prepared in ultrapure water and methanol (4:1, v/v).

M3: Calculation equation

The adsorption capacity of BPA on microplastics:

$$q_e = \frac{C_0 - C_e}{m}V \tag{1}$$

where q_e (μg/g) refers to the equilibrium adsorption capacity of microplastics for BPA; C_0 and C_e (μg/L) are the initial concentration and equilibrium concentration of BPA in the solution respectively; m (mg) is the mass of plastics and V (mL) is the volume of the solution used in adsorption experiments.

Pseudo-first-order model:

$$q_t = q_e(1 - e^{-k1t}) \tag{2}$$

Pseudo-second-order model:

$$q_t = \frac{q_e{}^2 k_2 t}{1 + q_e k_2 t} \tag{3}$$

where q_t (μg/g) is the adsorption amount of BPA per gram of microplastics at a given time t (h); k_1 and k_2 represent the rate constant for pseudo-first order and pseudo-second order kinetics respectively.

The desorption efficiency:

$$\%D = \left(\frac{C_{desorb}}{C_{adsorb}}\right) \times 100 \tag{4}$$

where C_{desorb} (µg/L) is the desorption concentration of BPA from microplastics and

C_{adsorb} (µg/L) is the adsorbed equilibrium concentration of bisphenols on plastics at

the beginning of the desorption experiment.

The desorption capacity:

$$q_{desorb} = \frac{C_{desorb}}{m}V \tag{5}$$

Where q_{desorb} (µg/g) is the desorption capacity of BPA from microplastics.

Table S1. Kinetic parameters for BPA adsorption by PVC microplastics.

Types		pseudo-first order parameters			pseudo-second order parameters		
		q_e	k_1	R^2	q_e	k_2	R^2
PVC$_1$	Fresh	1.48	1.00×10^{-2}	**0.971**	2.09	3.77×10^{-2}	0.962
	UV	1.77	9.93×10^{-2}	0.963	1.87	9.70×10^{-2}	**0.985**
	B-Fresh	1.60	2.01×10^{-2}	0.963	1.90	1.26×10^{-2}	**0.980**
	B-UV	3.18	1.22×10^{-2}	0.988	4.16	1.65×10^{-2}	**0.990**
PVC$_2$	Fresh	2.11	2.34×10^{-2}	**0.978**	2.52	1.02×10^{-2}	0.957
	UV	2.06	2.45×10^{-2}	**0.988**	2.40	1.46×10^{-2}	0.970
	B-Fresh	3.16	1.11×10^{-2}	0.978	2.72	2.90×10^{-2}	**0.994**
	B-UV	2.72	9.39×10^{-3}	0.982	3.19	2.51×10^{-2}	**0.992**

B-Fresh and B-UV represent fresh and UV aged microplastics colonized biofilms
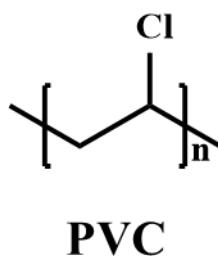
Figure S1. The structures of PVC plastics.
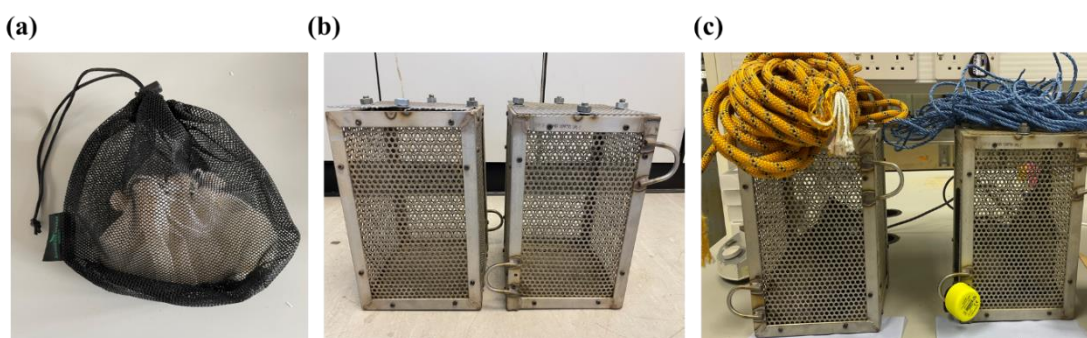
Figure S2. Design of the field work device for fresh and UV aged microplastics immersion. (a) the nylon and filter bags with microplastics inside; (b) the metal cages; (c) the installed device for microplastics exposure.
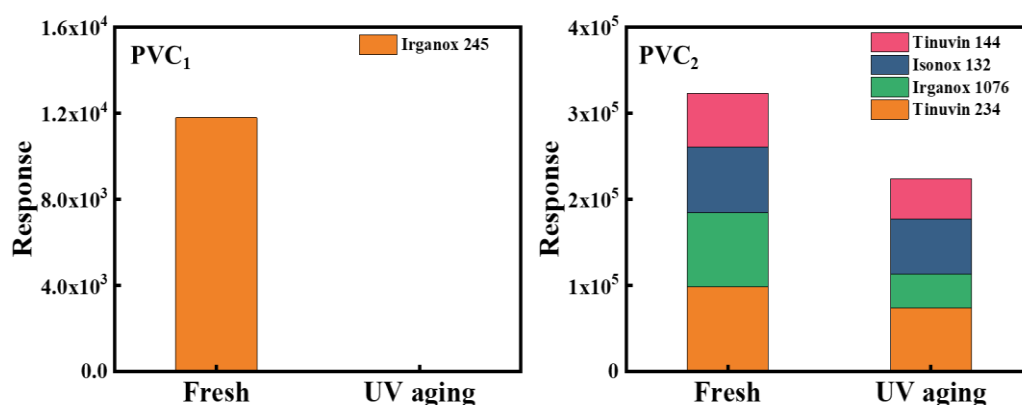
Figure S3. The response of antioxidants and light stabilizers in the ME extracts of fresh and UV aged PVC_1 and PVC_2 microplastics.

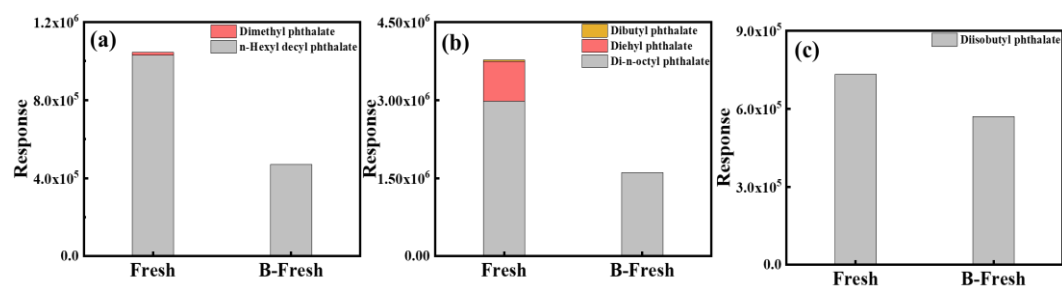**Figure S4.** The response of plasticizers in the ME (a), n-hexane (b) and DCM (c) extracts of fresh and biofilms colonized fresh PVC_2 microplastics. B-fresh represent the fresh microplastics colonized biofilms.
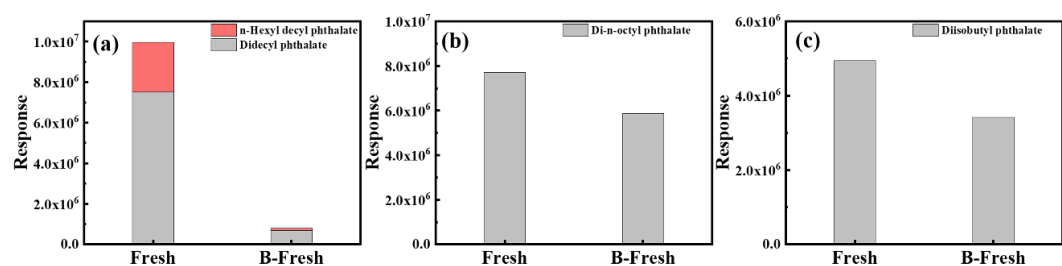
Figure S5. The response of plasticizers in the ME (a), n-hexane (b) and DCM (c) extracts of fresh and biofilms colonized fresh PVC_1 microplastics. B-fresh represent the fresh microplastics colonized biofilms.
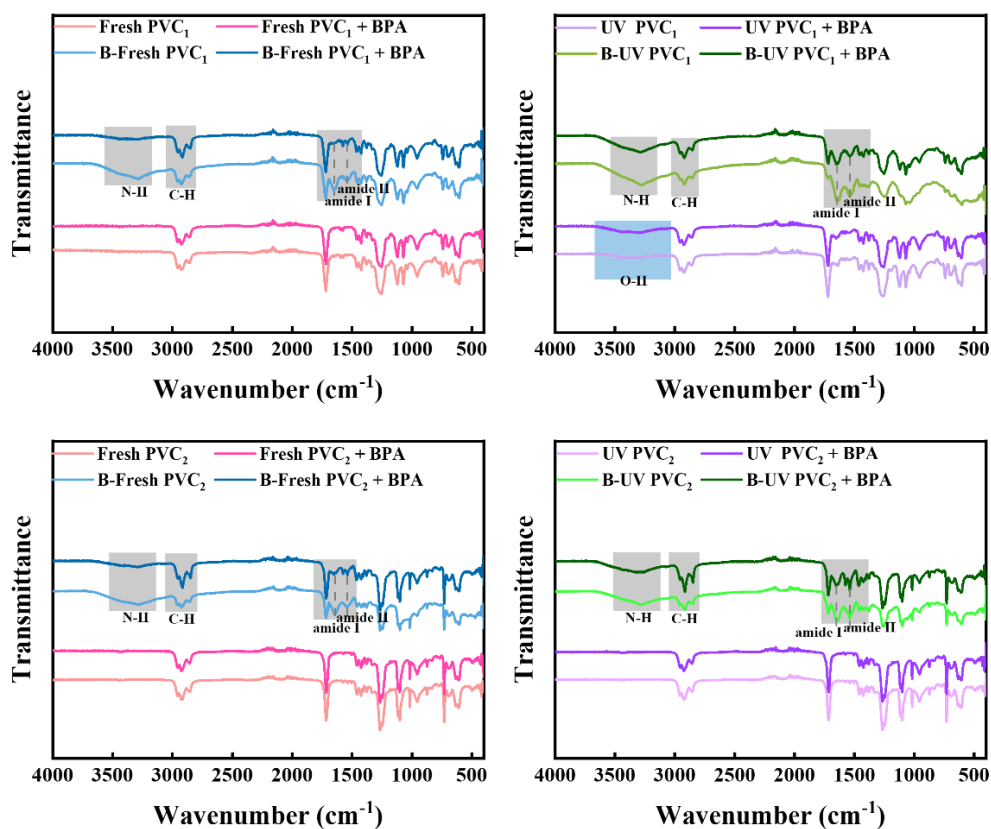
Figure S6. FTIR of PVC$_1$ and PVC$_2$ microplastics before and after adsorption BPA.

B-Fresh and B-UV represent biofilms colonized fresh and UV aged microplastics.
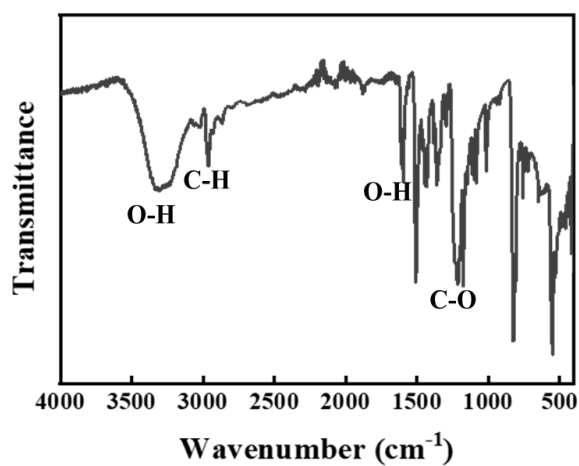
Figure S7. The FTIR spectra of BPA.
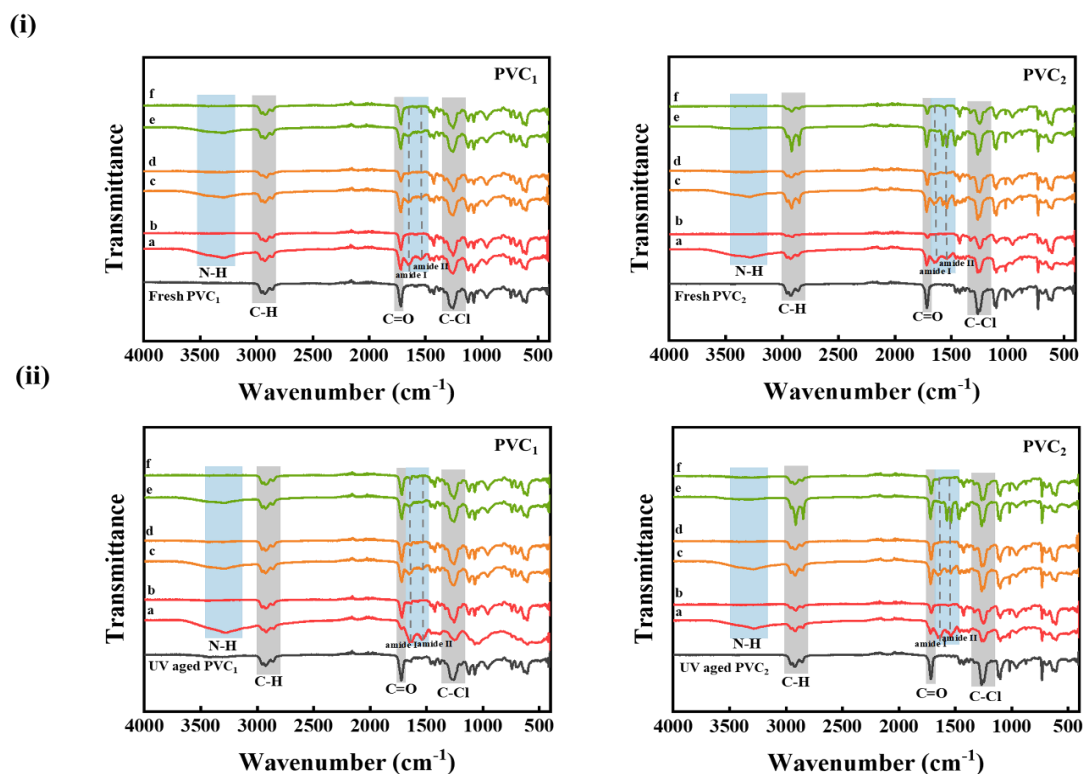
Figure S8. FTIR spectrum of fresh (i) and UV aged (ii) PVC_1 and PVC_2 microplastics colonization (a, c, e) and removing biofilms (b, d, f). Black spectrum: fresh or UV aged microplastic samples; red spectrum: fresh or UV aged microplastic samples incubated in laboratory; orange spectrum: fresh or UV aged microplastic samples incubated in River Conder.; green spectrum: fresh or UV aged microplastic samples incubated in WWTP. The blue shade represents the changes of biochemical signal after removing biofilms. The gray shade represents the biodegradation of microplastics.
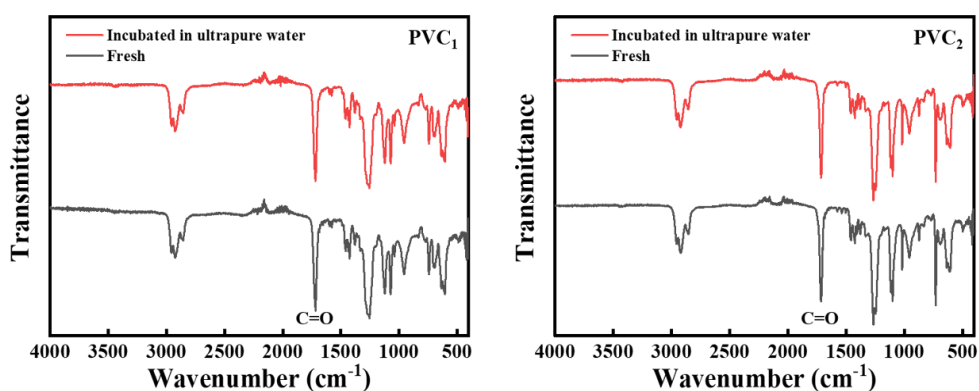
Figure S9. FTIR spectrum of PVC microplastics that incubated in ultrapure water for four weeks.

References

Ali, S.S., Elsamahy, T., Al-Tohamy, R., Zhu, D., Mahmoud, Y.A., Koutra, E., Metwally, M.A., Kornaros, M., Sun, J., 2021. Plastic wastes biodegradation: Mechanisms, challenges and future prospects. Science of the Total Environment 780, 146590.

Altenhofen da Silva, M., Adeodato Vieira, M.G., Gomes Maçumoto, A.C., Beppu, M.M., 2011. Polyvinylchloride (PVC) and natural rubber films plasticized with a natural polymeric plasticizer obtained through polyesterification of rice fatty acid. Polymer Testing 30, 478-484.

Arthur, C., Baker, J., Bamford, H., 2009. Proceedings of the international research workshop on the occurrence, effects, and fate of microplastic marine debris, September 9-11, 2008.

Barboza, L.G.A., Cunha, S.C., Monteiro, C., Fernandes, J.O., Guilhermino, L., 2020. Bisphenol A and its analogs in muscle and liver of fish from the North East Atlantic Ocean in relation to microplastic contamination. Exposure and risk to human consumers. J. Hazard. Mater. 393.

Bhagwat, G., Tran, T.K.A., Lamb, D., Senathirajah, K., Grainge, I., O'Connor, W., Juhasz, A., Palanisami, T., 2021. Biofilms Enhance the Adsorption of Toxic Contaminants on Plastic Microfibers under Environmentally Relevant Conditions. Environ. Sci. Technol. 55, 8877-8887.

Chen, C.-F., Ju, Y.-R., Lim, Y.C., Hsu, N.-H., Lu, K.-T., Hsieh, S.-L., Dong, C.-D., Chen, C.-W., 2020. Microplastics and their affiliated PAHs in the sea surface connected to the southwest coast of Taiwan. Chemosphere 254.

Chen, X., Chen, C., Guo, X., Sweetman, A.J., 2022. Sorption and desorption of bisphenols on commercial plastics and the effect of UV aging. Chemosphere 310, 136867.

Debroy, A., George, N., Mukherjee, G., 2021. Role of biofilms in the degradation of microplastics in aquatic environments. Journal of Chemical Technology and Biotechnology.

Fan, X., Gan, R., Liu, J., Xie, Y., Xu, D., Xiang, Y., Su, J., Teng, Z., Hou, J., 2021. Adsorption and desorption behaviors of antibiotics by tire wear particles and polyethylene microplastics with or without aging processes. Science of the Total Environment 771, 145451.

Geyer, R., Jambeck, J.R., Law, K.L., 2017. Production, use, and fate of all plastics ever made. Sci. Adv.

Gorman, D., Moreira, F.T., Turra, A., Fontenelle, F.R., Combi, T., Bícego, M.C., de Castro Martins, C., 2019. Organic contamination of beached plastic pellets in the South Atlantic: Risk assessments can benefit by considering spatial gradients. Chemosphere 223, 608-615.

Hahladakis, J.N., Velis, C.A., Weber, R., Iacovidoua, E., Purnell, P., 2015. An overview of chemical additives present in plastics: Migration,release, fate and

environmental impact during their use, disposal and recycling. J. Hazard. Mater. 344, 179-199.

Hanun, J.N., Hassan, F., Theresia, L., Chao, H.-R., Bu, H.M., Rajendran, S., Kataria, N., Yeh, C.-F., Show, P.L., Khoo, K.S., Jiang, J.-J., 2023. Weathering effect triggers the sorption enhancement of microplastics against oxybenzone. ENVIRON TECHNOL INNO. 30.

He, S., Tong, J., Xiong, W., Xiang, Y., Peng, H., Wang, W., Yang, Y., Ye, Y., Hu, M., Yang, Z., 2023. Microplastics influence the fate of antibiotics in freshwater environments: Biofilm formation and its effect on adsorption behavior. J. Hazard. Mater. 442, 130078.

Ho, W.K., Law, J.C., Zhang, T., Leung, K.S., 2020. Effects of Weathering on the Sorption Behavior and Toxicity of Polystyrene Microplastics in Multi-solute Systems. Water Research 187, 116419.

Hossain, M.R., Jiang, M., Wei, Q., Leff, L.G., 2019. Microplastic surface properties affect bacterial colonization in freshwater. Journal of Basic Microbiology 59, 54-61.

Jiang, T., Mao, Z., Qi, Y., Wu, Y., Zhang, J., 2021. The effect of two different UV absorbers combined with antioxidants on UV resistance of HDPE. Polym. Adv. Technol. 32, 4915-4925.

Liu, Y., Zhou, C., Li, F., Liu, H., Yang, J., 2020. Stocks and flows of polyvinyl chloride (PVC) in China: 1980-2050. Resour. Conserv. Recycl. 154.

Lobelle, D., Cunliffe, M., 2011. Early microbial biofilm formation on marine plastic debris. Marine Pollution Bulletin 62, 197-200.

Luo, H., Liu, C., He, D., Sun, J., Li, J., Pan, X., 2022. Effects of aging on environmental behavior of plastic additives: Migration, leaching, and ecotoxicity. Science of the Total Environment 849, 157951.

Mohan, D., Singh, K.P., Singh, V.K., 2006. Trivalent chromium removal from wastewater using low cost activated carbon derived from agricultural waste material and activated carbon fabric cloth. J. Hazard. Mater. 135, 280-295.

Net, S., Sempere, R., Delmont, A., Paluselli, A., Ouddane, B., 2015. Occurrence, fate, behavior and ecotoxicological state of phthalates in different environmental matrices. Environ. Sci. Technol. 49, 4019-4035.

Patil, S.S., Jena, H.M., 2021. Performance assessment of polyvinyl chloride films plasticized with Citrullus lanatus seed oil based novel plasticizer. Polymer Testing 101.

Pischedda, A., Tosin, M., Degli-Innocenti, F., 2019. Biodegradation of plastics in soil: The effect of temperature. Polym. Degrad. Stab. 170.

Qiu, S.Q., Huang, G.Y., Fang, G.Z., Li, X.P., Lei, D.Q., Shi, W.J., Xie, L., Ying, G.G., 2021. Chemical characteristics and toxicological effects of leachates from plastics under simulated seawater and fish digest. Water Research 209, 117892.

Qiu, X., Ma, S., Zhang, J., Fang, L., Guo, X., Zhu, L., 2022. Dissolved Organic Matter Promotes the Aging Process of Polystyrene Microplastics under Dark and

Ultraviolet Light Conditions: The Crucial Role of Reactive Oxygen Species. Environ. Sci. Technol. 56, 10149-10160.

Ragaert, K., Delva, L., Van Geem, K., 2017. Mechanical and chemical recycling of solid plastic waste. Waste Manag. 69, 24-58.

Rani, M., Shim, W.J., Han, G.M., Jang, M., Al-Odaini, N.A., Song, Y.K., Hong, S.H., 2015. Qualitative analysis of additives in plastic marine debris and its new products. Arch. Environ. Con. Tox. 69, 352-366.

Rani, M., Shim, W.J., Han, G.M., Jang, M., Song, Y.K., Hong, S.H., 2017. Benzotriazole-type ultraviolet stabilizers and antioxidants in plastic marine debris and their new products. Science of the Total Environment 579, 745-754.

Rochman, C.M., Lewison, R.L., Eriksen, M., Allen, H., Cook, A.-M., Teh, S.J., 2014. Polybrominated diphenyl ethers (PBDEs) in fish tissue may be an indicator of plastic contamination in marine habitats. Science of the Total Environment 476, 622-633.

Ru, J., Huo, Y., Yang, Y., 2020. Microbial Degradation and Valorization of Plastic Wastes. Front. microbiol. 11, 442.

Sandt, C., Waeytens, J., Deniset-Besseau, A., Nielsen-Leroux, C., Rejasse, A., 2021. Use and misuse of FTIR spectroscopy for studying the bio-oxidation of plastics. Spectrochim. Acta - A: Mol. Biomol. Spectrosc. 258, 119841.

Singh Jadaun, J., Bansal, S., Sonthalia, A., Rai, A.K., Singh, S.P., 2022. Biodegradation of plastics for sustainable environment. Bioresource Technology 347, 126697.

Singla, M., Diaz, J., Broto-Puig, F., Borros, S., 2020. Sorption and release process of polybrominated diphenyl ethers (PBDEs) from different composition microplastics in aqueous medium: Solubility parameter approach. Environmental Pollution 262.

Sun, P., Liu, X., Zhang, M., Li, Z., Cao, C., Shi, H., Yang, Y., Zhao, Y., 2021. Sorption and leaching behaviors between aged MPs and BPA in water: the role of BPA binding modes within plastic matrix. Water Research 195, 116956.

Sutkar, P.R., Gadewar, R.D., Dhulap, V.P., 2023. Recent trends in degradation of microplastics in the environment: A state-of-the-art review. J. Hazard. Mater. Adv. 11.

Takada;, H., Bell, L., 2021. ipen-plastic-waste-management-hazards.

Wang, H., Yu, P., Schwarz, C., Zhang, B., Huo, L., Shi, B., Alvarez, P.J.J., 2022. Phthalate Esters Released from Plastics Promote Biofilm Formation and Chlorine Resistance. Environ. Sci. Technol. 56, 1081-1090.

Wang, L., Guo, C., Qian, Q., Lang, D., Wu, R., Abliz, S., Wang, W., Wang, J., 2023. Adsorption behavior of UV aged microplastics on the heavy metals Pb(II) and Cu(II) in aqueous solutions. Chemosphere 313, 137439.

Wu, X., Liu, P., Shi, H., Wang, H., Huang, H., Shi, Y., Gao, S., 2021. Photo aging and fragmentation of polypropylene food packaging materials in artificial seawater. Water Research 188.

Yao, S., Ni, N., Li, X., Wang, N., Bian, Y., Jiang, X., Song, Y., Bolan, N.S., Zhang, Q., Tsang, D.C.W., 2023. Interactions between white and black carbon in water: A case study of concurrent aging of microplastics and biochar. Water Research 238.

Zafar, R., Arshad, Z., Eun Choi, N., Li, X., Hur, J., 2023. Unravelling the complex adsorption behavior of extracellular polymeric substances onto pristine and UV-aged microplastics using two-dimensional correlation spectroscopy. J. Chem. Eng. 470.

Zhou, L., Wang, T., Qu, G., Jia, H., Zhu, L., 2020. Probing the aging processes and mechanisms of microplastic under simulated multiple actions generated by discharge plasma. J. Hazard. Mater. 398, 122956-122956.

6. An investigation into the leaching behavior of chemical additives from microplastics with different aging treatments

This chapter investigates the role of the aging process on the leaching behavior of additives, providing new insights into the potential transfer and fate of additives of microplastics debris in the natural environment. These results could be useful for better understanding of environmental exposure to hazardous chemicals through plastic pollution.

Graphical abstract
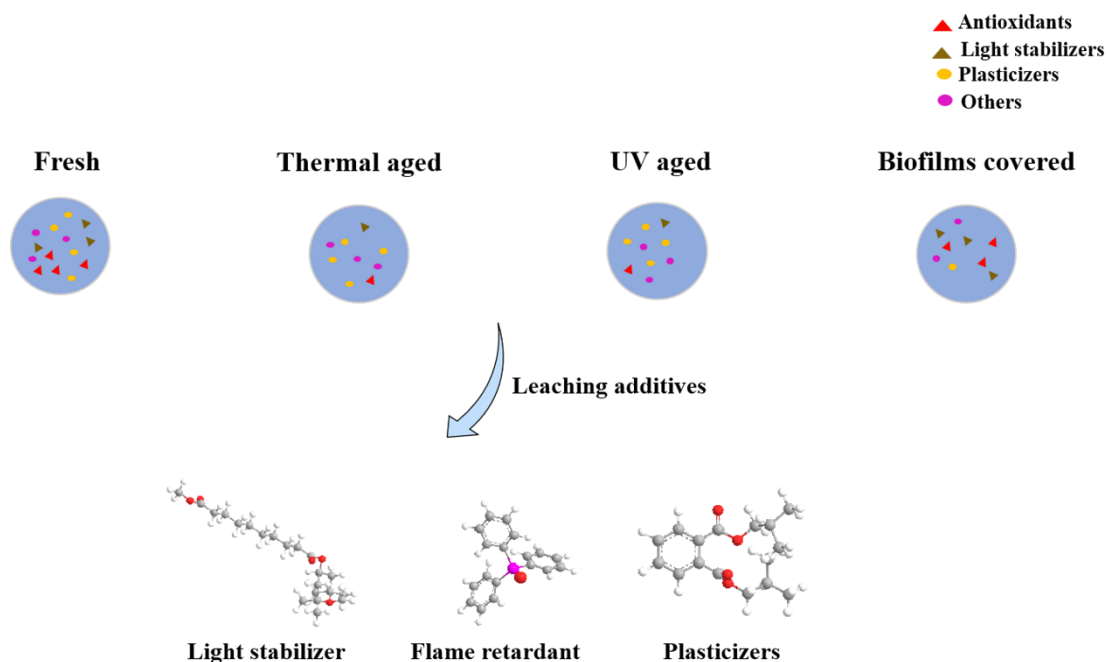
Abstract

Plastic debris makes up a large proportion of waste materials in the aquatic environment, yet little is known about their degradation and the role it plays in the fate of additives. This study investigated environmentally relevant aging for polyurethane (PU) and polyvinyl chloride (PVC) microplastics, along with changes to their respective additive chemical profile, together with their potential for additive leaching behavior. Fourier-transform infrared spectroscopy (FTIR) and scanning electron microscopy (SEM) studies suggested that physicochemical property changes (such as generation of new functional groups, erosion) occurs after the microplastic aging process. Between 33 and 36 chemical additives were tentatively identified in extracts of PU and PVC microplastics, respectively. The results indicate that additives are more likely leached in an artificial gastric solution compared with in artificial seawater. Fresh

and aged microplastic materials exhibit different leaching behaviors for additives, with increasing abundance of plasticizers and decreasing abundance of light stabilizers in leachates of microplastics after thermal and UV aging. It was also observed that additives (e.g., plasticizers, flame retardants, etc.) showed decreased leaching ability after colonization by biofilms. This study strengthens our understanding about the leaching behavior of additives from microplastics and explores the potential relationship between the aging of microplastics and the release behavior of additives.

6.1 Introduction

The issue of microplastic debris has received growing global attention. It has been reported that plastic debris are the major component of solid waste in the marine environment, accounting for 75 % of all marine litter (Napper and Thompson, 2020). Owing to the widespread and small size of microplastics, they are easily be ingested by marine organisms (e.g., fish, turtles, seabirds, etc.) (Steer et al., 2017; Tourinho et al., 2010). It is known that chemical additives such as plasticizers, flame retardants, antioxidants, etc. are applied in plastic products to modify and enhance their properties (Murphy, 2001). Many such additives have been identified as endocrine-disrupting chemicals (EDCs) and associated with endocrine disorders, cardiovascular diseases, reproductive disorders and various cancers. As additives are not chemically bound to the polymers, they leach into the marine ecosystems resulting in potential toxicity to aquatic wildlife. For example, a previous study demonstrated that phthalates can be detected in the leachate of polyvinyl chloride (PVC) plastics which might result in the

toxicity for the embryo development and larval growth of sea cucumber (Wang et al., 2023a). Therefore, consideration of the leaching ability of additives is essential for evaluating the fate and potential exposure risk of microplastics debris in the environment.

Most microplastic debris within the environment are likely to be highly aged due to biotic (e.g., microorganism colonization) and abiotic factors (e.g., light aging, thermal aging). It has estimated that with 80 - 90 % marine plastic debris has been in the environment for more than 2 years (Koelmans et al., 2016). Up to now, within the wide range of studies assessing the extracts or leachates of fresh microplastics, only a few studies have reported the effect of degradation on the extent of additive leaching under environmentally relevant conditions, warranting further investigation (Bridson et al., 2021).

In this study, organic solvent extracts of PU and PVC microplastics were analysed by using suspect screening analysis with ultra-performance liquid chromatography-quadrupole time-of-flight-mass spectrometry (UPLC-QTOF/ MS) to reveal the occurrence of additives in microplastics. Leachates from fresh and aged microplastics using artificial seawater and simulated gastric fluid were analysed to assess leaching behavior of additives during the aging process. The objectives of the study were to: 1). investigate changes to the additives during the aging process, clarify the relationship between aging of microplastics and additives leaching behavior; 2). assess the potential exposure risk of microplastic debris in aquatic environment.

6.2 Materials and methods

6.2.1 Chemicals and plastic materials

Ethyl acetate, n-hexane, methanol (ME), acetonitrile (ACN) and ethanol were purchased from Fisher Scientific Ltd (UK), dichloromethane (DCM) were purchased from Rathbun Chemicals Ltd (UK). All the solvents applied in the extraction and chemical analysis were of HPLC grade.

PU and PVC plastics were purchased in the market (Guangzhou, China) and Hilltop Products Ltd (UK), respectively. Plastics were cut into small pieces around 3-5 mm to obtain the micro-sized plastics before further study.

6.2.2 Aging treatment of microplastics

6.2.2.1 UV irradiation

Samples of PU and PVC microplastics were placed in quartz glass tubes (8 pieces microplastics were placed in each glass tube). UV exposure experiments were performed using an Atlas Suntest CPS+ instrument fitted with a Xenon lamp and sunlight filter, with intensity regulated using the emission range between 300 and 800 nm. Irradiation was conducted at an intensity of 750 W/m^2, while the temperature in the exposure chamber was maintained at 35 °C.

6.2.2.2 Biofilms colonization

PU and PVC microplastics (4.0 g/L) were incubated in shaken flasks (110 rpm) containing of activated sludge collected from the Lancaster Wastewater Treatment Plant at 23 °C for 28 days. Catton balls were used to seal the shaken flasks to prevent

the extreme volatilization. After 28 days incubation in sludge, the biofilms colonized microplastics were separated from sludge and washed thoroughly with ultrapure water to remove any salt residue or attached organic matter and kept sealed at 4 ℃ until further analysis.

6.2.2.3 Thermal treatment

For the accelerated thermal aging experiment, 10 pieces microplastics were put into each petri dish and then placed in thermostatic oven (Memmert GmbH & Co. KG, Germany) for 3 months. the temperature was set to 50 ℃. According to the previous report, the land surface temperature can reach above 45 ℃ in the hot summer for many regions, the temperature measured on dark sandy beaches may even reach above 60 ℃ and surpass the air temperature by 30 – 50 ℃ (Running et al., 2011). Thus, 50 ℃ is a reasonable temperature to for the accelerated thermal aging test.

6.2.2.4 Microplastics characterization

Spectra were recorded using a Fourier-transform infrared spectroscopy (FTIR, Agilent, USA), the spectra were recorded in a 4000−400 cm^{-1} region. To identify aging-induced changes to the microplastic, we compared the spectrum of the fresh PU and PVC microplastics to identify the presence of chemical bonds indicative of aging. The surface changes of the microplastics were inspected by scanning electron microscopy (SEM).

6.2.3 Microplastics extraction

To determine the chemical additives that present in the PU and PVC microplastics, fresh and aged samples of each microplastic type (100 mg) were extracted with 5 mL DCM, n-hexane, and ME respectively by ultrasonication for 30 min at room temperature (n=3). The solvents without microplastics were used as blank to eliminate interference of the additives that potentially leached through the entire experimental procedures (e.g., leached from pipette tips, filter syringes, etc.). DCM, n-hexane and ME represent different polarity from low to high, which could show different extraction efficiencies for chemical additives. Solvent extracts were dried up by gentle evaporation under a stream of N_2 and reconstituted in 800 μL ME prior to liquid chromatography–mass spectrometry (LC–MS) analysis.

6.2.4 Artificial seawater and simulated gastric fluid leachates

6.2.4.1 Leaching experiments

Artificial seawater and simulated gastric fluid were used as leaching media. Artificial seawater was obtained from Brightwell Aquatics (USA), the pH value = 8.2 ± 0.1. The pepsin A was purchased from Sigma-Aldrich Co. LLC (UK), and the simulated gastric fluid was prepared according to the recipes in a previous study (Liu et al., 2020c). In brief, 1.6 g pepsin was added into 500 mL and the pH of the solution was adjusted to 2.0 by the addition of 1 M HCl to simulate the acidic stomach environment. 100 mg of fresh and aged PU and PVC microplastics were immersed into 20 mL freshly prepared artificial seawater and simulated gastric fluid and shaken at 100

rpm at 24 °C in the dark for 16 h. This incubation duration was based on the retention time of food in the fish gastrointestinal tract (Coffin et al., 2019).The simulated solutions without microplastics were used as controls. All the experiments were performed in triplicate.

6.2.4.2 Solid phase extraction

After the leaching experiments, the pH of the artificial seawater was then adjusted to 2.0 with 1 M HCl. The solutions were extracted by solid phase extraction (SPE). During the SPE, glassware was used to prevent the contamination of exogenous plastic additives. Prior to loading 20 mL leaching liquid at an approximate speed of 1 mL/min, each hydrophilic-lipophilic balance (HLB) cartridge (Waters Oasis, 500 mg, 6 mL) was rinsed with 10 mL ME and 10 mL ultrapure water. Afterwards, columns were washed with 10 mL ultrapure water to remove impurities and dried for 2 h under vacuum. Due to differences in polarities of the additives in the plastic products, 6 mL DCM, 6 mL ethyl acetate and 6 mL ME with low to high elution intensity were performed sequentially. After elution, the extracts were filtered (0.22 μm nylon) and dried up under N_2 before reconstituted in 800 μL ME. Samples were stored at -20 °C until chemical analysis.

6.2.5 Instrument conditions and additives identification

The qualitative analysis of the chemicals in the extracts were performed using an ultra-performance liquid chromatography system (UPLC, Waters ACQUITY™, USA) coupled to a QTOF MS system (Waters Xevos G2-S, USA). The UPLC column (Waters

BEH C18 column ,1.7 μm, 2.1 × 50 mm) was kept at 30 °C and the injection volume was 5 μL. The UPLC was performed according to a previously published method (Qiu et al., 2021). The mobile phase consisted of ME (solvent A) and ultrapure water containing 0.1% formic acid (solvent B). The UPLC program was as follows: started at 20 % A, ramped to 99% in 12 min and held until 13 min, then returned to original ratio in 13.5 min and maintained 1.5 min for equilibrium until next injection. In addition, the capillary voltage was set at 3.0 KV in positive-ion (ESI+) and 2.5 KV in negative-ion (ESI−) modes. The source temperature was set to 120 °C and the desolvation gas temperature to 450 °C with a flow rate of 1000 L/h. The acquisition mode was MS^E with scan range from 50 to 1200m/z, which could obtain the parent and daughter ions of the compound through one injection. Leucine-enkephalin (0.2 ng/μL) was selected to calibrate the whole data acquisition process (every 20 s), referencing mass 556.2766m/z in ESI+ mode and 554.2620m/z in ESI−. To check and prevent laboratory contamination, a procedural blank containing ME was applied in every eight samples.

Waters UNIFI software was used to acquire and process the data (Waters, Milfor, MA USA). A library of 78 additives including plasticizers, antioxidants, flame retardants, etc. has been established in our laboratory, with detailed information contained in our previous study (Qiu et al., 2021). Three additional libraries were also referenced to identify more potential additives (Chen et al., 2021a; Zhang et al., 2016; Zimmermann et al., 2019), in which a total of 462 chemicals were available for searching. Features with response of at least 10000 and detector counts greater than

3000 were selected and features less than those in the samples were removed. When analysing complex samples with heavy matrix, the drift in the signals due to instrumental restrictions can be challenging and sometimes lead to the escape of chemicals and the generation of artefacts. Features were only considered if: i) response at least three times higher than the blank response (if present in the blank) ii) they were present in at least two of the three replicates.

UNIFI aided in the creation of a scientific library for plastic additives that contains all the critical detection criteria, such as accurate molecular weight, retention time, structural formula, fragment ions and other properties. Moreover, a series of critical detection criteria were set up according to our previous method to raise the correctness of determination. In the referential libraries, the compounds were determined upon satisfying these requirements: detector counts > 3000, isotope match intensity RMS (root mean square) percent < 20, isotope match Mz RMS ppm < 6, and MS error ranging from -5 ppm to 5 ppm, MS/MS error < 10 ppm. In the self-building library, the compounds were identified if they met these standards: isotope match intensity RMS (root mean square) percent < 20, isotope match Mz RMS ppm < 6, MS error ranging from -5 ppm to 5 ppm, MS/MS error < 10 ppm, number of fragment ions $\geq$ 1, and retention time error < 0.1 min. The candidates that meet above requirement were considered tentatively identified. Figure S1 shows the interface of UNIFI platform where the data are processed and matched as follow as: (A) template of workflow, (B) component identification list, (C) selected ion chromatogram of a single component

corresponding to (B), and finally (D) the respective mass spectrum and fragmentation (example of Tinuvin 292-2 identified by the library).

The presence of chemical additives was quantified according to changes in response. The higher response number indicate higher concentration of the compound. In order to ensure the accuracy and credibility of the data, all extraction samples were run in one batch that ensure the instrument could with the same running conditions.

6.2.6 Statistical analysis

T-test and one-way analysis of variance (ANOVA) were used to analyse significant differences, data were considered significantly different when $p < 0.05$. All statistical analysis was performed using SPSS 22.0 software and Microsoft Office Excel 2020. Figures were plotted with Origin 2020.

6.3 Results and discussion

6.3.1 Characteristics of extracted additives

The workflow for the identification strategy for additives (Figure S2) was as follows: peak alignment and picking, library searching followed by mass error, retention time error, isotope pattern filtering, MS/MS spectra interpretation with

characteristic fragment matching. Examples of additives identified process is self-building library and referential libraries are listed in Figure S3 and Figure S4.
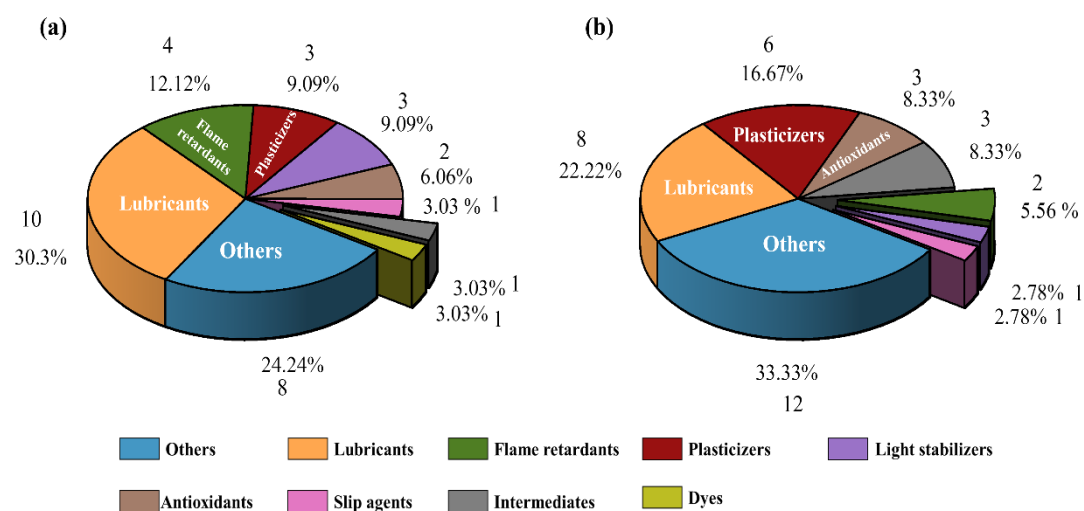
Figure 1. Number and percentage of tentative identified features in PU (a) and PVC (b) microplastics.

33 and 36 features be tentatively identified in PU and PVC microplastics, which were classified into 9 categories of additives according to their functionalities and properties, including plasticizers, antioxidants, flame retardants, etc. (Table S1 and Tables S2). The number of features identified in positive mode was higher than in negative mode. As illustrated in Figure 1, with the exception of the unclassified additives, the predominant additives were lubricants, plasticizers, flame retardants. In addition, antioxidants, light stabilizers, slip agents (friction control), dyes, etc. were also identified in PU and PVC microplastics. Most of identified features are functional additives, which are play important role in change/enhance the functional properties of plastic products (Hahladakis et al., 2015).

6.3.2 Characterization and additives changes after aging treatment

6.3.2.1 Thermal aging

The FTIR spectrum of PU microplastics before and after ageing are shown in Figure 2a.

(a)

(b)
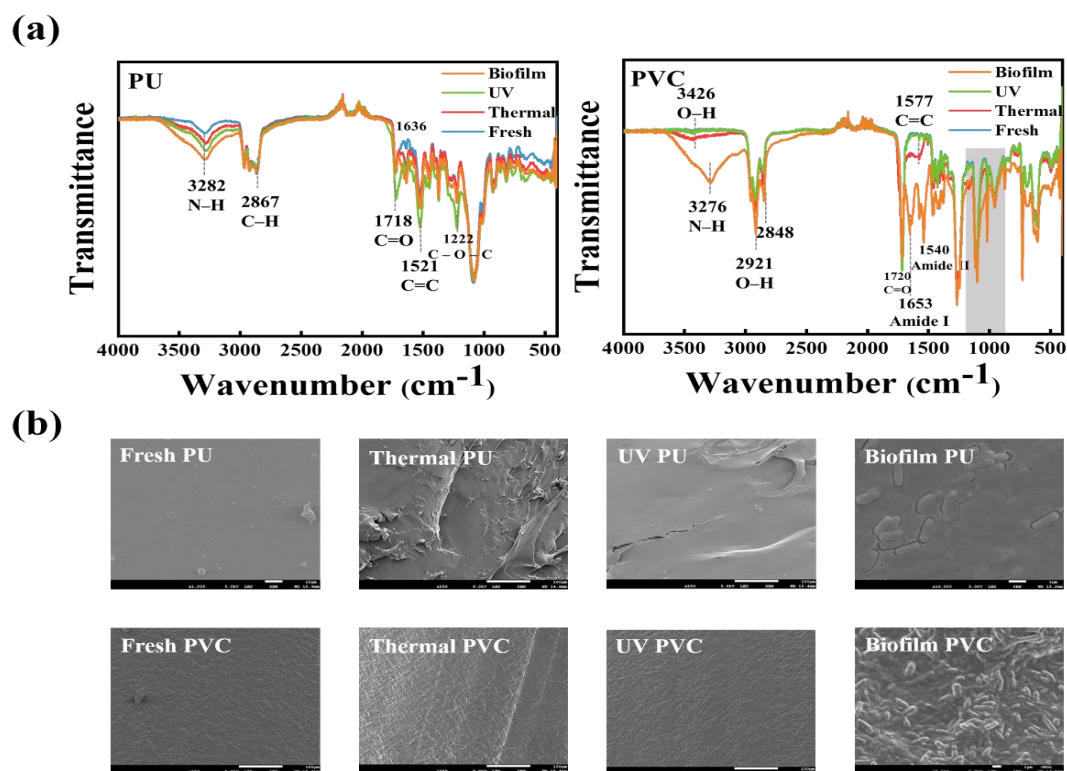
Figure 2. (a) FTIR spectrum of PU and PVC microplastics with different aging treatments. (b) SEM images of microplastics with different aging treatments.

The peaks observed at around 1718 cm^{-1} and 3282 cm^{-1} were attributed to the stretching vibration of characteristic urethane groups (C=O–N–H). The peaks identified around 2864 cm^{-1} were attributed to the stretching vibration of the C–H group (Boubakri et al., 2009). Moreover, the spectrum also showed bands C=O and C–O–C stretching around 1718 cm^{-1} and 1222 cm^{-1} (Xue et al., 2021). After thermal aging treatment, the intensity of N–H stretching band (3282 cm^{-1}) and C=O stretching band

(1636 cm^{-1}) were enhanced. As shown in Figure S5a, PU microplastics obviously yellowed after thermal aging treatment, which might be related to oxidization of the molecular structure and formation chromophores (e.g., methylene oxidation to form quinone-imide structures) (Rosu et al., 2009). The SEM images (Figure 2b) also suggest changes after thermal aging as the surfaces of fresh PU microplastics were smooth, whilst in contrast, more pits were generated after thermal aging treatment. For PVC microplastics (Figure 2a), the peak at around 2914 cm^{-1} and 2848 cm^{-1} represents C–H stretching. Compared with fresh PVC microplastics, the intensity of C–H stretching (2921 cm^{-1} and 2848 cm^{-1}) increased with thermal aging (Fan et al., 2021b). In addition, new peak generation occurred at 3424 cm^{-1} (O–H stretching band) and 1577 cm^{-1} (C=C stretching band) after thermal aging (Ouyang et al., 2022; Pagacz et al., 2015), which indicates the oxidation of PVC microplastics. The surface colour slightly yellowed for PVC microplastics after thermal aging (Figure S5b). The previous study suggested that the formation of conjugated polyene sequences leading to yellowing of PVC plastics, and indicates the dehydrochlorination and formation of aromatic compounds after thermal aging treatment (Pagacz et al., 2015). In addition, the surfaces of PVC microplastics generated more crinkles after thermal aging treatment according to the SEM images (Figure 2b), which indicates the morphological changes of PVC microplastics.

6.3.2.2 UV aging

The enhanced vibration of N–H stretching band (3282 cm^{-1}) and C=O stretching

band (1636 cm^{-1}) could also be observed for PU microplastics after UV aging treatment

(Figure 2a). In addition, increased vibration intensity occurred for C=O stretching band

(1718 cm^{-1}), C=C stretching band (1521 cm^{-1}) and C–O–C stretching band (1222 cm^{-1})

(Boulaouche et al., 2019; Rosu et al., 2009). In addition, obviously yellowed (Figure

S5a) and surfaces cracks could also be observed for UV aged PU microplastics (Figure

2b).

However, few changes could be characterized by FTIR spectra and SEM images

for PVC microplastics after UV aging treatment (Figure 2a and 2b). The PVC

microplastics used in this study were same with the PVC$_2$ microplastics used in chapter

5. As we illustrated in Chapter 5, the present of light stabilizers (Tinuvin 234) and

antioxidants (Irganox 1076, Isonox 132, Tinuvin 144) in PVC microplastics can absorb

UV and transfer irradiation to heat or capturing and removing free radicals (e.g., R•,

RO•, ROO•, etc.), which might inhibit the UV degradation and result in few

physiochemical property changes of PVC microplastics.

6.3.2.3 Biofilms colonization

As shown in Figure 2a, after biofilm colonization, a widened and enhanced bend

was observed at around 3282 cm^{-1} (N–H stretching) for PU microplastics. Further, the

increasing vibration characterized at around 1636 cm^{-1}, which might attributed to C=O

stretching of amide I group (Maquelin et al., 2002), is considered to represent the

characteristic peaks from proteins (Sandt et al., 2021). For PVC microplastics, new peaks were observed at 3286 cm^{-1} (N–H stretching band), 1653 cm^{-1} (amide I band) and 1540 cm^{-1} (amide II band) after biofilm colonization. In addition, the intensity of a spectral region between 1180−900 cm^{-1} (shaded in grey) obviously altered after biofilm colonization, which represents vibrations from polysaccharides (Sandt et al., 2021). For both PU and PVC microplastics surface changes and microorganisms (e.g., rod-like bacteria) were observed in SEM images (Figure 2b), which confirmed biofilm formation on microplastics.

6.3.3 Leaching of additives before and after aging treatments

6.3.3.1 Categories of leached additives from microplastics

Compared with solvent extraction, only small number of features be identified in the leachates of PU and PVC microplastics. For example, 11 types of additives leached to artificial seawater from fresh PU microplastics (Figure 3a), accounting for around 33 % of the identified features. Octanol-water partition coefficients (log K_{ow}) are used to represent the hydrophobicity of compounds. A substance is considered to exhibit relative hydrophobic properties when log $K_{ow} > 2$ and classified as high hydrophobicity when log $K_{ow} > 3.5$ (Huerta-Fontela et al., 2011; Razanajatovo et al., 2018). According to the log K_{ow} values of identified additives illustrated in Table S1 and S2, nearly all additives have hydrophobic properties, with 90 % and 80 % of chemical additives being highly hydrophobic in PU and PVC microplastics, respectively. Chemical additives showing hydrophobic properties would be expected to show lower solubility in water

and higher solubility in general organic solvents. Water is not efficient at extracting hydrophobic additives from a plastic matrix. In addition, in increased salinity can further decrease the water solubility of hydrophobic compounds which restricts the leaching behavior of additives from microplastics (Li et al., 2022). Compared to the artificial seawater, microplastics leach more additives in simulated gastric fluid (Figure 3), with this increased leaching ability also reported in a previous study (Li et al., 2022). Acidic pepsin solution may facilitate the release of chemical additives as it is sufficiently hydrophobic to extract organic additives mixed in plastic products (Li et al., 2022).
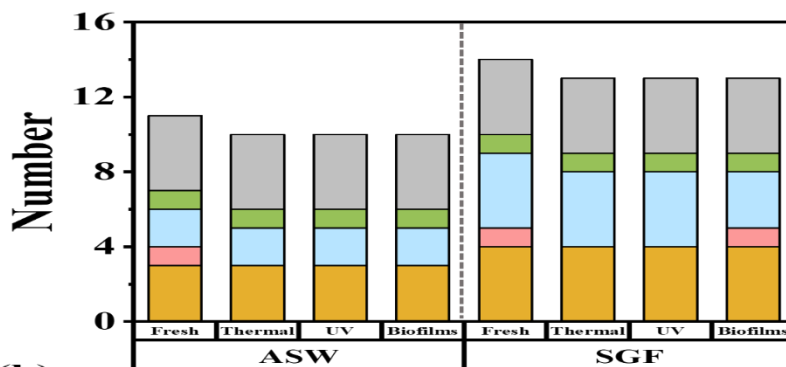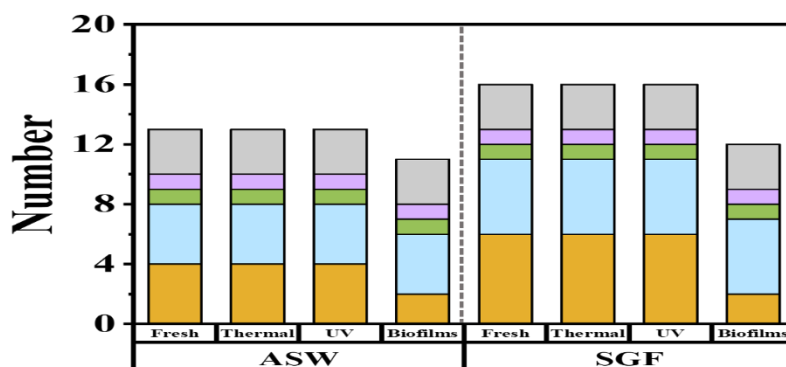
Figure 3. Number of identified features leached from fresh and aged PU (a) and PVC (b) microplastics to artificial seawater and simulated gastric fluid.

As illustrated in Figure 3a and Table S3, the light stabilizer Tinuvin 292-2 was detected in leachates from fresh PU microplastics, whilst it wasn't identified in the leachate after thermal and UV aging treatments. Tinuvin 292-2 as a hindered amine light stabilizer (HALS) which scavenges and reacts with radicals created by UV irradiation and thermal aging, hence restricting the degradation process (Luyt et al., 2021). Tinuvin 292-2 can undergo reaction with R• /ROO• converting to degradation products during UV and thermal aging treatments, resulting in the considerable reduction of Tinuvin 292-2 in PU microplastics. This could be verified using the solvent extracts (Figure S6), as Tinuvin 292-2 could be detected in fresh PU microplastics, but not after thermal and UV aging. As Tinuvin 292-2 appeared to be degraded during the aging process, it wasn't identified in the leachates of PU microplastics after UV irradiation and thermal aging treatments. As demonstrated in Figure 3b, PVC microplastics leached minimal plasticizers in both artificial seawater and simulated gastric fluid after colonization by biofilms. Plasticizers such as dimethyl phthalate (DMP), diethyl phthalate (DEP) and Dibutyl phthalate (DBP)) appeared to be metabolized during the microorganism colonization process (illustrated in chapter 5), which result in decreased leaching of plasticizers from biofilm colonized PVC microplastics (Table S4). These results suggest that the additives are being consumed

during microplastics aging process, which would further affect their leaching behavior from microplastic debris.

6.3.3.2 Leaching ability for fresh and aged microplastics

In order to assess the potential for additive leaching further, we used the response for those identified features found in fresh and aged groups to explore which additives contributed to the significant difference between fresh and aged microplastics. Volcano plots combine the measure of statistical significance from statistical tests (p values from T-test) with the magnitude of the change ($\log_2$ Fold Change, this value is reported on a logarithmic scale to base 2, which indicates how much the additive response changes between fresh and aged microplastics), could quick visual identification of those data-points (additives) that show large magnitude changes that are also statistically significant, and are commonly used in non-target analysis studies for the statistical analysis of two experimental groups. The related data of the volcano plot for PU and PVC microplastics are suggested in Table S5 and S6.

The leaching ability of additives to artificial seawater and simulated gastric fluid significantly increased (e.g., di-n-octyl phthalate (DnOP), etc.) for PU microplastics after thermal/UV aging treatments and PVC microplastics after thermal aging treatment (Figure 4). As the aging process of microplastics can lead to polymer chain breakage and formation of surface pores and cracks (Figure 2), this in turn accelerates the leaching ability of additives (Luo et al., 2022b). In addition, the FTIR data showed that polar functional groups (e.g., C=O, C–O–C, etc.) were created after aging treatments

(Figure 2a), which will have increased the surface polarity of the polymers. As a result, these changes might have affected the distribution (partition coefficients) of the additives between artificial seawater/simulated gastric fluid and microplastics, resulting in changes the leaching behavior (Paluselli et al., 2019).
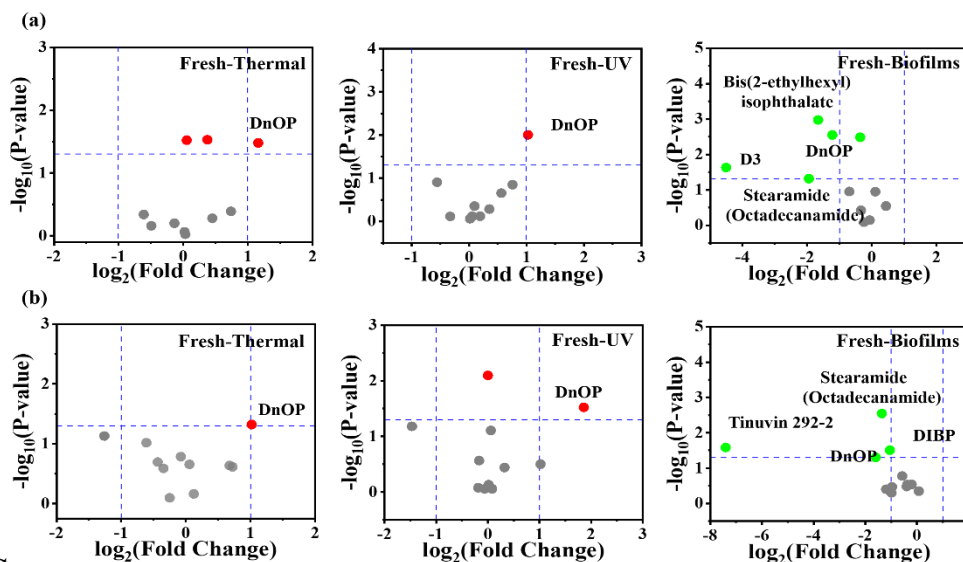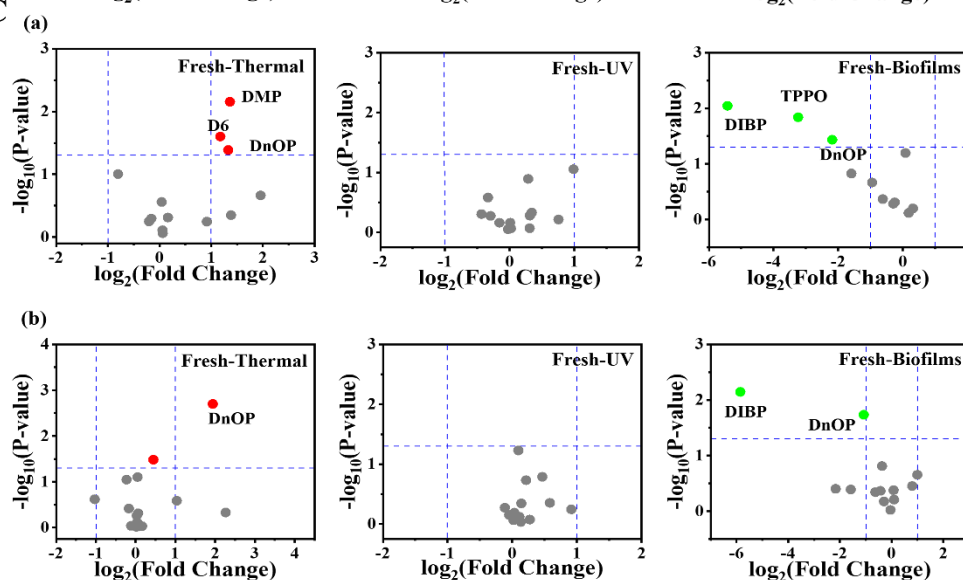
Figure 4. Volcano plots comparing fresh and aged microplastics leachates in artificial seawater (a) and simulated gastric fluid (b). Additives with a positive value in the x-axis (red dots) have an average response across aged microplastics that is significantly

higher ($p < 0.05$) than that of fresh microplastics. Additives with a negative value in the x-axis (green dots) have an average response that is significantly lower ($p < 0.05$) than that of fresh microplastics. Characteristic additives with higher significance levels are labelled.

It worth noting that leaching ability showed few changes for PVC microplastics after UV aging treatment. Due to the protection of light stabilizers and antioxidants the degradation of PVC microplastics was reduced (Figure2), leading to few changes to their physicochemical characteristics and resulting in no significant changes to leaching behavior of UV aged PVC microplastics to artificial seawater and simulated gastric fluid. All characteristics features (labelled) that leached from PU and PVC microplastics colonized with biofilms to artificial seawater and simulated gastric fluid suggest significant lower leaching ability compared with fresh microplastics (Figure 4). Those additives included plasticizers, flame retardants, light stabilizers, etc. In addition to the potential metabolism by microorganisms leading to the decrease leaching behavior, biofilm formation can also act as an additional mass transfer resistance, which might also reduce the leaching process of additives from microplastics (Daniel et al., 2008).

6.3.4 Risk assessment

The enhanced leaching potential demonstrated in this study indicates that ecological risk may increase after microplastics undergoing UV irradiation and thermal aging. For example, the phthalate DnOP, identified as a characteristic feature, showed

enhanced leaching after thermal and UV aging treatments (Figure 4). This substance has been identified as a priority pollutant by the US Environmental Protection Agency and the European Commission as its presence in the environment has been linked to potential risks to organisms (Huan-Yu et al., 2022). Further studies are required to accurately quantify the leaching of additives after aging treatment to better assess the potential exposure risks and biotoxicity of plastic debris in the environment.

However, the leaching and exposure risk of additives might also be decreased for microplastics after colonization by biofilms (Figure 4). This decreased leaching ability indicates that reduced amounts of additives might be released from biofilm colonized microplastics to the environment or biota. However, as we mentioned in Chapter 3, the presence of microorganisms has also been linked to microplastics acquiring chemical signals that attract species that use chemosensory mechanisms when locating, identifying, and ingesting food (Procter et al., 2019; Savoca et al., 2016). So, although the leaching ability of additives might become weaker after biofilms colonization, their presence might enhance bioavailability of microplastics to marine organisms and therefore increase the bioavailability of additives in microplastics increasing the potential ecological risk.

According to the Stockholm Convention, chemicals with a log K_{ow} greater than 5 can be considered to bioaccumulate. As shown in Table S1 and Table S2, more than 72 % and 69 % of identified features in PU and PVC microplastics have the potential to bioaccumulate, although only small number of additives were found to leach

according to this study. Microplastic debris will be undergo long-term and more complicated degradation process in the real environment systems, which could result in more physiochemical property changes. Owing to most additives not being tightly bound into polymers, more additives could be expected be released to the environment, posing a potential long-term exposure risk that cannot be ignored.

6.4 Conclusions

This study identified the presence of a wide range of organic additives in PU and PVC microplastics. With the exception of the unclassified additives, the most frequently detected additives were lubricants, plasticizers, flame retardants and antioxidants/light stabilizers. The number of additives detected in different leaching media indicated that gastric fluid increased microplastics leaching behavior compared to seawater, which suggests higher exposure ecological risks could be expected once microplastics are accidently ingested by organisms. The number of leached additives decreased after aging treatments, which might be related to the degradation of the additives during the aging process. Owing to the protection from light stabilizers and antioxidants, the leaching behavior didn't significantly change for PVC microplastics after UV irradiation under experimental conditions. As a result, this study suggests that additives might play an important role in the aging process of plastic debris in the natural environment, which could further affect their leaching behavior. This study will help to increase our understanding of the leaching behavior of additives in aquatic

environments as microplastics age, and thereby lays a foundation for further study on

the fate, potential exposure risk and toxicity of plastic debris in the natural environment.

Supporting information

Table S1. Identified additives in PU microplastics

Category	CAS	Additive name	Log K_{ow}	Formula	Molecular weight	Mass error (ppm)	RT (min)	RT error
Light stabilizers	41556-26-7	Tinuvin 292-1 a	6.92	$C_{30} H_{56} N_2 O_4$	508.79	0.2	4.35	-
	82919-37-7	Tinuvin 292-2 a	5.14	$C_{21}H_{39}NO_4$	369.54	1.8	6.11	-
	52829-07-9	Tinuvin 770 a	6.50	$C_{28} H_{52} N_2 O_4$	480.74		5.02	
Antioxidants	125643-61-0	Irganox 1135 b	8.50	$C_{25} H_{42} O_3$	390.61	0.4	12.08	-
	6683-19-8	Irganox 1010 b	19.60	$C_{73} H_{108} O_{12}$	1177.67		13.13	
Plasticizers	117-84-0	Di-n-octyl phthalate a	8.54	$C_{24} H_{38} O_4$	390.57	3	12.01	-
	84-69-5	Diisobutyl phthalate a	4.46	$C_{16} H_{22} O_4$	278.35	2.1	9.29	0.02
	137-89-3	Bis(2-ethylhexyl) isophthalate a	8.39	$C_{24}H_{38}O_4$	390.56	1.1	12.07	
Flame retardants	791-28-6	Triphenylphosphine oxide a	2.87	$C_{18}H_{15}O_1P_1$	278.29	1.9	6.82	0.03
	126-73-8	Tributyl phosphate a	3.82	$C_{12} H_{27} O_4 P_1$	266.32	2.1	9.45	-
	19186-97-1	Tris (tribromo neopentyl) phosphate a	8.05	$C_{15} H_{24} Br_9 O_4 P_1$	1018.47	-1.5	13.08	
	115-86-6	Triphenyl phosphate a	4.70	$C_{18} H_{15} O_4 P_1$	326.29	0.1	8.75	0.00
Slip agents	124-26-5	Stearamide (Octadecanamide) a	6.70	$C_{18} H_{37} N_1 O_1$	283.50	2	12.03	
Lubricants	373-49-9	9-Hexadecenoic acid a	6.75	$C_{16} H_{30} O_2$	254.42		11.67	
	301-02-0	9-octadecenamide (z)- a	6.48	$C_{18}H_{35}NO$	281.48	1.1	11.58	
	1113-92-4	Ethylmalonic acid dibutyl ester a	3.77	$C_{13} H_{24} O_4$	244.33	0.5	8.93	
	112-79-8	Elaidic Acid a	7.73	$C_{18} H_{34} O_2$	282.47	3.9	11.76	
	302912-17-0	Tetracosanoic acid b	10.89	$C_{24} H_{48} O_2$	368.65	1.2	12.18	
	60-33-3	Linoleic acid a	7.51	$C_{18} H_{32} O_2$	280.45	0.2	11.65	
	10436-09-6	trans-13-Docosenamide a	8.44	$C_{22}H_{43}N_1O_1$	337.59	2.5	12.60	
	628-97-7	Hexadecanoic acid, ethyl ester b	7.74	$C_{18} H_{36} O_2$	284.49	-0.7	13.41	
	20290-75-9	SDA, stearidonic acid, moroctic acid a	7.08	$C_{18} H_{28} O_2$	276.42	2.2	11.13	
	10417-94-4	cis-5,8,11,14,17-Eicosapentaenoic acid a	7.85	$C_{20}H_{30}O_2$	302.45	4.6	11.70	
Dyes	119-90-4	3,3'-Dimethoxybenzidine (Dianisidine) b	2.08	$C_{14} H_{16} N_2 O_2$	244.30	-2.5	8.66	
Intermediates	14035-33-7	1-(3,5-ditert-butyl-4-hydroxyphenyl) ethenone a	4.16	$C_{16} H_{24} O_2$	248.37	2.4	8.86	
Others	623563-19-9	Methyl 9-eicosenoate b	23.63	$C_{59} H_{102} O_6$	907.47	-2.1	12.12	
	103-95-7	3-(4-Isopropylphenyl)-2-methylpropionaldehyde b	3.91	$C_{13} H_{18} O_1$	190.29	-0.5	7.81	
	83-40-9	2-Anisic acid a	2.79	$C_8 H_8 O_3$	152.15	1.0	12.02	
	541-05-9	Hexamethylcyclotrisiloxane (D3) a	5.64	$C_6 H_{18} O_3 Si_3$	222.47	2.9	7.41	
	540-97-6	Dodecamethylcyclohexasiloxane (D6) a	9.08	$C_{12}H_{36}O_6Si_6$	444.92	-1.8	13.24	
	29761-21-5	Phosphoric acid, isodecyl diphenyl ester a	7.28	$C_{22} H_{31} O_4 P_1$	390.46	-0.3	11.13	
	141-02-6	BIS(2-ETHYLHEXYL) FUMARATE a	7.94	$C_{20} H_{36} O_4$	340.51	-2.9	13.22	
	23470-00-0	Hexadecanoic acid, 2-hydroxy-1-(hydroxymethyl)ethyl ester a	5.63	$C_{19}H_{38}O_4$	330.5	-0.4	11.58	-

RT: retention time (minute)

Log K_{ow} from Estimation Program Interface (EPI) Suite, V 4.11 (EPA,2012)

a: identified by ESI +

b: identified by ESI –

red color represents the additives leached from fresh PU microplastics in ASW or SGF

Table S2. Identified additives in PVC microplastics

Category	CAS	Additive name	Log K_{ow}	Formula	Molecular weight	Mass error (ppm)	RT	RT error
Light stabilizers	70321-86-7	Tinuvin 234 b	7.67	$C_{30}H_{29}N_3O_1$	447.57	2.3	6.92	
Antioxidants	2082-79-3	Irganox 1076 b	13.41	$C_{35}H_{62}O_3$	530.88	2.4	12.87	
	17540-75-9	Isonox 132 a	6.43	$C_{18}H_{30}O_1$	262.44	1.9	11.34	
	63843-89-0	Tinuvin 144 a	10.03	$C_{42}H_{72}N_2O_5$	685.03	-2.0	13.35	
Plasticizers	131-11-3	Dimethyl phthalate a	1.66	$C_{10}H_{10}O_4$	194.18	0.8	4.26	0.04
	25724-58-7	n-Hexyl decyl phthalate a	8.54	$C_{24}H_{38}O_4$	390.57	-0.4	10.28	
	84-69-5	Diisobutyl phthalate a	4.46	$C_{16}H_{22}O_4$	278.35	1.5	9.30	0.01
	84-74-2	Dibutyl phthalate a	4.61	$C_{16}H_{22}O_4$	278.35	2.7	12.04	0.06
	117-84-0	Di-n-octyl phthalate a	8.54	$C_{24}H_{38}O_4$	390.57	1.2	12.01	
	84-66-2	Diethyl phthalate a	2.65	$C_{12}H_{14}O_4$	222.24	0.4	6.23	0.04
Flame retardants	78-51-3	Tris(2-butoxyethyl) phosphate a	3.00	$C_{18}H_{39}O_7P_1$	398.48	0.8	12.47	
	791-28-6	Triphenylphosphine oxide a	2.87	$C_{18}H_{15}O_1P_1$	278.29	2.4	6.87	0.01
Lubricants	506-30-9	Arachidic acid a	8.93	$C_{20}H_{40}O_2$	312.54	1.2	10.96	
	301-02-0	9-octadecenamide (z)- a	6.48	$C_{18}H_{35}NO$	281.48	2.8	11.58	-
	20290-75-9	SDA, stearidonic acid, moroctic acid a	7.08	$C_{18}H_{28}O_2$	276.42	0.1	11.14	
	2363-71-5	Heneicosanoic acid b	9.42	$C_{21}H_{42}O_2$	326.57	2.1	12.98	
	112-84-5	trans-13-Docosenamide a	8.44	$C_{22}H_{43}N_1O_1$	337.59	1.2	12.54	
	123-94-4	1-Stearoylglycerol a	6.62	$C_{21}H_{42}O_4$	358.56	0.5	12.17	
	110-30-5	N, N-Ethylenebis(stearamide) a	13.98	$C_{38}H_{76}N_2O_2$	593.04	0.5	12.37	
	60-33-3	Linoleic acid a	7.51	$C_{18}H_{32}O_2$	280.45	0.8	11.35	
Slip agents	124-26-5	Stearamide (Octadecanamide)	6.70	$C_{18}H_{37}N_1O_1$	283.50	2.2	11.03	
Intermediates	85-44-9	Phthalic anhydride a	2.07	$C_8H_4O_3$	148.12	2.5	12.77	
	14035-33-7	1-(3,5-ditert-butyl-4-hydroxyphenyl) ethanone a	4.16	$C_{16}H_{24}O_2$	248.37	1.6	8.85	
	85-44-9	Retarder AK a	2.07	$C_8H_4O_3$	148.12	-2.5	12.78	
Others	10340-21-3	Methyl 9-eicosenoate	9.00	$C_{21}H_{40}O_2$	324.55	2.5	12.08	
	822-23-1	Acetic acid n-octadecyl ester b	8.72	$C_{20}H_{40}O_2$	312.54	2.3	13.03	
	1673-08-1	Hexadecanoic acid, cyclohexyl ester b	9.52	$C_{22}H_{42}O_2$	338.58	1.1	12.95	
	14290-23-4	Myristin, 1,3-diaceto-2- a	6.26	$C_{21}H_{38}O_6$	386.53	1.3	8.60	
	135861-56-2	1,3,2,4-bis(3,4-dimethylbenzylidene)-sorbitol a	3.57	$C_{24}H_{30}O_6$	414.50	1.5	7.22	

	141-02-6	BIS(2-ETHYLHEXYL) FUMARATE a	7.94	$C_{20}H_{36}O_4$	340.51	-2.2	13.21	
	66037-03-4	Avocadyne 1-acetate a	2.32	$C_9H_9Cl_1O_3$	200.62	2.5	8.69	
	541-05-9	Hexamethylcyclotrisiloxane (D3) a	5.64	$C_6H_{18}O_3Si_3$	222.47	2.1	7.41	
	540-97-6	Dodecamethylcyclohexasiloxane (D6) a	9.08	$C_{12}H_{36}O_6Si_6$	444.92	0	13.24	
	57156-91-9	2,5-Octadecadiynoic acid, methyl ester a	6.80	$C_{19}H_{30}O_2$	290.45	1.8	9.84	
	33795-18-5	Isophthalic acid, butyl 10-chlorodecyl ester a	6.50	$C_{17}H_{25}Cl_1O_2$	296.84	0	13.55	
	39111-19-8	Oxiraneoctanoic acid, 3-octyl-, methyl ester, cis- a	22.42	$C_{57}H_{108}O_7$	905.49	1.4	11.35	

RT: retention time (minute)

Log Kow from Estimation Program Interface (EPI) Suite, V 4.11 (EPA,2012)

a: identified by ESI +

b: identified by ESI –

Table S3. Additives leached from PU microplastics to ASW and SGF after aging treatment.

		Fresh	**Thermal**	**UV**	**Biofilms**
ASW	**Plasticizers**	Diisobutyl phthalate	Diisobutyl phthalate	Diisobutyl phthalate	Diisobutyl phthalate
		Di-n-octyl phthalate	Di-n-octyl phthalate	Di-n-octyl phthalate	Di-n-octyl phthalate
		Bis(2-ethylhexyl) isophthalate	Bis(2-ethylhexyl) isophthalate	Bis(2-ethylhexyl) isophthalate	Bis(2-ethylhexyl) isophthalate
	Light stabilizers	Tinuvin 292-2	-	-	-
	Lubricants	SDA, stearidonic acid, moroctic acid	SDA, stearidonic acid, moroctic acid	SDA, stearidonic acid, moroctic acid	SDA, stearidonic acid, moroctic acid
		trans-13-Docosenamide	trans-13-Docosenamide	trans-13-Docosenamide	trans-13-Docosenamide
	Slip agents	Stearamide (Octadecanamide)	Stearamide (Octadecanamide)	Stearamide (Octadecanamide)	Stearamide (Octadecanamide)
	Others	Hexamethylcyclotrisiloxane (D3)	Hexamethylcyclotrisiloxane (D3)	Hexamethylcyclotrisiloxane (D3)	Hexamethylcyclotrisiloxane (D3)
		Dodecamethylcyclohexasiloxane (D6)	Dodecamethylcyclohexasiloxane (D6)	Dodecamethylcyclohexasiloxane (D6)	Dodecamethylcyclohexasiloxane (D6)
		BIS(2-ETHYLHEXYL) FUMARATE	BIS(2-ETHYLHEXYL) FUMARATE	BIS(2-ETHYLHEXYL) FUMARATE	BIS(2-ETHYLHEXYL) FUMARATE
		Hexadecanoic acid, 2-hydroxy-1-(hydroxymethyl)ethyl ester	Hexadecanoic acid, 2-hydroxy-1-(hydroxymethyl)ethyl ester	Hexadecanoic acid, 2-hydroxy-1-(hydroxymethyl)ethyl ester	Hexadecanoic acid, 2-hydroxy-1-(hydroxymethyl)ethyl ester
SGF	**Plasticizers**	Diisobutyl phthalate	Diisobutyl phthalate	Diisobutyl phthalate	Diisobutyl phthalate
		Di-n-octyl phthalate	Di-n-octyl phthalate	Di-n-octyl phthalate	Di-n-octyl phthalate
		Dicyclohexyl phthalate	Dicyclohexyl phthalate	Dicyclohexyl phthalate	Dicyclohexyl phthalate
		Bis(2-ethylhexyl) isophthalate	Bis(2-ethylhexyl) isophthalate	Bis(2-ethylhexyl) isophthalate	Bis(2-ethylhexyl) isophthalate
	Light stabilizers	Tinuvin 292-2	-	-	Tinuvin 292-2
	Lubricants	SDA, stearidonic acid, moroctic acid	SDA, stearidonic acid, moroctic acid	SDA, stearidonic acid, moroctic acid	SDA, stearidonic acid, moroctic acid
		cis-5,8,11,14,17-Eicosapentaenoic acid	cis-5,8,11,14,17-Eicosapentaenoic acid	cis-5,8,11,14,17-Eicosapentaenoic acid	-
		trans-13-Docosenamide	trans-13-Docosenamide	trans-13-Docosenamide	trans-13-Docosenamide
		9-Octadecenamide, (Z)-	9-Octadecenamide, (Z)-	9-Octadecenamide, (Z)-	9-Octadecenamide, (Z)-
	Slip agents	Stearamide (Octadecanamide)	Stearamide (Octadecanamide)	Stearamide (Octadecanamide)	Stearamide (Octadecanamide)
	Others	Hexamethylcyclotrisiloxane (D3)	Hexamethylcyclotrisiloxane (D3)	Hexamethylcyclotrisiloxane (D3)	Hexamethylcyclotrisiloxane (D3)
		Dodecamethylcyclohexasiloxane (D6)	Dodecamethylcyclohexasiloxane (D6)	Dodecamethylcyclohexasiloxane (D6)	Dodecamethylcyclohexasiloxane (D6)
		BIS(2-ETHYLHEXYL) FUMARATE	BIS(2-ETHYLHEXYL) FUMARATE	BIS(2-ETHYLHEXYL) FUMARATE	BIS(2-ETHYLHEXYL) FUMARATE
		Hexadecanoic acid, 2-hydroxy-1-(hydroxymethyl)ethyl ester	Hexadecanoic acid, 2-hydroxy-1-(hydroxymethyl)ethyl ester	Hexadecanoic acid, 2-hydroxy-1-(hydroxymethyl)ethyl ester	Hexadecanoic acid, 2-hydroxy-1-(hydroxymethyl)ethyl ester

Table S4. Additives leached from PVC microplastics to ASW and SGF after aging treatment.

		Fresh	Thermal	UV	Biofilms
ASW	**Plasticizers**	Diethyl phthalate	Diethyl phthalate	Diethyl phthalate	-
		Dimethyl phthalate	Dimethyl phthalate	Dimethyl phthalate	-
		Di-n-octyl phthalate	Di-n-octyl phthalate	Di-n-octyl phthalate	Di-n-octyl phthalate
		Diisobutyl phthalate	Diisobutyl phthalate	Diisobutyl phthalate	Diisobutyl phthalate
	Flame retardants	Triphenylphosphine oxide	Triphenylphosphine oxide	Triphenylphosphine oxide	Triphenylphosphine oxide
	Lubricants	9-Octadecenamide, (Z)-	9-Octadecenamide, (Z)-	9-Octadecenamide, (Z)-	9-Octadecenamide, (Z)-
		trans-13-Docosenamide	trans-13-Docosenamide	trans-13-Docosenamide	trans-13-Docosenamide
		1-Stearoylglycerol	1-Stearoylglycerol	1-Stearoylglycerol	1-Stearoylglycerol
		N,N'-Ethylenebis(stearamide)	N,N'-Ethylenebis(stearamide)	N,N'-Ethylenebis(stearamide)	N,N'-Ethylenebis(stearamide)
	Slip agents	Stearamide (Octadecanamide)	Stearamide (Octadecanamide)	Stearamide (Octadecanamide)	Stearamide (Octadecanamide)
	Others	Hexamethylcyclotrisiloxane (D3)	Hexamethylcyclotrisiloxane (D3)	Hexamethylcyclotrisiloxane (D3)	Hexamethylcyclotrisiloxane (D3)
		Dodecamethylcyclohexasiloxane (D6)	Dodecamethylcyclohexasiloxane (D6)	Dodecamethylcyclohexasiloxane (D6)	Dodecamethylcyclohexasiloxane (D6)
		BIS(2-ETHYLHEXYL) FUMARATE	BIS(2-ETHYLHEXYL) FUMARATE	BIS(2-ETHYLHEXYL) FUMARATE	BIS(2-ETHYLHEXYL) FUMARATE
SGF	**Plasticizers**	Diethyl phthalate	Diethyl phthalate	Diethyl phthalate	-
		Dimethyl phthalate	Dimethyl phthalate	Dimethyl phthalate	-
		n-Hexyl decyl phthalate	n-Hexyl decyl phthalate	n-Hexyl decyl phthalate	-
		Di-n-octyl phthalate	Di-n-octyl phthalate	Di-n-octyl phthalate	Di-n-octyl phthalate
		Diisobutyl phthalate	Diisobutyl phthalate	Diisobutyl phthalate	Diisobutyl phthalate
		Dibutyl phthalate	Dibutyl phthalate	Dibutyl phthalate	-
	Flame retardants	Triphenylphosphine oxide	Triphenylphosphine oxide	Triphenylphosphine oxide	Triphenylphosphine oxide
	Lubricants	SDA, stearidonic acid, moroctic acid	SDA, stearidonic acid, moroctic acid	SDA, stearidonic acid, moroctic acid	SDA, stearidonic acid, moroctic acid
		trans-13-Docosenamide	trans-13-Docosenamide	trans-13-Docosenamide	trans-13-Docosenamide
		1-Stearoylglycerol	1-Stearoylglycerol	1-Stearoylglycerol	1-Stearoylglycerol
		N,N'-Ethylenebis(stearamide)	N,N'-Ethylenebis(stearamide)	N,N'-Ethylenebis(stearamide)	N,N'-Ethylenebis(stearamide)
		9-Octadecenamide, (Z)-	9-Octadecenamide, (Z)-	9-Octadecenamide, (Z)-	9-Octadecenamide, (Z)-
	Slip agents	Stearamide (Octadecanamide)	Stearamide (Octadecanamide)	Stearamide (Octadecanamide)	Stearamide (Octadecanamide)
	Others	Hexamethylcyclotrisiloxane (D3)	Hexamethylcyclotrisiloxane (D3)	Hexamethylcyclotrisiloxane (D3)	Hexamethylcyclotrisiloxane (D3)
		Dodecamethylcyclohexasiloxane (D6)	Dodecamethylcyclohexasiloxane (D6)	Dodecamethylcyclohexasiloxane (D6)	Dodecamethylcyclohexasiloxane (D6)
		BIS(2-ETHYLHEXYL) FUMARATE	BIS(2-ETHYLHEXYL) FUMARATE	BIS(2-ETHYLHEXYL) FUMARATE	BIS(2-ETHYLHEXYL) FUMARATE

Table S5. Related data of the volcano plot for PU microplastics

	Additives	Fresh-Thermal		Fresh-UV		Fresh-Biofilms	
		log2 Fold Change	p-value	log2 Fold Change	p-value	log2 Fold Change	p-value
ASW	trans-13-Docosenamide	0.054	**0.029**	0.093	0.442	0.112	0.113
	Diisobutyl phthalate (DIBP)	0.020	0.865	0.015	0.870	-0.062	0.720
	Tinuvin 292-2	-	**0.015**	-	**0.015**	-	**0.015**
	Stearamide (Octadecanamide)	0.739	0.407	0.191	0.760	-1.945	**0.048**
	Hexamethylcyclotrisiloxane (D3)	0.450	0.525	0.756	0.141	-4.507	**0.023**
	Di-n-octyl phthalate (DnOP)	1.160	**0.033**	1.025	**0.009**	-1.218	**0.002**
	Dodecamethylcyclohexasiloxane (D6)	0.032	0.943	0.523	0.286	0.440	0.286
	BIS(2-ETHYLHEXYL) FUMARATE	-0.136	0.631	-0.556	0.124	-0.332	0.380
	SDA, stearidonic acid, moroctic acid	-0.493	0.694	0.351	0.520	-0.242	0.820
	Hexadecanoic acid, 2-hydroxy-1-(hydroxymethyl)ethyl ester	-0.611	0.458	-0.329	0.767	-0.693	0.112
	Bis(2-ethylhexyl) isophthalate	0.373	**0.029**	0.054	0.759	-1.659	**0.001**
SGF	trans-13-Docosenamide	0.060	0.222	0.057	0.078	0.071	0.449
	Diisobutyl phthalate (DIBP)	0.126	0.692	0.002	**0.008**	-1.048	**0.031**
	Tinuvin 292-2	-	**0.001**	-	**0.001**	-7.401	**0.026**
	Stearamide (Octadecanamide)	0.319	0.740	0.081	0.877	-1.357	**0.002**
	Hexamethylcyclotrisiloxane (D3)	0.204	0.820	0.323	0.363	-0.373	0.292
	Di-n-octyl phthalate (DnOP)	1.019	**0.047**	1.858	**0.030**	-1.595	**0.049**
	9-Octadecenamide, (Z)-	0.680	0.231	-0.062	0.874	-0.077	0.933
	Dodecamethylcyclohexasiloxane (D6)	0.041	0.924	0.0163	0.738	-0.400	0.330
	BIS(2-ETHYLHEXYL) FUMARATE	-0.073	0.165	-0.168	0.272	-0.203	0.290
	SDA, stearidonic acid, moroctic acid	-1.26	0.074	-1.471	0.066	-0.964	0.340
	Hexadecanoic acid, 2-hydroxy-1-(hydroxymethyl)ethyl ester	-0.342	0.259	-0.187	0.838	-0.568	0.167
	Bis(2-ethylhexyl) isophthalate	0.726	0.245	1.021	0.315	-1.192	0.397

Red bold text represents with significant difference ($p < 0.05$)

Table S6. Related data of the volcano plot for PVC microplastics

	Additives	Fresh-Thermal		Fresh-UV		Fresh-Biofilms	
		log2 Fold Change	p-value	log2 Fold Change	p-value	log2 Fold Change	p-value
ASW	trans-13-Docosenamide	0.043	0.276	0.008	0.691	0.083	0.063
	Stearamide (Octadecanamide)	0.915	0.568	0.756	0.611	-0.619	0.429
	N,N'-Ethylenebis(stearamide)	-0.801	0.099	-0.295	0.530	-0.291	0.519
	Diethyl phthalate	-0.202	0.563	0.313	0.526	-	**0.010**
	BIS(2-ETHYLHEXYL) FUMARATE	-0.158	0.508	-0.335	0.262	-0.250	0.491
	Hexamethylcyclotrisiloxane (D3)	0.063	0.866	-0.158	0.690	-0.949	0.215
	Dimethyl phthalate (DMP)	1.362	**0.007**	0.020	0.859	-	**0.033**
	Di-n-octyl phthalate (DnOP)	1.329	**0.041**	0.287	0.128	-2.182	**0.036**
	Diisobutyl phthalate (DIBP)	0.058	0.778	-0.026	0.886	-5.425	**0.009**
	1-Stearoylglycerol	1.957	0.217	-0.436	0.494	0.314	0.632
	Dodecamethylcyclohexasiloxane (D6)	1.175	**0.025**	0.989	0.088	0.180	0.761
	Triphenylphosphine oxide (TPPO)	1.383	0.447	0.342	0.467	-3.236	**0.014**
	9-Octadecenamide, (Z)-	0.163	0.488	0.309	0.852	-1.591	0.148
SGF	trans-13-Docosenamide	0.049	0.079	0.095	0.059	0.799	0.352
	Stearamide (Octadecanamide)	0.026	0.955	0.915	0.568	0.096	0.619
	Dimethyl phthalate (DMP)	0.446	**0.033**	0.022	0.863	-	**0.005**
	N,N'-Ethylenebis(stearamide)	-0.114	0.914	0.466	0.163	-0.626	0.454
	Diethyl phthalate (DEP)	0.065	0.488	0.017	0.815	-5.853	**0.007**
	BIS(2-ETHYLHEXYL) FUMARATE	-0.170	0.384	-0.114	0.535	-0.365	0.154
	SDA, stearidonic acid, moroctic acid,	-1.031	0.241	-0.047	0.702	-0.428	0.430
	Hexamethylcyclotrisiloxane (D3)	-0.228	0.090	0.112	0.756	0.997	0.221
	n-Hexyl decyl phthalate	0.038	0.773	0.020	0.737	-	**0.004**
	Di-n-octyl phthalate (DnOP)	1.940	**0.002**	0.021	0.866	-1.074	**0.018**
	Diisobutyl phthalate (DIBP)	0.028	0.549	0.033	0.646	0.077	0.418
	Dibutyl phthalate (DBP)	2.264	0.469	0.141	0.452	-	**0.0001**
	1-Stearoylglycerol	0.161	0.933	0.133	0.920	-1.577	0.407
	Dodecamethylcyclohexasiloxane (D6)	0.019	0.966	0.214	0.185	-0.292	0.666
	Triphenylphosphine oxide (TPPO)	1.035	0.259	0.584	0.443	-2.161	0.395

|	0.053	0.950	0.273	0.843	-0.042	0.948
9-Octadecenamide, (Z)-						

Red bold text represents with significant difference ($p < 0.05$)
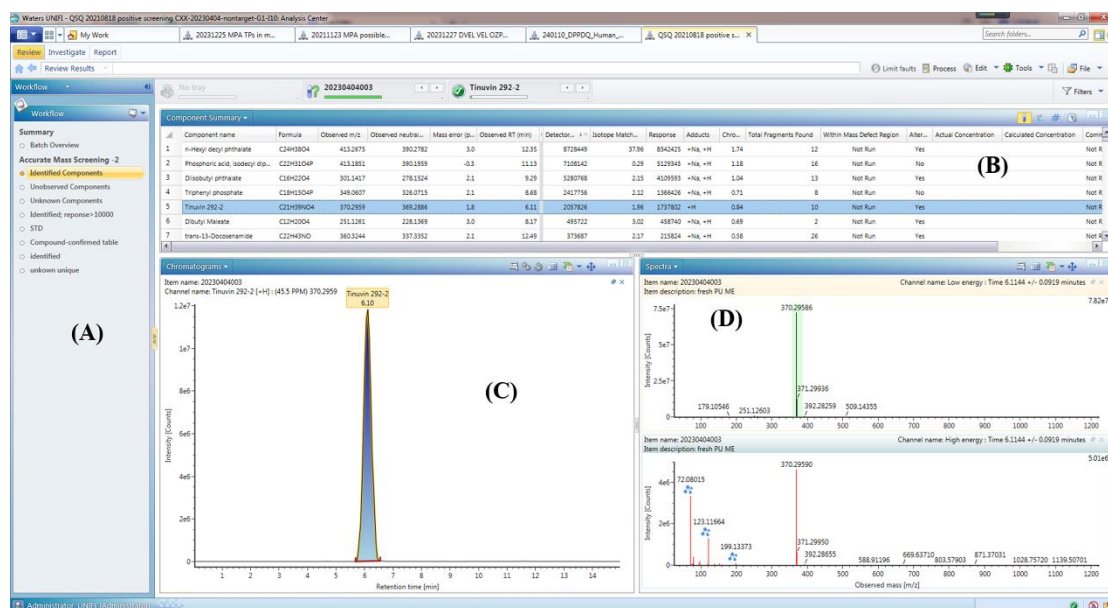
Figure S1. UNIFI platform interface. (A) template of workflow, (B) component identification list, (C) selected ion chromatogram of a single component corresponding to B, and (D) the upper figure is a low energy spectrum (MS spectrum) while the lower figure is a high energy spectrum (MS/MS spectrum) collected immediately after the low energy spectrum by the MSE technique used by waters.
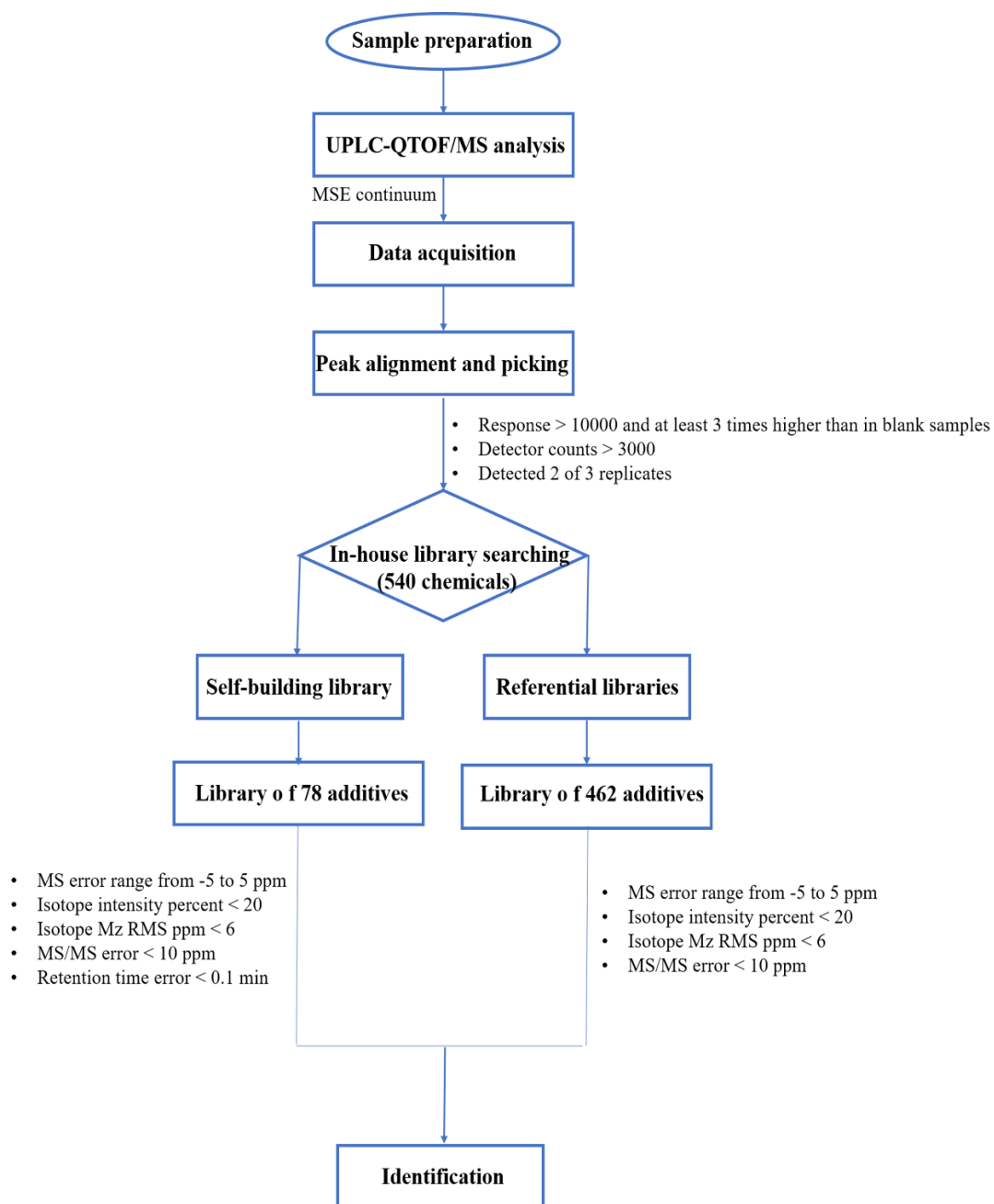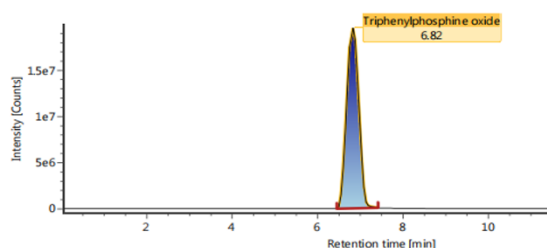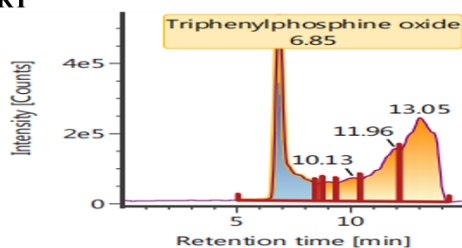
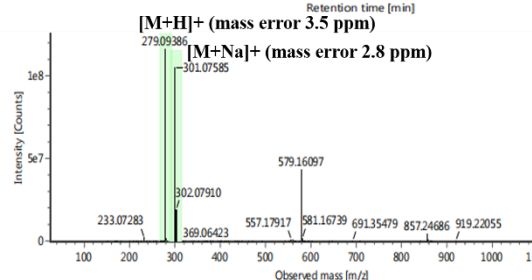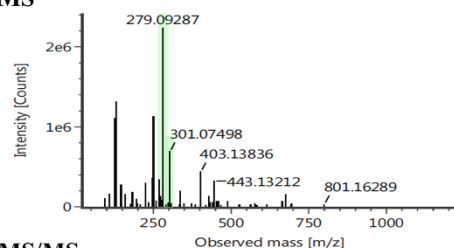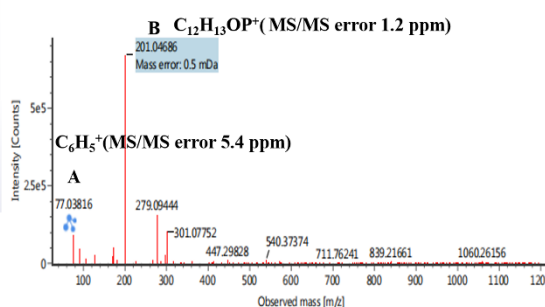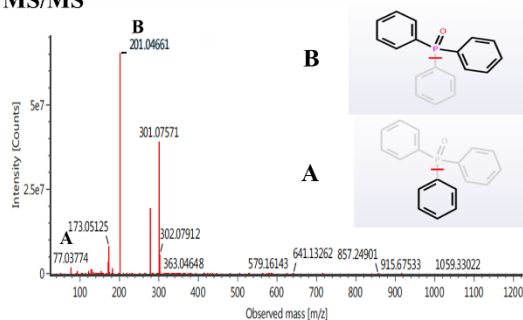**Figure S2** Workflow of additives identification.

Triphenylphosphine oxide

Figure S3. Identification of triphenylphosphine oxide form the self-building library included: chromatographic and fragmentation comparison of triphenylphosphine oxide in the sample and standard. (In ESI+ mode, the accurate m/z of [M+H] $^+$ and [M+Na] $^+$of obtained from the standard at low energy was 279.09287 and 301.07498, the RT (retention time) was 6.85 min. In the sample, a plausible compound with adduct of H^+ and Na^+, accurate m/z of 279.09386 and 301.07585, respectively, RT of 6.82 min was detected. Their RT error was 0.03 min and mass error were 3.5 and 2.8 ppm. The isotope match Mz RMS PPM of the plausible compound was 2.97. Additionally, two major fragment ions $C_{12}H_{13}OP^+$ (m/z 201.04661), $C_6H_5^+$ (m/z 77.038126) were generated at high energy from the triphenylphosphine oxide precursor ion of the standard. Two

fragment ions of the plausible compound at m/z 301.04686 and 77.038126 could be matched to the standard and their MS/MS errors were 1.2 and 5.4 ppm, respectively. The above results show that identification parameter errors met the screening criteria and identified the presence of triphenylphosphine oxide in microplastics.

Tinuvin 292-2
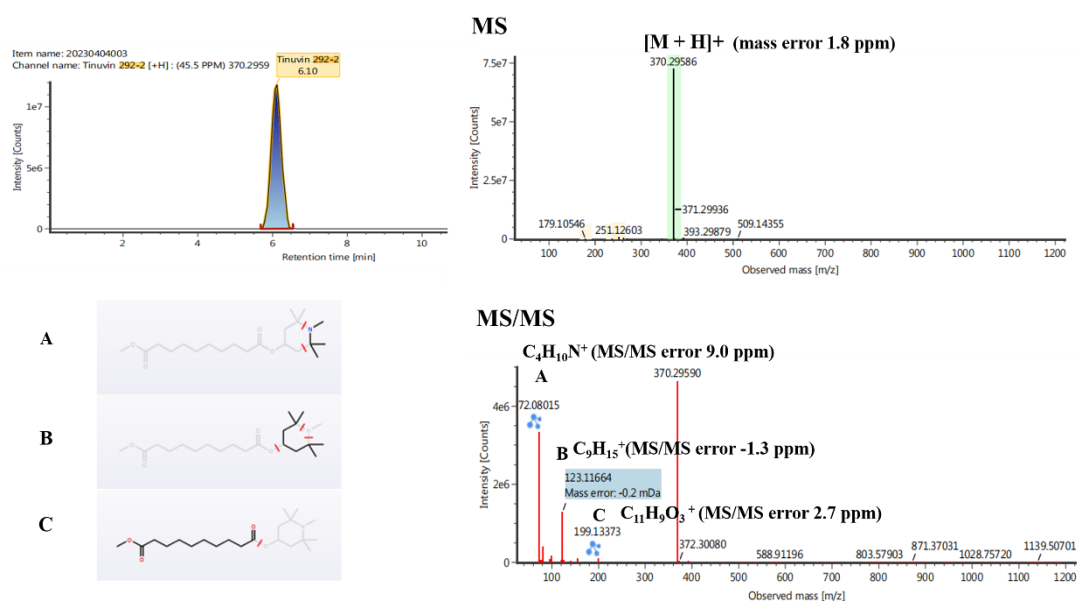
Figure S4. Identification of Tinuvin 292-2 from the referential libraries included: fragmentation comparison of Tinuvin 292-2 in the sample and theoretical MS/MS library. (In the sample, a plausible compound with adduct of H^+ accurate m/z of 370.29586 was detected. Their mass error was 1.8 ppm. The isotope match Mz RMS PPM of the plausible compound was 1.96. Additionally, three major fragment ions $C_4H_{10}N^+$ (m/z 72.08015), $C_9H_{15}^+$ (m/z 123.11664) and $C_{11}H_9O_3^+$ (199.13373) were generated at high energy from precursor ion of the plausible compound, which could be matched to the theoretical MS/MS database and their MS/MS errors were 9.0, -1.3 and 2.7 ppm, respectively. The above results show that identification parameter errors

met the screening criteria and tentatively identified the presence of Tinuvin 292-2 in microplastics.
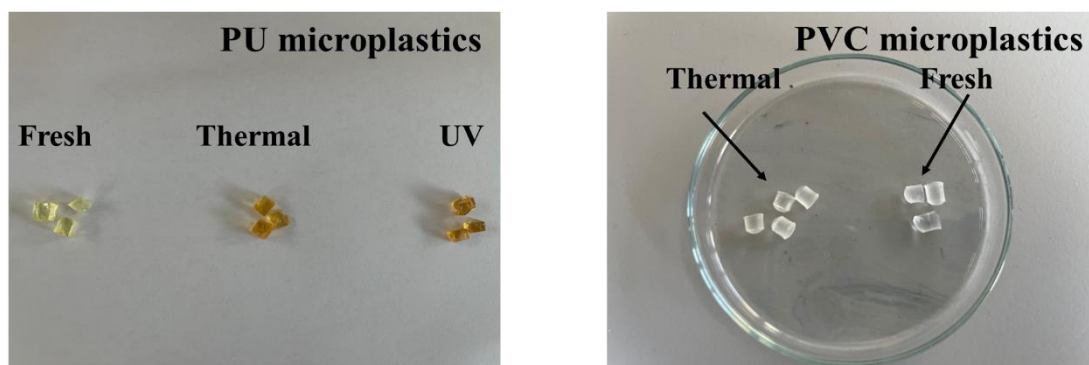
Figure S5. Color changes for PU (a) and PVC (b) microplastics after aging treatment.
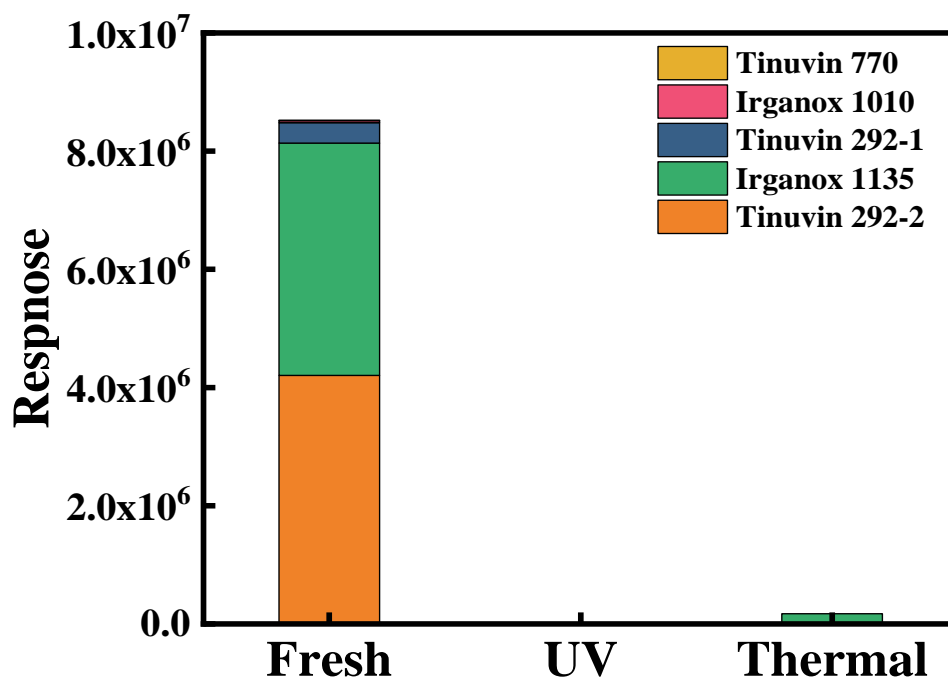
Figure S6. Response of light stabilizers in PU extracts.

References

Boubakri, A., Elleuch, K., Guermazi, N., Ayedi, H.F., 2009. Investigations on hygrothermal aging of thermoplastic polyurethane material. Materials & Design 30, 3958-3965.

Boulaouche, T., Kherroub, D.E., Khimeche, K., Belbachir, M., 2019. Green strategy for the synthesis of polyurethane by a heterogeneous catalyst based on activated clay. Research on Chemical Intermediates 45, 3585-3600.

Bridson, J.H., Gaugler, E.C., Smith, D.A., Northcott, G.L., Gaw, S., 2021. Leaching and extraction of additives from plastic pollution to inform environmental risk: A multidisciplinary review of analytical approaches. J Hazard Mater 414, 125571.

Chen, Q., Santos, M.M.D., Tanabe, P., Harraka, G.T., Magnuson, J.T., McGruer, V., Qiu, W., Shi, H., Snyder, S.A., Schlenk, D., 2021. Bioassay guided analysis coupled with non-target chemical screening in polyethylene plastic shopping bag fragments after exposure to simulated gastric juice of Fish. J. Hazard. Mater. 401, 123421.

Coffin, S., Huang, G.Y., Lee, I., Schlenk, D., 2019. Fish and Seabird Gut Conditions Enhance Desorption of Estrogenic Chemicals from Commonly-Ingested Plastic Items. Environ Sci Technol 53, 4588-4599.

Fan, X., Zou, Y., Geng, N., Liu, J., Hou, J., Li, D., Yang, C., Li, Y., 2021. Investigation on the adsorption and desorption behaviors of antibiotics by degradable MPs with or without UV ageing process. J. Hazard. Mater. 401, 123363.

Hahladakis, J.N., Velis, C.A., Weber, R., Iacovidoua, E., Purnell, P., 2015. An overview of chemical additives present in plastics: Migration,release, fate and environmental impact during their use, disposal and recycling. J. Hazard. Mater. 344, 179-199.

Huan-Yu, T., Jiawei, Z., Hui, G., Mengtao, Z., Wei, G., Jianghong, S., Xiao-yan, L., 2022. Development of ecological risk assessment for Diisobutyl phthalate and di-n-octyl phthalate in surface water of China based on species sensitivity distribution model. Chemosphere 307, 135932.

Huerta-Fontela, M., Galceran, M.T., Ventura, F., 2011. Occurrence and removal of pharmaceuticals and hormones through drinking water treatment. Water Res 45, 1432-1442.

Koelmans, A.A., Bakir, A., Burton, G.A., Janssen, C.R., 2016. Microplastic as a Vector for Chemicals in the Aquatic Environment: Critical Review and Model-Supported Reinterpretation of Empirical Studies. Environ Sci Technol 50, 3315-3326.

Li, Y., Lu, Z., Abrahamsson, D.P., Song, W., Yang, C., Huang, Q., Wang, J., 2022. Non-targeted analysis for organic components of microplastic leachates. Sci Total Environ 816, 151598.

Liu, P., Wu, X., Liu, H., Wang, H., Lu, K., Gao, S., 2020. Desorption of pharmaceuticals from pristine and aged polystyrene microplastics under simulated gastrointestinal conditions. J. Hazard. Mater. 392, 122346.

Luo, H., Liu, C., He, D., Sun, J., Li, J., Pan, X., 2022. Effects of aging on environmental behavior of plastic additives: Migration, leaching, and ecotoxicity. Sci Total Environ 849, 157951.

Luyt, A.S., Gasmi, S.A., Malik, S.S., Aljindi, R.M., Ouederni, M., Vouyiouka, S.N., Porfyris, A.D., Pfaendner, R., Papaspyrides, C.D., 2021. Artificial weathering and accelerated heat ageing studies on low-density polyethylene (LDPE) produced via autoclave and tubular process technologies. Express Polymer Letters 15, 121-136.

Maquelin, K., Kirschner, C., Choo-Smith, L.P., Braak, N.v.d., Endtz, H.P., Naumann, D., Puppels, G.J., 2002. Identification of medically relevant microorganisms by vibrational spectroscopy. Journal of Microbiological Methods, 255–271.

Murphy, J., 2001. Additives for plastics handbook. Elsevier.

Napper, I.E., Thompson, R.C., 2020. Plastic Debris in the Marine Environment: History and Future Challenges. Global Challenges 4.

Ouyang, Z., Zhang, Z., Jing, Y., Bai, L., Zhao, M., Hao, X., Li, X., Guo, X., 2022. The photo-aging of polyvinyl chloride microplastics under different UV irradiations. Gondwana Research 108, 72-80.

Pagacz, J., Chrzanowski, M., Krucińska, I., Pielichowski, K., 2015. Thermal aging and accelerated weathering of PVC/MMT nanocomposites: Structural and morphological studies. Journal of Applied Polymer Science 132, n/a-n/a.

Paluselli, A., Fauvelle, V., Galgani, F., Sempere, R., 2019. Phthalate Release from Plastic Fragments and Degradation in Seawater. Environ Sci Technol 53, 166-175.

Procter, J., Hopkins, F.E., Fileman, E.S., Lindeque, P.K., 2019. Smells good enough to eat: Dimethyl sulfide (DMS) enhances copepod ingestion of microplastics. Marine Pollution Bulletin 138, 1-6.

Qiu, S.Q., Huang, G.Y., Fang, G.Z., Li, X.P., Lei, D.Q., Shi, W.J., Xie, L., Ying, G.G., 2021. Chemical characteristics and toxicological effects of leachates from plastics under simulated seawater and fish digest. Water Research 209, 117892.

Razanajatovo, R.M., Ding, J., Zhang, S., Jiang, H., Zou, H., 2018. Sorption and desorption of selected pharmaceuticals by polyethylene microplastics. Marine Pollution Bulletin 136, 516-523.

Rosu, D., Rosu, L., Cascaval, C.N., 2009. IR-change and yellowing of polyurethane as a result of UV irradiation. Polym. Degrad. Stab. 94, 591-596.

Running, S.W., Zhao, M., Mildrexler, D.J., 2011. Satellite Finds Highest Land Skin Temperatures on Earth. Bulletin of the American Meteorological Society 92, 855-860.

Sandt, C., Waeytens, J., Deniset-Besseau, A., Nielsen-Leroux, C., Rejasse, A., 2021. Use and misuse of FTIR spectroscopy for studying the bio-oxidation of plastics. Spectrochim. Acta - A: Mol. Biomol. Spectrosc. 258, 119841.

Savoca, M.S., Wohlfeil, M.E., Ebeler, S.E., Nevitt, G.A., 2016. Marine plastic debris emits a keystone infochemical for olfactory foraging seabirds. Sci. Adv. 2, 1-8.

Steer, M., Cole, M., Thompson, R.C., Lindeque, P.K., 2017. Microplastic ingestion in fish larvae in the western English Channel. Environ Pollut 226, 250-259.

Tourinho, P.S., Ivar do Sul, J.A., Fillmann, G., 2010. Is marine debris ingestion still a problem for the coastal marine biota of southern Brazil? Mar Pollut Bull 60, 396-401.

Wang, H., Liu, H., Zhang, Y., Zhang, L., Wang, Q., Zhao, Y., 2023. The toxicity of microplastics and their leachates to embryonic development of the sea cucumber Apostichopus japonicus. Mar Environ Res 190, 106114.

Xue, X.D., Fang, C.R., Zhuang, H.F., 2021. Adsorption behaviors of the pristine and aged thermoplastic polyurethane microplastics in Cu(II)-OTC coexisting system. J. Hazard. Mater. 407, 124835.

Zhang, Y., Sun, S., Xing, X., Du, Z., Guo, Q., Yu, W., 2016. Detection and Identification of Leachables in Vaccine from Plastic Packaging Materials Using UPLC-QTOF MS with Self-Built Polymer Additives Library. Anal. Chem. 88, 6749-6757.

Zimmermann, L., Dierkes, G., Ternes, T.A., Volker, C., Wagner, M., 2019. Benchmarking the in Vitro Toxicity and Chemical Composition of Plastic Consumer Products. Environ. Sci. Technol. 53, 11467-11477.

7. Conclusions and further perspectives

This chapter presents a synopsis of the results gathered from the previous chapters. It also discusses the environmental implication of the research and provides an outlook for further research on the topic.

7.1 Synopsis of results and conclusions

Whilst the plastic contamination has drawn a lot of attention and concern in recent years, very few studies have systematically discussed different aging pathways for commercial plastics and how that affects environmental behavior processes such as adsorption/desorption and leaching. Aging of plastics particles has been demonstrated to result in morphology and property changes, which is very likely to have consequences for the fate and behavior of chemicals on plastic debris.

Results from Chapter 2 suggested that UV irradiation could produce surface cracks and breakage of polymer chains, and this might be a key factor that effects the adsorption/desorption capacity after UV aging treatment. In addition, this study also illustrated that hydrophobicity, electrostatic interaction, competitive adsorption are also important factors affect the adsorption/desorption behavior of bisphenols on commercial microplastics. Results in Chapter 3 showed that biofilms colonization would slightly enhance the adsorption capacity at a relatively low BPA exposure concentration (≤ 100 μg/L). Generally, BPA and other organic pollutants exist at low concentrations in the aquatic environment. Therefore, improved adsorption capacity could be expected for microplastics colonized with biofilms in the natural environment. In addition, UV irradiation could also enhance biofilms colonization and lead to the enhanced adsorption ability for BPA. Abiotic degradation processes are usually considered prior to biotic degradation, and so plastic debris colonized with biofilms is expected to have undergone initial abiotic degradation (e.g., UV irradiation, washing

of waves, etc.) in the natural environment, which might result in an increased pollutant loading capacity. Meanwhile, as microorganisms' colonization can enhance bioavailability, biofilms colonized microplastics might be more easily ingested accidently by organism, resulting in higher potential exposure risk in the natural environment. Samples used in Chapter 4 are naturally aged microplastics collected from estuarine and beach environments, and so the results in this chapter could be considered to best reflect microplastics interaction behavior with bisphenols in the true environment. These results suggested that aged microplastics showed higher adsorption capacities than fresh ones, although the involved mechanisms were similar with we demonstrated in Chapter 2 and Chapter 3. As a result, more pollutants could be excepted loading on degraded microplastics debris in the natural environment. Although the desorption efficiency decreased after aging, the desorption capacity might still show an increased trend. As a result, aged microplastics might represent a higher potential risk than fresh materials, as they could not only load more pollutants, but also exhibit a stronger release potential to the environment system. According to the study in Chapter 2, Chapter 3 and Chapter 5, heteroatomic plastics (PU, PA) showed obviously better adsorption capacity for bisphenols compared to C–C backbone plastics (PE, PVC, PP, PS) as strong H-bonding interaction exist between amide group of heteroatomic plastics and bisphenols. This indicates that heteroatomic plastic debris might act as an important carrier for pollutants in the aquatic system. However, it worth noting that microplastic debris that collected in the environment were all C–C backbone polymers, which suggests that C–C backbone plastics might be the main types of plastics that distribute

and accumulate in the environment. Thus, most microplastics might show relatively low adsorption ability in the real environment. The exposure risk still cannot be ignored, however, as the aging of microplastics would generate new functional groups and surface cracks, which could enhance the chemical bonding interaction and offer more available adsorption sites, leading to adsorption capacity significantly increasing after aging. Results in Chapter 5 and Chapter 6 helped to clarify the relationship between aging of microplastics debris and their related chemicals (additives and co-existing pollutants). Additives (e.g., light stabilizers, antioxidants, plasticizers) might be vital to control the aging degree of microplastics and further impact the leaching behavior of additives and interaction behavior with co-existing chemicals. In addition, additives might be degraded during the aging process, which could result in exhaustion of additives in polymer resulting in conversion to by-products, which could also alter leaching behavior. In summary, this study has clearly demonstrated that the aging of microplastics has fundamental effects on the environmental behavior of microplastics, providing new insights for microplastic debris' release and their interaction with chemicals in the natural environment.

7.2 Shortcomings and further perspectives

Although this study is helpful to understand the weathering behavior of microplastics and its influence of weathering on the environmental behavior of microplastics, there are still some shortcomings and potential areas for further research. The following suggestions are made for future work based on our current research:

1). The concentration of spiked bisphenols was much higher than those reported in the natural environments. For example, the spiked concentration of bisphenols was 1000 µg/L in Chapter 2, which is dozens of times higher than the maximum detected concentration in the natural environment. Owing to HPLC instrument was used in this study, and in order to get accurate results, the concentration was generally higher than real concentrations. Further studies should adjust the concentration to closer to realistic environmental levels for potentially more credible results.

2). This study has carried out series batch experiments to explore different exposure environments for the effect of adsorption/desorption and leaching behavior. For example, both Chapter 3 and Chapter 6 assessed the risks of BPA and additives from microplastics to simulated gastric fluid. Whilst all of the work were laboratory-based experiments, the results represented a surrogate for the ingestion aged microplastics by real biota. Due to the small particle size, microplastics are easily to be accidentally ingested by organisms, which might be an important pathway for microplastics releasing chemicals to organisms and resulting in toxicity. Further studies should be expanded to fish, birds and other organisms to probe the accumulation process of chemicals in biota (e.g., in liver, gastric fluid, abdominal adipose tissue, etc.) to help better assess the biotoxicity and exposure risks of aged microplastic debris in biota.

3). This study has characterized the surface morphological changes and functional groups changes by Raman, FTIR, SEM instruments. While other properties such as crystallinity, specific surface area, hydrophobicity, etc. might also be altered after aging

treatments. In Chapter 4, although naturally aged PE1 and PE2 microplastics both suggested better adsorption behavior than fresh microplastics, the adsorption difference between PE1 and PE2 cannot be clearly explained, although such data could have provided more insights. The properties e.g., crystallinity, specific surface area, hydrophobicity, etc. should be quantitatively characterized in further studies and correlations with microplastics adsorption/desorption and leaching capacities explored to better understanding the factors affect the interaction behavior between pollutants and aged microplastics.

4). Future studies should encourage the use of more naturally aged microplastics rather than laboratory aged microplastics. As plastic debris in the natural environment might undergoing a series complex aging process compared to our laboratory aging treatments (e.g., undergoing several aging pathways simultaneously and aging much more time), which could result in a higher degree of aging of microplastics and lead to more obviously changes for the adsorption and released behavior of chemical pollutants and additives. As a result, experiments based on laboratory aged microplastics are not enough to comprehensively assess aging for the effect of microplastics environmental behavior in the real environment, more environmental-related natural aged microplastics should be used for the further risk assessment.

5). Chapter 5 and Chapter 6 were helpful to understand the present of additives in microplastics during the aging process. Structure assignments based on exact mass, isotope pattern and fragmentation are an important step towards identifying chemicals.

However, its theoretical nature sometimes matched false positives in terms of mass accuracy, or fragmentation. As a result, tentative structural assignments should be better confirmed with their authentic standards in the further study. Further work is needed for target-screening analysis to provide quantitative data support for evaluating the ecological risks of aged microplastics debris in the environment.

7.3 Concluding remarks

Plastic material manufacturing and buildup over the past 50 years has significantly increased pollution levels. Micro-sized plastics have become one of the most pressing environmental issues among the numerous types of plastic pollution. These tiny plastic flakes enter water systems from a variety of sources, where additives and other sorbed chemicals may be released throughout the entire life cycle of plastics resulting in contamination of aquatic systems. Since microplastics can be consumed by people and aquatic species and eventually make their way into the food chain, their presence in the environment poses a serious concern. This study has assessed the adsorption and release behavior of bisphenols and other chemical additives from microplastics during different aging process. As the aging of microplastics and the increased abundance of microplastics in real environments are inevitable trends these factors need to be considered in our life cycle assessments. This study will be helpful to understand the environmental behavior of microplastics as a carrier for the migration and transformation of chemicals, also potentially to the assessment of exposure risk of microplastic debris in the environment.